REPORT 49

GOVERNMENT OF WESTERN AUSTRALIA

GEOLOGY AND GEOCHEMISTRY OF GRANITOID ROCKS IN THE SOUTHWEST EASTERN GOLDFIELDS PROVINCE

by W. K. Witt and R. Davy

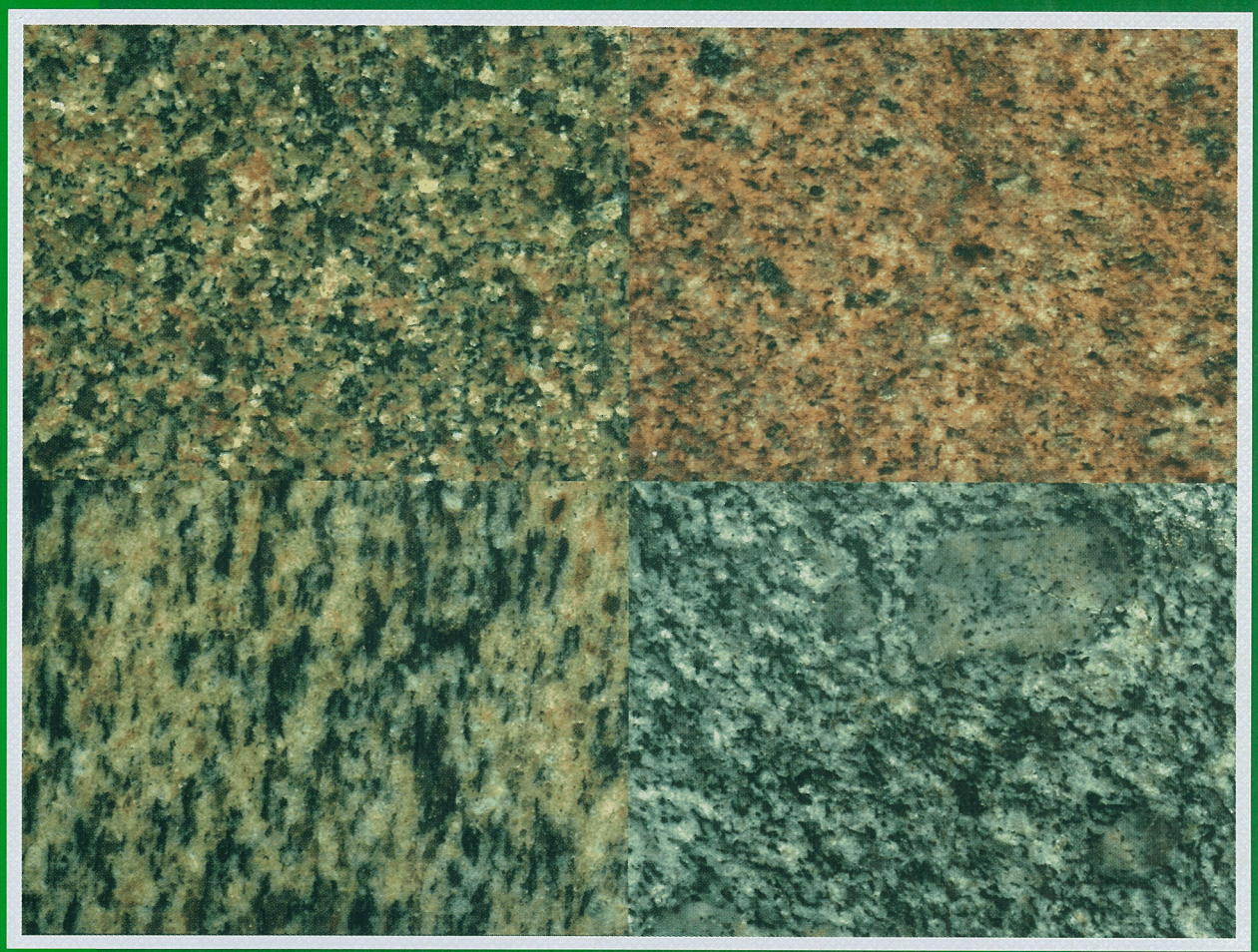

GEOLOGICAL SURVEY OF WESTERN AUSTRALIA

DEPARTMENT OF MINERALS AND ENERGY

GEOLOGICAL SURVEY OF WESTERN AUSTRALIA

REPORT 49

GEOLOGY AND GEOCHEMISTRY OF GRANITOID ROCKS IN THE SOUTHWEST EASTERN GOLDFIELDS PROVINCE

by
W. K. Witt and R. Davy

Perth 1997

MINISTER FOR MINES
The Hon. Norman Moore, MLC

ACTING DIRECTOR GENERAL
L. C. Ranford

DIRECTOR, GEOLOGICAL SURVEY OF WESTERN AUSTRALIA
Pietro Guj

REFERENCE

The recommended reference for this publication is:

WITT, W. K., and DAVY, R., 1997, Geology and geochemistry of granitoid rocks in the southwest Eastern Goldfields Province: Western Australia Geological Survey, Report 49, 137p.

National Library of Australia
Cataloguing-in-publication entry

Witt, W. K.
Geology and geochemistry of granitoid rocks in the southwest Eastern Goldfields Province.

Bibliography.
Includes index
ISBN 0 7309 6548 1

1. Granite - Western Australia - Yilgarn Craton.
2. Geology - Western Australia - Yilgarn Craton.
3. Geochemisty - Western Australia - Yilgarn Craton.
I. Davy, R. (Richard), 1935–
II. Geological Survey of Western Australia.
III. Title. (Series: Report (Geological Survey of Western Australia); no. 49).

553.52099416

ISSN 0508–4741

Cover picture:

Slab surfaces of some representative samples of granitoids in the southwest Eastern Goldfields Province: Woolgangie supersuite, GSWA 100938 (top Left); Dairy supersuite, GSWA 100924 (top right); Twin Hills suite, GSWA 100927 (bottom left); Rainbow suite, GSWA 93904 (bottom right).

Contents

Chapter 5 Whole-rock chemistry of SWEGP granitoids

Chapter 6 Petrogenesis of SWEGP granitoids

Appendices

Plates

Figures

Tables

Geology and geochemistry of granitoid rocks in the southwest Eastern Goldfields Province

by W. K. Witt and R. Davy

Abstract

Granitoids comprise approximately 40–50% of the southwest Eastern Goldfields Province (SWEGP). They are mainly biotite(–hornblende) granodiorite and monzogranite, with minor two-mica(–garnet) monzogranite and syenogranite, tonalite, trondhjemite and syenite.

Two main episodes of granitoid magmatism are recognized. Pre-regional folding granitoid (pre-RFG) complexes commonly form composite, elongate domes in the cores of F_2 anticlines. They were emplaced as broadly conformable, sheet-like bodies, at or near the base of the exposed greenstone sequences, during D_1 compression. Preferential exposure in the northern part of the SWEGP may reflect subsequent gravitational collapse of the thickened greenstone pile, and domal uplift of the granitoid substrate. Available geochronological data indicate pre-RFG magmatism occurred at 2690–2685 Ma. Circular to ovoid post-regional folding granitoid (post-RFG) plutons were emplaced mainly at 2665–2660 Ma, but intrusion probably continued until about 2600 Ma. Late plugs and dykes of alkaline granitoids yield emplacement ages as young as 2360 Ma, substantially later than regional deformation. A third granitoid group, granitoid gneiss, occurs mainly along the western margin of the SWEGP greenstone belt and as xenoliths in post-RFG plutons. The age range and origin of the granitoid gneiss are unknown, but available data indicate the gneiss is deformed and metamorphosed pre-RFG.

There are four calc-alkaline pre-RFG suites, three calc-alkaline post-RFG supersuites and one alkaline post-RFG supersuite in the SWEGP. The granitoids belong to the magnetite-series, and primary mineral assemblages suggest crystallization under relatively high fO_2 conditions ($fO_2 >$ QFM). All are I-type granitoids, except for the alkaline Gilgarna supersuite, which has A-type characteristics.

Parent melts for pre-RFG suites were derived by hydrous melting of tonalite, granodiorite and monzogranite in a layered lower crust. The volumetrically predominant post-RFG (Woolgangie) supersuite was derived by hydrous melting of a more uniform granodioritic to monzogranitic source in the mid-crust. The Gilgarna supersuite may have formed by anhydrous melting of residual source rocks in the lower crust during post-orogenic extension. Following anatexis, pre-RFG and post-RFG (super)suites evolved mainly by fractional crystallization of biotite, feldspars and, in the more mafic magmas, hornblende. Chemical variation in the pre-RFG Minyma suite and the post-RFG Dairy supersuite cannot be adequately explained by fractional crystallization alone. A second process, possibly crustal contamination, may have influenced these suites.

Relatively mafic pre-RFG suites and post-RFG plutons contain microgranitoid xenoliths and synplutonic dykes of weakly alkalic composition. They have geochemical affinities with lamprophyres and are interpreted as synplutonic intrusions.

Lithium-rich pegmatites, some of which have been mined for lithium, tin and tantalite, are genetically related to fractionated members of the Woolgangie supersuite (including particularly the Bali suite). Bali suite granitoids acted as centres of heat and fluid flux that drove synmetamorphic fluids through greenstone belt-scale hydrothermal systems. These fluids deposited gold in late-tectonic structures. Most characteristics of the SWEGP granitoids do not favour the formation of genetically related metalliferous deposits. The most likely orthomagmatic deposits (apart from pegmatites) are small Mo, W and base-metal (Cu, Pb, Zn) concentrations associated with fractionated post-RFG plutons.

Granitoids in the SWEGP were emplaced during, and immediately after, a major tectonic event involving regional compression. However, the absence of S-type granitoids contrasts with other syn-collisional granitoid provinces. The predominantly I-type compositions of the SWEGP granitoids probably reflects an absence of large sedimentary accumulations in the middle to lower crust.

KEYWORDS: Archaean, Yilgarn Craton, Eastern Goldfields Province, igneous petrology, geochemistry, geophysical interpretation, xenolith, granite, tectonics, petrogenesis, supersuites

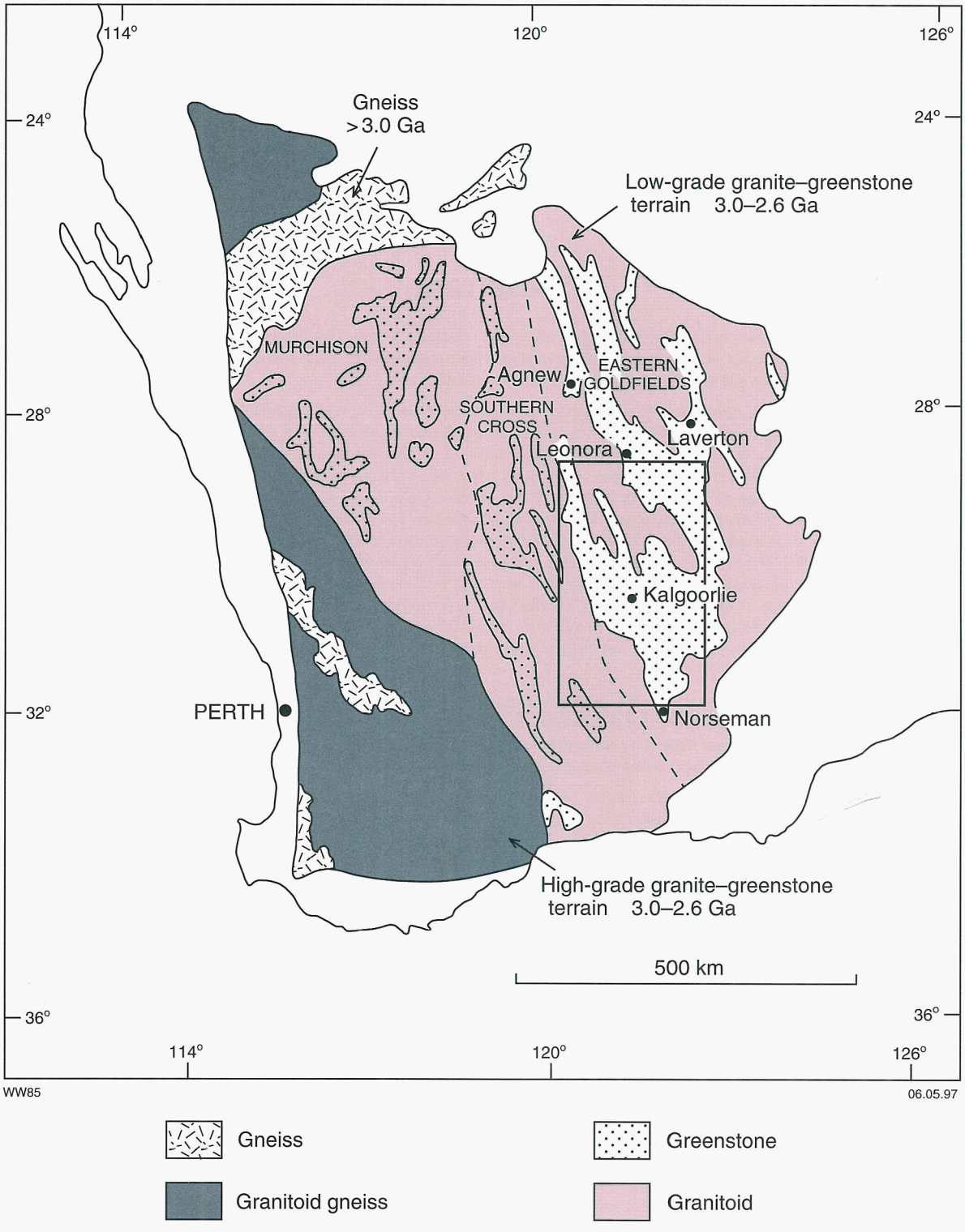

Figure 1. Regional map showing the Yilgarn Craton, and the study area (southwest Eastern Goldfields Province — SWEGP). Also shown are the Eastern Goldfields Province and the Norseman–Wiluna Belt. Note that a small part of the Southern Cross Province is included in the SWEGP but the study area is here referred to as the SWEGP for convenience. Modified from Myers (1992)

Chapter 1

Introduction

The southwest Eastern Goldfields Province (SWEGP) forms part of the Archaean Yilgarn Craton (Geological Survey of Western Australia (GSWA), 1990) in Western Australia (Fig. 1). It lies mostly within the Norseman–Wiluna belt, a linear zone of 'rift-related' greenstones that occupies approximately the western two thirds of the Eastern Goldfields Province (Williams, 1974). The area includes all or parts of MENZIES*, EDJUDINA, KALGOORLIE, KURNALPI, BOORABBIN and WIDGIEMOOLTHA (1:250 000 sheets), and covers approximately 50 000 km^2, 40–50% of which is underlain by granitoids. Although exposure of granitoids is sparse (Plate 1), observations and fresh samples were obtained from numerous small, flat pavements and rubbly outcrop.

The study area (Figs 1–3) is characterized by a pronounced north-northwesterly structural grain, defined by elongate granitoid bodies, regional shear zones, contacts between rock units, and a regional foliation. It has been divided into several terranes, each with distinct lithostratigraphic and structural associations, and separated by regional shear zones (Swager and Ahmat, 1992; Swager et al., 1995). The division of the SWEGP into terranes is based on studies of greenstone belts and is independent of granitoid data. A summary of the main lithostratigraphic associations in the study area is given in Table 1.

A limited number of precise U–Pb zircon ages (Pidgeon, 1986; Claoue-Long et al., 1988; Campbell and Hill, 1988) suggest formation of greenstones in the Kalgoorlie Terrane in the period 2700–2690 Ma. These greenstones appear to overlie older felsic volcanic rocks of the Penneshaw Formation, in the Norseman Terrane (Fig. 2), which have been dated at c. 2900 Ma (Campbell and Hill, 1988). When this work was compiled there were no other published precise age data for formation of greenstones in areas outside the Kalgoorlie Terrane.

* Capitalized names refer to standard map sheets.

Table 1. Lithostratigraphic characteristics of terranes identified in the southwest Eastern Goldfields Province

Terrane	*Lithological association*	*Stratigraphic relations*	*References*
Barlee	Tholeiitic basalt, banded iron-formation, sedimentary rocks (including basal quartzite and conglomerate)	Relatively simple ('layer-cake') stratigraphy	Griffin (1990)
Kalgoorlie	Abundant komatiite, high-Mg and tholeiitic basalts; thick dolerite sills; felsic volcaniclastic and sedimentary rocks	Relatively simple ('layer-cake') stratigraphy; felsic rocks overlie mafic to ultramafic rocks	Swager et al. (1992, 1995)
Norseman	Felsic volcaniclastic sedimentary rocks; banded iron-formation; tholeiitic basalt; komatiite minor to absent	Relatively simple ('layer-cake') stratigraphy; older felsic rocks and amphibolite (2.90 Ga) overlain by younger banded iron-formation and mafic volcanic rocks (2.7 Ga)	Campbell and Hill (1988); Swager et al. (1995)
Gindalbie	Bimodal basalt and dacitic to rhyolitic volcanic rocks; subordinate dolerite and volcaniclastic sedimentary rocks; komatiite rare to absent, except where structurally emplaced	Complex interfingering of all units in the north; tendency for mafic rocks to occur in lower part of sequence to the south	Swager and Ahmat (1992); Witt (1994); Ahmat (in prep.)
Jubilee	Basalt, komatiite, felsic volcanic and sedimentary rocks	Complex interfingering of all rock types	Swager and Ahmat (1992)
Kurnalpi	Basalt, sedimentary rocks with lenses of komatiite, and some banded iron-formation	Mafic to ultramafic rocks are overlain by felsic rocks and banded iron-formation	Swager and Ahmat (1992)


Conglomerate and greywacke

GREENSTONE TERRANES


Barlee


Edjudina
(no details of granitoid geology shown)


Gindalbie


Kalgoorlie


Kurnalpi (Jubilee domain)


Kurnalpi (Mulgabbie domain)


Kurnalpi (Steeple Hill domain)


Menzies


Norseman

GRANITES


Post-folding granitoids


Pre-folding granitoids


Granitoid gneiss
(mainly deformed pre-folding granitoids)


Fault, shear zone

FAULTS

BMF	Boorara–Menzies Fault
BLF	Boulder–Lefroy Fault
KF	Kunanalling Fault
MMF	Monger–Moriaty Fault
BFF	Butcher's Flat Fault
ZF	Zuleika Fault

GEOCHEMICAL AFFILIATION OF WHOLE–ROCK SAMPLES

Pre-folding suites

- □ Rainbow
- ◇ Twin Hills
- ○ Goongarrie
- △ Minyma

Post-folding supersuites

- \+ Woolgangie
  - ✳ Bali suite
- ▽ Dairy
  - Liberty
    - ☆ Liberty Granodiorite
    - ☆ Doyle Granodiorite
    - ☆ Bonnie Vale Tonalite
    - ☆ Kambalda Trondhjemite
    - ✲ Depot Granodiorite
    - ◈ Other plutons
- × Gilgarna

POST-FOLDING PLUTONS

B	Bullabulling Monzogranite
BK	Balarky Monzogranite
BL	Bali Monzogranite
BM	Battery Monzogranite
BV	Bonnie Vale Tonalite
CS	Carpet Snake Syenogranite
D	Doyle Granodiorite
DK	Donkey Rocks Monzogranite
DP	Depot Granodiorite
DR	Dairy Monzogranite
G	Galah Monzogranite
L	Liberty Granodiorite
M	Menangina Monzogranite
S	Siberia Monzogranites
SM	Six Mile Well Monzogranite

WW82AA 26.05.97

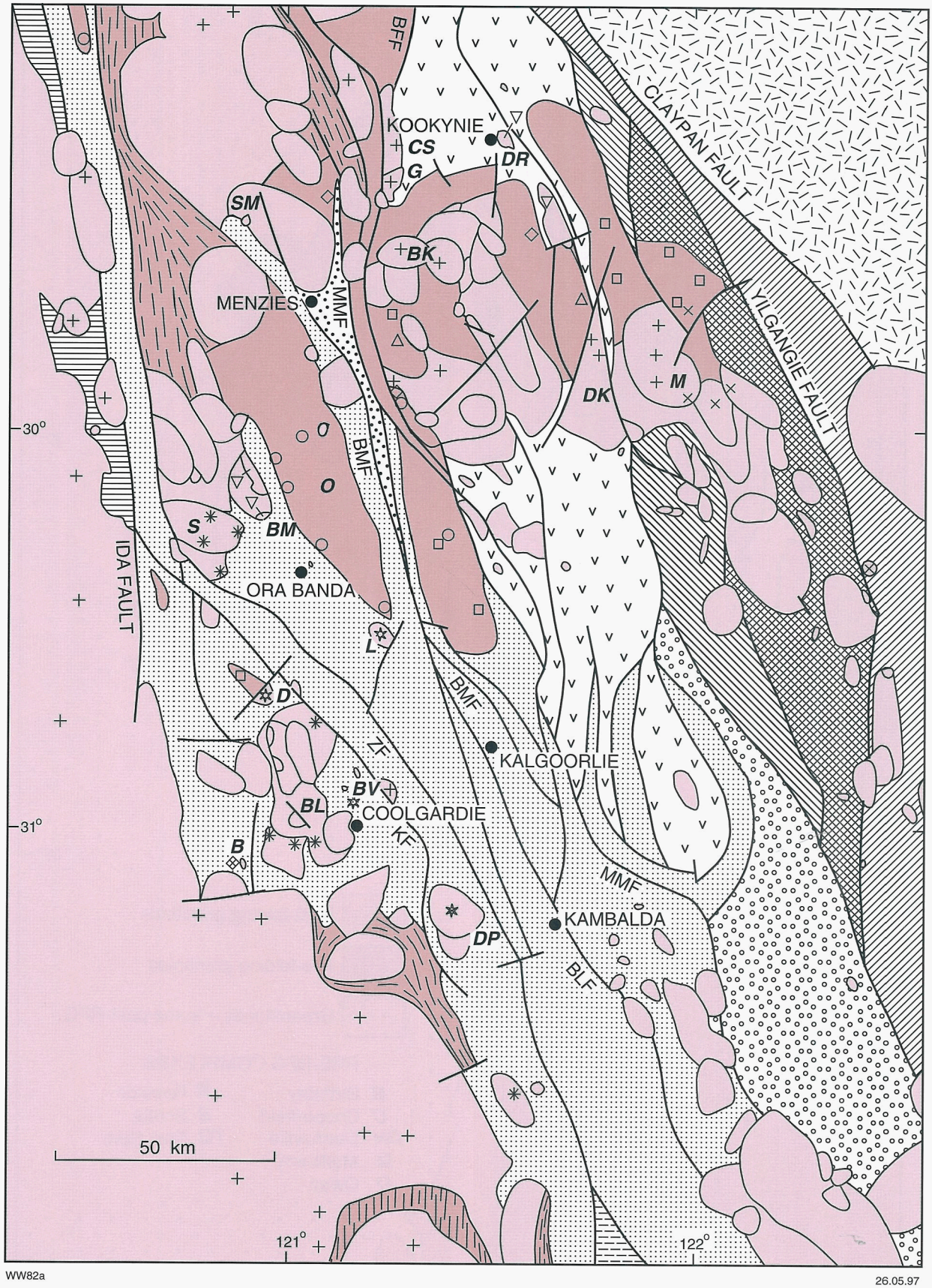

Figure 2. Interpreted geology of the southwest Eastern Goldfields Province (SWEGP), showing granitoid gneiss, pre-RFG complexes and post-RFG plutons. Also shown are major shear zones and greenstone terranes (from Swager and Ahmat, 1992; van der Hor and Witt, 1992; and Swager et al., 1995)

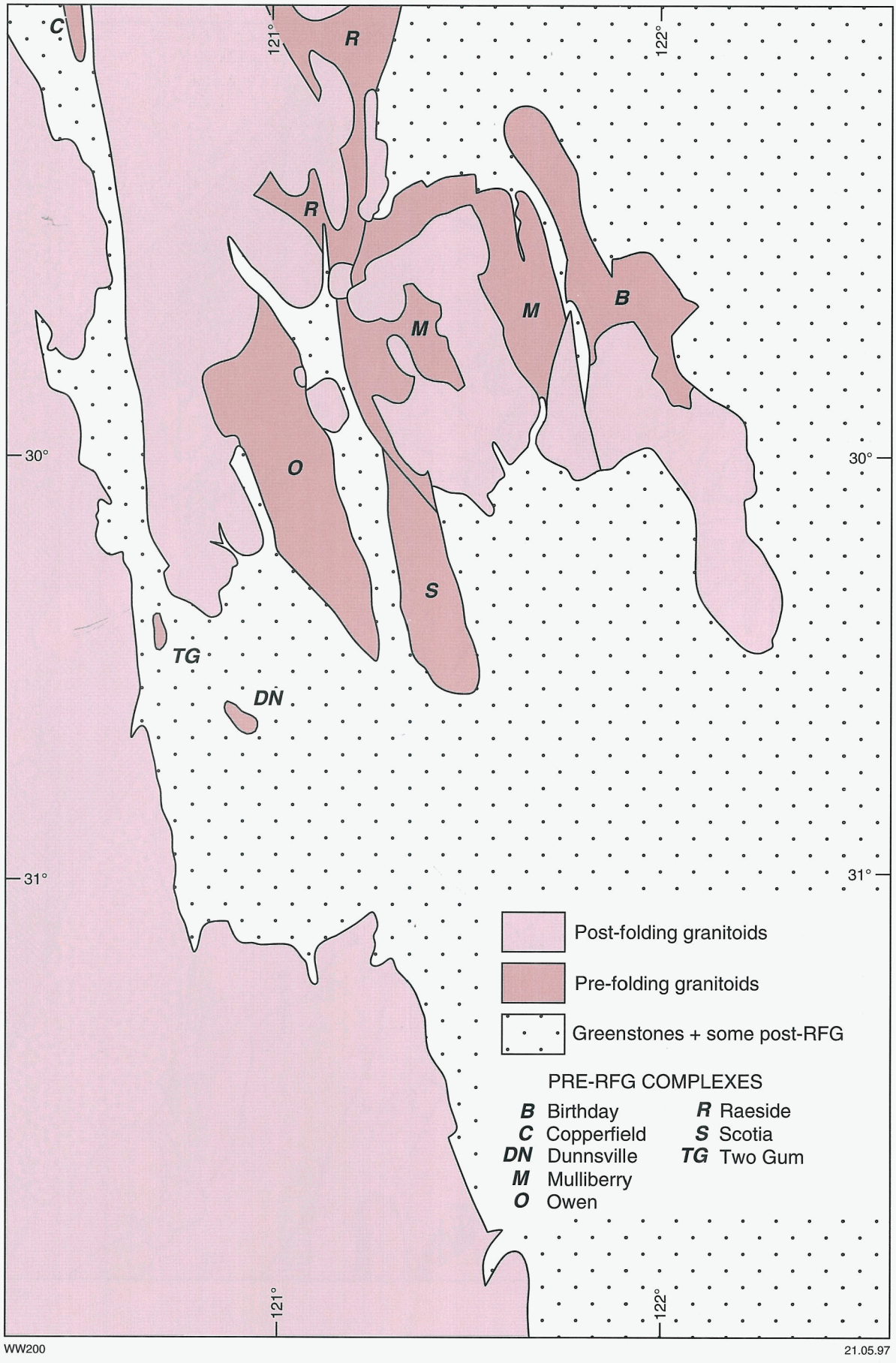

Figure 3. Pre-regional folding granitoid complexes in the SWEGP

Previous studies of SWEGP granitoids

Early studies on the felsic rocks of the Kalgoorlie area were reported by O'Bierne (1968), Glikson and Sheraton (1972) and Oversby (1975). Oversby (1975) made the important observation that Pb-isotope data indicated a significant crustal prehistory (at least 600 Ma) for the source rocks of the granitoids she sampled. The earliest regional study of granitoid rocks was carried out in the central Yilgarn Craton by Bettenay (1977), in an area that overlaps the western part of the SWEGP. At about the same time, large parts of the Yilgarn Craton were mapped by the GSWA for the State 1:250 000 map series, and some geochemical data for granitoids collected during this period were discussed by Davy (1976, 1978). These projects led to similar subdivisions of Yilgarn granitoids, based on their age of emplacement with respect to regional deformation or structural settings (Gee et al., 1981; Archibald et al., 1981).

More recent studies of granitic rocks in the Eastern Goldfields Province include those of Foden et al. (1984), Hallberg and Wilson (1983), Hallberg (1985) and Cassidy et al. (1991). Cassidy et al. (1991) summarized much of the currently available information on granitic rocks in the Eastern Goldfields Province. In recent years, the Sensitive High Resolution Ion Microprobe (SHRIMP) at the Australian National University has provided the first precise dates for the emplacement of granitoid intrusions in the Yilgarn Craton, including a few within the SWEGP and adjacent areas. These dates have been combined with new and existing geochemical data to stimulate new models for the crustal evolution of the Yilgarn Craton (Hill et al., 1989; 1992a,b). Although geochronological data are limited, published ages have been resolved into two main periods of granitic magmatism, at 2690–2685 Ma and 2665–2660 Ma (Hill et al., 1992a,b). Some younger dates suggest that, although the second peak of magmatism occurred at 2665–2660 Ma, granitoids may have been emplaced intermittently as late as 2600 Ma. SHRIMP U–Pb zircon data for the SWEGP granitoids available at the time of writing are summarized in Table 2.

Libby (1989) summarized data on an alkaline group of granitoids, mainly syenite and quartz syenite, which occurs in the eastern part of the Eastern Goldfields Province. Some alkaline granitoids also occur within the SWEGP, but structural and Rb–Sr age data suggest they are significantly younger (<2600 Ma) than other granitoids in the Eastern Goldfields Province.

Samples collected by O'Bierne (1968) and Bettenay (1977) were re-analysed, along with new samples collected by Perring (1989) and Cassidy (1992), by the Bureau of Mineral Resources (now the Australian Geological Survey Organisation (AGSO)). Results of the AGSO analyses, which included subvolcanic and volcanic porphyry samples, as well as granitic rocks, were discussed by Wyborn (1993).

Methods and aims

This study commenced in 1986, and has progressed in parallel with geological mapping for the GSWA 1:100 000 map series in the Eastern Goldfields Province. Poor

Table 2. SHRIMP U–Pb in zircon ages for granitoids in the southwest Eastern Goldfields Province (from Hill et al., 1992a)

Pluton	*Structural group*	*Locality*	*Latitude*	*Longitude*	*Sample age (Ma)*	*Pluton age (Ma)*
Unnamed granodiorite	Pre-RFG	Norseman	32°35.7'S	121°3.6'E	2691 ± 8	–
Unnamed granodiorite	Pre-RFG	Norseman	32°4.7'S	122°2.0'E	2689 ± 22	2686 ± 6
Unnamed granodiorite	Pre-RFG	Norseman	32°4.7'S	122°2.0'E	–	2686 ± 6
Unnamed monzogranite	Pre-RFG	Norseman	32°12.6'S	121°55.0'E	2686 ± 6	–
Unnamed monzogranite	Pre-RFG	Queen Victoria Rocks	31°17.5'S	121°55.3'E	2687 ± 6	–
Bonnie Vale Tonalite	Post-RFG	Bonnie Vale	30°51.9'S	121°9.6'E	2680 ± 5	–
Theatre Rocks Monzogranite	Post-RFG	Theatre Rocks	32°8.4'S	121°33.3'E	2672 ± 7	?c. 2665
Porphyry Granodiorite	Post-RFG	Porphyry	29°4.6'S	122°16.8'E	2667 ± 4	–
Liberty Granodiorite	Post-RFG	Lady Bountiful	30°30.2'S	121°12.4'E	–	?c. 2665
Menangina Monzogranite	Post-RFG	Menangina Rocks	29°50.3'S	121°56.4'E	c. 2665	–
Woolgangie Monzogranite	Post-RFG	Woolgangie	31°10.8'S	120°29.0'E	2646 ± 6	–
Mungari Monzogranite	Post-RFG	Mungari	30°53.1'S	21°15.1'E	2603 ± 19; 2600 ± 2	2602 ± 11; 2602 ± 11

exposure has been countered, to some extent, by commercially available aeromagnetic data, which cover approximately 80% of the study area. Survey flights were made at a 200 m line spacing and an average height of 60 m. Regional mapping, supported by aeromagnetic data, has been used to establish relationships between granitoid intrusions and greenstone country rocks with a view to determining the timing and mode of emplacement. Petrographic observations have been made in the field and by microscope examination of thin sections. One hundred and thirty-two geochemical samples were collected by drilling and blasting the freshest available outcrops. New analyses have been supplemented by published data from within the study area, bringing the total database to 194 samples. The analytical data and methods have been published separately (Witt et al., 1996).

Field, petrographic and chemical data have been combined to investigate the nature and origin of the granitoids, and the extent to which they are related to economic mineralization. Implications for the tectonic evolution of the SWEGP and the nature of the underlying crust are discussed in this Report.

Map references to all localities mentioned below in the text or tables are listed in Appendix 1.

Definitions

Complexes and plutons are geographical entities, whereas suites are defined mainly on petrographic and geochemical criteria.

Complex and pluton nomenclature

Three *structural* groupings of granitoids are recognized in the SWEGP: granitoid gneiss, pre-regional folding granitoids (pre-RFGs), and post-regional folding granitoids (post-RFGs). Most pre-RFGs are found in composite bodies termed complexes (Fig. 3). Pre-RFG complexes comprise several intrusive pulses, which have been named in some areas (Table 3). However, the aerial extent of the individual intrusive phases is difficult to determine. Individual post-RFG magmatic pulses (plutons) are more readily recognized, particularly where aeromagnetic data are available. Granitoid gneiss, pre-RFG complexes and post-RFG plutons together form large masses of granitoid rock. In younger terranes, these larger masses would be termed batholiths, but batholith terminology is inappropriate in the Yilgarn Craton where isolated greenstone belts occur in a single, large expanse of granitoid rock.

Table 3. Individual intrusive pulses within pre-RFG complexes

Complex	*Component granitoids*	*Reference*
Owen	Goongarrie Monzogranite	Witt (1990)
	Cawse Monzogranite	Witt (1990)
	Credo Granodiorite	Witt (1990)
Scotia	Crowbar Granodiorite	Witt (1990)
	Nine Mile Monzogranite	Hunter (1993)

For convenience, a single name has been attributed to some multiple post-RFG intrusive centres (e.g. Bali Monzogranite). The more important complexes and plutons have been informally named (Plate 1, Fig. 3). Some pre-RFG complexes form elongate domes in the cores of regional anticlines. Thus the Owen complex, which occurs in the core of the Goongarrie–Mount Pleasant anticline, may be referred to as the Owen dome when the structural entity, rather than the collection of granitoid rocks, is being referred to.

Suites and supersuites

A suite is a group of granitoids that share distinctive textural, modal, chemical and isotopic features, and a specific source-rock composition (Chappell, 1978; Wyborn and Chappell, 1986; Chappell and White, 1992). The primary geochemical tool used for distinguishing granitoid suites in the SWEGP has been the Harker diagram, in which major and trace elements are plotted against SiO_2 (Chappell, 1978; Hine et al., 1978; Griffin et al., 1978). Supersuites are less precise groupings of suites or granitoids that cannot be related collectively to the same source rock but which nevertheless share similar petrographic and chemical characteristics that distinguish them from other suites and supersuites.

In this study, five supersuites are recognized (Gilgarna, Dairy, Woolgangie, Liberty, Morapoi; Table 4). The Morapoi supersuite is subdivided into four suites (Minyma, Goongarrie, Twin Hills, Rainbow), and the Bali suite is defined as a distinctive component of the Woolgangie supersuite. Although defined mainly on petrographic and chemical criteria, these subdivisions are introduced here because they are referred to below when describing structural relations between granitoids and greenstones, and related topics. All supersuites in the SWEGP have calc-alkaline chemical affinities, except the alkaline Gilgarna supersuite.

Table 5 summarizes the distribution of named complexes and plutons within the suite and supersuite nomenclature.

Dykes, enclaves and xenoliths

Some granitoids in the SWEGP contain smaller, texturally and modally distinct bodies collectively referred to as enclaves, which include dykes and xenoliths. Some dykes are believed to have been emplaced while the host granitoid was at least partly molten and, consequently, are referred to as synplutonic dykes. Rounded enclaves, up to 1 m across, of material that is lithologically similar to, but finer grained and more mafic than that which forms the host granitoid, are referred to as cognate xenoliths and may

Table 4. Summary of the main features of granitoid suites and supersuites in the southwest Eastern Goldfields Province

Suite	*Estimated percent of SWEGP granitoids, by area*	*SiO_2 (%)*	*Non-quartzofeldspathic mineralogy (a)*	*Microgranitoid xenoliths, synplutonic dykes*	*Negative anomalies on mantle-normalized spidergrams*	*Probable source rock*	*Predominant fractionation mechanism*
Post-regional folding granitoid suites and supersuites							
Gilgarna supersuite	<5	54.0–67.1	Clinopyroxene (amphibole)	Present	Not investigated	Granulite	Uncertain
Dairy supersuite	<5	75.3–76.7	Biotite (hornblende, muscovite)	Not observed	Nb, ?Sr, P, Ti	Monzogranite	Fractional crystallization, ?contamination
Woolgangie supersuite	60	70.5–76.5	Biotite (muscovite, garnet)	Not observed	Nb, P, Ti, Y	Granodiorite	Fractional crystallization
Bali suite (b)	10	71.9–76.5	Biotite (muscovite, garnet)	Not observed	Nb, P, Ti, Y	Granodiorite	Fractional crystallization, ?metasomatism
Liberty Granodiorite (c)	5	66.4–71.7	Biotite, hornblende	Present	Nb, P, Ti, Y	Tonalite	Fractional crystallization
Pre-regional folding granitoid suites (Morapoi supersuite)							
Minyma suite	<5	76.4–77.3	Biotite, hornblende	Not observed	Nb, ?Sr, P, Ti	Monzogranite	Fractional crystallization, ?contamination
Goongarrie suite	10	71.0–76.5	Biotite	Locally only	Nb, P, Ti, Y	Granodiorite	Fractional crystallization
Twin Hills suite	10	71.3–75.1	Biotite	Present	Nb, P, Ti, Y	Granodiorite	Fractional crystallization
Rainbow suite	10	66.1–71.3	Biotite, hornblende (clinopyroxene)	Relatively common	Nb, P, Ti, Y	Tonalite	Fractional crystallization

NOTE: (a) Brackets indicate mineral is present (typically in minor amounts) in some samples only
(b) The Bali suite is a subgroup within the Woolgangie supersuite. Percentage for the Woolgangie supersuite includes the area of the Bali suite
(c) The Liberty Granodiorite is described as a representative of the Liberty supersuite

Table 5. Summary of the relationships between structural and chemical groupings of granitoids in the southwest Eastern Goldfields Province

Structural group	*Supersuite*	*Suite*	*Examples of plutons (post-RFG) or complexes (pre-RFG)*
Post-regional folding granitoids	Gilgarna		Gilgarna Syenite, McAuliffe Well Syenite, and several small, unnamed intrusions (e.g. near Twelve Mile Well, Princess Bore, Tassy Well, southwest of Hamdorf Bore and east of Cement Well)
	Liberty		Bonnie Vale Tonalite, Bullabulling Monzogranite, Comet Vale Monzogranite, Depot Granodiorite, Doyle Dam Granodiorite, Federal Granodiorite, Kambalda Trondhjemite, Kintore Tonalite, Liberty Granodiorite, Porphyry Quartz Monzonite
	Dairy		Dairy Monzogranite, Jungle Monzogranite, Old Monzogranite
	Woolgangie	Bali	Bali Monzogranite, Pioneer Monzogranite, Siberia Monzogranites, Widgiemooltha Monzogranite
	Woolgangie	Other (undefined) suites	Balarky Monzogranite, Carpet Snake Syenogranite, Donkey Rocks Monzogranite, Galah Monzogranite, Menangina Monzogranite, Mulline Monzogranite, Mungari Monzogranite, Ularring Monzogranite and most plutons to the west of the Kalgoorlie Terrane
Pre-regional folding granitoids	Morapoi	Minyma	Mulliberry
		Goongarrie	Goongarrie, Mulliberry, Scotia
		Twin Hills	Mulliberry, Raeside
		Rainbow	Birthday, Scotia
Granitoid gneiss	Uncertain origin; partly derived from deformation of pre-RFG complexes and post-RFG plutons; may include some occurrences of basement, but such occurrences have not yet been identified		

be either igneous-textured (microgranitoid) or gneiss-textured. Angular xenoliths derived from greenstone, gneiss and granitoid country rock are referred to as accidental xenoliths.

Structural history of the greenstones

The primary three-fold division of granitoids adopted in this study is based on timing of emplacement relative to regional deformation events. It is therefore important to establish the structural history of the SWEGP before proceeding with a description of the granitoids. Structural studies at numerous localities within the western part of the Eastern Goldfields Province indicate similar deformation histories, involving early thrust faulting and/or recumbent folding, followed by upright regional folding and strike-slip faulting (Archibald et al., 1978, 1981; Platt et al., 1978; Gresham and Loftus-Hills, 1981; Spray, 1985; Swager, 1989; Williams et al., 1989). This regional deformation history was applied to the entire Kalgoorlie Terrane by Swager et al. (1995). Ongoing mapping and structural studies (Rattenbury, 1991; Ahmat, 1994; Morris, 1994; Swager, 1994; Witt, 1994; Wyche, in prep.) indicate that adjacent terranes, to the east and west of the Kalgoorlie Terrane, record a similar deformation history. However, some recent studies (Hammond and Nisbet, 1992; Williams and Currie, 1993; Witt, 1994) recognize an extensional event, the timing of which is still being debated. The regional deformation history is summarized in Table 6.

Low-angle thrust faults, recumbent folds and a bedding-parallel foliation are assigned to D_{1c}. The movement direction during D_{1c} stacking was south to north (Swager et al., 1992). In the Kalgoorlie and Gindalbie Terranes, extension most probably occurred before D_2 and may have resulted from gravitational collapse of overthickened crust, following D_{1c}. Extension in the greenstones was accompanied by broad doming of extensive granitoid sheets in the northern part of the SWEGP (Witt, 1994). The thickness of greenstones removed during granitoid doming may have varied widely. Williams and Currie (1993) estimated at least 9 km of crust had been excised at Leonora. Witt (1994) estimated that 2.5 to 4 km of crust had been excised, west of Kookynie.

D_2 to D_4 can be viewed as successive stages of progressive regional east-northeast–west-southwest regional compression.

Table 6. Summary of regional deformation in the southwest Eastern Goldfields Province

Deformation	*Structures*	*Locality or example*	*References*
D_1 D_{1c}	Low-angle thrust faults and recumbent folds; (?)deformed contacts between early granitoid complexes and greenstones	Between Kalgoorlie and Democrat (south of Kambalda)	Swager and Griffin (1990); Gresham and Loftus-Hills (1981)
D_{1e}	Deformed contacts between early granitoid complexes and greenstones; N–S lineations in contact zone; recumbent folds in overlying greenstones	Jeedamya–Kookynie area	Witt (1994)
D_2	Upright folds with shallowly plunging, NNW fold axes	Kambalda Anticline, Goongarrie–Mt Pleasant Anticline, Kurrawang Syncline	Swager and Griffin (1990); Witt (1990); Hunter (1993)
D_3	Tightening of F_2 folds	–	Swager (1989); Swager et al. (1995)
	NW to NNW sinistral strike-slip faults and shear zones	Boorara–Menzies Fault	Witt (1990); Swager et al. (1995)
		Boulder–Lefroy Fault	Swager (1989); Swager and Griffin (1990)
	N to NNE dextral strike-slip faults and shear zones	Butchers Flat Fault	Witt (1994)
	En echelon folds adjacent to strike-slip faults	Kunanalling, Celebration	Swager (1989)
Late D_3	Steeply plunging lineations on strike-slip faults	Goongarrie, Bardoc Tectonic Zone	Witt (1990)
	Steeply dipping reverse faults	Melita, Niagara	Witt (1994)
D_4	NW to WNW sinistral oblique faults	Paddington area	Witt (1990)
	NE to ENE dextral oblique faults	Mount Charlotte (Kalgoorlie), Black Flag Fault (Mount Pleasant)	Swager (1989); Witt (1990)

Although some D_3 shear zones and faults (e.g. the Kunnanalling Fault, the Boulder–Lefroy Fault north of Kambalda) were initiated during D_3, those which form domain and terrane boundaries are believed to be older structures that were reactivated during D_3 (Swager et al., 1995). The two sets of regional structures can be viewed as conjugate faults, formed in an east-northeast–west-southwest compressional stress regime. Opposite movement directions on the conjugate D_3 fault set caused northward and southward displacement of intervening greenstone wedges, where north-northwest and north-trending faults converge. Two examples of this process can be cited. Northward displacement of greenstones has occurred near Menzies, where the Boorara–Menzies Fault (sinistral) and the Moriaty Fault (dextral) converge (Swager, 1991). Southward displacement of the Melita greenstone is related to the convergence of the Butchers Flat Fault (dextral) and the Keith–Kilkenny Shear Zone (sinistral), near Leonora, immediately to the north (Witt, 1994). In both areas, displacement was opposed by rigid granitoid bodies, resulting in local stress anomalies.

During late D_3, subhorizontal movements gave way to subvertical movements on regional faults and on newly-formed, oblique faults. Reverse faults are also common in the Melita and Niagara areas where movements reflect simultaneous east-northeast–west-southwest compression, and north–south compression (Plate 1; Witt, 1994).

Interpretation of aeromagnetic data

The interpretation of the subsurface granitoid geology shown on Plate 1 relies heavily on aeromagnetic data. Although magnetic character alone cannot consistently

differentiate between granitoid gneiss, pre-RFGs and post-RFGs, some generalizations can be made.

Internal structure

Steep magnetic gradients within areas underlain by granitoids are shown as a purple dashed line on Plate 1 and are interpreted as possible geological contacts. These may be either intrusive contacts or more gradational, within-pluton transitions related to inwards fractionation of the granitoid magma (Bateman and Chappell, 1979; Gastil et al., 1990).

Granitoid gneiss and pre-RFG complexes commonly display a variegated magnetic pattern, which at some localities (e.g. Riverina, Twin Hills) coincides with a distinct compositional banding. Although the scale of visible banding is relatively small (metres to tens of metres), it is presumed that the variegated magnetic patterns reflect a compositional banding that is either too coarse or too subtle (variable magnetite content) to be observed at individual outcrops.

Steep magnetic gradients within post-RFG plutons are commonly concentric with respect to pluton margins (for example, within the Bali and Silt Dam Monzogranites) and probably record compositional variations caused by inward fractionation. However, there are few instances where this interpretation can be confirmed because normally only one of the magnetically-distinct zones is well exposed. In one pluton (the Menangina Monzogranite), there is little difference in the petrography or magnetic susceptibility of outcrops from inner and outer zones that are magnetically distinct on aeromagnetic data imagery.

Linear anomalies of relatively low magnetic intensity are common in all three structural groupings of granitoid. They can be correlated with offset contacts and faults in adjacent greenstones in some cases (e.g. Coolgardie, Davyhurst, Broad Arrow areas), and are typically interpreted as faults and fractures that acted as pathways for oxidizing fluids.

Magnetic susceptibility

The magnetic susceptibility of a representative range of samples (Plate 1) was measured, to compare granitoids, and to investigate the extent to which variations in this parameter could be correlated with lithology and variations in the total magnetic intensity measured by airborne survey. The results, given in Figure 4, show that although some suites in the SWEGP tend to be more (or less) magnetic than others, there is considerable overlap, and magnetic susceptibility, by itself, cannot be used to separate suites.

The total range of magnetic susceptibility measurements is from 0 to 5000 $\times 10^{-5}$ SI (Fig. 4). The magnetic susceptibility of most granitoids in the SWEGP is similar to values for magnetite-series granitoids but a few plutons have values that are typical of ilmenite-series granitoids (Ishihara, 1981; Gastil et al., 1990). Mineralogically, the low magnetic-susceptibility samples cannot be classified as ilmenite-series granitoids because, although they have a low opaque-oxide content, the oxide is magnetite (where not totally altered by weathering). Where it cannot be attributed to weathering or alteration, low magnetic susceptibility is attributed to the fractionation of magnetite-series granitoid magma to yield magnetite-poor, ilmenite-absent monzogranite and syenogranite.

Attempts to correlate variations in magnetic susceptibility with rock type and total magnetic intensity (as recorded by airborne survey) have met with only limited success. There are several possible reasons for this, including differences in the depth of penetration by the two methods of measurement, lithological heterogeneity in many granitoid gneiss and pre-RFG units, and sparse, possibly unrepresentative exposure. Even apparently homogenous post-RFG intrusions display a considerable range in magnetic susceptibility that is not evident on aeromagnetic images (e.g. Donkey Rocks Monzogranite, 0–300 $\times 10^{-5}$ SI). Low magnetic susceptibility in samples from near the margins of some granitoid bodies may be due to demagnetization related to fluid activity and oxidation of magnetite to hematite (Gastil et al., 1990). For example, the magnetic susceptibility of the Copperfield complex increases from 40 $\times 10^{-5}$ SI at the contact to 500 $\times 10^{-5}$ SI 200 m inside the contact.

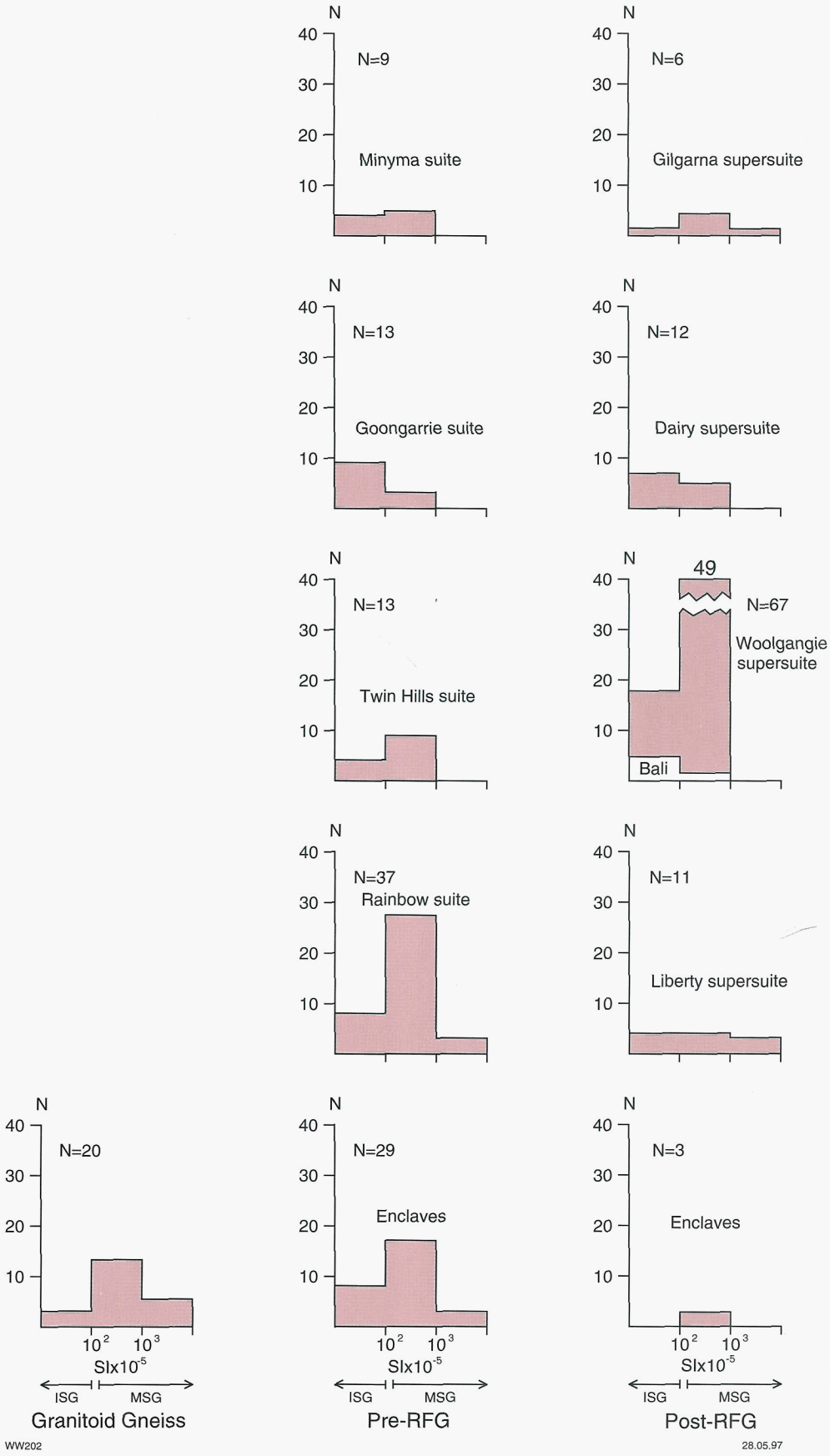

Figure 4. Histograms showing frequency of magnetic susceptibility measurements for granitoid gneiss, pre-RFGs (by suite), post-RFGs (by supersuite), and enclaves in the SWEGP. Range of magnetite-series granitoids (MSG) and ilmenite-series granitoids (ISG) from Gastil et al. (1990)

Chapter 2

Relationships of granitoids with greenstones, regional structures and regional metamorphism

Granitoid gneiss, pre-regional folding granitoid complexes and post-regional folding granitoid plutons are described below in terms of their shape, contact relationships and relationships to regional structures. The presence of sedimentary rocks containing granitoid clasts has important implications for the tectonic evolution of the area, and is also discussed. Finally, a close spatial relationship between granitoid intrusions and regional metamorphic grade (Binns et al., 1974) suggests an important role for granitoid magmatism in the regional metamorphism of the greenstones.

Relative emplacement ages of granitoids are based on relationships with regional structures, and on the degree of deformation and recrystallization. Conclusions based entirely on the degree of deformation and recrystallization observed in limited exposures are potentially subject to error because of the heterogeneous distribution of strain during regional deformation. Therefore, where possible, large-scale relationships between plutonic units and regional structures (fold hinges, shear zones) have been emphasized in an attempt to determine the relative ages of intrusions.

Reliable absolute age data for the crystallization of granitoid intrusions in the Eastern Goldfields Province are scarce. Early K–Ar, Rb–Sr and Nd–Sm age determinations record metamorphic and post-metamorphic events, or are influenced by source-rock compositions and/or ages. Precise SHRIMP U–Pb zircon ages have been published for a few samples, but most of these are from the Norseman area. However, since the regional deformation history and pluton–structure relationships at Norseman appear similar to those in the study area, published dates from Norseman are tentatively applied to comparable intrusions described below.

Structural subdivision of granitoids

Witt and Swager (1989) recognized three periods of granitoid emplacement in the Bardoc–Coolgardie area (part of the Kalgoorlie Terrane): 1) pre- to syn-D_2 granitoids, 2) post-D_2 to syn-D_3 granitoids, and 3) late- to post-tectonic granitoids. The distinction of post-D_2 to syn-D_3 granitoids from late- to post-tectonic granitoids has proven difficult outside the Kalgoorlie Terrane because contact zones between these intrusions and D_3 shear zones are rarely exposed. Furthermore, F_2 fold axes cannot be identified in areas dominated by late granitoid intrusions. Concordant and discordant relationships between intrusions and country rocks cannot be distinguished for plutons that were emplaced into earlier granitoids. Therefore, in this study, two broad groups of intrusive granitoid are recognized:

1. Pre-regional folding granitoid (pre-RFG) complexes, which are equivalent to the pre- to syn-D_2 granitoids of Witt and Swager (1989).

2. Post-regional folding granitoid (post-RFG) intrusions, which include post-D_2 to syn-D_3 granitoids and late- to post-tectonic granitoids of Witt and Swager (1989).

A third group of granitoid rocks comprising granitoid gneiss was not discussed by Witt and Swager (1989). The distribution of these three structural groups is shown in Plate 1 and Figure 2.

Granitoid gneiss

Granitoid rocks with a widespread granoblastic fabric, and millimetre- to metre-scale metamorphic banding, are assigned to the granitoid gneiss classification. Strongly foliated granitoids with a pronounced lepidoblastic fabric, and those in which metre-scale compositional banding is of igneous origin, have been termed granitoid gneiss in some publications (Kriewaldt, 1970; Swager, 1991; Williams and Whitaker, 1993) but are not included here. Also excluded are relatively narrow marginal zones of some granitoid intrusions, which are characterized by intense deformation and a gneissic structure. Thus defined, granitoid gneiss occurs mainly in a broad zone along the western margin of the Kalgoorlie Terrane, west of Menzies, and south of Coolgardie (Fig. 2). It also occurs in a narrow strip north of Menzies, and as xenoliths in intrusive granitoids, as far east as Six Mile Rocks (75 km east-southeast of Menzies; Plate 1).

North of Davyhurst, the Ballard Fault separates gneiss from greenstones of the Kalgoorlie Terrane (Rattenbury, in press). The contact between greenstones and granitoid gneiss, south of Coolgardie, is not exposed, but a discordant relationship west of the Depot Granodiorite (Plate 1) suggests this also is a tectonic contact. There are no exposures or other evidence to indicate the nature of contact relationships between granitoid gneiss and pre-RFG complexes. South of Donkey Rocks Well (65 km north of Menzies) there are gradational contacts between monzogranitic gneiss and post-regional folding biotite

monzogranite. The latter contains irregular schlieren, wispy lenses, and tapered bands of gneissic material. Bettenay (1977) also describes gradational contacts, via increasingly extensive migmatitic structures, between granitoid gneiss and post-RFG intrusions.

Pre-RFG complexes

Pre-RFGs form elongate domes and more irregularly-shaped bodies, mainly in the northern part of the study area (Fig. 2). The term complex is used to indicate that these bodies are not simple plutons but consist of several petrographically distinct intrusive phases, as described in Appendix 2. The southern-most pre-RFG complex is the Dunnsville dome, north of Coolgardie. Descriptions of granite–greenstone relationships and contact zones (Platt et al., 1978; Spray, 1985) suggest similar early granitoid complexes are exposed at Norseman and Agnew, south and north of the study area respectively (Fig. 1).

Pre-RFG complexes are regionally conformable with primary layering in the greenstones, but low-angle discordances are common (e.g. the Owen dome). They commonly form the cores of F_2 anticlines, although the more areally extensive Raeside and Mulliberry complexes probably also contain synclinal axes. Most complexes are cut, or partly bounded, by D_3 shear zones and/or later faults. A pervasive to spaced, north-northwest regional foliation (S_2/S_3) occurs throughout the complexes, and locally overprints the contact-parallel S_1 fabric.

Contacts between pre-RFG complexes and greenstones are zones of intense ductile deformation (D_1) and interleaving of granitoid rocks with greenstones. Deformed contact zones vary from a few metres wide (north- to northwest-trending margins of the Owen and Scotia domes) to several kilometres wide (the northern margin of the Mulliberry complex). Within these zones, granitoids vary from strongly schistose and fissile, to gneissic or mylonitic. At some localities, there is evidence of small-scale partial melting of deformed granitoid rocks (Spray, 1985; Witt, 1987). A linear fabric (L_1) is subhorizontal to shallowly plunging on northerly to northwesterly trending contacts, and down-dip to steeply oblique in F_2 fold closures. Witt (1994) proposed that D_1 movement on some pre-RFG–greenstone contacts involved both compressional (D_{1c}) and extensional (D_{1e}) phases. Steep lineations developed locally on north- to northwest-trending contacts are interpreted as L_2.

The distribution of analysed samples suggests individual pre-RFG suites are concentrated in one or another of the fault-bound pre-RFG complexes. However, three suites occur in more than one complex and most complexes contain granitoids belonging to more than one suite (Plate 1). Rainbow suite granitoids occur mainly in the Birthday and Scotia complexes, although one sample from the Mulliberry complex also belongs to the Rainbow suite. Twin Hills granitoids occur in the Twin Hills area of the Raeside complex and at Granite Dam and Naismith Bore in the Mulliberry complex. Petrographic characteristics suggest that Twin Hills suite granitoids may dominate the northern part of the Mulliberry complex where no geochemical samples have been collected. Samples of Goongarrie suite granitoids come mainly from within the Owen complex. Other samples have been identified in the Copperfield, Mulliberry and Scotia complexes. Minyma suite granitoids have been identified mainly within the Mulliberry complex, at Black Gin Rocks and east of Alexandria Bore.

Post-RFG plutons

Post-RFG plutons form numerous ovoid to circular plutons that have been emplaced within greenstones, pre-RFG complexes and granitoid gneiss. They are commonly distributed in elongate clusters, subparallel to the north-northwesterly trending tectonic grain of the SWEGP (Fig. 2). Some are localized by D_3 shear zones, but, unlike the pre-RFGs, there is no systematic association with F_2 anticlines. Internal fabric and contact relationships vary widely among the better-exposed intrusions. Five examples of post-regional folding granitoids will be described to give an idea of this variability.

Post-D_2 to syn-D_3 granitoid diapirs

A series of ovoid to elliptical plutons, classified as post-D_2 to syn-D_3 granitoids by Witt and Swager (1989), occur along the western margin of the Kalgoorlie Terrane. This group of intrusions extends southwards to Norseman where it includes the Theatre Rocks and Goodia plutons (McGoldrick, 1993). The belt containing most of these intrusions is a high-strain zone characterized by relatively high-grade metamorphic assemblages.

Aeromagnetic data have been used to identify the margins of individual plutons in multiple intrusive centres at Coolgardie and Siberia (northwest of Ora Banda). Interpretation of contact relationships suggests progressive westward migration of the locus of intrusion at Coolgardie, and eastward migration at Siberia.

The plutons deform or transect F_2 fold axes, but deflect, and are partly bounded by, D_3 shear zones. Primary layering in the greenstones is partly concordant with pluton margins. A contact-parallel foliation is developed in the greenstones for up to several kilometres, and increases in intensity towards the granitoid contacts. At Siberia, contact-parallel shear zones, up to 1 m wide, cut primary layering in the greenstones at a low angle and become more closely spaced towards the granitoid contact.

The margins of these intrusions are zones of intense ductile deformation and flattening, resulting in alternating bands of coarse- and fine-grained quartzofeldspathic schist, commonly with coarse feldspar porphyroclasts. Extensive interleaving of granitoid and greenstone lithologies is not commonly observed, but thin screens of greenstone may separate individual plutons within a cluster (e.g. Wangine Soak, Siberia; Wyche and Witt, 1992). Down-dip lineations are common within marginal zones of deformation, and where preserved, S–C fabrics and porphyroclast–matrix relations are consistent with pluton movement upwards, relative to greenstones.

Subvertical movement indicators are obliterated where they are overprinted by D_3 strike-slip shear zones (e.g. the western side of the Siberia Monzogranite; the northeast margin of the Bali Monzogranite). Deformation decreases rapidly away from the contacts. Pluton interiors are variably recrystallized but the regional S_2/S_3 foliation is poorly developed or absent.

This group of intrusions includes all analysed members of the Bali suite, and the Depot Granodiorite (Plate 1).

Late-tectonic granitoids emplaced into regional shear zones

Post-RFG plutons east and north of Menzies (including the Carpet Snake Syenogranite and the Galah Monzogranite) have intruded the D_3 Moriaty Fault and the Butchers Flat Fault, and related structures (Plate 1). Contact zones are typically undeformed and cut primary layering in greenstones adjacent to the shear zones. Although variably recrystallized, the granitoids do not display a regional S_2/S_3 foliation.

These plutons are equivalent to the late- to post-tectonic granitoids of Witt and Swager (1989). The Carpet Snake Syenogranite and the Galah Monzogranite belong to the Woolgangie supersuite.

Small, late-tectonic granitoids emplaced in linear zones of non-ductile strain

Another group of granitoids were emplaced along linear north-northwest trends that are not readily identified as faults or shear zones at the surface, but which may reflect deep-seated zones of crustal weakness. Examples occur between Mount Pleasant (Liberty Granodiorite) and Siberia, and south-southeast from Kookynie. Most intrusions are small (<100 km^2) and have sharp, undeformed contacts that cut across primary layering in the greenstones. They are massive, except where cut by late faults, and typically display unrecrystallized igneous textures. Examples of local deformation are displayed by the Comet Vale Monzogranite (south of Menzies) where its eastern margin is sheared against the Boorara–Menzies Fault, and by the Lone Hand Syenogranite (east of Ora Banda), which contains abundant quartz veins, presumably related to movement on the adjacent Cashmans Fault (Witt, 1990).

These plutons, which include members of the Liberty and Dairy supersuites, are equivalent to the late- to post-tectonic granitoids of Witt and Swager (1989).

Post-RFGs west of the Kalgoorlie Terrane

Post-RFGs bordering the study area to the west are variably recrystallized and little deformed. Hunter (1991) distinguished two main phases of biotite monzogranite in this vast area of granitoid-dominated outcrop. The aerial extent of these phases suggest they are not individual intrusions, but represent distinct intrusive episodes. The Burra Monzogranite, the dominant granitoid, is intruded by the Woolgangie Monzogranite. Although mostly undeformed and homogenous, granitoids are increasingly foliated and heterogeneous towards pluton margins. Marginal zones (up to 1 km wide) contain biotite schlieren, irregular rafts of granitoid gneiss, and xenoliths of amphibolite and tonalitic granofels. Deformed, heterogeneous marginal zones outline oblate plutons with long axes oriented approximately 150°. Contacts cut across primary layering in the greenstones. Many other post-RFG plutons, intrusive into the pre-RFG Raeside and Mulliberry complexes, display several features in common with this group of granitoids.

These intrusions include most members of the Woolgangie supersuite.

Alkaline intrusions

Small, late-tectonic intrusions of alkaline granitoids, mostly syenite and quartz syenite, are concentrated in the eastern part of the SWEGP, and their distribution extends east of the Keith–Kilkenny Shear Zone (Libby, 1989). However, syenite also occurs as an isolated intrusion between Kalgoorlie and Coolgardie (Hallberg, 1982), and as xenoliths in a small porphyry intrusion, southeast of Ora Banda (Witt, 1990). Granitoids are typically undeformed, though variably recrystallized, and form small plugs, sills and dykes, intrusive into greenstones and earlier granitoid rocks. Numerous angular greenstone xenoliths southwest of Hamdorf Bore occur against a sharp, flat-lying, lower contact with underlying monzogranite of the Rainbow suite. Alkaline intrusions emplaced within greenstones (e.g. McAuliffe Well, east of Yerilla Homestead) cut across lithological contacts and D_3 shear zones.

Metasedimentary rocks containing granitoid clasts

Two zones of metasedimentary rocks containing detritus possibly derived from granitoid sources are recognized. The first is a northerly trending zone of conglomerates that extends from near Kalgoorlie to Menzies, and possibly as far north as Agnew. The second occurrence is a more restricted unit at Wongi Hills, north and west of Siberia.

The first zone is represented by massive, equigranular, coarse-grained (1–3 mm) granitoid clasts in weathered outcrops of metaconglomerate at the base of the Black Flag Group, near Mount Hunt (locality 3 of Griffin et al., 1983), and 2.5 km northwest of Arrow Lake, near the Panglo opencut mine. The matrix-supported, polymictic conglomerate also contains clasts (≤10 cm across) of felsic porphyry, chert and quartz. Clasts from the Arrow Lake locality include quartz–plagioclase–hornblende porphyry and biotite–hornblende tonalite. These clasts contain less K-feldspar than most exposed granitoids in the SWEGP. Percussion drilling near Panglo indicates that the conglomerate matrix is chloritic.

Similar conglomerate containing granitoid clasts has been identified at Jennys Reward openpit, in the Bardoc Tectonic Zone, near Goongarrie (about 35 km south of Menzies). The zone of granitoid clast-bearing conglomerate extends northwards to Menzies, where hornblende-bearing granodiorite clasts (comparable to some members of the Rainbow suite) occur in an arkosic matrix (Swager, 1991; Witt, 1993a,b). The matrix is locally ultramafic to mafic. Platt et al. (1978) described similar arkose, and tonalite clast-bearing conglomerate, from the Agnew area, 200 km north of Menzies.

The second zone is represented by felsic-derived metasedimentary rocks close to the base of the exposed greenstone sequence in the Wongi Hills, north of Siberia (Wyche and Witt, 1992). Thin units of coarse grit contain clasts of quartz and feldspar reaching 1 mm across. Although the detritus could have been derived from volcanic rocks, the coarse mineral clasts and milky white quartz are more compatible with a granitic source.

Relationships between regional metamorphism and granitoid intrusion

There is an important but as yet incompletely understood link between granitoid magmatism and regional metamorphism in the Eastern Goldfields Province (Binns et al., 1974). Two main periods of regional metamorphism are indicated by distinct metamorphic fabrics and spatial association with granitoids of different ages. High-grade M_1 assemblages define an S_1 fabric, and are spatially associated with pre-RFG complexes. High-grade M_2 assemblages define and partly overprint S_3 fabrics and are spatially associated with post-RFGs. Both sets of isograds are subparallel to the contacts of their associated granitoids, implying intersecting M_1 and M_2 isograds in the Ora Banda and Menzies areas (Fig. 5).

Metamorphism on the margins of pre-RFG complexes (M_1)

Narrow, possibly discontinuous zones of anomalously high-grade metamorphism (up to the amphibolite–granulite facies transition) occur around the margins of pre-RFG complexes. The width of this high-grade M_1 metamorphic zone is variable, but no more than 100 m in most places. The best-documented zone occurs adjacent to the Mulliberry complex, west of Kookynie (Witt, 1994). Similar zones occur adjacent to the Raeside Complex, near Leonora (Williams et al., 1989; Williams and Currie, 1993), and south of Norseman (Spray, 1985). Metamorphic conditions in relatively thin zones of M_1 metamorphism adjacent to the Owen and Scotia complexes are not well constrained but appear to be less extreme than those at Leonora and west of Kookynie.

In the Niagara area, west of Kookynie, estimated metamorphic conditions of pressure (P) greater than 5 kb and temperature (T) between 650 and 750°C are based mainly on evidence of partial melting in mafic gneiss/migmatite units containing clinopyroxene–hornblende–plagioclase assemblages (Fig. 6). Metamorphic banding in the gneiss defines an S_1 fabric, indicating that M_1 occurred during D_1. Witt (1994) argued that D_1 thrust stacking was required to achieve these high pressures (>5 kb). Temperatures of greater than 600°C could be achieved at the base of the greenstones, following thrust stacking, assuming a geothermal gradient of 40°C/km, or more. However, thermal equilibration is commonly believed to be sluggish (England and Richardson, 1977), and the close spatial association between high-grade assemblages and pre-RFG contacts at Niagara suggest that extra heat from the emplacement and crystallization of syn-D_1 granitoid sheets may have been an essential component of M_1.

Similar high P–T conditions have been recorded in greenstones elsewhere in the Yilgarn Craton, but typically only in thin greenstone slices within predominantly granitic terranes (Gee et al., 1981). Such occurrences may be tectonic slices of greenstone material that became interleaved with early granitoids and were buried during D_1 thrust stacking of the greenstones. The thin slice of predominantly amphibolitic rocks in the Mulliberry complex, east of Menzies, may be an example of this relationship.

Late syntectonic metamorphism (M_2)

The bulk of the greenstones in the SWEGP have been metamorphosed at greenschist to lower amphibolite grade (Fig. 5). Detailed studies at several localities have established peak metamorphic conditions of 2–4 kb and 250–600°C. M_2 metamorphic assemblages define an S_3 foliation in zones of 'dynamic' metamorphism, but garnet, chloritoid and andalusite porphyroblasts and randomly oriented amphibole prisms contain non-rotated inclusion trails that are continuous with a S_2/S_3 fabric in the matrix. These observations suggest that M_2 metamorphism occurred late in the tectonic history of the greenstones, and that metamorphic recrystallization outlasted regional deformation. Witt (1991) showed that M_2 isograds throughout much of the Kalgoorlie Terrane were controlled by proximity to post-D_2 to syn-D_3 granitoids (Fig. 5). Furthermore, these isograds were not influenced by the pre-regional folding Owen and Scotia complexes. The close spatial relationship between M_2 and post-D_2 to syn-D_3 granitoids suggests peak metamorphism occurred during D_3 (Archibald et al., 1981; Witt, 1991).

Metamorphic (M_2) conditions of 3–5 kb and 500–600°C have been established for the Widgiemooltha area (McQueen, 1981; Bickle and Archibald, 1984). Bickle and Archibald (1984) argued that heat generated by crystallization of the post-D_2 to syn-D_3 granitoid diapirs was not sufficient to account for the high-grade metamorphic belt. However, whereas post-D_2 to syn-D_3 diapirs were not primarily responsible for regional M_2 metamorphism in the Kalgoorlie Terrane, it is clear that addition of heat from the crystallization of granitoids

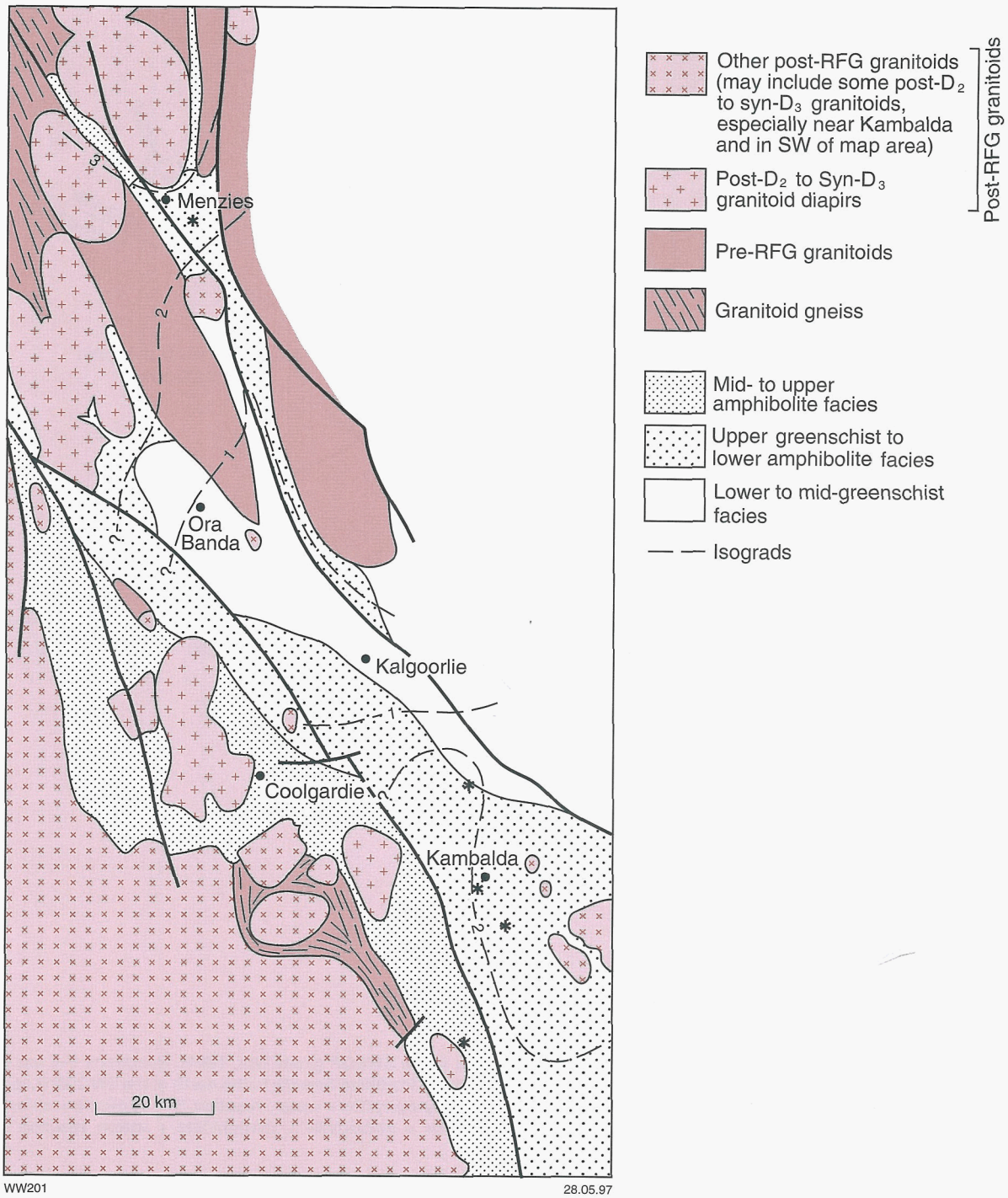

Figure 5. Distribution of metamorphic grade in the Kalgoorlie Terrane (modified from Witt, 1991). Isograds 1–3 are based on M_2 alteration assemblages in gold mines and separate, progressively higher temperature assemblages (Witt, 1991). Asterisks represent localities of detailed metamorphic studies (see Witt, 1991 for details). Narrow M_1 metamorphic aureoles are not shown but occur around the margins of pre-RFG granitoid complexes

emplaced during peak dynamothermal metamorphism strongly influenced the distribution of M_2 isograds.

Controls on M_2 metamorphism in areas east of the Kalgoorlie Terrane are less well understood but current mapping indicates an increase in grade towards the contacts of some post-RFGs (e.g. along the southern margins of the Mulliberry and Birthday complexes; Ahmat, A. L., 1992, pers. comm.).

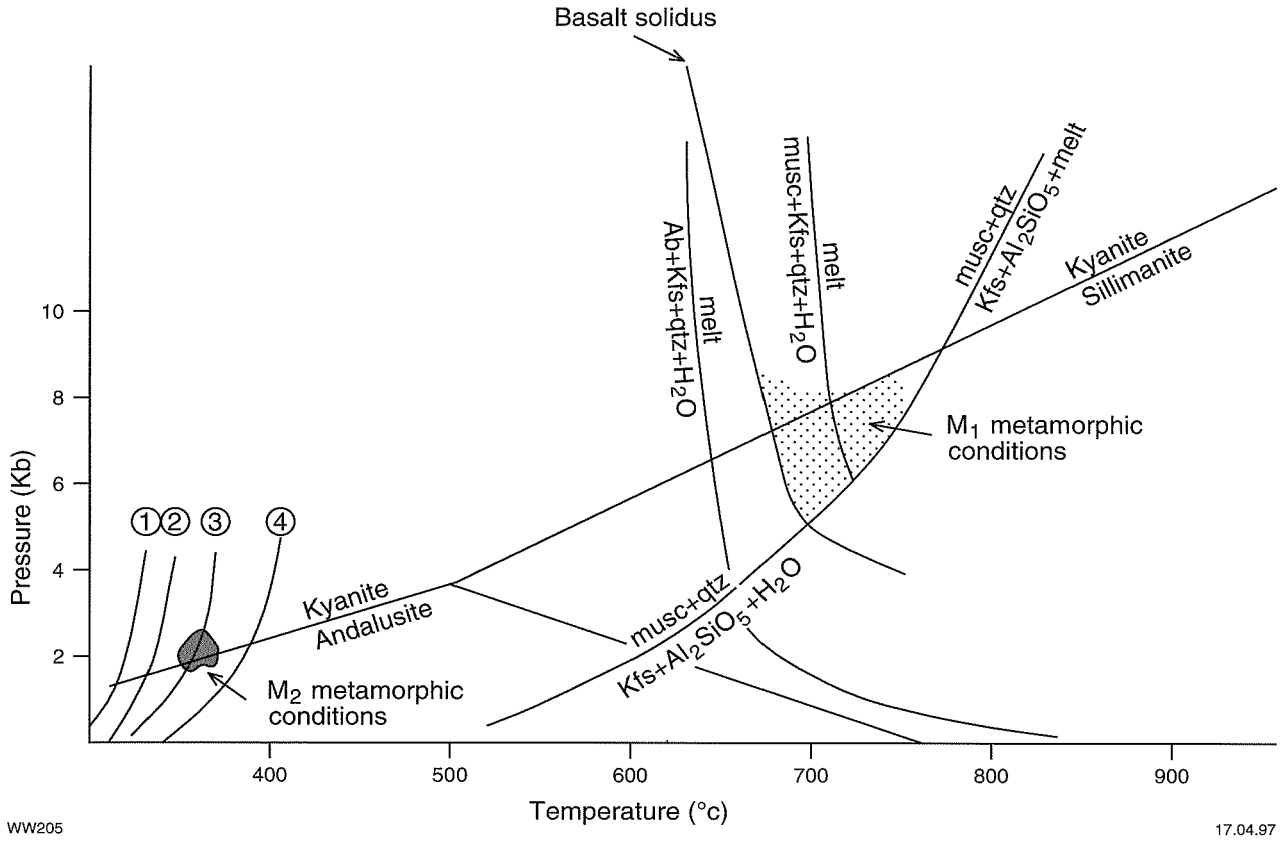

Ab	Albite
Al_2SiO_5	Aluminosilicate mineral (Andalusite, Kyanite, Sillimanite)
Kfs	K-Feldspar
musc	Muscovite
qtz	Quartz

Figure 6. P–T grid indicating M_1 and M_2 metamoprhic conditions in the SWEGP (from Witt, 1994). Reactions 1–4 are from Wallmach and Meyer (1990) and define M_2 at Melita and other localities directly to the north of the SWEGP (Leonora and Mount Malcolm). Reaction 1 — kaolinite + quartz = pyrophyllite + water; reaction 2 — kaolinite + chlorite = chloritoid + pyrophyllite + water; reaction 3 — kaolinite = andalusite + pyrophyllite + water; reaction 4 — pyrophyllite = andalusite + quartz + water

Chapter 3

Granitoid emplacement mechanisms, timing, and relationships to tectonics and regional metamorphism

Granitoid intrusion was an integral part of the tectono-thermal evolution of the SWEGP. In this section, the field observations and relationships described above are used to interpret the timing and emplacement mechanisms of different granitoid groups, and the ways in which plutonism, deformation and metamorphism were related.

Granitoid gneiss

Granitoid gneiss is intruded by post-regional folding monzogranite south of Coolgardie and north of Menzies (Bettenay, 1977; Witt, 1994), and also occurs as xenoliths in some post-RFG intrusions (e.g. Depot Granodiorite). The gneiss is therefore older than post-RFG magmatism. However, age relations with pre-RFGs are more difficult to determine because intrusive contacts between gneiss and pre-RFG units have not been observed. Gneissic banding and a granoblastic fabric reflect relatively high-temperature deformation and recrystallization relative to that in pre-RFGs, but this does not necessarily imply an age difference.

Archibald and Bettenay (1977) and Archibald et al. (1978) concluded that granitoid gneiss exposed along the eastern margin of the Pioneer Monzogranite contained evidence of an early deformation event, defined by the gneissic banding, which did not appear in the greenstones. They proposed that the gneiss may represent basement to the greenstone sequence. This conclusion has been disputed by Glikson (1979), and remains equivocal because an early gneissic fabric, equivalent to D_1, has been observed within the greenstones adjacent to some pre-RFG complexes (Williams and Whitaker, 1993; Witt, 1994). No unconformities, or conglomerates containing gneiss clasts, have been observed in the lower part of the greenstone succession. Therefore, geochronological data are required to determine whether granitoid gneiss is basement, or remnants of highly deformed and metamorphosed pre-RFG complexes.

McCulloch et al. (1983) obtained Rb–Sr and Sm–Nd whole-rock ages of approximately 2800 Ma for gneiss in the Pioneer Monzogranite and Depot Granodiorite. Hill et al. (1992a,b) reported a similar age for zircon xenocrysts in plutons (Theatre Rocks, Widgiemooltha Monzogranite), which are temporally and spatially associated with the Pioneer Monzogranite and Depot Granodiorite. On the other hand, Williams (1993) reported U–Pb zircon ages for granitoid gneiss west of Leonora (north of, but along strike from, gneiss in the northern SWEGP; Fig. 2) that are equivalent to or younger than those for pre-RFG. These dates are 2684 ± 9 Ma (Blueys Well) and 2680 ± 5 Ma (Peters Bore).

Pre-regional folding granitoids

Emplacement of pre-RFG complexes took place in two stages: intrusion as sheet-like magmas at deep (P >5 kb) crustal levels, and subsequent solid-state emplacement as domes in relatively shallow (P = 2–3 kb) greenstone country rocks.

Magmatic emplacement

Pre-RFGs were actively involved in the extensional phase of D_1, and were buckled and sheared by subsequent phases of deformation. They were probably emplaced during D_{1c}. Accurate age determinations for pre-RFGs in the study area are not yet available. However, granodiorite in the Norseman area, with petrographic, geochemical and some structural characteristics of the pre-RFG Rainbow suite, yields ages of 2691 ± 6 Ma and 2686 ± 8 Ma (Hill et al., 1992a,b). These ages are equivalent to those of felsic volcanic rocks (the Mount Kirk Formation) in the same area, which, in turn, are correlated with the Black Flag Group in the Kalgoorlie Terrane (Swager et al., 1992, 1995).

Conceptual pre-D_2 and D_3 geometry indicates that the contacts with greenstones were originally subhorizontal. The broadly concordant relations with primary layering in the greenstones, and their common location in the cores of F_2 anticlines, suggest that the granitoid complexes were emplaced as sheet-like bodies near the base of the exposed greenstones, prior to regional folding (D_2). Aeromagnetic data (particularly the Owen, Scotia and northern Birthday complexes; Plate 1), and exposures in the Twin Hills area (Appendix 2), further suggest that individual intrusive components of the granitoid complexes had a sheet-like form. The granitoid complexes probably formed an extensive sheet-like body at the base of all, or most, of the greenstone sequences in the study area, including those in the south. Recent results of a single deep-crustal seismic traverse across the SWEGP have cast some doubt upon the lateral extent of the pre-RFG complexes (Goleby et al., 1993).

Granitoid magmas may rise diapirically through the lower crust, but spread laterally when they encounter less ductile crust at the brittle–ductile transition (Williams and Whitaker, 1993). Emplacement of pre-RFGs as sheets at the base of the thickened, relatively dense greenstone pile may have been further facilitated by active, subhorizontal D_{1c} thrust surfaces. Ponding of magmas beneath subhorizontal structures would allow time for further crystallization, which would increase the viscosity of the melt. The increase in viscosity may have been sufficient to overcome any tendency toward continued ascent due to negative buoyancy (Walker, 1989), provided the relatively dense overlying crust was not ruptured by steep fractures.

Solid-state emplacement (doming)

Preferential exposure of pre-RFGs in the north of the study area is attributed to broad, asymmetric doming during D_{1e}. Metamorphic conditions in narrow M_1 aureoles adjacent to pre-RFG complexes (P >5 kb, T = 650–750°C) contrast markedly with those established for M_2 assemblages (P = 2–3 kb, T = 250–600°C). Transitions between M_1 and M_2 zones are very sharp, implying unreasonably steep temperature gradients and impossible pressure gradients. The gradients are difficult to quantify, but relationships at Leonora (Williams and Currie, 1993) and Niagara (Witt, 1994) demand a tectonic contact between the two metamorphic zones. Williams and Currie (1993) concluded that at least 9 km of crust was excised during extensional movement on the granitoid–greenstone contact. Witt (1994) suggested a more limited excision of crust (>2.5 km) across the margins of the Mulliberry complex.

Witt (1994) attributed extension to broad doming of regionally extensive granitoid sheets, in the north of the study area, prior to regional folding (D_2). The cause of doming is not known, but may have been a consequence of gravitational instability and collapse, following thickening of the crust by thrust stacking (Fig. 7). In common with some other granitoid domes (Davis, 1980), uplift was asymmetric, producing much steeper contacts on the northern margins of the domal complex. A northerly to north-northeasterly trending felsic dyke swarm west of Kookynie may be related to stresses caused by uplift of the granitoid complex.

Near Kookynie and Leonora, the main zone of extension was located within the greenstones, resulting in the preservation of a narrow, high-grade metamorphic carapace adjacent to the granitoid complex. High-grade metamorphic rocks also occur in a narrow zone adjacent to granitoid complexes on the more gently dipping, southern margin of the uplifted area (e.g. the Owen dome). However, the difference between metamorphic conditions in the carapace and those in the overlying greenstones appears to have been less extreme than that in the Leonora–Kookynie area, and the stratigraphic succession appears to be little disturbed across the metamorphic break. These observations suggest either that there was little or no associated excision of crust on the southern face of the uplifted granitoid dome, or that if a significant thickness of crust was excised, its original position was directly adjacent to the contact with the granitoid complex (i.e. extensional deformation was focused on the granite–greenstone contact, in contrast to Kookynie where extensional deformation was focused just above the contact).

Following broad domal uplift, the shallowly south-dipping upper surface of the regionally extensive pre-RFG sheets was folded during D_2 to produce elongate domes (e.g. the Owen dome, the Scotia dome), which form the cores of regional anticlines.

Evidence against pre-RFG magmatic diapirism

Gee et al. (1981) envisaged pre-RFG complexes as magmatic diapirs and attributed their elongate shape to strain during regional deformation. Typical features of granitic diapirs, and other plutons forcefully emplaced during regional compression, have been described by Dixon (1975), Barriere (1977), Bateman (1985), Brun and Pons (1981) and Lagarde et al. (1990). Although pre-RFG complexes display some characteristics of magmatic diapirs (e.g. deformed contact zones), the features described below are not consistent with emplacement as diapirs:

1. Early granitoid complexes commonly form the cores of D_2 anticlines. Therefore, if they were emplaced as diapirs, the logical timing for emplacement was during D_2. However, the early granitoids record all phases of regional deformation detected in the greenstones, including D_1.

2. Thin greenstone screens (tectonic slices) and a contact-parallel foliation (S_1) within the northern margin of the

Figure 7. Schematic diagram illustrating D_{1c} and D_{1e} in the SWEGP

A. Development of greenstones on sialic basement; a–d represent stratigraphic units within the undisturbed greenstone sequence

B. D_{1c}: northerly directed thrusting along contacts within greenstones and along or near contact between greenstones and basement (solid arrows indicate direction of movement). Intrusive granitoid sheets emplaced at or near base of greenstones. High-pressure metamorphism of greenstones at base of thickened greenstone pile. 1–4 represent thrust slices of all, or parts of the original greenstone sequence a–d. Dotted lines and arrows represent future planes and directions of movement during D_{1e}

C. D_{1e}: gravitational collapse of thickened crust, and extension of stacked greenstones

D. Asymmetric domal uplift of intrusive granitoid complex (and underlying basement?) following unloading of greenstones during D_{1e}. Note juxtaposition of low-pressure greenstones (thrust slice 3) against high-pressure metamorphic assemblages on north side of dome. Vertical scale at right is a notional scale only

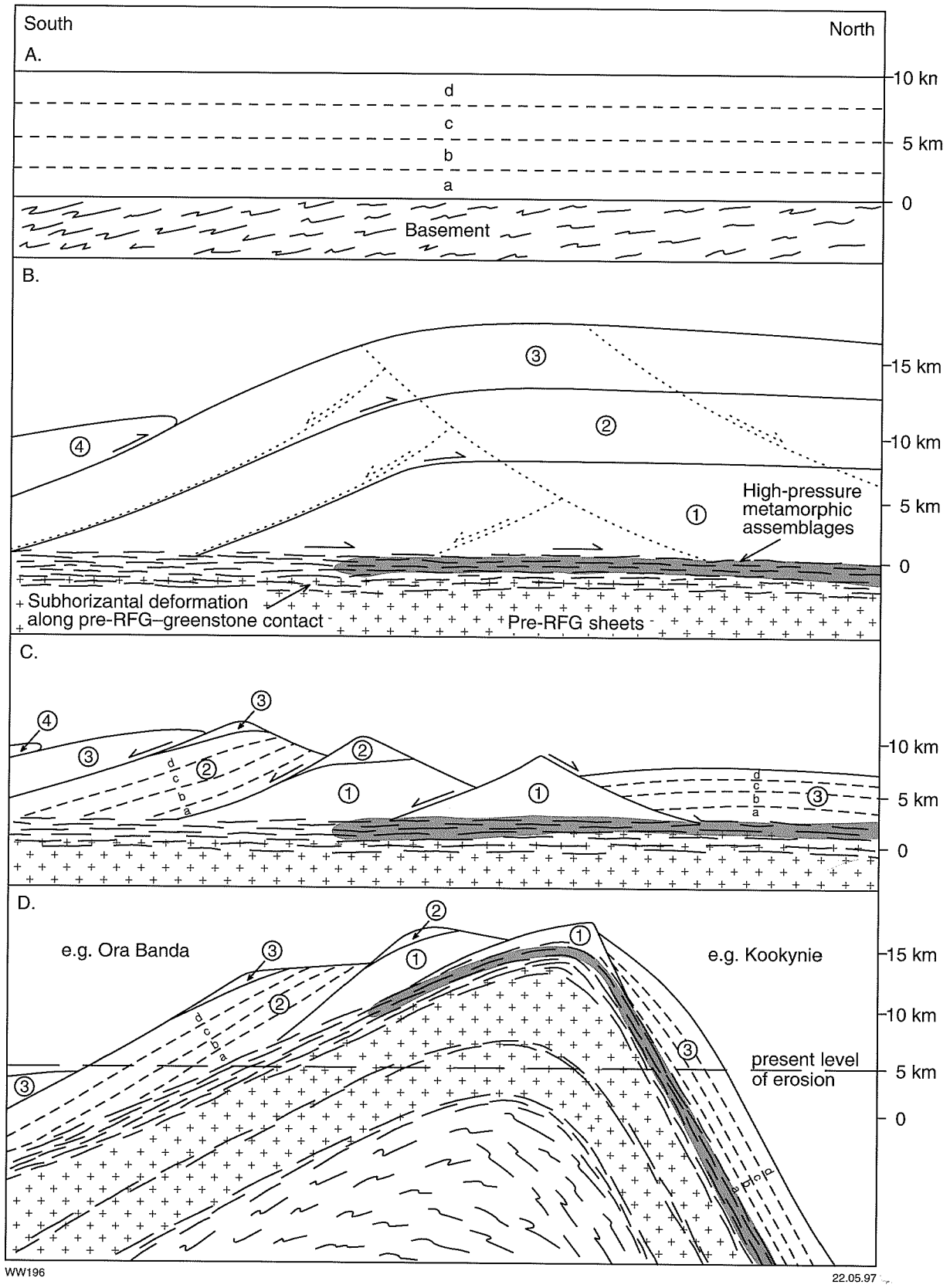
South
North
A.
d
c
b
a
Basement
10 km
5 km
0
B.
③
②
④
①
High-pressure metamorphic assemblages
Subhorizantal deformation along pre-RFG–greenstone contact
Pre-RFG sheets
15 km
10 km
5 km
0
C.
④
③
②
①
d
c
b
a
10 km
5 km
0
D.
e.g. Ora Banda
e.g. Kookynie
present level of erosion
15 km
10 km
5 km
0
WW196
22.05.97

Mulliberry Complex are crenulated by D_2. This relationship would not be expected if the granitoid magma was forcefully emplaced during D_2.

3. Strongly deformed greenstones in the contact zones adjacent to the granitoid complexes are unusually narrow, compared with the flattening aureoles around well-documented diapirs. Aureoles around some later granitoids in the SWEGP, which are interpreted to have been emplaced as diapirs (post-D_2 to syn-D_3 granitoid diapirs, described below), contain a diverse set of foliations due to complex interaction between ballooning of the intrusion and regional deformation (Wyche and Witt, 1992). In contrast, there is no evidence of flattening or accommodation structures that overprint S_1 in greenstones adjacent to the early granitoid complexes.

4. Critical evidence for emplacement mechanisms should be sought along the northern and southern margins of pre-RFG complexes where structures related to emplacement would not have been overprinted by D_3 deformation. Down-dip lineations at the northern end of the Mulliberry Complex are equally compatible with diapiric emplacement or north–south D_1 movement on a subhorizontal granite–greenstone contact. Oblique to shallowly plunging lineations at the northern end of the Dunnsville dome (Fig. 8) are incompatible with diapiric emplacement, and must have formed during northwesterly directed D_1 movement on the contact between a subhorizontal granitoid sheet and overlying greenstones.

5. An easterly trending contact between two petrographically and chemically distinct phases of the Scotia Complex (at Split Rocks) is overprinted by the north-northwesterly trending S_2/S_3 fabric but there is no evidence of the contact-parallel foliation typically associated with coalesced diapiric intrusions.

6. Although early granitoid complexes commonly occupy the cores of F_2 anticlines, the extensive aerial extent represented by the Raeside, Mulliberry and Birthday complexes suggest that they are also exposed in some (partly sheared out) synclinal positions. This situation requires that the early granitoid complexes formed an extensive sheet at the base of the greenstones, prior to D_2 folding.

Similar arguments have been used to reject diapirism, in favour of sheet-like intrusions, for early granitoids in the Laverton area (Williams and Whitaker, 1993) and at Agnew (Platt et al., 1978).

Post-regional folding granitoids

The wide range of contact relationships for post-RFG plutons reflects variable timing of emplacement with respect to regional deformation, and a diversity of emplacement mechanisms. Available geochronological data suggest that post-RFG magmatism peaked early at around 2665–2660 Ma, but may have continued until around 2600 Ma (Hill et al., 1992a,b).

Post-D_2 to syn-D_3 granitoids

Displacement and transection of F_2 fold axes indicate that post-D_2 to syn-D_3 granitoid intrusions were emplaced after F_2. However, emplacement did not post-date D_3, since D_3 shear zones deform the margins of several diapirs. Near Menzies, northward displacement of the greenstone wedge between the Boorara–Menzies Fault and the Moriaty Fault, during D_3, was blocked by the Jorgenson Monzogranite. This resulted in thin slices of greenstone being thrust upwards over the Jorgenson Monzogranite and the Federal Granodiorite, along shallowly dipping, curved reverse faults (Fig. 9). The Theatre Rocks Monzogranite has an emplacement age of c. 2665 (Table 2).

The contact features and relationships with greenstones displayed by this group of granitoids are indicative of diapiric emplacement (see also Archibald et al., 1978, 1981). There is ample evidence of forceful emplacement in greenstones adjacent to the diapiric intrusions, including contact-parallel foliation(s) and accommodation faults. Plutons at Coolgardie and Siberia have deflected F_2 fold-hinge lines. At Siberia, the hinge of the Kurrawang Syncline has been deflected eastwards by about 15 km. This displacement has been accommodated by east-northeasterly trending faults. Easterly trending accommodation faults occur at the northern and southern margins of the Silt Dam Monzogranites. Expansion of the diapirs was thus mainly in an east–west direction, against the principal regional stress axis. Deeper structural and stratigraphic levels of the greenstone pile have been uplifted around the margins of all diapirs.

In addition to uplift of country rocks, there is further evidence that the diapirs have actively deformed the greenstones, and not just acted passively as rigid bodies against which F_2 fold hinge lines were deflected (i.e. the F_2 fold hinges pre-dated the intrusions, not vice versa).

1. The Bali Monzogranite actually transects an F_2 anticline in the Coolgardie area, as well as displacing it (Plate 1).

2. The Siberia group of diapirs has deflected the hinge of the F_2 Kurrawang Syncline, but has had much less effect, if any, on the F_2 Goongarrie–Mount Pleasant Anticline (Fig. 10). The Owen dome, in the core of the anticline, acted as a rigid buttress, against which the uplifted greenstones in the Wongi Hills belt were compressed.

3. The Kurrawang Syncline is located close to the Zuleika Fault, northeast of Coolgardie. As these two structures approach the Siberia granitoids, only the Zuleika Fault is deflected to the west of the intrusions (Fig. 10). Displacement of the F_2 fold hinge to the east could only occur if the fold pre-dated the shear, and was actively pushed across progressively by intrusions that were emplaced sequentially further to the east.

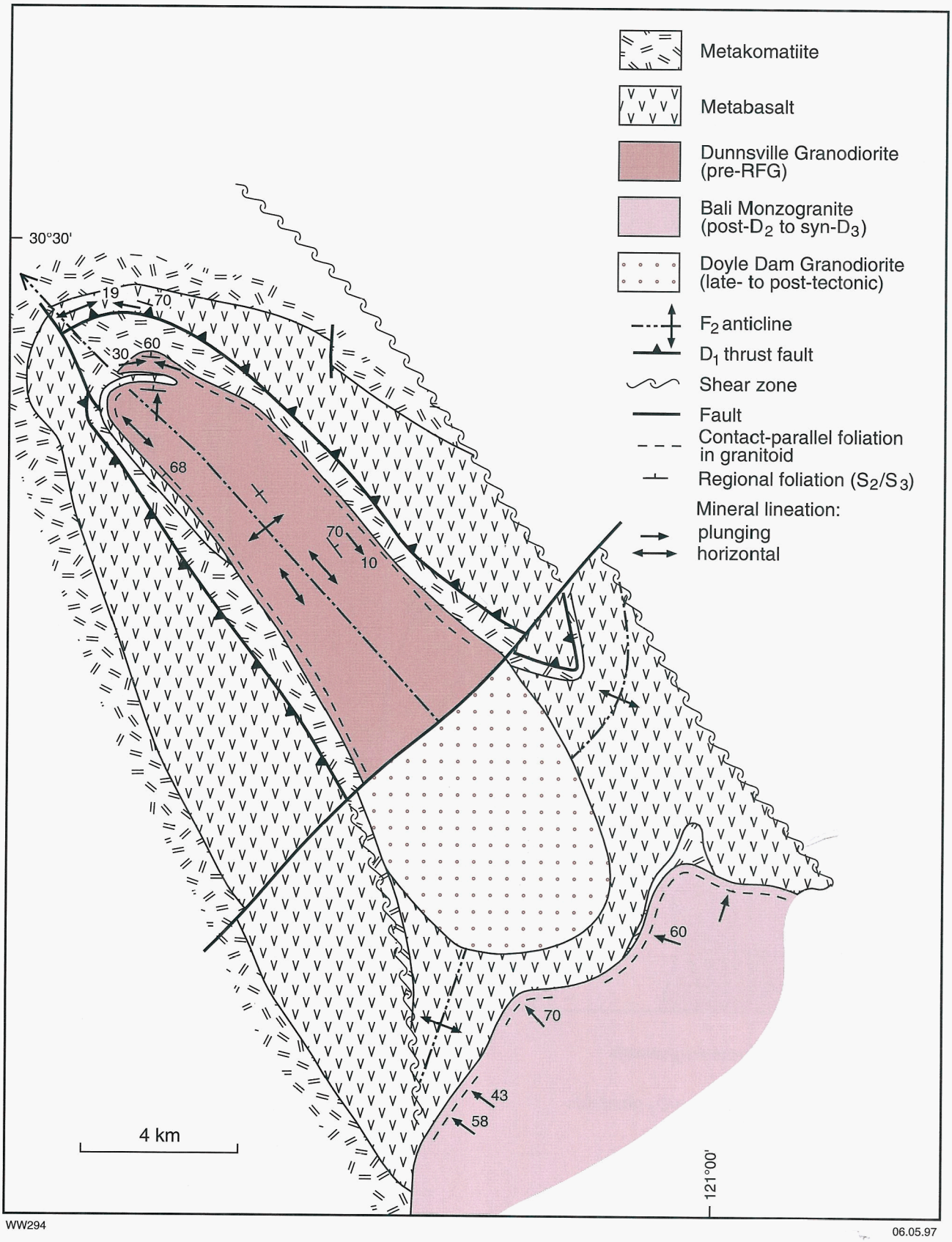

Figure 8. Geological relationships in the Doyle Dam Granodiorite area (from Witt and Swager, 1989)

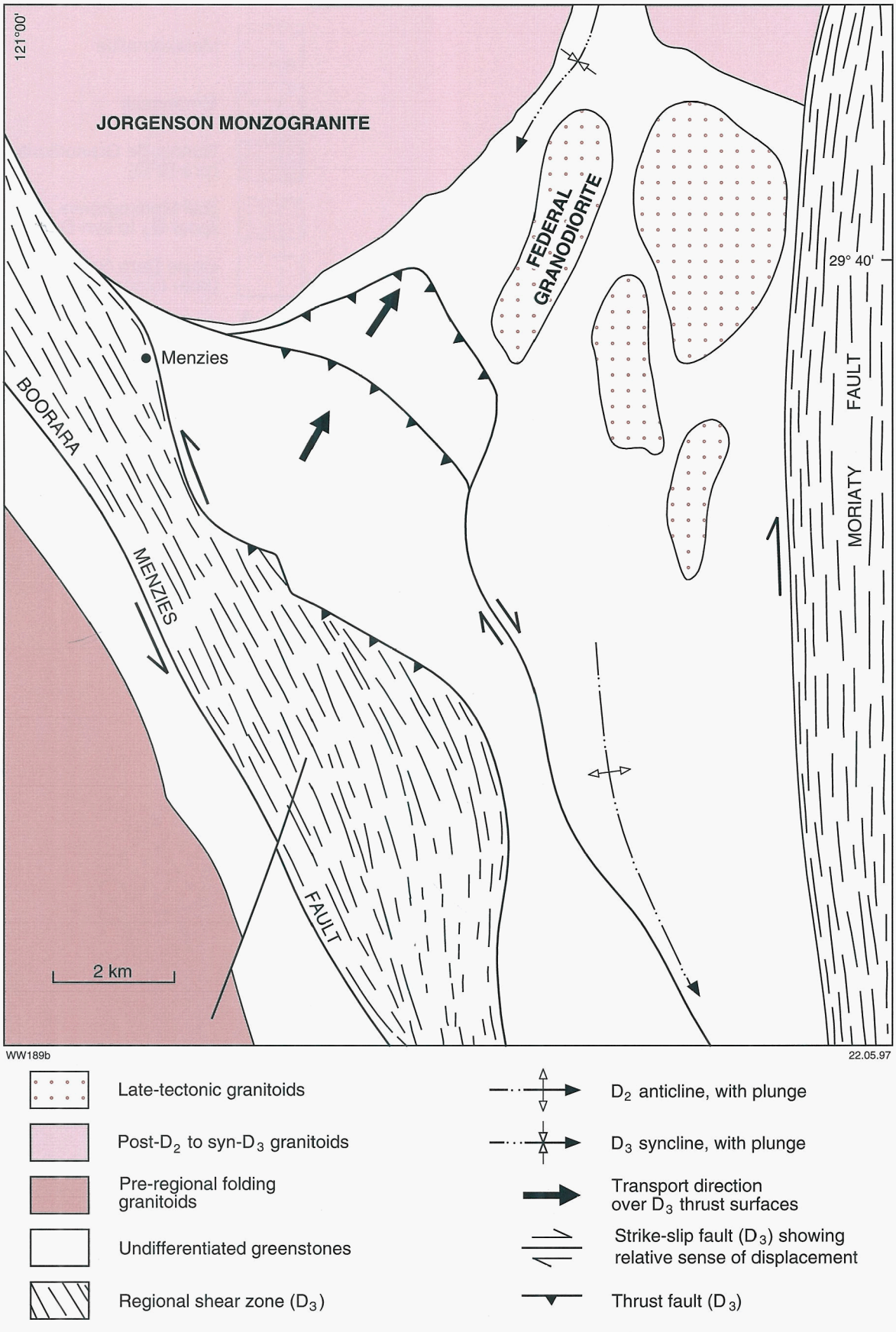

Figure 9. Relationships between D_3 shear zones, post-RFG intrusions and late, low-angle thrusts in the Menzies area (modified from Witt, 1993a)

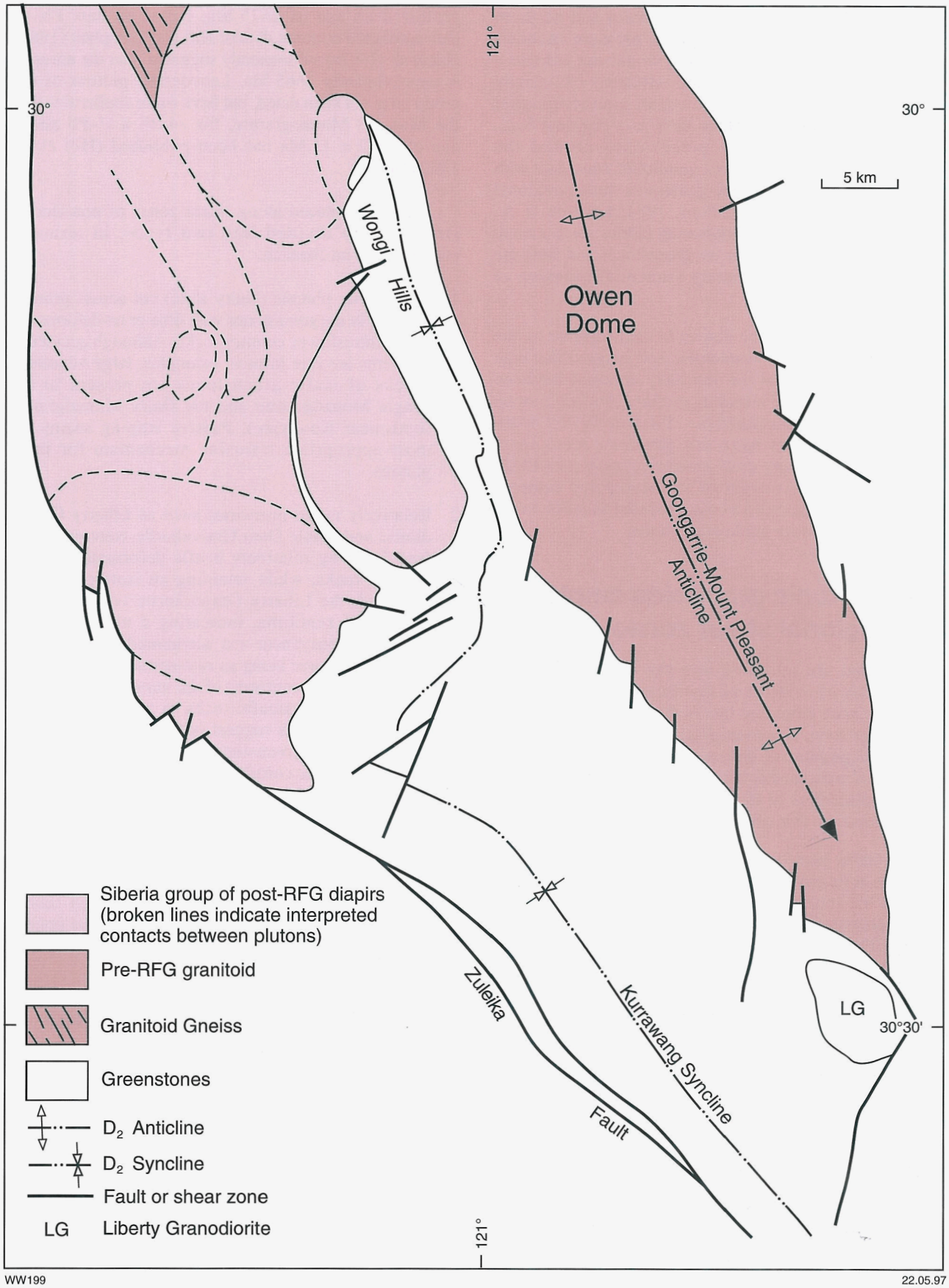

Figure 10. Geological relationships in the Siberia area

Greenstones adjacent to the southern and northern margins of plutons were located in pressure shadows during regional compression, and would not contain a contact-parallel foliation(s) if the intrusions had simply deflected regional strain. However, contact-parallel foliations and shear zones, as well as a regional S_2/S_3 foliation, are present in greenstones around the southern margins of the Siberia granitoids, consistent with forceful emplacement of the granitoids during regional compression (cf. Brun and Pons, 1981; Lagarde et al., 1990). The contact-parallel flattening fabrics are at a small angle to primary layering in the greenstones and there are several generations, reflecting sequential intrusion of successive diapirs.

The distribution of the diapirs in, and adjacent to, the 'dynamic' high-grade metamorphic belt suggests that high temperatures lowered the ductility contrast between country rocks and the intruding granites, thus promoting diapiric intrusive mechanisms (Pitcher, 1979). Well-documented diapirs have not yet been recognized elsewhere in the study area. However, some post-RFGs along the southern margin of the Mulliberry complex appear to have imparted a contact-parallel foliation to the adjacent, amphibolite-grade greenstones.

Late-tectonic granitoids emplaced into regional shear zones

Plutons that are intrusive into the D_3 Butchers Flat Fault display no evidence of significant ductile strain and must have been emplaced late in the deformation history of the shear zone. However, displacement and boudinage of related pegmatite dykes, intrusive into adjacent greenstones, indicate that minor strike-slip movement post-dated emplacement of the granitoid intrusions. Absolute age dates are not available.

The Galah Monzogranite contains numerous accidental xenoliths at its present level of exposure, interpreted to be close to the roof of the intrusion. Abundant pegmatitic dykes penetrate basaltic country rocks via a reticulate joint system. The contact between basalt and monzogranite is a broad (500 m) zone containing alternating layers of monzogranite, pegmatite and basalt. There is no evidence of deformation related to emplacement of the Carpet Snake Syenogranite and Galah Monzogranite in adjacent greenstones, and it is concluded that they were emplaced passively, by piecemeal stoping.

Small, late-tectonic granitoids emplaced along linear zones of non-ductile strain

The unmodified igneous textures of small, late tectonic granitoids emplaced along linear zones of non-ductile strain suggest late- or post-tectonic emplacement. The age of the Liberty Granodiorite is controversial. Hill and Campbell (1989) originally published a U–Pb zircon age of 2593 Ma. McNaughton and Cassidy (1990) recalculated the data to give an age of 2645 Ma, but preferred an age of 2675 Ma, based on new Pb–Pb data combined with the data of Hill and Campbell (1989). Hill et al. (1992a) subsequently suggested that the intrusion is approximately 2665 Ma. Leucocratic plutons of this group have not been dated, but have some similarities with the Mungari Monzogranite, for which a U–Pb zircon age of 2602 ± 11 Ma has been published (Hill et al., 1992a,b).

Plutons emplaced along linear zones of non–ductile strain can be divided into two types, in terms of emplacement mechanism:

1. Leucocratic plutons (Dairy suite) cut across primary layering in the greenstones with little or no deformation of the intrusion or country rocks. Although accidental xenoliths are rare in most examples, large xenolithic blocks of mafic greenstones are present in the Jungle Monzogranite and the Dairy Monzogranite (both near Kookynie). Passive stoping seems the most appropriate intrusive mechanism for these plutons.

2. Relatively mafic intrusions such as Liberty Granodiorite and Doyle Dam Granodiorite were emplaced forcefully, by relatively brittle deformation of the country rocks, while retaining an isotropic fabric. Although the Liberty Granodiorite contains some accidental xenoliths, indicating a minor role for stoping, emplacement was accommodated mainly by dextral movement along an east-northeasterly trending fault zone to the northwest of the intrusion, and intense flattening of ultramafic rocks to the east (Fig. 11). These observations suggest predominantly east–west dilation of the greenstones, a conclusion which is supported by the correlation of contacts and zones of the Mount Ellis Sill, to the east and west of the pluton (Fig. 11).

An east-northeasterly trending fault appears to have accommodated emplacement of the Doyle Dam Granodiorite. Forceful emplacement of the intrusion caused folding in greenstones adjacent to the northeast contact (Fig. 8).

Post-regional folding granitoids west of the Kalgoorlie Terrane

Poor exposure and intrusion into granitic country rocks prevent confident assessment of the timing and mechanism of emplacement of post-RFG intrusions west of the Kalgoorlie Terrane. Hunter (1991) interpreted the lithologically heterogenous margins of these intrusions to have developed by a combination of stoping, dyke intrusion and deformation caused by magma ballooning. The plutons thus display some similarities with the post-D_2 to syn-D_3 intrusions that occur in a linear belt along the western margin of the Kalgoorlie Terrane. However, other granitoids west of Coolgardie appear to post-date the D_3 Ida Fault, indicating a later age of emplacement. The Woolgangie Monzogranite has been dated at 2646 ± 6 Ma (Table 2).

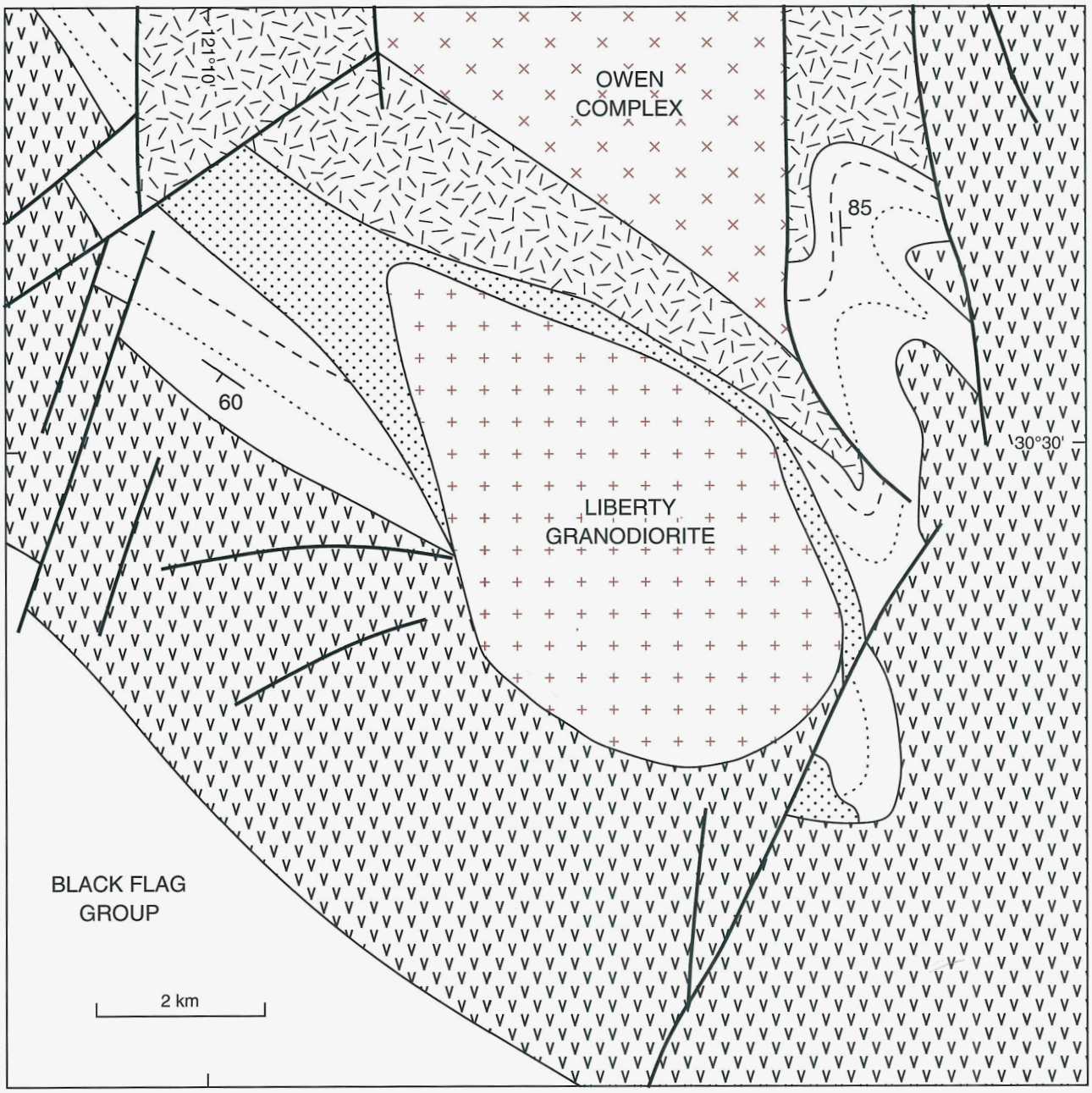

Figure 11. Geological relationships in the Liberty Granodiorite area. Forceful emplacement of the pluton caused compression of komatiitic rocks and east–west dilation of the overlying greenstones (see marker horizons in the Mount Ellis Sill)

Alkaline intrusions

The absence of a regional foliation, and transgressive relations with respect to D_3 shear zones and lithological layering in the greenstones, suggest late emplacement of alkaline intrusions in the SWEGP. There are no published U–Pb zircon data for alkaline granitoids in the SWEGP. Rb–Sr data yield much younger ages than for other granitoids. These young ages substantially post-date peak regional metamorphism (c. 2660 Ma: Swager et al., 1992, 1995) and cratonization, and have typically been interpreted as emplacement ages. Syenite at Twelve Mile

Well yielded a Rb–Sr whole-rock date of 2489 ± 82 Ma (Libby, 1989). Similarly young Rb–Sr ages for alkaline intrusions in the Eastern Goldfields Province (but outside the SWEGP) include 2520 ± 113 Ma (Woorana Well; Libby, 1989), 2360 ± 96 Ma (Fitzgerald Peaks; Libby, 1989); and 2542 ± 14 Ma and 2627 ± 41 Ma (Gilgarna Rock; Johnson and Cooper, 1989).

The presence of xenoliths and the apparent lack of evidence in the country rocks for forceful emplacement suggest that the alkaline intrusions were passively emplaced by piecemeal stoping.

Chapter 4

Petrography of SWEGP granitoids

General petrographic characteristics

Collectively, granitoid gneiss, pre-RFGs and post-RFGs have many petrographic features in common and cannot be distinguished using petrographic criteria alone. However, individual pre-RFG suites and post-RFG supersuites display some petrographic features that can be used to help distinguish them from one another.

Although accurate modal analyses of granitoid samples have not been carried out, modal estimates from most thin sections are consistent with geochemical data (Fig. 12). Rock types (including some unanalysed samples) vary from tonalite to syenogranite, and from diorite to syenite, with a marked predominance of monzogranite and granodiorite. The dominance of monzogranite and granodiorite is underestimated by Figure 12 because sampling has been slightly biased toward localities displaying petrological diversity. Sample points in Figure 12 may be shifted slightly toward Or, and Q (especially in low-SiO_2 samples), because biotite is not accounted for in the CIPW norms. In Figure 12, the albitic component in perthitic K-feldspar is assigned to plagioclase, resulting in a significant displacement of syenitic rocks toward the Pl apex. By comparison, most samples plot in the trondhjemite and granite fields on the orthoclase–anorthite–albite triangular diagrams in Figure 13.

Granitoid gneiss

Granitoid gneiss is a medium- to coarse-grained rock in which banding is defined by the variation in grainsize, and the distribution of dark minerals and feldspars. Although a granoblastic texture is dominant, oriented biotite defines a weak to strong foliation parallel to gneissic banding. Strain is also preserved irregularly, as elongate quartz grains and boudins of deformed plagioclase grains. Relict igneous grains in low-strain domains are common, and indicate a medium- to coarse-grained igneous precursor for the gneiss. However, pelitic assemblages, and amphibolite, occur within gneiss at some localities, suggesting tectonic interleaving of granitoids with greenstones. Metapelitic assemblages include sillimanite–phlogopite–cordierite–muscovite, west of Coolgardie (Bettenay, 1977), and garnet–biotite–staurolite–K-feldspar, west of Menzies (Rattenbury, in prep.).

Biotite is typically the only common mafic silicate. Hornblende occurs in a biotite-rich diorite enclave within gneiss, south of Donkey Rocks Well, and is dominant in amphibolite bands west of 29 Mile Well (the two localities are north and west, respectively, of Menzies). Biotite, hornblende and clinopyroxene occur in gneiss enclaves within the Depot Granodiorite. Accessory minerals in granitoid gneiss are apatite, zircon, opaque oxide minerals, allanite and, less commonly, epidote. Tonalitic gneiss, north of Menzies, also contains titanite.

Bulk gneiss compositions

South of Breakaway Well

The most mafic granitoid gneiss occurs south of Breakaway Well, north of Menzies, where gneissic banding is oriented approximately 160°, but locally shows evidence of having been folded. The overall composition is tonalitic, but individual bands vary from biotite tonalite to biotite granodiorite. Gneissic banding is cut by thin diorite dykes, some of which display small-scale fold structures.

Riverina area

Monzogranite and granodiorite gneiss, with conspicuous compositional banding, occurs in a zone from the Riverina Homestead area, north towards Mount Ida. Good exposures at 18 Mile Well and west of 29 Mile Well have been described by Bettenay (1977) and Rattenbury (1990, pers. comm.). A distinct, subvertical gneissic banding trends north, subparallel to a tectonic contact with greenstones to the west. Individual bands, tens of centimetres to a few metres wide, are mostly straight and regular, but there are low-angle discordances in some places. Bettenay (1977) documented the presence of tight, rootless folds within individual bands, and aeromagnetic data also indicate complex structural relationships (see Plate 1). At 18 Mile Well, the volumetrically dominant bands are medium- to coarse-grained (0.5–2 mm) monzogranite and granodiorite that contain 10–20% biotite, and porphyroclasts of K-feldspar.

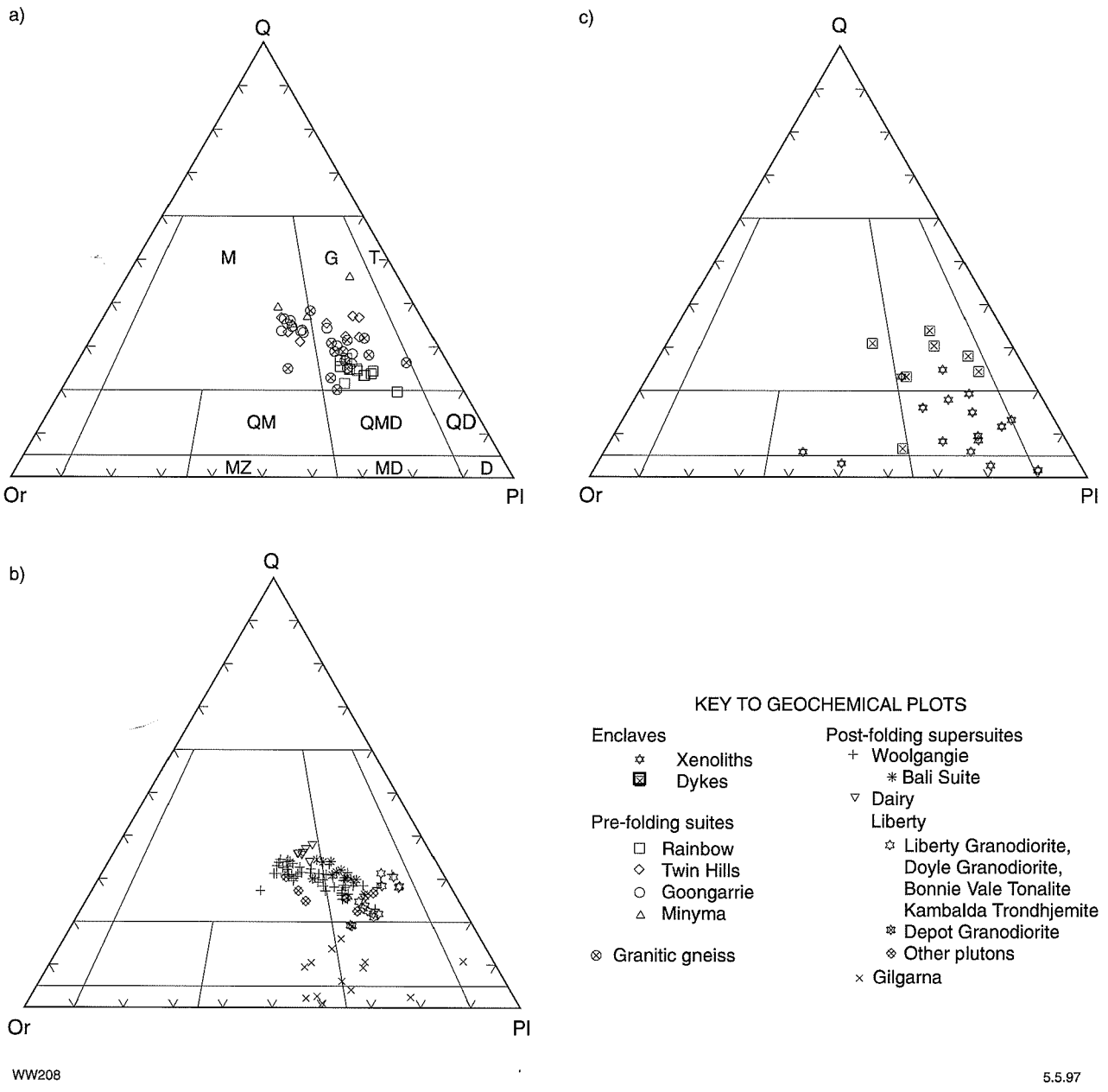

Figure 12. Normative plagioclase–quartz–orthoclase triangular diagrams showing: (a) gneiss and pre-RFGs, (b) post-RFGs, and (c) dykes and xenoliths. Divisions are from Streckeisen (1976). Diorite (D), Granodiorite (G), Monzogranite (M), Monzodiorite (MD), Monzonite (MZ), Quartz diorite (QD), Quartz monzodiorite (QDM), Quartz monzogranite (QM), Tonalite (T)

Relatively leucocratic bands (<5% biotite) are subordinate, and finer grained tonalitic bands (20–40% biotite) form a minor component. At 29 Mile Well, similar granitoid gneiss is interleaved with bands of clinopyroxene-bearing amphibolite.

Other areas

Relatively leucocratic monzogranite to granodiorite gneiss occurs at many other localities, including south of Donkey Rocks Well, at Quairnie Rock (south of Coolgardie), and on the eastern side of the Pioneer Monzogranite. A granoblastic texture is dominant, but gneissic banding is less obvious because the outcrops are dominated by a leucocratic monzogranite to granodiorite component (about 10% biotite). A north to north-northwesterly trending gneissic banding is only locally distinct, where compositional variation is enhanced by mafic-rich bands of granodiorite and tonalite (up to 50% biotite). At 50 Mile Rocks (the Pioneer Monzogranite locality), numerous pegmatite dykes are subparallel to the gneissic banding, and some have been deformed with the gneiss.

Leucocratic tonalite gneiss also occurs as xenoliths within the Depot Granodiorite.

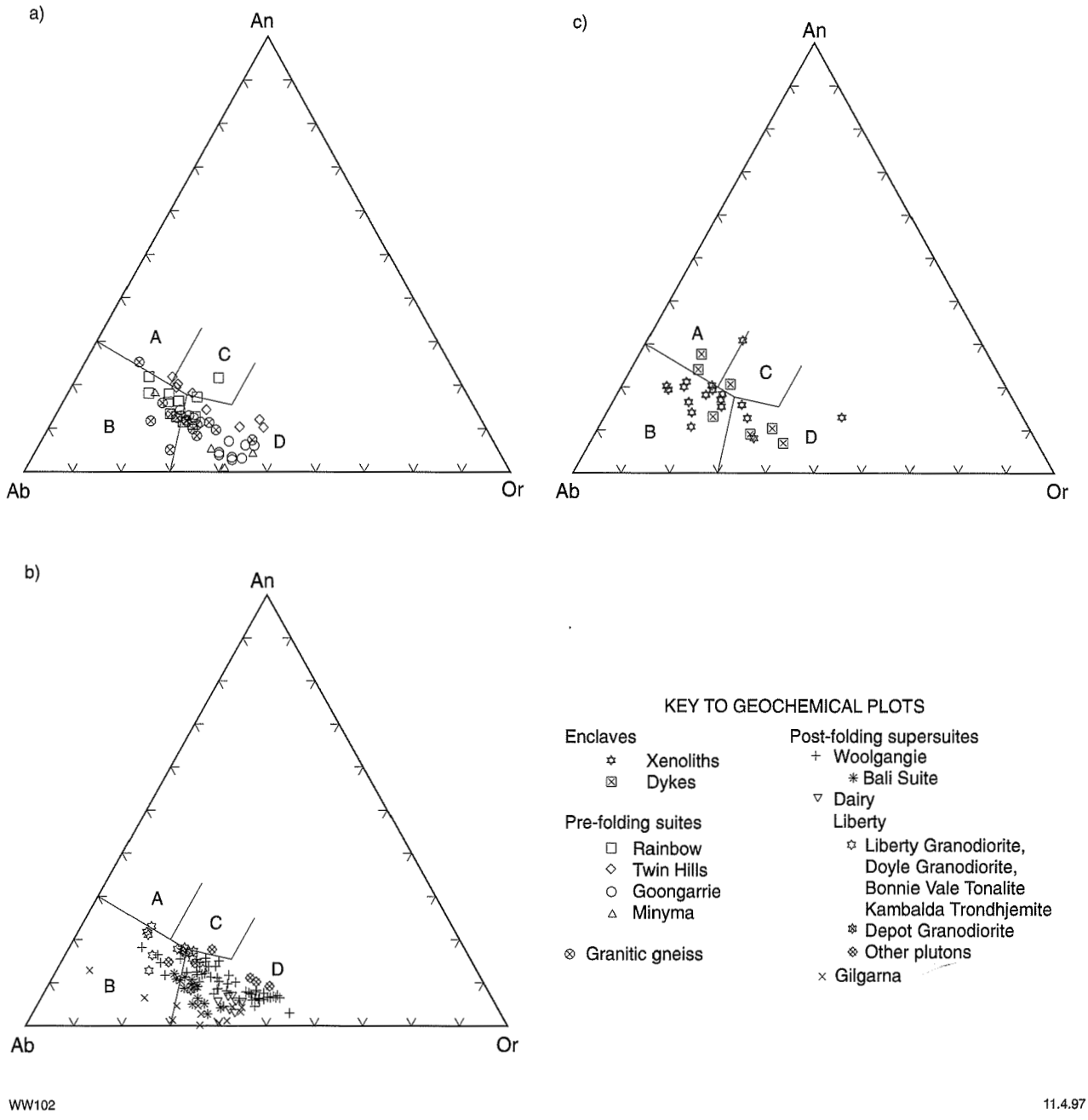

Figure 13. Normative orthoclase–anorthite–albite triangular diagrams (after Barker, 1979) showing: (a) gneiss and pre-RFGs, (b) post-RFGs, and (c) dykes and xenoliths. A = Tonalite, B = Trondhjemite, C = Granodiorite, D = Granite

Pre-regional folding granitoids (Morapoi supersuite)

One of the most striking features of many pre-RFG outcrops is their lithological diversity (see Appendix 2), which contrasts with the relative uniformity displayed by most post-RFG outcrops. Lithological diversity takes the form of compositional banding (in some cases involving granitoids of more than one suite), hypabyssal intrusive dykes, synplutonic dykes, and rounded mafic (cognate) xenoliths. Some or all of these features are evident in most pre-RFG outcrops, with the exception of outcrops of the Goongarrie suite, especially those along the western margin of the Owen complex (e.g. the Cawes Monzogranite of Witt, 1990). Pegmatite dykes occur at some localities, but irregular internal segregations of pegmatite are rare or absent.

Pre-RFGs (Morapoi supersuite) are coarse-grained (2–6 mm), and seriate to porphyritic. Porphyritic rocks are characterized by tabular K-feldspar phenocrysts, up to several centimetres long. Although there is some overlap, pre-RFGs tend to be slightly coarser grained than most

post-RFGs. They range in composition from tonalite to syenogranite, but are dominantly granodiorite and monzogranite. Microgranitoid xenoliths and synplutonic dykes are commonly present. They are most abundant in exposures of Rainbow suite granitoids where they occupy <5% of the outcrop area but more typically comprise <1% of most pre-RFG complexes. The main petrographic features of the pre-RFG suites are summarized below.

Rainbow suite

Granitoids range from granodiorite to monzogranite, and are relatively mafic compared to other pre-RFG suites. Ferromagnesian minerals commonly comprise around 10% of the rock, and the most mafic variants contain approximately 20% ferromagnesian minerals (e.g. east of Scotia, in the Scotia Complex). Cognate microgranitoid xenoliths and synplutonic dykes are common, and are locally abundant (Appendix 2). The granitoids are characterized by the presence of biotite and hornblende and, more rarely, clinopyroxene. Hornblende is the dominant ferromagnesian mineral in some samples, but is rare in some of the more fractionated members of the suite. Textural observations (Appendix 3) suggest late-magmatic reaction of hornblende with the melt to form biotite in the more fractionated granitoids. Sample 90967099 (66.1% SiO_2) contains only biotite, but was collected from the strongly deformed margin of the Copperfield complex, where hornblende was probably destroyed during metamorphic recrystallization. Clinopyroxene has only been observed in samples collected adjacent to some microgranitoid xenoliths. Magnetite, titanite, apatite and zircon are the main accessory phases. Allanite and ilmenite are relatively rare, and ilmenite appears to be metastable with respect to titanite.

Twin Hills suite

The Twin Hills locality is characterized by compositional banding (Appendix 2), in which rock types range from mafic granodiorite to leucocratic syenogranite. Cognate microgranitoid xenoliths are rare, but some of the more mafic granitoids may be synplutonic dykes. The most mafic granitoids contain about 15% biotite, which is typically the only ferromagnesian mineral. Hornblende occurs only in small mafic aggregates within the most mafic granitoids at Twin Hills, and as a minor component of sample 101361. Titanite coexists with magnetite in less fractionated members of the suite, but magnetite occurs alone, or with minor titaniferous oxide minerals, in the more fractionated granitoids. Other accessory phases are apatite and zircon.

Goongarrie suite

The Goongarrie suite is the most leucocratic of the pre-RFG suites, rarely containing more than 5% ferromagnesian minerals. Biotite is the only common ferromagnesian silicate, and hornblende has not been observed. Outcrops are generally relatively homogenous monzogranite or granodiorite (Appendix 2). Cognate, microgranitoid xenoliths and synplutonic dykes are locally common, but are more generally rare to absent. Magnetite coexists with titanite or ilmenite–hematite intergrowths, except in the more fractionated members of the suite, in which opaque minerals are relatively rare. Other accessory phases are apatite and zircon.

Minyma suite

The Minyma suite granitoids commonly contain 5–10% ferromagnesian minerals, including both hornblende and biotite. They are typically less leucocratic than Goongarrie suite granitoids, and in some samples ferromagnesian minerals form distinctive aggregates, up to 1 cm across. Magnetite coexists with ilmenite in most samples, and titanite is absent. Other accessory minerals are apatite and zircon. Cognate microgranitoid xenoliths and synplutonic dykes have not been observed.

Primary muscovite has been observed in only one pre-RFG sample (101006). This sample contains biotite-rich aggregates, and is probably a fractionated member of the Minyma suite.

Post-regional folding granitoids

Calc-alkaline post-RFG suites

Granitic pegmatite dykes, and internal pegmatitic segregations, are common in many outcrops of post-RFG plutons, particularly those of the Bali suite and Woolgangie supersuite. Most post-RFG outcrops display little lithological diversity, beyond pegmatitic segregations and minor amounts of mafic schlieren. Exceptions are some tonalite and granodiorite plutons of the Liberty supersuite (e.g. Liberty Granodiorite and Depot Granodiorite), which contain some cognate xenoliths.

Calc-alkaline post-RFGs are coarse-grained (1–3 mm), and vary from equigranular to seriate to porphyritic. Phenocrysts are mainly tabular K-feldspar. Granitoids range in composition from tonalite to syenogranite, although the great majority are monzogranite. A small intrusion at Kambalda (the Red Hill Granitoid Complex) has been identified as a trondhjemite (Perring, 1988). Although pre-RFGs and post-RFGs have similar modal ranges, relatively mesocratic (>5% mafic minerals, approximately) rocks are volumetrically dominant in the former. Post-RFGs are dominantly leucocratic (<5% mafic minerals, approximately) with biotite the only mafic silicate. The main petrographic features of post-RFG suites are summarized below.

Woolgangie supersuite

Most post-RFG samples belong to the Woolgangie supersuite, which occurs extensively throughout most of the SWEGP. The granitoids are rather homogenous, medium-grained biotite syenogranite, monzogranite and

granodiorite, which were variably recrystallized during metamorphism. K-feldspar phenocrysts up to several centimetres long are common. The granitoids are leucocratic, rarely containing greater than 5% biotite. Hornblende has not been observed but (?primary) muscovite and, more rarely, garnet occur in some of the more fractionated members of the suite. Magnetite commonly coexists with ilmenite or ilmenite–hematite intergrowths, although minor magnetite occurs alone in the more fractionated members of the supersuite. Titanite is rare. Other accessory minerals are apatite, zircon and, more rarely, monazite. Cognate microgranitoid xenoliths and synplutonic dykes have not been observed, but some plutons contain biotite-rich schlieren and xenoliths of granitoid gneiss and tonalitic granofels.

The Woolgangie supersuite also includes some granitoid porphyries, which contain phenocrysts of quartz and plagioclase, as well as biotite(–hornblende) aggregates up to several millimetres across. These rocks (including samples 101360 and 101366), which probably come from volumetrically minor intrusions, crop out mainly between Kookynie and Menangina Homestead. Bali suite granitoids occur along the western margin of the Kalgoorlie Terrane, and largely correspond to the post-D_2 to syn-D_3 granitoid diapirs, described above. They are petrographically similar to Woolgangie supersuite granitoids but are distinguished on geochemical criteria.

Dairy supersuite

Dairy supersuite granitoids form small intrusions of massive, equigranular syenogranite and monzogranite that occur in linear trends of non-ductile deformation. They are virtually unmodified by metamorphic recrystallization and have multigrain elongate aggregates of quartz. However, in some cases there is microtextural evidence for extensive modification of feldspars by a pervasive hydrothermal fluid. Ferromagnesian minerals commonly comprise less than 5% of the granitoids. The ferromagnesian assemblage includes biotite, with or without hornblende, and muscovite coexists with biotite in some samples. Magnetite and ilmenite make up the typical opaque oxide mineral assemblage, but are rare in more evolved members of the supersuite. Other accessory minerals are zircon, apatite, and rare allanite: primary titanite has not been observed. Cognate microgranitoid xenoliths and synplutonic dykes are absent.

Liberty supersuite

Plutons within this supersuite are a volumetrically minor component of the post-RFG group. They include biotite monzogranite and granodiorite (Bullabulling Monzogranite), hornblende–biotite monzogranite and granodiorite (Liberty Granodiorite, Doyle Dam Granodiorite, Comet Vale Monzogranite), hornblende granodiorite (Depot Granodiorite), biotite tonalite (Bonnie Vale Tonalite, Kintore Tonalite), trondhjemite (Kambalda Trondhjemite) and quartz monzonite (Porphyry Quartz Monzonite; Allen, 1987). Most intrusions contain igneous textures, largely unmodified by metamorphic recrystallization. However, the Depot Granodiorite is characterized by a well-developed granoblastic texture. Ferromagnesian minerals achieve a maximum modal abundance of about 10% in the Liberty Granodiorite and Bonnie Vale Tonalite. Magnetite and titanite coexist with apatite, zircon and rare allanite in most plutons. The Bullabulling Monzogranite contains minor fluorite and monazite. Mafic microgranitoid xenoliths are relatively common (but less than 1% by volume) in the Liberty and Doyle Dam Granodiorites.

Alkaline post-RFG suites

Gilgarna supersuite

Late alkaline intrusions of the Gilgarna supersuite range in composition from syenite to monzodiorite. They are texturally variable, from medium grained, and equigranular to seriate, to coarse grained, and equigranular to porphyritic. Coarse-grained varieties commonly display a cumulate-like texture, comprising tightly packed, tabular K-feldspar euhedra. Fine-grained rocks, and interstitial domains in the cumulate-like rocks, typically display an allotriomorphic fabric with convolute, interpenetrating grain boundaries reflecting extensive (?deuteric) recrystallization. Coarse-grained rocks are unfoliated, but some finer grained varieties display mineralogical (?igneous) banding and a trachytic texture.

Mafic minerals, chiefly clinopyroxene, but in some cases with subordinate amphibole, form up to 10% of these rocks, and minor melanite garnet occurs in some samples. Magnetite, titanite and apatite are widespread whereas zircon (and possibly monazite) are less common.

Late-magmatic to metamorphic, mineralogical and textural modifications in granitoids

Many of the granitoids described in this report were emplaced before or during regional metamorphism (M_2). Although systematic changes in mineralogy and texture with metamorphic grade (cf. Wyborn and Page, 1983) have not been recognized, there are a variety of textural and mineralogical modifications in most granitoid samples that reflect this event. It is not always possible to distinguish the effects of deuteric alteration and metamorphism from those of late-magmatic reaction between crystals and melt. To some extent, late-magmatic reactions can be resolved by studying the ferromagnesian mineral inclusions in K-feldspar (and less commonly plagioclase and quartz) phenocrysts (Appendix 3). Naturally, earlier granitoids display more profound textural and mineralogical modification than those emplaced late in the tectono-thermal history of the study area. Table 7 summarizes late-magmatic and post-magmatic (?deuteric, ?metamorphic) modifications identified in the granitoids. A more complete description is given in Appendix 3.

Table 7. Late-magmatic and metamorphic modifications of granitoid minerals

Mineral	*Igneous form*	*Late magmatic to early post-magmatic modifications*	*Post-magmatic (?metamorphic) modifications*
Quartz	Subequant, anhedral	Strained extinction and suturing of grain boundaries?	Strained extinction, subgrain growth, quartz ribbons in highly deformed granitoids
K-feldspar	Anhedral, interstitial to porphyritic	Perthitic intergrowth textures	Coarsening of perthitic textures; ultimately segregation of microcline and albite into distinct grains. Recrystallization (grain size reduction; 120° triple points in high-strain zones)
Plagioclase	Subhedral, tabular, with normal to oscillatory	Fine-grained, secondary ?sericite; ?myrmekitic intergrowths	Alteration to fine- and coarse-grained muscovite, epidote and zoning carbonate. Narrow, irregular, intragranular veins of unzoned plagioclase that cross-cut compositional zoning. Fracturing, and bending of twin planes; recrystallization to anhedral, granoblastic grains in strongly deformed zones
Biotite	Anhedral to subhedral, tabular to platy	Alteration to green biotite, with expulsion of Ti to form titanite and/or ilmenite	Recrystallization to aggregates of smaller, irregularly shaped grains, oriented in foliated granitoids. Alteration to green biotite, epidote, chlorite, muscovite; expulsion of Ti, Fe, F to form titanite, rutile, ilmenite, hematite and/or fluorite
Amphibole	Subhedral, prismatic	Reaction with melt to form biotite	Recrystallization in highly deformed granitoids only. Irregular colour zoning, and patchy replacement of magmatic amphibole by actinolitic amphibole. Alteration of magmatic amphibole to biotite and epidote
Clinopyroxene	Relict grains in magmatic amphibole	Reaction with melt to form magmatic amphibole	Alteration of clinopyroxene to secondary amphibole
Magnetite	Subhedral to euhedral, subequant	–	Cleavage-, and grain-boundary-controlled alteration to hematite
Titanomagnetite	Anhedral to subhedral	'Oxidation' exsolution to form compound, sandwich and trellis intergrowths between magnetite and ilmenite	Continuation of late-magmatic processes
Ilmenite–hematite solid-solution	Anhedral to subhedral	Exsolution to ilmenite–hematite intergrowths	Exsolution to ilmenite–hematite intergrowths

Recrystallization of pre-RFGs

Although a gross igneous texture and fabric is widely preserved in pre-RFGs, the development of an anastomosing foliation was accompanied by metamorphic recrystallization. Recrystallization involves grain size reduction, and orientation of biotite and, less commonly, hornblende. Recrystallization of quartz and feldspars varies from minor subgrain growth at the margins of igneous grains, to the development of irregular, anastomosing zones (up to several millimetres wide) with a fine-grained, granoblastic texture. Recrystallization is accompanied by (mostly minor) development of secondary epidote, chlorite, muscovite, carbonate and (rarely) fluorite.

Recrystallization of post-RFGs

Igneous textures are dominant in post-RFGs, although some recrystallization, mainly at igneous grain boundaries, characterizes most intrusions. Recrystallization becomes more intense and pervasive in the more strongly deformed marginal zones of some intrusions (notably the post-D_2 to syn-D_3 diapirs of the Bali suite and the Depot

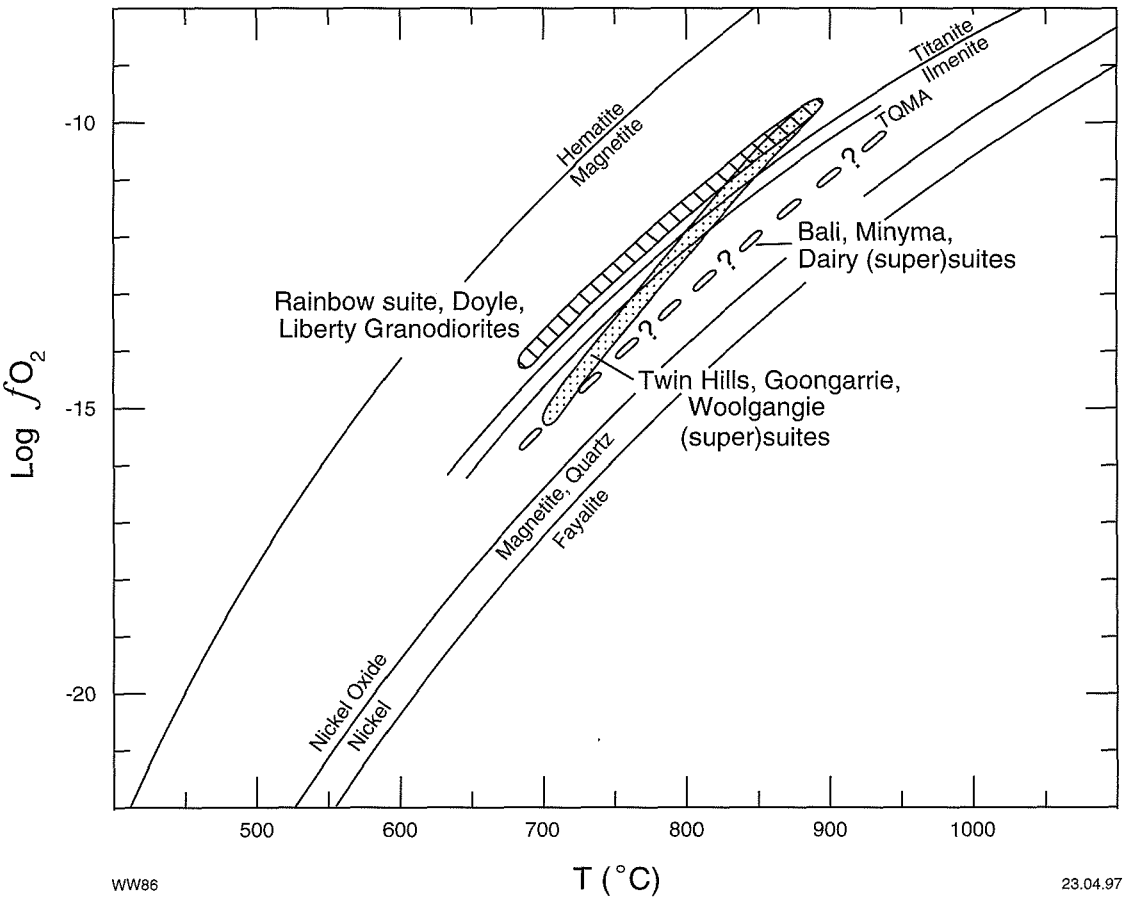

Figure 14. Temperature–oxygen fugacity diagram showing oxygen fugacity buffers and approximate conditions for granitoid (super)suites in the SWEGP. The oxygen-fugacity buffers shown are hematite–magnetite, titanite–ilmenite, titanite–magnetite–quartz–amphibole, nickel–nickel oxide, fayalite–magnetite–quartz, and are taken from Dilles (1987), except for titanite–magnetite–quartz–amphibole (TQMA), which is taken from Barnes (1987). The approximate temperature range for crystallization (700–900°C) is based on experimental studies by Piwinskii (1968). Note that the T–fO_2 range for the Liberty supersuite is based on data from the Liberty and Doyle Dam Granodiorites

Granodiorite). Recrystallization is accompanied by the development of secondary minerals, including muscovite, epidote, chlorite, carbonate and, in more fractionated members, fluorite.

Although gross igneous textures of the alkaline granitoids are preserved, microtextural features suggest substantial strain-free recrystallization, possibly due to interaction with an aqueous (?deuteric) fluid phase. Secondary minerals include amphibole, biotite, carbonate and, in some samples, fluorite.

Oxygen fugacity of granitoid magmas

Various oxide, and oxide–silicate mineral assemblages that buffer fO_2 in granitoid magmas have been described by Haggerty (1976), Wones (1981, 1989) and Noyes et al. (1983). Much of these data are summarized in Figure 14 which also shows estimated magmatic fO_2 conditions for granitoid suites in the SWEGP, based on primary mineral assemblages. The assemblage titanite–magnetite–quartz–amphibole defines the oxygen fugacity for the Rainbow suite and the Liberty and Doyle Dam Granodiorites. Amphibole is absent from the Goongarrie, Twin Hills and Woolgangie (super)suites, but less fractionated members of these (super)suites contain titanite and magnetite, whereas more fractionated members contain ilmenite and magnetite. These observations indicate a trend in these (super)suites toward relatively reducing conditions with fractionation. The absence of titanite in ilmenite–magnetite–quartz(–amphibole) assemblages of the Bali, Minyma and Dairy (super)suites indicates lower fO_2, compared to the Rainbow and Liberty (super)suites. The assemblage titanite–magnetite–clinopyroxene in alkaline granitoids of the Gilgarna supersuite suggests relatively oxidizing conditions, which cannot be more accurately constrained. These assemblages and fO_2 conditions are similar to those of other magnetite-series granitoids, and are distinctly more oxidized than ilmenite-series granitoids (Wones, 1981; Czamanske et al., 1981; Whalen and Chappell, 1988).

The widespread development of post-magmatic epidote, hematite, titanite and green biotite indicates a trend toward relatively high fO_2 during metamorphic recrystallization.

Xenoliths

Three main types of xenolith are recognized in granitoid rocks in the SWEGP: greenstone xenoliths, gneiss-textured xenoliths, and microgranitoid xenoliths.

Greenstone xenoliths

Xenoliths of greenstone country rocks are a feature of relatively few granitoids in the study area, and are confined to post-RFG plutons. They are most common in late-tectonic, leucocratic monzogranite and syenogranite plutons, such as the Galah Monzogranite, the Jungle Monzogranite and the Dairy Monzogranite, in the Kookynie area. Xenoliths of amphibolite also occur in marginal zones of post-RFG monzogranite plutons, south and southwest of Coolgardie, and at Siberia.

Gneiss-textured xenoliths

Monzogranite to granodiorite gneiss xenoliths are moderately common in some post-RFGs (e.g. Depot Granodiorite, Pioneer Monzogranite, and other monzogranitic plutons south and southwest of Coolgardie). They are associated with xenoliths of tonalitic granofels in some granitoids.

Relatively mafic, gneiss-textured xenoliths are uncommon but have been recognized in some pre-RFGs where they are associated with microgranitoid xenoliths and dykes (see below), and appear to encompass a similar range of compositions. A tonalitic to granodioritic gneiss xenolith (sample 93905) occurs within foliated granodiorite at Sunday Soak, in the Scotia Complex. Other fine- to medium-grained, mafic xenoliths, which contain a foliation oriented obliquely to the regional foliation in the host granitoid (e.g. near Goongarrie Homestead, Appendix 2), may also be gneissic, but these occurrences have not been confirmed by thin-section observations.

A large enclave in a quartz monzonite intrusion 18 km southeast of Menangina Homestead (south of Princess Bore) is a banded, quartz–alkali feldspar–clinopyroxene–hornblende granofels in which mafic minerals comprise about 50%. The enclave is modally equivalent to a mafic quartz syenite.

Microgranitoid xenoliths

Rounded microgranitoid xenoliths (Figures 2.1 and 2.2, Appendix 2) are most widely distributed in the more mafic pre-RFGs and post-RFGs (e.g. Rainbow suite granitoids, Liberty Granodiorite). They are also present in some late alkaline intrusions of the Gilgarna supersuite, but these have not been studied in detail.

Microgranitoid xenoliths are texturally and modally diverse. Igneous textures vary from seriate to porphyritic with quartz and/or plagioclase phenocrysts (typically <6 mm long), and more rarely K-feldspar (<2 cm long). These textures are commonly well preserved in xenoliths hosted by post-RFGs, such as the Liberty Granodiorite and Doyle Dam Granodiorite. Xenoliths in pre-RFGs display evidence of varying degrees of deformation and recrystallization, in some cases exceeding that for the host granitoid.

Microgranitoid xenoliths range in composition from granodiorite to tonalite through monzonite to diorite (see Figure 12 for analysed samples only). Mafic minerals form up to about 40% of the xenoliths, and are either hornblende or biotite, or both. Clinopyroxene is a minor constituent of some xenoliths in the Birthday Complex. As documented in other areas (Holden et al., 1991; Poli and Tommasini, 1991), the ferromagnesian mineral assemblage in the xenoliths is strongly influenced by the composition of the host granitoid: xenoliths commonly contain the same ferromagnesian mineral assemblage as the host granitoid. Some biotite granitoids contain hornblende–biotite xenoliths, but the reverse situation rarely occurs. Typical accessory minerals are opaque oxide minerals, titanite and apatite, and more rarely allanite. Apatite is very common to abundant in some microgranitoid xenoliths. Although more mafic than the host granitoid, microgranitoid xenoliths do not necessarily contain more opaque oxide minerals, and are, in some cases, essentially devoid of these phases. Secondary minerals include (?biotite), epidote and chlorite, and less commonly, carbonate, sericite and fluorite. Clots of mafic minerals, from a few millimetres to several centimetres across, within xenoliths and synplutonic dykes, are concentrations of hornblende, biotite, or both, with or without opaque oxides, apatite and titanite (Figure 3.1d,g,h, Appendix 3). The ferromagnesian assemblage in the clots is influenced by the composition of the xenolith, in a manner similar to that described above, between xenoliths and host granitoids.

Other xenoliths

A xenolith (sample 101019) at Cement Well in foliated granodiorite of the Birthday Complex displays two distinct textural domains. A monzonite gneiss domain occurs within an igneous-textured microgranitoid domain. The gneiss-textured domain is K-feldspar rich, quartz poor and contains about 10% clinopyroxene (modal abundance). Other modal differences between the two textural domains are summarized in Table 8.

In addition, a number of texturally diverse, biotite-rich xenoliths, of uncertain origin, have been identified in pre-regional folding monzogranite near Goongarrie Homestead, and in the Liberty Granodiorite. Some of these xenoliths contain anomalous concentrations of magnetite, apatite and calcite, and have been described in detail by Witt (1990). They have been referred to as possible surmicaceous enclaves in Witt and Swager (1989).

Table 8. Modal differences between gneiss-textured and microgranitoid-textured portions of sample 101019

	Gneiss-textured monzonite	*Microgranitoid-textured quartz monzodiorite*
Quartz	Rare to absent	~15%
K-feldspar	Common	Subordinate
Plagioclase	Common	Dominant
Biotite	Minor	Moderately common
Hornblende	Common	Common
Clinopyroxene	~10%	Absent
Apatite	Absent	Minor
Magnetite	Minor	Minor
Ilmenite	Minor	Absent

Dykes

Dykes in pre-RFG complexes (Figures 2.1 and 2.2, Appendix 2) range from biotite monzogranite to biotite(–hornblende) tonalite to hornblende(–clinopyroxene) monzodiorite. Accessory minerals and textures cover a similar range to those of the pre-RFGs, though the dykes are typically finer grained. Additionally, plagioclase is rarely a phenocryst phase in pre-RFGs, but some dykes are plagioclase-phyric. Dyke textures vary from unmodified igneous textures to strongly deformed and recrystallized. As with some microgranitoid xenoliths, strain in some dykes is more intense than in the host granitoids (e.g. Birthday complex, Appendix 2).

Proterozoic dolerite dykes intrude granite and greenstones of the Yilgarn Craton (Plate 1), but are poorly exposed within areas of granitoid. They are not discussed in this Report.

Chapter 5

Whole-rock chemistry of SWEGP granitoids

Whole-rock analyses of samples from the SWEGP are presented in Witt et al. (1996). The data are summarized in Table 9 and Appendix 4. Samples were collected by drilling and blasting to avoid the effects of weathering. With the exception of sample 90967099, sample sites did not display evidence of significant hydrothermal alteration. Petrographic observations indicate that most whole-rock geochemical samples have undergone very little hydrothermal alteration, other than regional metamorphism.

Possible effects of regional metamorphism on granitoid chemistry

Several studies have indicated that metamorphism of granitoid rocks, to amphibolite grade, is approximately isochemical (Ferry, 1979; Wyborn and Page, 1983; Studmeister, 1985; Feng and Kerrich, 1992). Mineralogical modifications attributed to metamorphism of granitoids in the SWEGP (described in Appendix 3, and summarized in Table 7) indicate that hydration reactions are common, but that the volume of secondary minerals is small (mostly <3%, approximately). The trends and groupings displayed by most of the data presented here are coherent and overall are consistent with magmatic processes, although individual samples display possible evidence of substantial mobility for some elements.

Petrographic evidence described above indicates that post-magmatic modification of the granitoids took place under relatively oxidizing conditions. One important chemical effect of metamorphism may have been to increase the $Fe_2O_3/(FeO+Fe_2O_3)$ ratio of the granitoids. Whole-rock $Fe^{+3}/(Fe^{+2}+Fe^{+3})$ data are plotted, in histogram form, in Figure 15. Although data for several (super)suites are sparse, most samples have $Fe^{+3}/(Fe^{+2}+Fe^{+3})$ between 0.3 and 0.6, with slightly higher values (up to 0.9) in some samples of the Gilgarna, Bali and Goongarrie (super)suites. These values overlap, but are on the whole even higher than, those of magnetite-rich I-type granitoids of the Lachlan Fold Belt (Whalen and Chappell, 1988), most of which have $Fe^{+3}/(Fe^{+2}+Fe^{+3})$ between 0.2 and 0.4. They are more comparable with, but still higher than, those of the much more mafic Uasilau–Yau Yau Intrusive Complex, New Britain (Whalen, 1985). Although primary mineral assemblages indicate that the granitoids are intrinsically 'oxidized' (fO_2 >FMQ buffer; terminology of Wones, 1981), the very high whole-rock values may reflect partial to complete equilibration with an oxidized fluid, consistent with the presence of post-magmatic epidote and green biotite (Table 7). Magmatic trends towards lower fO_2, at least for the Twin Hills, Goongarrie and Woolgangie (super)suites, are reversed as a result of interaction with post-magmatic fluids. This reversal suggests post-magmatic modification was due to metamorphic rather than deuteric fluids. For example, the very high $Fe^{+3}/(Fe^{+2}+Fe^{+3})$ values for some Bali suite granitoids may reflect their unique role as centres of fluid and heat flux during regional metamorphism (Witt, 1991). The high $Fe^{+3}/(Fe^{+2}+Fe^{+3})$ values for some samples of the Gilgarna supersuite must be intrinsic to the magma because they were emplaced after regional metamorphism.

Aluminium saturation index (ASI) and alkalinity

The great majority of analysed granitoids straddle the boundary between metaluminous and peraluminous compositions (Fig. 16). Only intrusions of the Gilgarna supersuite plot in, or close to, the peralkaline field. Xenoliths and some dykes define a trend away from the bulk of the granitoid population, in the metaluminous field. All granitoids have A/CNK ratios (the molecular ratio $Al_2O_3/(CaO+Na_2O+K_2O)$, equivalent to the aluminium saturation index, or ASI; Zen, 1986) less than 1.1. This value separates most I-type from most S-type granitoids in the Lachlan Fold Belt (Chappell and White, 1992).

Most granitoids plot on a calc-alkaline trend on an AFM diagram (Fig. 17). Some Gilgarna supersuite intrusions, some dykes and most enclaves, plot in the alkalic field of Coleman and Donato (1979). The total granitoid population also defines a modified calc-alkaline trend in Figure 18. The trend is offset towards the Na apex compared with typical calc-alkaline granitoids. Dykes and xenoliths define a weak trend from the main granitoid population towards the Ca apex.

Debon and Le Fort (1982) published several diagrams, based on major element contents, for distinguishing granitoid populations within the broad calc-alkaline field, with possible implications for tectonic setting and petrogenesis. SWEGP granitoids are not uniquely assigned to either the CAFEMIC (cafemic) group or the ALCAFEMIC (aluminocafemic) group by the A(Al-(K-Na+2Ca)) versus B(Fe+Mg+Ti) diagram (not reproduced), although they clearly do not belong to the ALUM (aluminous) group. However, the triangular

Table 9. Selected granitoid analyses, southwest Eastern Goldfields Province, Western Australia

	Granitoid gneiss			*Pre-regional folding granitoids*								
Supersuite				*Morapoi*								
Suite				*Rainbow*	*Rainbow*	*Twin Hills*	*Twin Hills*	*Twin Hills*	*Goon-garrie*	*Goon-garrie*	*Minyma*	*Minyma*
Sample no.	*101370*	*82167*	*82061*	*93901*	*101375*	*100931*	*101361*	*100928*	*93903*	*98250*	*101358*	*100944*
						Percentage						
SiO_2	68.80	73.05	73.71	68.50	71.00	71.30	73.40	75.10	71.00	76.00	77.10	77.30
TiO_2	.41	.11	.18	.40	.20	.26	.28	.12	.32	<.05	.10	.05
Al_2O_3	16.10	14.44	14.44	15.00	15.10	14.60	13.20	12.90	15.60	13.00	12.10	12.00
Fe_2O_3	1.19	.40	.71	1.24	.62	.71	1.49	.35	.76	.47	.59	.31
FeO	1.59	.45	.55	1.60	.79	1.38	.88	.71	1.00	<.10	.49	.42
MnO	.05	.17	.03	.06	<.05	.04	.05	.03	<.05	.06	<.05	.03
MgO	1.05	.17	.48	1.93	.74	.62	.42	.25	.56	.12	<.05	.09
CaO	3.70	1.41	1.55	3.14	2.38	2.59	1.96	1.32	1.99	.51	.43	.50
Na_2O	5.13	4.90	4.65	4.85	5.21	4.40	4.01	3.28	5.03	4.43	4.37	3.57
K_2O	1.27	3.46	3.40	2.73	2.99	2.30	3.14	4.54	3.31	4.17	4.38	4.52
P_2O_5	.11	.04	.07	.17	.07	.09	.06	.05	.10	<.05	<.05	.01
H_2O^+	–	–	–	–	–	–	–	–	–	–	–	–
H_2O^-	–	–	–	–	–	–	–	–	–	–	–	–
CO_2	.14	–	–	–	.29	.20	.23	.41	–	.48	.10	.15
LOI	.74	.27	.62	1.20	.89	.45	.95	.76	.78	.90	.51	.42
Rest	.19	.20	.32	.34	.27	.18	.20	.18	.33	.11	.25	.08
Subtotal	100.47	99.07	100.71	100.16	100.55	99.12	100.27	100.00	100.78	100.25	100.42	99.45
O=F,S	.00	.00	.03	.00	.00	.02	.02	.00	.00	.00	.00	.00
Total	**100.47**	**99.07**	**100.68**	**100.16**	**100.55**	**99.10**	**100.25**	**100.00**	**100.78**	**100.25**	**100.42**	**99.45**
						Parts per million						
Ba	346	1 079	1 235	1 010	851	485	601	788	1 330	25	600	196
Ce	26	25	20	80	32	–	65	–	71	–	79	–
Cr	16	7	3	–	13	5	10	14	–	<10	10	3
Cs	3	–	–	5	2	4	2	6	2	–	3	4
Cu	9	–	311	11	<4	4	<4	1	8	<2	<4	<1
F	384	–	–	653	500	310	316	162	340	477	1 033	150
Ga	20	3	20	19	17	18	15	13	18	21	14	13
La	15	8	12	44	16	–	33	–	45	–	37	–
Li	50	16	16	40	39	39	46	36	32	4	19	23
Nb	<7	–	4	<7	<7	6	<7	8	<7	13	11	7
Nd	–	–	–	41	–	–	–	–	27.5	–	–	–
Ni	11	6	3	–	19	5	16	3	–	<4	29	2
Pb	11	57	37	24	22	18	13	33	28	18	21	20
Pr	–	–	–	9.5	–	–	–	–	9.2	–	–	–
Rb	62	95	100	94	78	75	93	133	87	247	160	177
S	<100	94	528	<100	<100	100	100	<100	<100	<100	<100	<100
Sc	5	6	3	–	2	3	5	2	–	2	4	2
Sn	–	24	–	–	–	–	–	–	–	–	–	–
Sr	310	246	310	657	596	269	114	125	608	22	18	14
Th	4	–	9	13	7	11	13	22	11	29	16	16
U	<2	8	3	5	<2	5	2	5	2	8	5	2
V	42	7	12	49	22	20	14	7	21	<2	<3	1
Y	9	3	16	11	7	12	21	13	7	14	49	14
Zn	64	28	46	59	35	34	41	21	50	<10	32	13
Zr	181	57	137	160	102	135	159	136	184	88	154	53

NOTES:

101370 Biotite tonalite gneiss, south of Breakaway Well
82167 Gneiss, 18 Mile Well
82061 Biotite monzogranite gneiss, Quairnie Rock
93901 Hornblende–biotite granodiorite, Split Rocks (Scotia complex)
101375 Biotite–hornblende granodiorite, Boundary Well (Birthday complex)
100931 Biotite monzogranite, Twin Hills (Raeside complex)
101361 Hornblende–biotite monzogranite, Naismith Bore (Mulliberry complex)
100928 Biotite syenogranite, Twin Hills (Raeside complex)
93903 Biotite monzogranite, Split Rocks (Scotia complex)
98250 Biotite monzogranite, NE of Ora Banda (Owen complex)
101358 Hornblende–biotite syenogranite, Black Gin Rocks (Mulliberry complex)
100944 Biotite monzogranite, E of Alexandria Bore (Mulliberry complex)

(*continued*)

Table 9. (*continued*)

	Post-regional folding granitoids											
Supersuite	*Woolgangie*						*Dairy*		*Liberty*			
Suite					*Bali*	*Bali*						
Sample no.	*105904*	*101348*	*100934*	*101349*	*98267*	*98261*	*101367*	*98254*	*97096*	*K3*	*98278*	*98263*
						Percentage						
SiO_2	70.70	72.10	74.10	75.00	72.90	75.70	75.90	75.90	66.40	66.94	69.10	70.50
TiO_2	.39	.22	.10	.11	.20	<.05	.17	.07	.48	.44	.19	.29
Al_2O_3	14.80	14.60	13.30	13.60	15.00	14.20	12.40	13.20	15.50	15.76	15.60	15.60
Fe_2O_3	1.10	.80	.43	.58	.92	.37	.86	.46	1.73	2.93	1.09	1.04
FeO	1.49	.58	.71	.31	.46	<.10	.67	.29	1.67	–	.71	1.22
MnO	<.05	<.05	.05	<.05	.05	.07	<.05	.05	.07	.03	.07	.06
MgO	.70	.46	.18	.11	.45	.13	.13	.22	1.62	.88	.66	1.02
CaO	2.15	1.65	.87	.80	1.52	.35	.88	.72	3.30	2.65	1.77	3.06
Na_2O	4.35	4.99	3.38	4.18	5.04	4.56	3.84	3.81	4.85	4.18	5.53	5.08
K_2O	3.38	3.72	5.01	4.70	3.08	3.90	4.04	4.41	2.85	3.40	3.87	1.61
P_2O_5	.12	.06	.04	<.05	.06	<.05	<.05	<.05	.28	.19	.09	.09
H_2O^+	–	–	–	–	–	–	–	–	–	–	–	–
H_2O^-	–	–	–	–	–	–	–	–	–	–	–	–
CO_2	.07	.23	.19	.03	.14	.24	.13	.19	.44	–	.45	.31
LOI	.82	.98	.62	.69	.52	.82	.74	.73	1.45	–	.93	1.01
Rest	.33	.35	.23	.16	.32	.13	.20	.15	.42	.41	.57	.20
Subtotal	100.40	100.74	99.21	100.27	100.66	100.47	99.96	100.20	101.06	97.81	100.63	101.09
O=F,S	.00	.06	.03	.01	.00	.00	.00	.00	.05	.00	.00	.00
Total	**100.40**	**100.68**	**99.18**	**100.26**	**100.66**	**100.47**	**99.96**	**100.20**	**101.01**	**97.81**	**100.63**	**101.09**
						Parts per million						
Ba	1 410	946	436	384	1 187	<20	613	745	1 227	1 533	3 025	462
Ce	145	41	–	52	60.5	–	96	–	134	–	–	–
Cr	7	8	2	<4	<10	<10	5	<10	18	24	12	20
Cs	2	15	12	4	–	–	3	–	2	–	–	–
Cu	11	4	1	<4	4	2	<4	2	17	–	2	11
F	270	620	680	193	504	500	440	149	1 010	–	363	306
Ga	18	19	19	18	19	32	13	14	18	–	19	20
La	88	22	–	28	47.2	–	50	–	–	52	–	–
Li	13	65	74	28	26	64	26	8	12	–	25	24
Nb	<7	10	18	<7	<10	10	8	<10	<7	7	<10	<10
Nd	–	–	–	–	28.1	–	–	–	–	–	–	–
Ni	5	14	2	14	4	<4	8	7	15	13	8	11
Pb	33	32	49	51	23	21	17	21	28	20	52	<10
Pr	–	–	–	–	–	–	–	–	–	–	–	–
Rb	103	183	306	256	79	376	159	98	74	99	106	41
S	<100	600	100	100	<100	<100	<100	<100	200	–	<100	<100
Sc	3	2	3	2	2	3	3	<2	5	–	2	4
Sn	<4	–	–	–	–	–	–	–	–	–	–	–
Sr	409	361	64	77	614	13	55	165	805	1 303	1 131	566
Th	21	11	44	31	15	13	15	11	13	11	16	<10
U	<2	5	8	6	<5	<5	5	<5	3	–	<5	<5
V	31	19	6	<3	11	<2	6	4	54	44	22	30
Y	10	15	29	38	10	36	38	10	12	12	16	6
Zn	66	43	39	29	45	49	34	17	68	79	42	47
Zr	230	131	124	82	140	40	149	67	172	181	169	122

NOTES:

105904 Biotite monzogranite, N of 26 Mile Rock
101348 Biotite monzogranite, Brady Well (Menangina Monzogranite)
100934 Muscovite–biotite monzogranite, Galah Rockhole (Galah Monzogranite)
101349 Muscovite–biotite monzogranite, Donkey Rocks (Donkey Rocks Monzogranite)
98267 Biotite monzogranite, Snot Rocks (Bali Monzogranite)
98261 Garnet–muscovite microgranite, Kunanalling (Bali Monzogranite)
101367 Biotite monzogranite, W of Dairy Well (Dairy Monzogranite)
98254 Biotite monzogranite, N of Bora Rock
97096 Biotite–hornblende granodiorite, Great Lady, Mt Pleasant (Liberty Granodiorite)
K3 Quartz monzonite, Porphyry gold mine (Porphyry Quartz Monzonite)
98278 Hornblende granodiorite, Horse Rocks (Depot Granodiorite)
98263 Biotite–hornblende granodiorite, N of Doyle Dam (Doyle Dam Granodiorite)

(*continued*)

Table 9. (*continued*)

	Post-regional folding granitoids						*Xenoliths*			*Dykes*	
Supersuite	*Liberty*			*Gilgarna*							
Suite											
Sample no.	*K4*	*105909*	*98259*	*101386*	*59022E*	*59024D*	*101357*	*101356*	*89928*	*101383*	*101354*
						Percentage					
SiO_2	71.41	71.50	71.70	54.00	61.70	67.40	50.40	58.60	62.20	60.10	74.50
TiO_2	.22	.40	.22	.40	.60	.20	1.16	.69	.62	.64	.08
Al_2O_3	15.43	14.40	14.90	10.80	17.00	16.50	11.40	15.90	15.20	14.80	13.60
Fe_2O_3	1.51	.99	.57	3.78	3.40	1.40	4.48	2.47	1.89	2.26	.46
FeO	–	1.35	1.15	2.71	1.08	.29	7.02	2.83	2.69	3.23	.28
MnO	.02	<.05	.05	.26	.29	.13	.42	.17	.11	.13	<.05
MgO	.79	.47	.79	2.51	.84	.55	8.98	3.56	3.07	3.07	.13
CaO	1.79	1.55	2.18	11.50	2.09	.70	8.65	4.23	4.50	5.01	.99
Na_2O	5.42	3.84	4.95	4.89	5.58	6.95	2.71	3.35	5.09	4.49	4.21
K_2O	2.18	5.00	1.95	4.31	5.93	4.30	1.56	6.29	2.12	4.35	4.58
P_2O_5	.04	.10	.06	1.23	.06	.03	.21	.32	.56	.50	<.05
H_2O^+	–	–	–	–	.32	.32	–	–	–	–	–
H_2O^-	–	–	–	–	.24	.13	–	–	–	–	–
CO_2	–	.07	.31	2.68	.12	–	.08	.16	–	.12	.27
LOI	–	.62	1.34	3.28	–	–	2.01	1.06	2.41	.74	.64
Rest	.28	.57	.25	.65	.76	.29	.63	.47	.50	.53	.16
Subtotal	99.09	100.86	100.42	103.00	100.01	99.19	99.71	100.10	100.96	99.97	99.90
O=F,S	.00	.00	.05	.07	.04	.01	.14	.06	.07	.00	.01
Total	**99.09**	**100.86**	**100.38**	**102.93**	**99.97**	**99.18**	**99.57**	**100.04**	**100.89**	**99.97**	**99.89**
						Parts per million					
Ba	1 177	1 724	598	1 419	3 400	1 300	110	1 315	1 016	1 343	624
Ce	41	246	23.1	263	230	42	79	108	181	160	17
Cr	13	<4	15	<4	–	–	561	40	–	32	16
Cs	–	2	–	2	–	–	7	7	5	4	7
Cu	–	5	16	7	–	–	58	12	13	42	9
F	–	1 940	147	1 400	960	300	3 155	1 375	1 350	1 100	75
Ga	–	18	19	11	20	18	24	17	191	17	19
La	11	149	16.2	110	140	18.2	34	59	107	79	7
Li	–	34	14	71	9	18	75	49	18	41	10
Nb	2	14	<10	24	6	2	14	13	<7	12	29
Nd	–	–	9.7	–	–	16.2	–	–	71.2	–	–
Ni	8	10	9	6	–	–	176	29	–	23	3
Pb	27	58	13	16	–	–	8	30	24	33	39
Pr	–	–	–	–	–	6.6	–	–	19.6	–	–
Rb	67	239	64	94	200	100	87	168	86	145	187
S	–	<100	800	200	–	–	100	100	200	<100	100
Sc	–	3	2	6	–	–	41	21	–	12	2
Sn	–	<4	–	–	–	–	–	–	–	–	–
Sr	847	185	344	1 541	1 200	600	217	424	875	1 046	131
Th	8	57	<10	13	15	5	4	8	14	18	5
U	–	9	<5	2	–	–	5	7	3	3	2
V	21	22	22	71	–	–	180	74	85	107	3
Y	3	20	7	51	60	6	27	25	13	38	35
Zn	47	41	41	114	–	–	359	135	96	87	19
Zr	123	376	105	259	440	120	149	180	214	276	77

NOTES:

K4	Trondhjemite, Kambalda (Kambalda Trondhjemite)
105909	Biotite monzogranite, Bullabulling (Bullabulling Monzogranite)
98259	Biotite tonalite, Bonnie Vale (Bonnie Vale Tonalite)
101386	Pyroxene melasyenite, E of Cement Well (Houses of the Holy Syenite)
59022E	Pyroxene syenite, southwest of Hamdorf Bore
59024D	Pyroxene syenite, McAuliffe Well (McAuliffe Well Syenite)
101357	Hornblende diorite, Rainbow Bore (Birthday complex)
101356	Biotite–hornblende monzonite, Rainbow Bore (Birthday complex)
89928	Hornblende–biotite tonalite, Mt Pleasant (Liberty Granodiorite)
101383	Hornblende(–clinopyroxene) monzonite, E of Cement Well (Birthday complex)
101354	Biotite monzogranite, Rainbow Bore (Birthday complex)

Rest is the sum of all trace elements after they are converted to oxides. The total is the sum of all components with the exception of F and S. The oxygen equivalent value (O=F,S) is subtracted from the subtotal. Some totals appear to be incorrect by 0.01% due to a rounding-off effect. Analytical methods and standards are given in Witt et al. (1996)

Figure 15. (opposite) Whole-rock $0.9Fe_2O_3/(0.9Fe_2O_3+FeO)$ histograms, by suites and supersuites: (a) gneiss and pre-RFGS; (b) post-RFGS; (c) enclaves

B(Fe+Mg+Ti)–Q(Si/3-(K+Na+2Ca/3))–F(555-(Q+B)) diagram (Fig. 19) suggests the bulk of the granitoids define a composite subalkalic trend, rather than a strictly calc-alkaline trend. The host granitoids comprise a light-coloured subalkaline association whereas the xenoliths and some synplutonic dykes fit a dark subalkaline association. Gilgarna supersuite samples tend to plot on the alkaline-saturated trend but most have silica-undersaturated compositions and plot just outside the triangle.

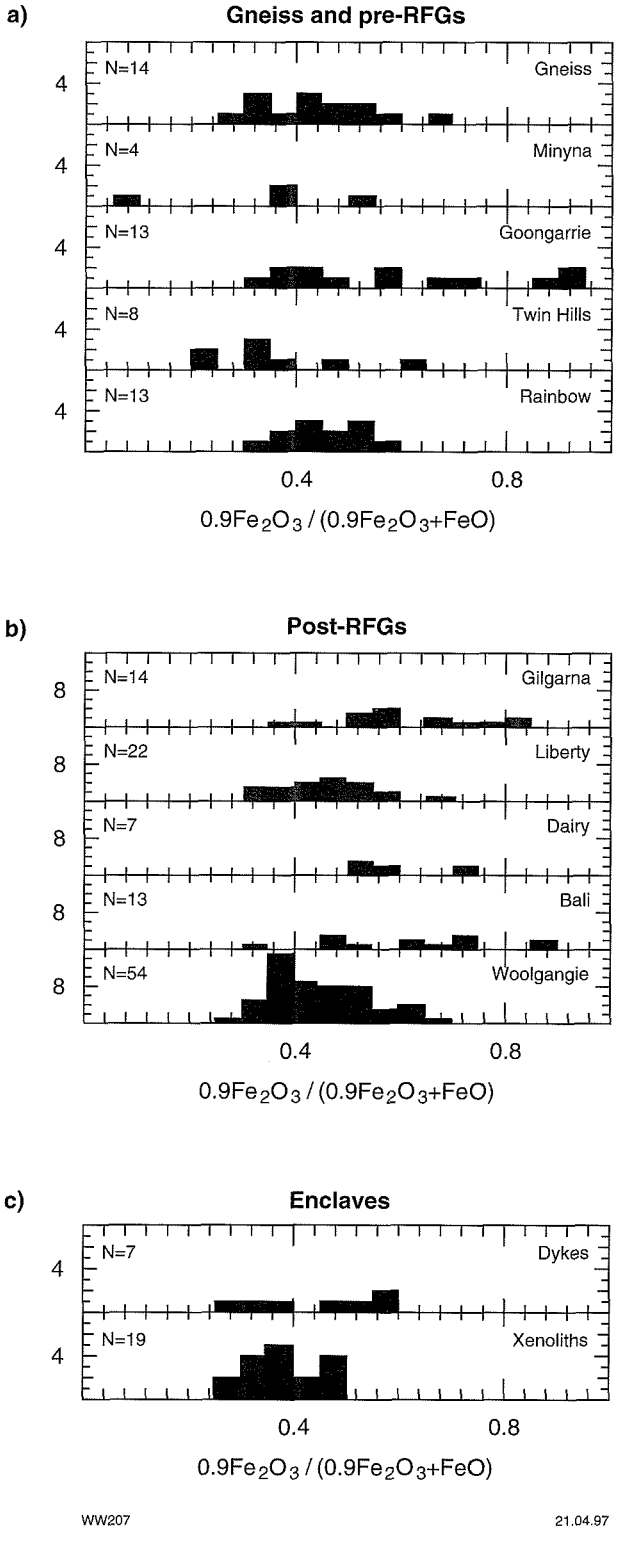

SiO_2 content

Percent SiO_2 for the total SWEGP sample population varies from 50 to 77%, although only xenoliths, some dykes, and alkaline granitoids contain less than 65% SiO_2 (Fig. 20). The majority of granitoids contain greater than 70% SiO_2. There is a weakly bimodal distribution of SiO_2 values among the pre-RFGs (Fig. 20). The gap in percent SiO_2 occurs at 73–74% . It is not known whether the SiO_2 gap among pre-RFGs is an intrinsic feature or can be attributed to limited sampling.

Identifying granitoid suites in the SWEGP

Most analysed samples can be assigned to one of several suites and supersuites, based on geological and geochemical characteristics (Appendix 4). There are four pre-RFG suites and four post-RFG supersuites. All suites and supersuites are calc-alkaline, except the Gilgarna supersuite, which has alkaline characteristics. The main features of these (super)suites are summarized in Table 4. Further work, including isotopic studies and more widespread sampling in adjacent areas, may lead to further refinement of the proposed suites. However, at the present level of investigation it is considered that the eight (super)suites proposed represent the most logical subdivision of granitoids in the SWEGP.

Although they generate linear to curvilinear geochemical trends, SWEGP granitoid (super)suites display more scatter than most suites from the Lachlan Fold Belt, New South Wales, where suites were first defined. However, the degree of scatter is comparable to that shown by the Boggy Plains supersuite (Wyborn et al., 1987). The main outliers for each suite are given in Appendix 4. This scatter can be attributed to one, or more, of the following:

1. Limited movement of some elements during regional metamorphism and deformation. Although coherent trends and groupings can be recognized on plots involving elements that are susceptible to mobility during metamorphism (e.g. Na, K, Rb, Sr, Ba), the data for these elements are more scattered than on plots involving the 'immobile' elements (e.g. Ti, Al, Zr; compare Fig. 21a with Fig. 21b).

2. Imperfect separation of cumulus crystals from the intercumulus melt during fractional crystallization. Perfect fractional crystallization generates tight, coherent trends on geochemical plots. However, imperfect separation of cumulus crystals from intercumulus melt produces samples containing variable proportions of each, with consequent scatter in geochemical plots (McCarthy and Hasty, 1976;Wyborn et al., 1987).

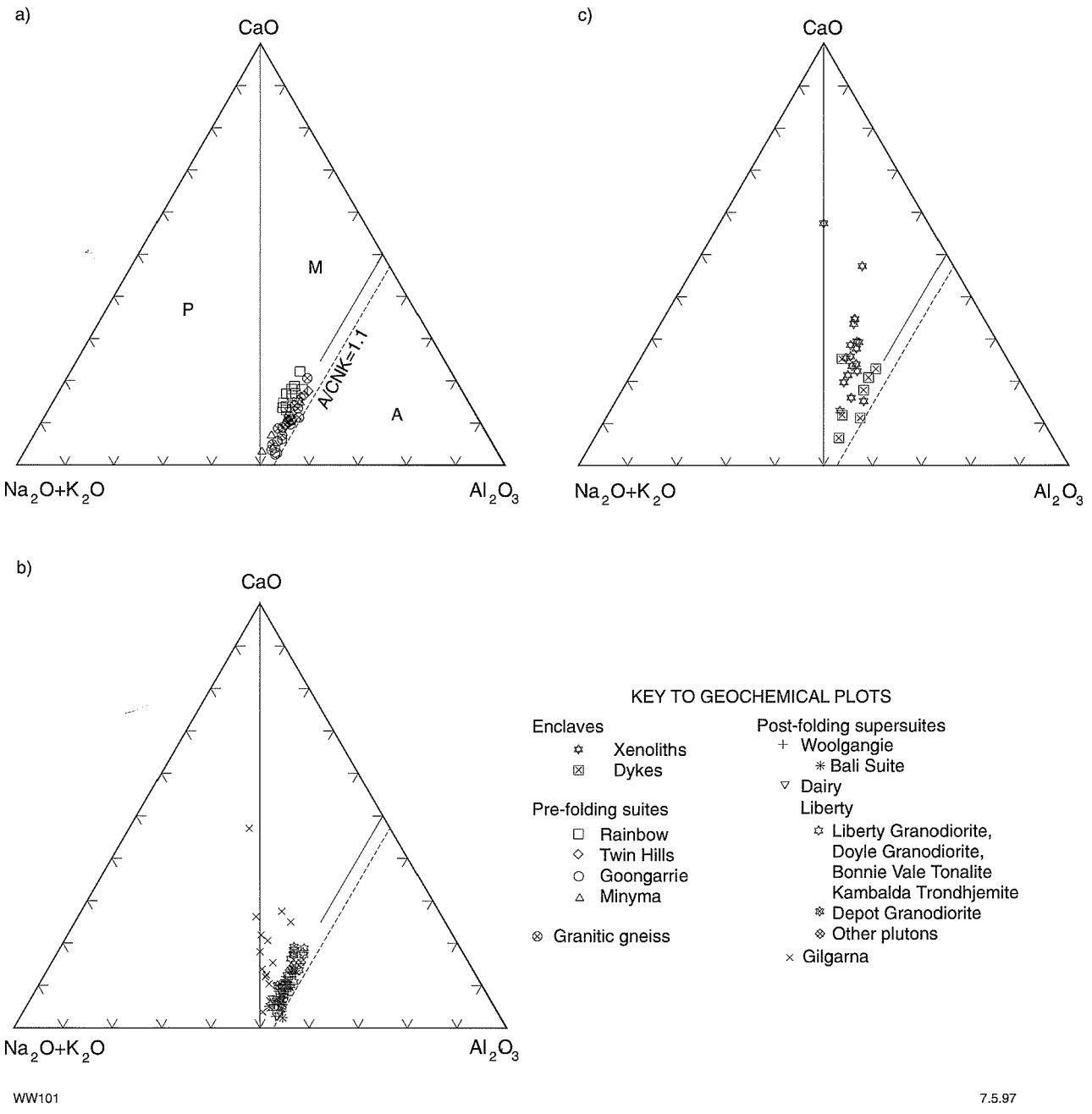

Figure 16. Molar $K_2O+Na_2O–CaO–Al_2O_3$ triangular diagrams showing whole-rock compositions for: (a) gneiss and pre-RFGs, (b) post-RFGs and (c) dykes and xenoliths. The line A/CNK=1.1 separates most I-type granitoids (A/CNK <1.1) from most S-type granitoids (A/CNK >1.1) in the Lachlan Fold Belt (Chappell and White, 1992). A/CNK is molar ratio of Al_2O_3/ $CaO+Na_2O+K_2O$

3. Heterogeneous source rocks. Miller et al. (1988) suggested that source-rock heterogeneity may be preserved in a granitoid, to some extent, after it has been extracted from the source and emplaced at higher levels of the crust. Geochemical plots reflect this heterogeneity as relatively broad groupings and trends, compared with those generated by granitoids derived from a homogenous source.

4. Contamination. Further scatter in geochemical plots may be induced by partial magmatic assimilation of accidental xenoliths or microgranitoid enclave magmas. These processes are assessed below.

Granitoid gneiss

Granitoid gneiss samples range from 65.8 to 73.9% SiO_2. They display considerable scatter on Harker variation diagrams, and none of the samples plot consistently within any of the granitoid suites (Fig. 22). Field evidence

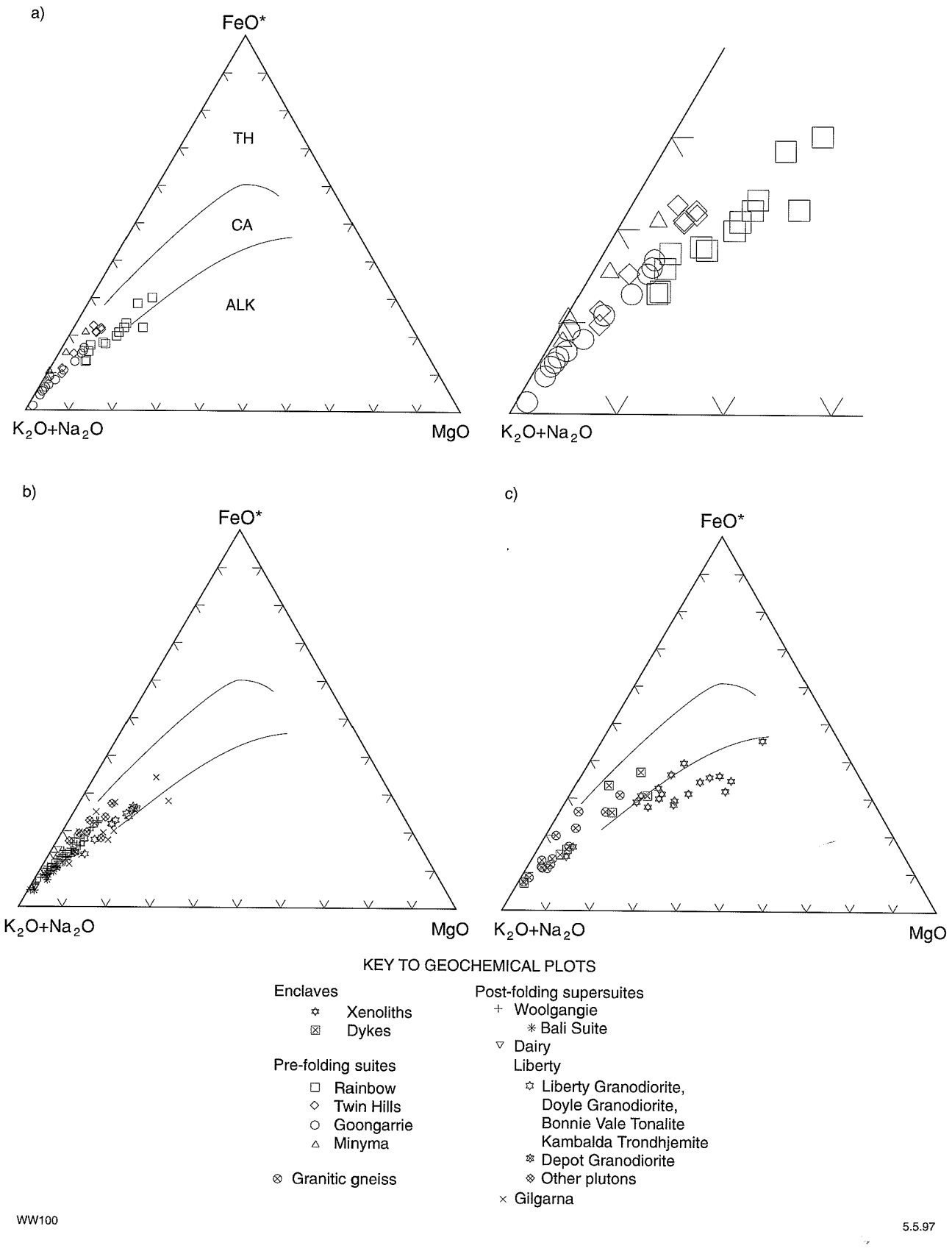

Figure 17. Weight percent Na_2O+K_2O–FeO–MgO (AFM) triangular diagrams showing whole-rock compositions for: (a) pre-RFGs, (b) post-RFGs, and (c) gneiss, dykes and xenoliths. FeO*=FeO+0.9Fe_2O_3. Tholeiitic (TH), calc-alkaline (CA), and alkalic fields (ALK) are from Coleman and Donato (1979). Upper right diagram shows detail of Figure 17a

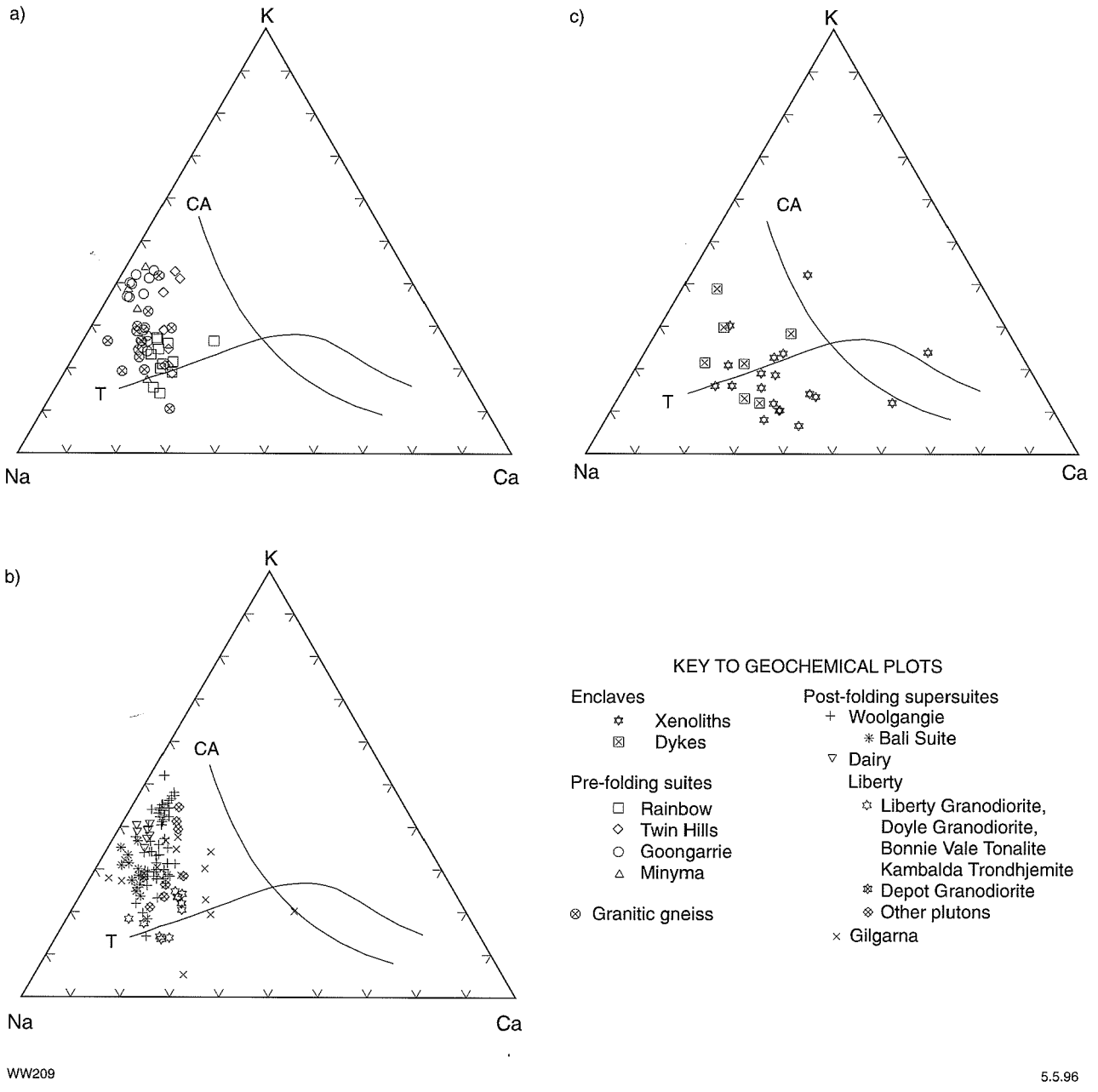

Figure 18. Na–K–Ca triangular diagrams (after Barker and Arth, 1976), showing whole-rock compositions compared to calc-alkalic (CA) and trondhjemitic (T) trends for: (a) gneiss and pre-RFGs, (b) post-RFGs, and (c) dykes and xenoliths

indicates that partial melting in situ of some gneiss has occurred, and analysed samples possibly contain variable proportions of leucosome and palaeosome. This could contribute to the observed scatter, and obscure possible geochemical affinities with other granitoid groups. Incompatible-element ratios in the newly formed melt should reflect those in the source rock (Hart and Allegre, 1980), and thus be immune to potential sampling problems.

Plots of Rb/Ce versus Th/Y, and Rb/Y versus Th/Y display substantial overlap between the granitoid gneiss and pre-RFG fields (Fig. 23), although some gneiss samples are slightly enriched in Rb compared to pre-RFGs. More carefully controlled sampling of granitoid gneiss, in conjunction with detailed mineral chemical studies of leucosome and palaeosome (cf. Tait and Harley, 1988; Sawyer, 1991), is required to determine if granitoid gneiss samples represent highly deformed and metamorphosed pre-RFGs.

Pre-RFG suites

Four pre-RFG suites are recognized. Selected Harker variation diagrams are shown in Figure 24. The suites

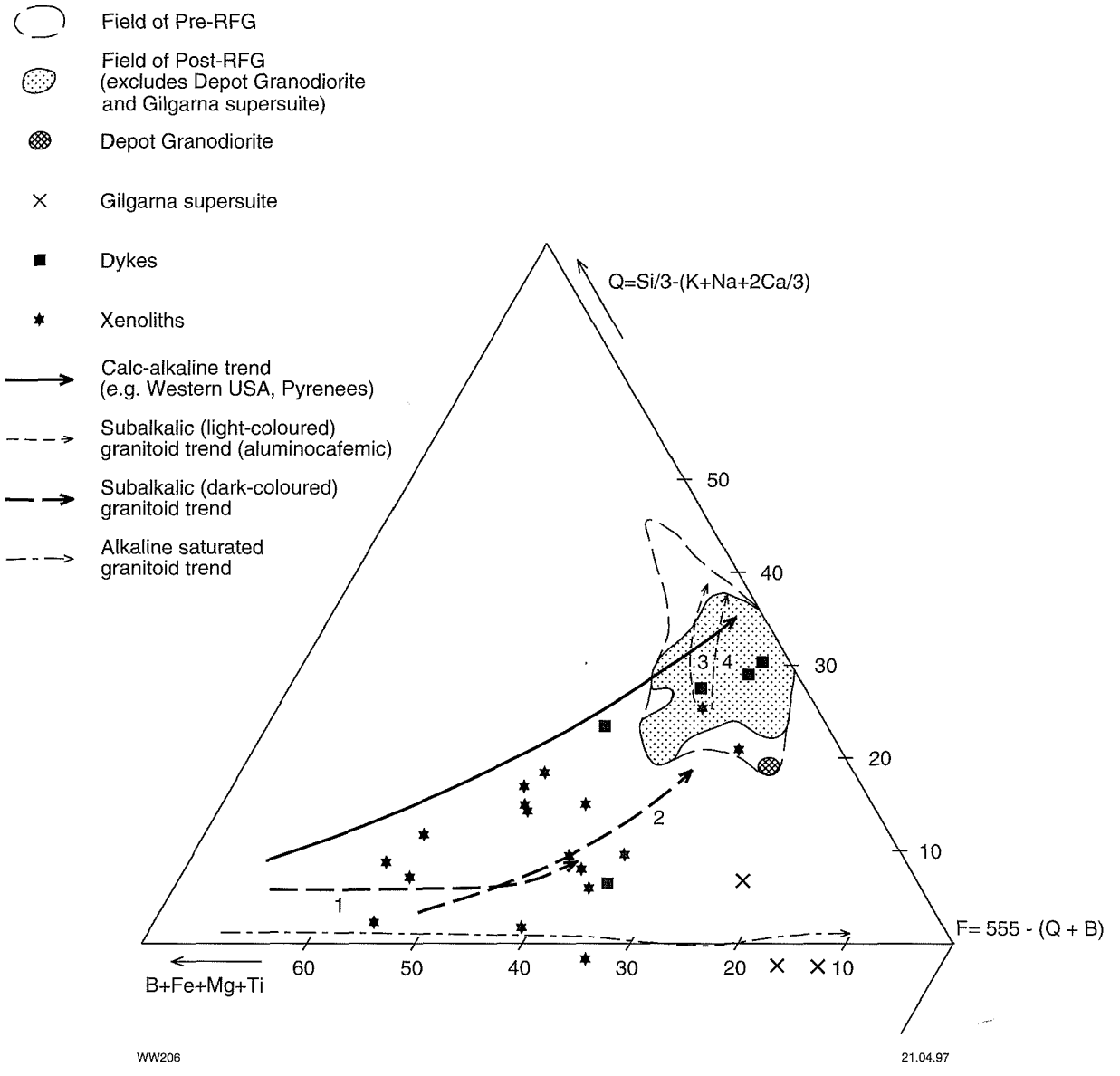

Figure 19. B–Q–F triangular diagram (after Debon and Le Fort, 1982), showing whole-rock compositions for pre-RFGs, post-RFGs, dykes and xenoliths. Calc-alkaline trend is composed of data from several plutons in the French and Spanish Pyrenees. Subalkalic granitoid trends 1 and 2 are the 'gabbroic' group of the Ploumanac'h complex, Brittany, and the external zone of the Ballons pluton, Vosges, France, respectively. Subalkalic trends 3 and 4 are the 'coarse-grained granitic' group of the Ploumanac'h complex and the Obe NW pluton, Feroz Koh, Afghanistan, respectively. Alkalic trend is the Nuku-Hiva volcanic series, Fiji

possess distinctive FeO*/(FeO* + MgO) ratios (Fig. 17a), as follows: Minyma > Twin Hills > Goongarrie > Rainbow.

Rainbow suite: SiO_2 contents in the Rainbow suite vary from 66.1 to 71.3%. The aluminium saturation index (ASI) and Na_2O+K_2O increase, whereas TiO_2, FeO*, CaO, MgO, P_2O_5, V and Zn decrease, with increasing SiO_2. Incompatible elements (Ba, Rb, Th, Zr, Y) display relatively little variation with increasing SiO_2 content.

Chondrite-normalized rare-earth element (REE) patterns are steeply fractionated, with a slight shoulder between Ce and Nd, and no Eu anomaly (Fig. 25a).

Twin Hills suite: The SiO_2 content of analysed Twin Hills suite samples varies from 71.3 to 75.1%. Barium, K_2O, Rb, Th and Nb increase, and TiO_2, Al_2O_3, FeO*, CaO, Na_2O, P_2O_5, Sr, Li and V decrease, with increasing SiO_2. The Twin Hills suite displays a wide scatter on many plots. The most coherent trends are shown by plots of Al_2O_3, P_2O_5, Zr and Sr versus SiO_2 (Fig. 24). There is commonly a large degree of overlap between the Twin Hills suite and the Goongarrie suite, but the Twin Hills suite contains higher CaO, Nb and Li, and lower Al_2O_3 and Sr. There are no REE data for Twin Hills suite granitoids.

Goongarrie suite: SiO_2 contents of the analysed samples from the Goongarrie suite fall between 71.0 and 76.5%.

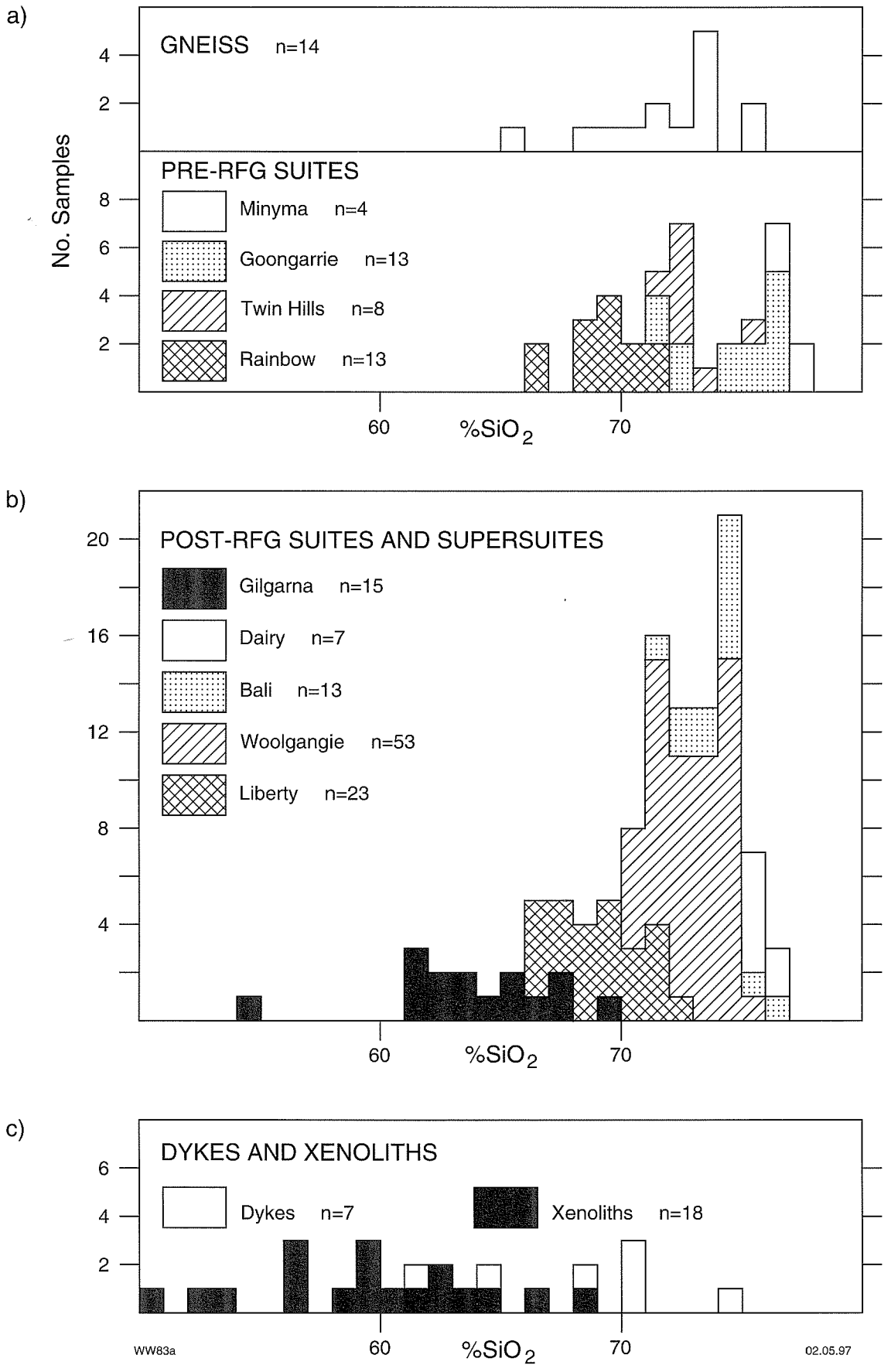

Figure 20. Histograms showing SiO_2 content (weight %) of granitoids (by suites and supersuites) in the SWEGP: (a) gneiss and pre-RFGs, (b) post-RFGs and (c) dykes and xenoliths

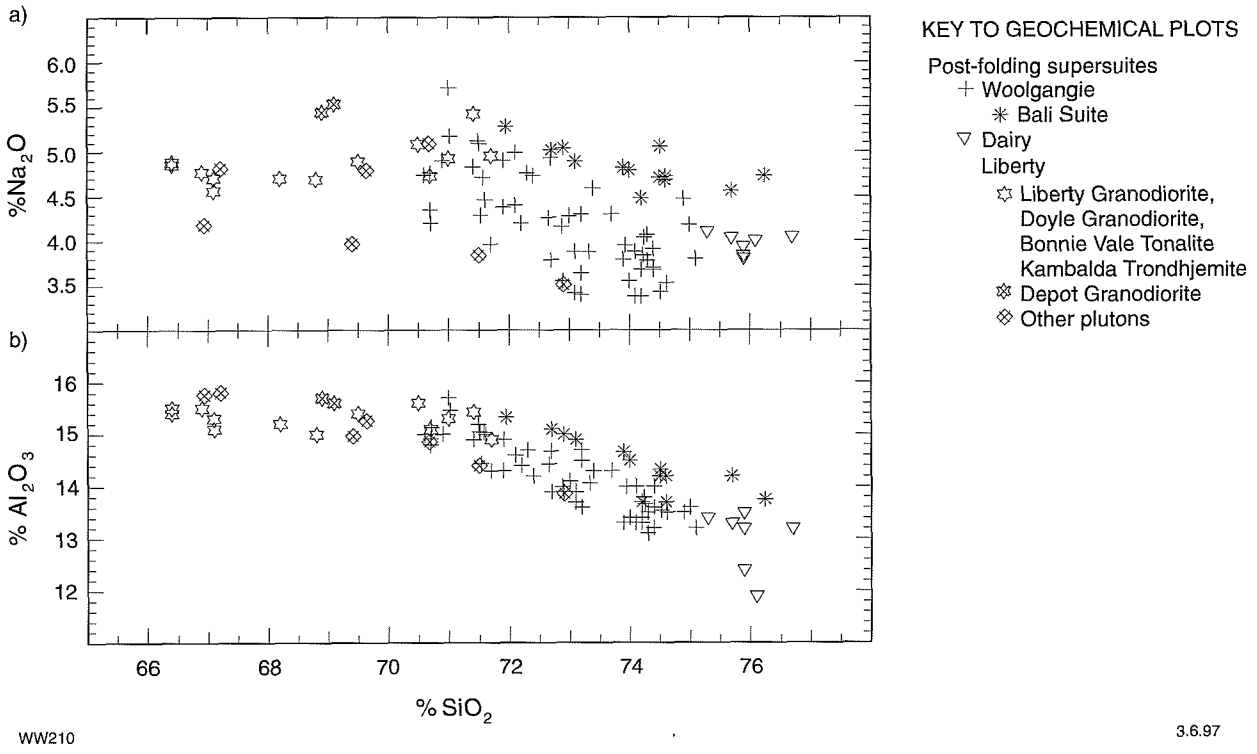

Figure 21. Post-RFGs only, showing relative scatter of data on: (a) Na_2O versus SiO_2 plot, and (b) Al_2O_3 versus SiO_2 plot

Although the suite defines a linear trend on most geochemical plots, it is distinctly bimodal with respect to many elements. Thus, the suite consists of two subgroups, one containing samples with less than 72.3% SiO_2, and the other containing samples with greater than 74.4% SiO_2. This bimodality is probably an artifact of limited data.

With increasing SiO_2, K_2O, Rb, Th, U and Y increase, whereas TiO_2, Al_2O_3, FeO*, CaO, Na_2O, P_2O_5, Ba, Sr, Zr, Li, V and Zn decrease. Barium, P_2O_5, Zr and Zn (versus SiO_2 diagrams) indicate that Goongarrie suite granitoids are not simply fractionated members of the Rainbow suite (Fig. 24).

Light rare-earth element (LREE) concentrations in the Goongarrie suite granitoids are similar to those of the Rainbow suite, and neither display Eu anomalies. However, REE patterns for the Goongarrie suite are more fractionated (Fig. 25b).

Minyma suite: SiO_2 values are uniformly high (76.4 to 77.3%) in the four samples analysed from the Minyma suite. Despite the restricted SiO_2 range, there is a relatively extended range of some major- and trace-element contents, giving rise to apparent steep trends on variation diagrams for TiO_2, FeO*, CaO, Na_2O, K_2O, Ba, Rb, Nb, Y, Zr, F and Zn (Fig. 24). These apparent steep trends serve to distinguish the Minyma suite from other pre-RFG suites. Harker variation diagrams for Zr, Th, U and Li indicate that Minyma suite granitoids are not fractionated members of the Goongarrie suite. There are no REE data for Minyma suite granitoids.

Post-RFG supersuites

Three calc-alkaline post-RFG supersuites and one alkaline post-RFG supersuite are recognized. Figure 26 illustrates chemical differences between the calc-alkaline supersuites.

Calc-alkaline post-RFG supersuites

Woolgangie supersuite: The Woolgangie supersuite yields relatively scattered geochemical plots. Silica contents vary between 70.5 and 75.0%. Silica, K_2O, Rb, Th, U, Nb, Y and Li increase, and TiO_2, Al_2O_3, FeO*, MgO, CaO, Na_2O, P_2O_5, Ba, Sr, Zr and V decrease, with increasing SiO_2.

Light rare-earth element contents of Woolgangie supersuite granitoids are similar to those of the Rainbow and Goongarrie suites. Chondrite-normalized plots are less fractionated, however, and most samples generate a moderate to distinct negative Eu anomaly (Fig. 27).

Bali suite granitoids have SiO_2 values between 71.9 and 76.5%. They are petrographically similar to other granitoids of the Woolgangie supersuite and there is a large degree of overlap between the two groups on most geochemical plots. However, Bali suite granitoids have less scattered geochemical trends than Woolgangie supersuite granitoids (Fig. 26). They also have higher Al_2O_3, Na_2O, Sr, and lower K_2O, Rb, Th and U, for given SiO_2 values.

Bali suite granitoids display slightly more fractionated REE curves than Woolgangie supersuite granitoids, due to

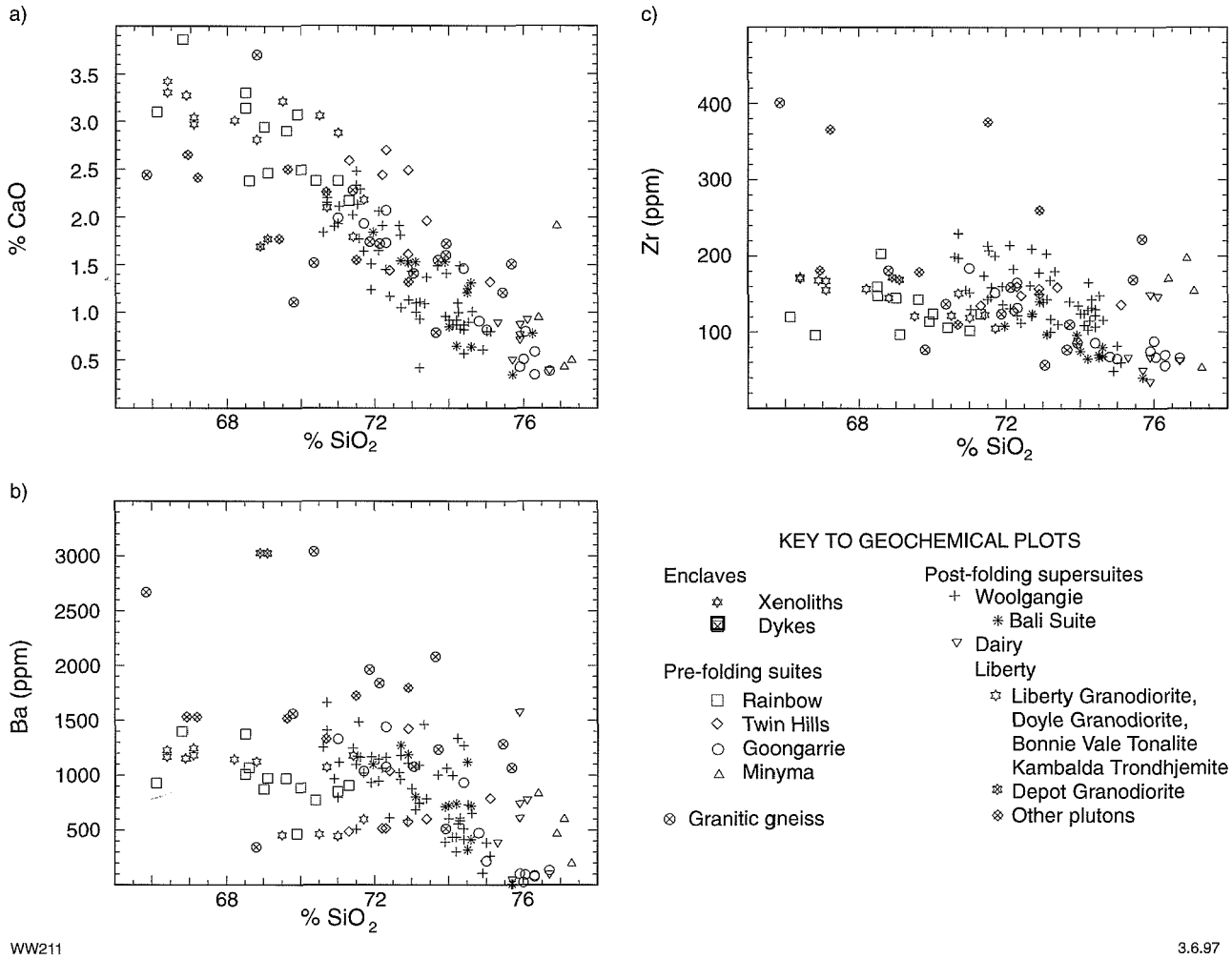

Figure 22. Comparison of whole-rock compositions for granitoid gneiss with those of other calc-alkaline granitoid (super)suites in the SWEGP: (a) CaO versus SiO_2, (b) Ba versus SiO_2, (c) Zr versus SiO_2

lower heavy rare-earth element (HREE) contents, and have weak to moderate negative Eu anomalies (Fig. 27).

Dairy supersuite: Silica contents are uniformly high (75.3–76.7%) in the Dairy supersuite and produce tight clusters and steep, linear apparent trends on variation diagrams. Harker variation diagrams for components such as TiO_2, FeO*, Ba, Nb and Zr indicate that Dairy supersuite granitoids are not fractionated members of the Woolgangie supersuite (Fig. 26).

Dairy supersuite granitoids contain lower LREE and total REE than other suites. They generate concave upward chondrite-normalized curves, and one of two analysed samples has a negative Eu anomaly (Fig. 27).

Liberty supersuite: This diverse group of plutons is characterized by relatively low SiO_2 (66.4–71.7%). The TiO_2, FeO*, MgO, CaO, P_2O_5, Sr, V and Zn contents decrease with increasing SiO_2 in plutons from which more than one sample has been analysed (e.g. Liberty Granodiorite, Doyle Dam Granodiorite). The Al_2O_3, Na_2O, K_2O, Ba, Rb, Th, U, Nb, Y, Zr, Li and Ga contents have relatively little within-pluton variation, giving rise to distinctive subhorizontal trends on plots involving these components (Fig. 26). Plots involving CaO, K_2O, P_2O_5, Na_2O+K_2O, Ba, Rb and Ga/Al establish the separate identity of the Liberty Granodiorite, Doyle Dam Granodiorite and Bonnie Vale Tonalite (i.e. they do not form a multi-pluton 'suite'. Variation of K/Rb within plutons is controlled by fractional crystallization, but Ga/Al only changes with extreme fractional crystallization (Möeller, 1989). Thus, the characteristic Ga/Al ratios for the different plutons suggest they were derived from different source-rock compositions (Fig. 28).

The Depot Granodiorite has low TiO_2, MgO, CaO, V and Zn, and high Na_2O, K_2O, Ba and Sr compared to most other granitoids with comparable SiO_2 in this study (Fig. 26). The single analysed sample of Larkinville Monzogranite has distinctive, high values of Rb, Sr and Li. The Bullabulling Monzogranite plots with the Woolgangie supersuite for many elements, but contains distinctively high contents of TiO_2, Rb, Th, Nb and Y, and especially F and Zr.

Liberty supersuite granitoids display a variety of chondrite-normalized REE curves (Fig. 27). The

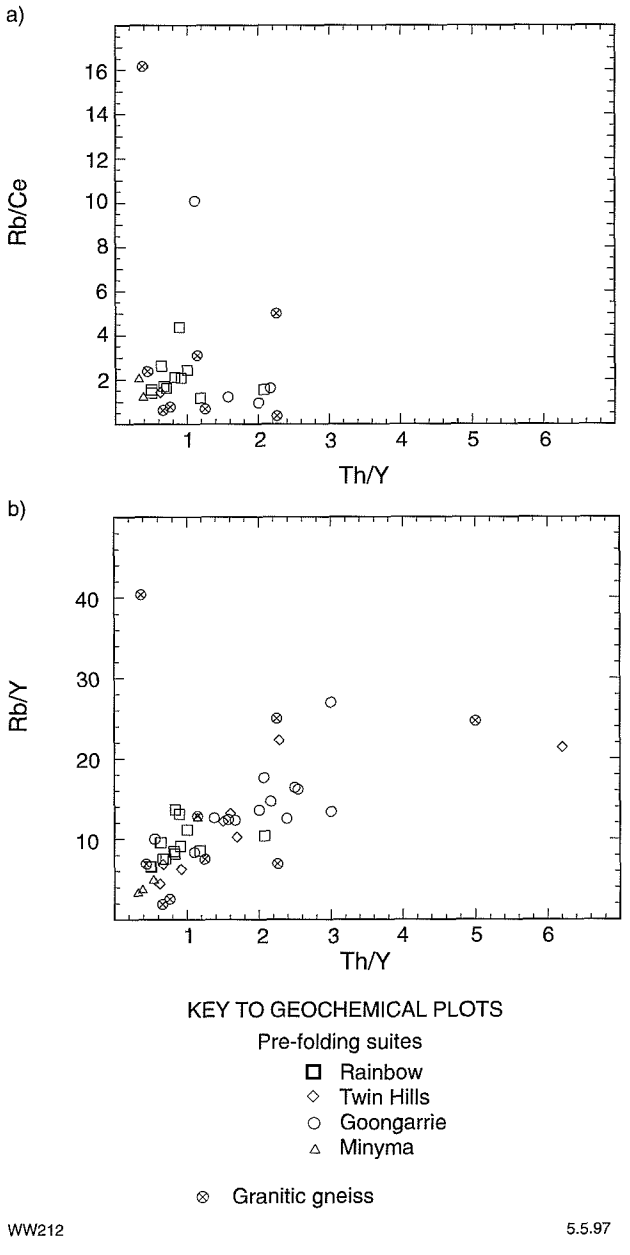

Figure 23. Incompatible trace-element ratio plots comparing granitoid gneiss with pre-RFG suites: (a) Rb/Ce versus Th/Y, (b) Rb/Y versus Th/Y

curves are variably fractionated, and do not have Eu anomalies.

Alkaline post-RFG supersuite

Gilgarna supersuite: The SiO_2 contents for granitoids of the Gilgarna supersuite, in the study area, range from 54.0 to 67.1%, lower than for most of the calc-alkaline granitoids. Analyses of alkaline granitoids for the whole of the Eastern Goldfields Province, published by Libby (1989), extend to 71.4% SiO_2. Gilgarna supersuite granitoids do not show coherent trends on Harker variation diagrams. As shown by Libby (1989), they are distinguished from calc-alkaline granitoid suites by higher K_2O and total alkalies (Fig. 29a,b). They also have a lower ASI (Fig. 30a) compared with calc-alkaline granitoid (super)suites, and are reasonably well separated from both calc-alkaline granitoids and xenoliths on diagrams plotting Al_2O_3, FeO* and MgO (Fig. 30b) against SiO_2.

Libby (1989) presented REE data for twelve alkaline (Gilgarna supersuite) granitoids in the Eastern Goldfields Province. The two examples from the study area (Fig. 27e) are taken from Libby (1989) and are reasonably typical. Rare-earth elements are less fractionated than for most calc-alkaline granitoid (super)suites in the study area, but are fractionated to a similar degree to those of the Dairy supersuite. Eu anomalies are not present. Libby (1989) noted a positive correlation between TiO_2 and REE, and interpreted this relationship to indicate a large part of the REE resided in titanite.

The alkaline granitoids of the Gilgarna supersuite have chemical and other features (anorogenic, anhydrous) of A-type granitoids described by Eby (1990). Chemical features include high Na_2O+K_2O and FeO*/MgO, and low CaO, compared to I- and S-type granitoids with comparable SiO_2 (Figs 29c,d).

Comparison of petrographically similar pre- and post-RFG supersuites

Collectively, post-RFGs and pre-RFGs display a high degree of overlap on all geochemical plots. However, individual, petrographically similar pre-RFG and post-RFG (super)suites can be distinguished from one another on selected geochemical plots. Although the distinction between the two major subdivisions of SWEGP granitoids is based on structural and timing relationships, these geochemical differences reinforce the primary subdivision of SWEGP granitoids into pre-RFG and post-RFG groups.

The Woolgangie supersuite and the Goongarrie suite have some common petrographic features, and overlap on many variation diagrams. However, the Woolgangie supersuite is characterized by a far greater enrichment of Th, U, Nb, Y and Li, and also has less Sr (Fig. 31a), at equivalent SiO_2, than the Goongarrie suite. The two suites are also clearly distinguished by different trends on Ba versus Y, and K/Rb versus Ga/Al diagrams.

The Dairy supersuite and Minyma suite are both characterized by a restricted range of high SiO_2 values. The Dairy supersuite is distinguished from the Minyma suite by an extended range in Al_2O_3, ASI, Ba, Rb, Th, U and Zn, and a tighter range in CaO, K_2O and F. In addition, on Harker diagrams, Dairy supersuite granitoids have steeper slopes than Minyma suite granitoids for some elements (FeO*, Ba, Zr, Li, V and Zn; cf. Figs 24 and 26).

The Liberty Granodiorite and Doyle Dam Granodiorite share some petrographic similarities with Rainbow suite

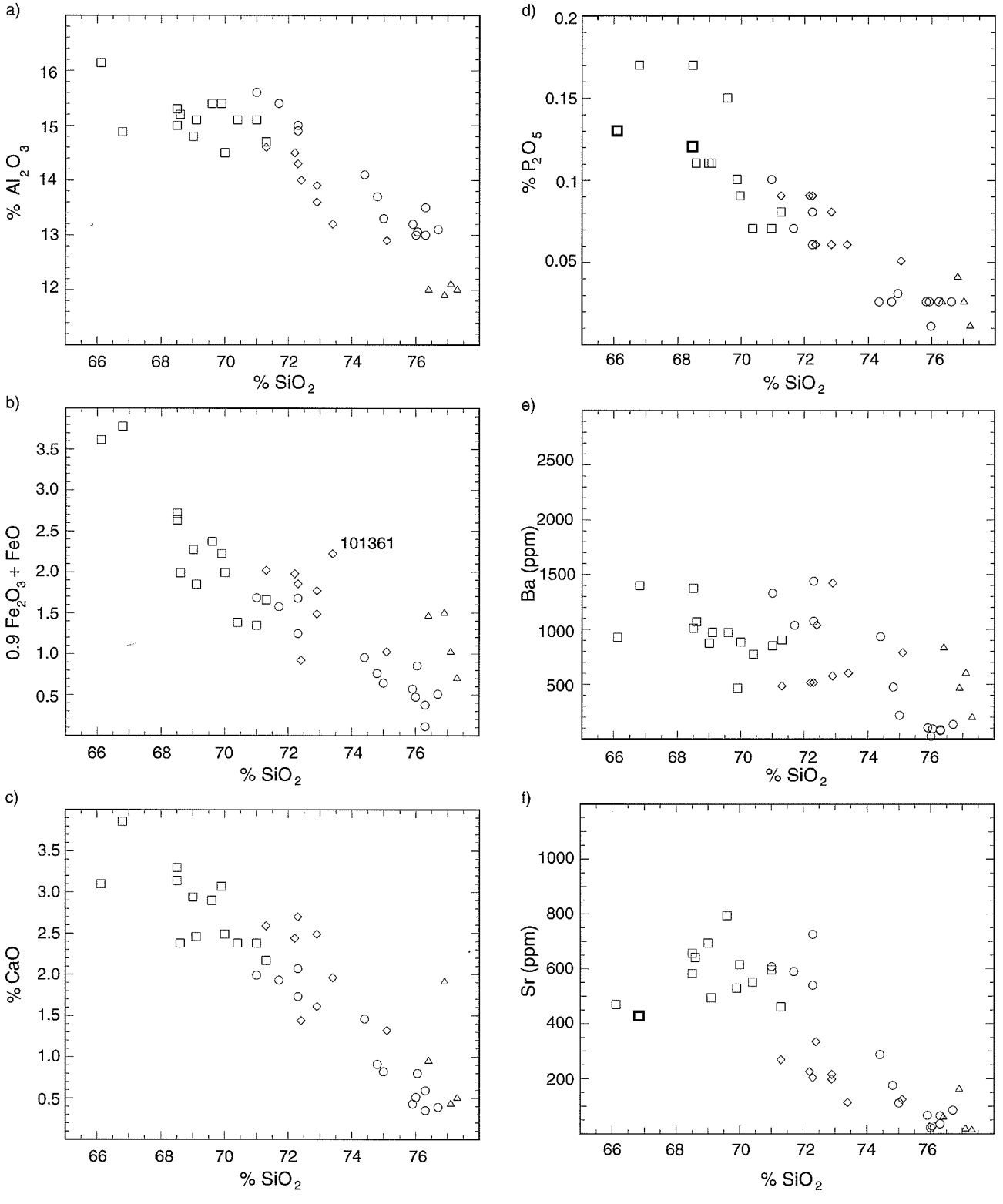

Figure 24. Harker variation diagrams for pre-RFG suites: (a) Al_2O_3, (b) $0.9Fe_2O_3$+FeO, (c) CaO, (d) P_2O_5, (e) Ba, (f) Sr, (g) Zr, (h) Li, (i) Th and (j) Zn

Figure 25. (opposite) Chondrite-normalized REE plots for: (a) the Rainbow suite and (b) the Goongarrie suite. The shaded envelope in a), representing data from five samples of Lawlers Tonalite near Agnew (from Cassidy et al., 1991), is shown for comparison. Sample 93904 from the Rainbow suite is shown in b) for reference (broken line)

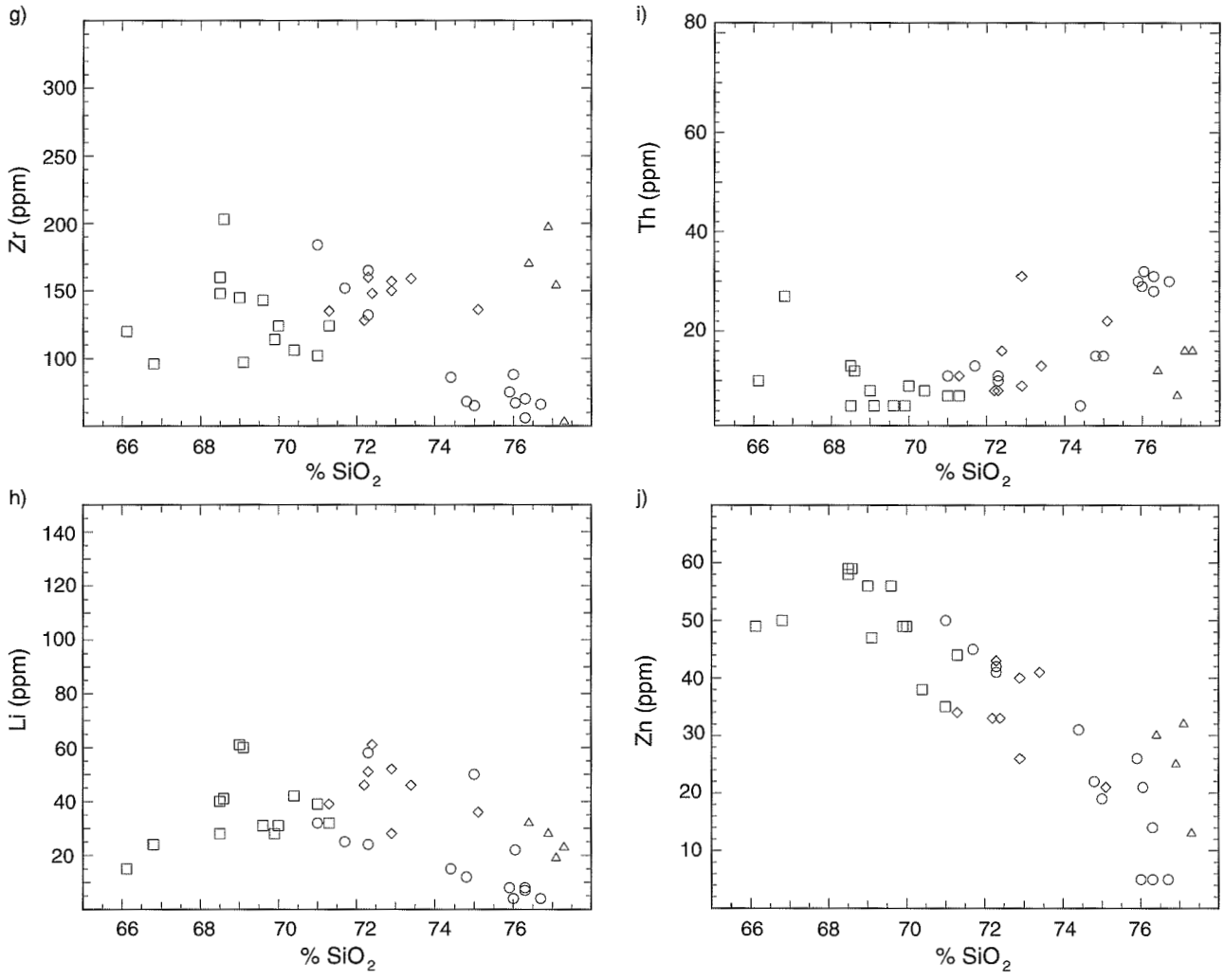

Figure 24. (continued)

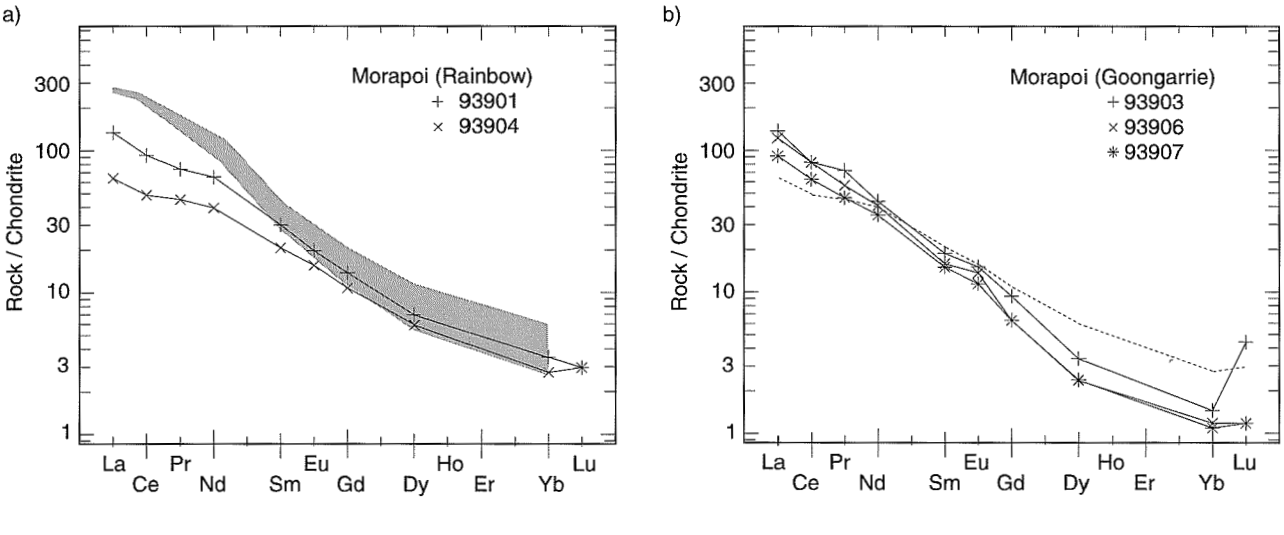

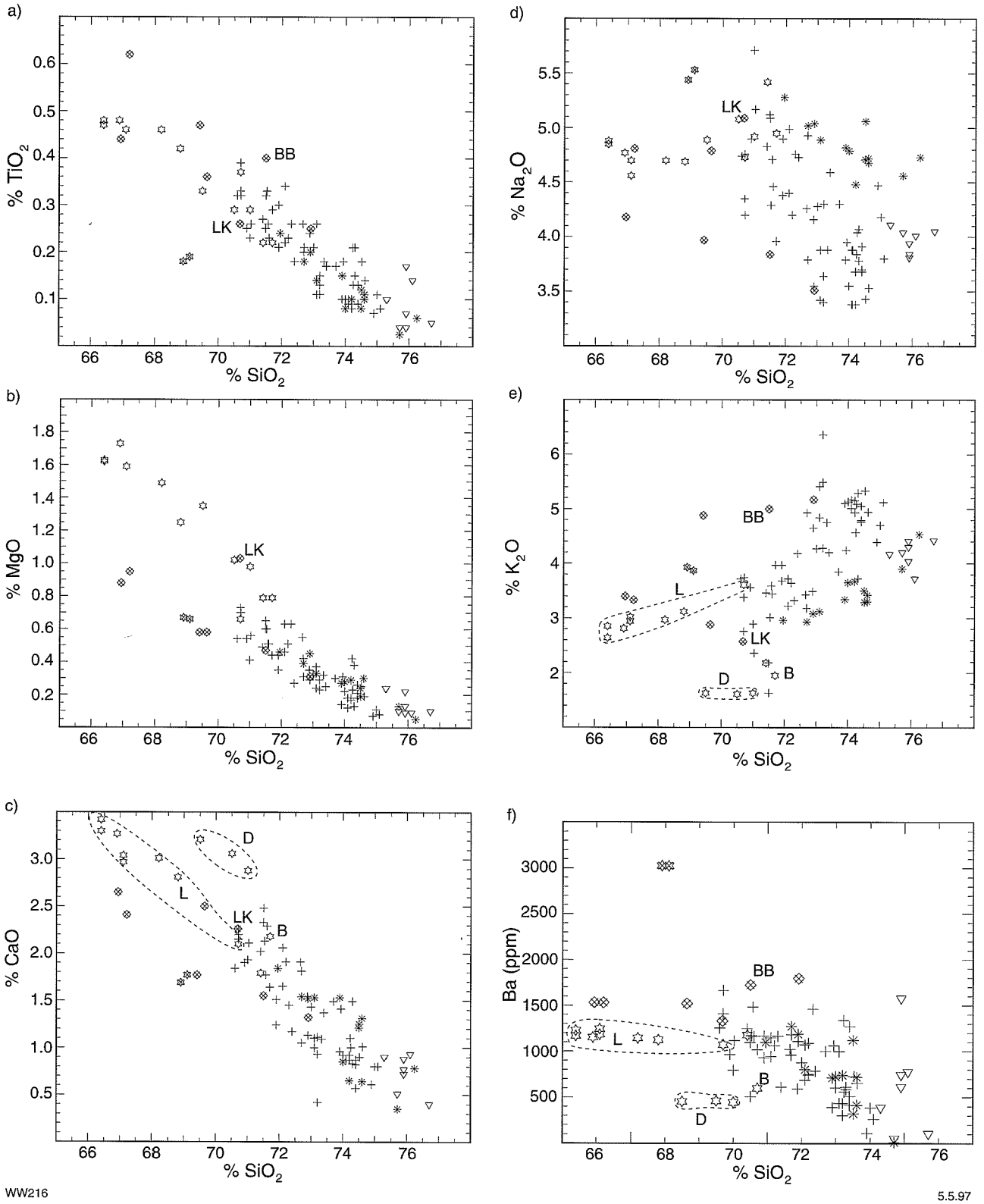

Figure 26. Harker variation diagrams for calc-alkaline post-RFGs: (a) TiO_2, (b) MgO, (c) CaO, (d) Na_2O, (e) K_2O, (f) Ba, (g) Sr, (h) Rb, (i) Th and (j) Nb. Liberty supersuite plutons are outlined or annotated on selected diagrams as follows: Bonnie Vale Tonalite (B), Bullabulling Monzogranite (BB), Doyle Dam Granodiorite (D), Liberty Granodiorite (L), Larkenville Monzogranite (LK)

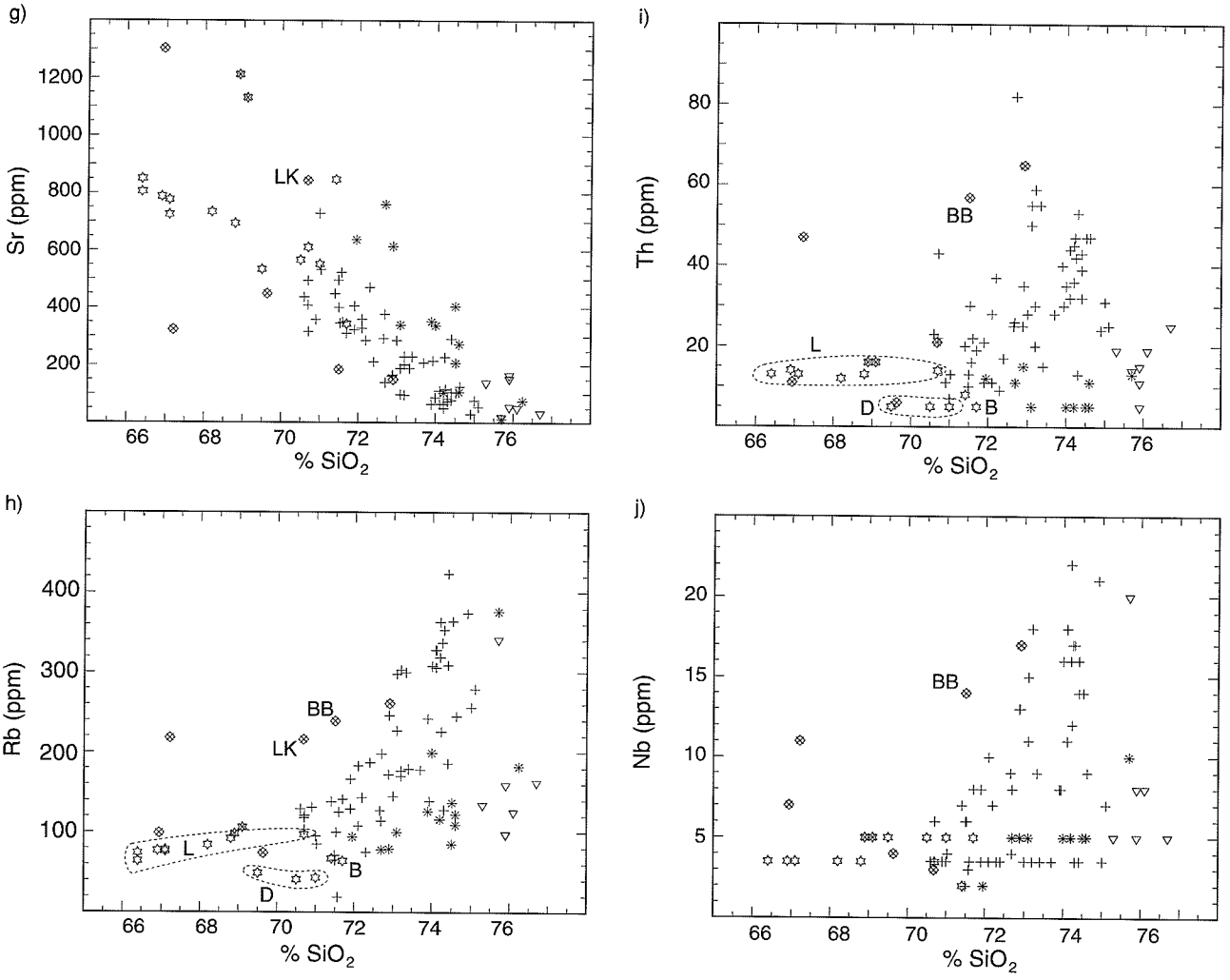

KEY TO GEOCHEMICAL PLOTS
Post-folding supersuites
+ Woolgangie
* Bali Suite
▽ Dairy
Liberty
☼ Liberty Granodiorite, Doyle Granodiorite, Bonnie Vale Tonalite Kambalda Trondhjemite
❄ Depot Granodiorite
⊗ Other plutons

WW217 5.5.97

Figure 26. (continued)

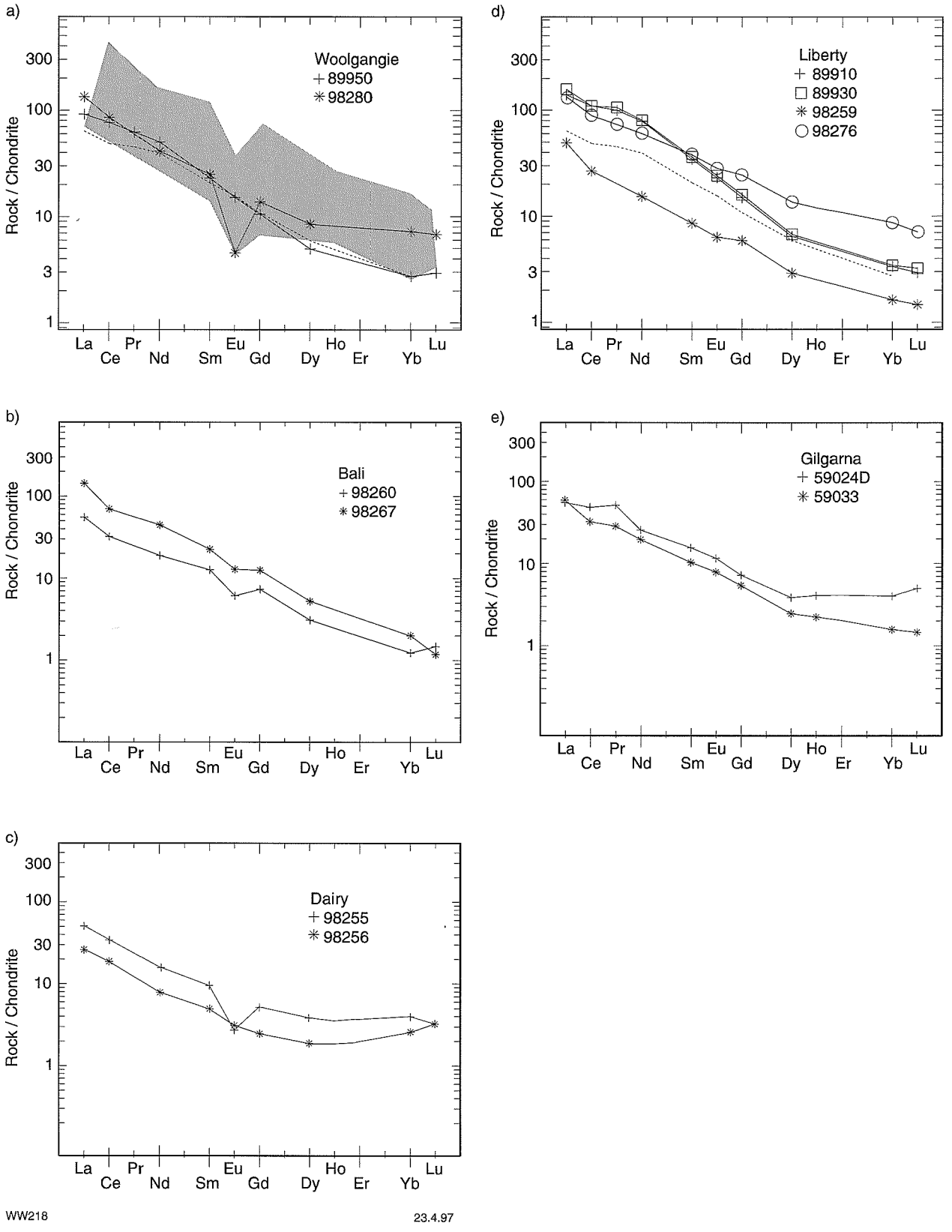

Figure 27. Chondrite-normalized REE plots for: (a) Woolgangie supersuite; (b) Bali suite; (c) Dairy supersuite; (d) Liberty supersuite (sample 98259 is the Bonnie Vale Tonalite, sample 98276 is the Depot Granodiorite, the other two samples are the Liberty Granodiorite); (e) Gilgarna supersuite (data from Libby, 1989). Sample 93904 (broken line) from the Rainbow suite is shown in (a) and (d) for reference. Pluton abbreviations as for Figure 26. Shading in Figure 27c includes data for samples equivalent to Woolgangie supersuite from Hill et al. (1992b)

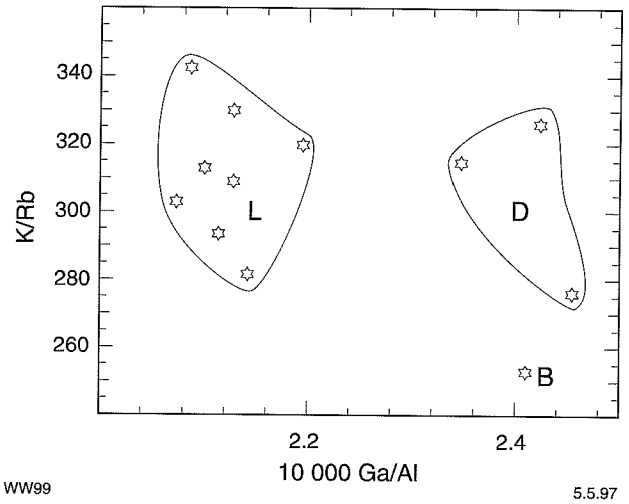

WW99 5.5.97

Figure 28. (left) Individual plutons of the Liberty supersuite are distinguished on a K/Rb versus 10 000 Ga/Al diagram. Pluton abbreviations as for Figure 26

Figure 29. (below) Gilgarna supersuite granitoids plotted with calc-alkaline granitoids on: (a) Na_2O+K_2O versus SiO_2, (b) K_2O versus Na_2O, (c) $(0.9Fe_2O_3+FeO)/MgO$ versus SiO_2, (d) Na_2O+K_2O versus 10 000 Ga/Al. Solid dots in (a), (b) and (c) are lamprophyres (minettes) from the Leonora–Laverton area (Hallberg, 1985). Envelope in (a) is for Boreas-type granitoids, northeast Eastern Goldfields Province (Libby, 1989). Square in lower left hand corner of (d) separates A-type granitoids (outside box) from unfractionated I-type and S-type granitoids (Whalen et al., 1987). Shaded envelope in (d) encloses all calc-alkaline granitoid samples

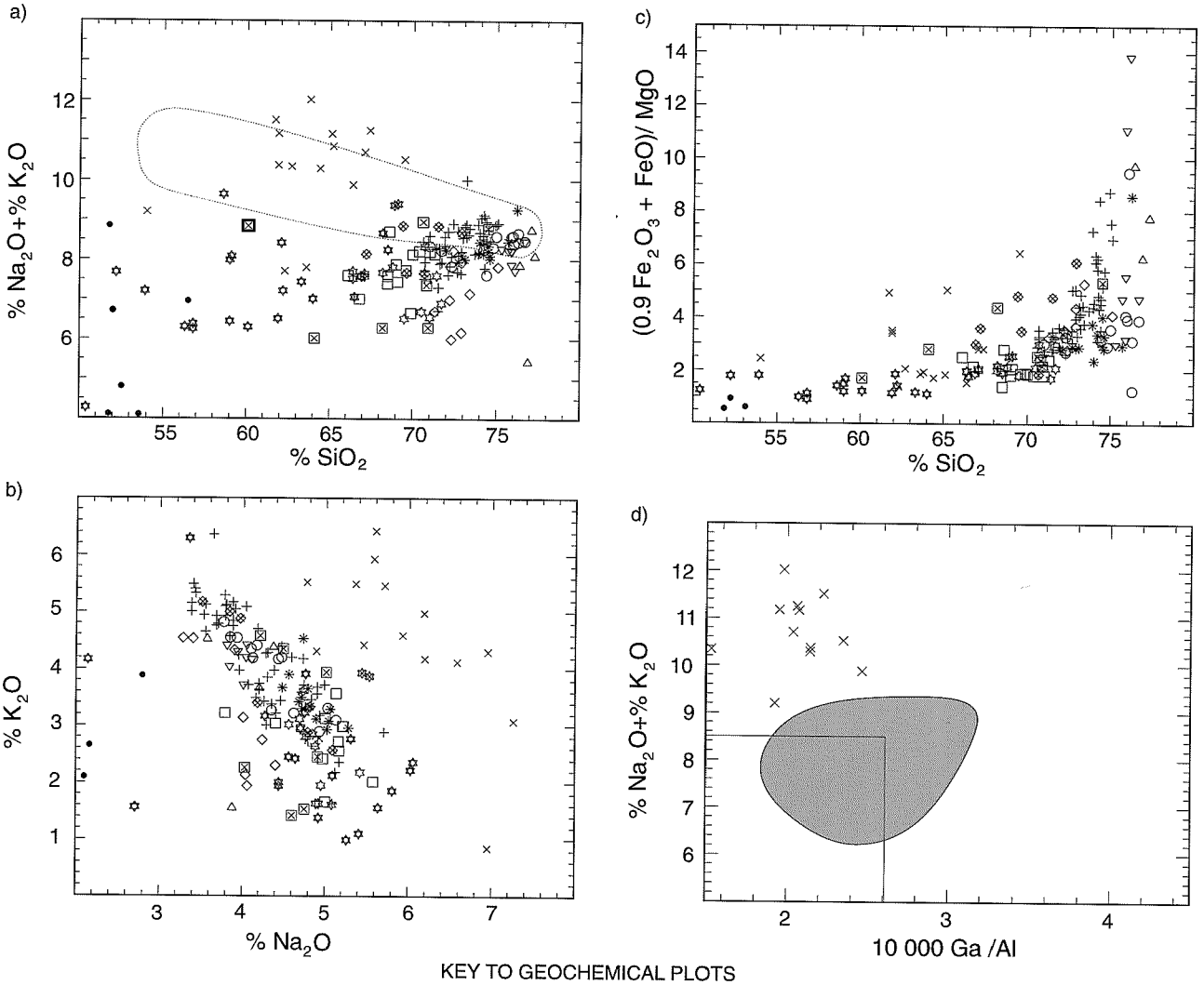

KEY TO GEOCHEMICAL PLOTS

Enclaves
- Xenoliths
- Dykes

Pre-folding suites
- Rainbow
- Twin Hills
- Goongarrie
- Minyma

Granitic gneiss

Post-folding supersuites
- Woolgangie
- Bali Suite
- Dairy

Liberty
- Liberty Granodiorite, Doyle Granodiorite, Bonnie Vale Tonalite Kambalda Trondhjemite
- Depot Granodiorite
- Other plutons

Gilgarna

WW219 5.5.97

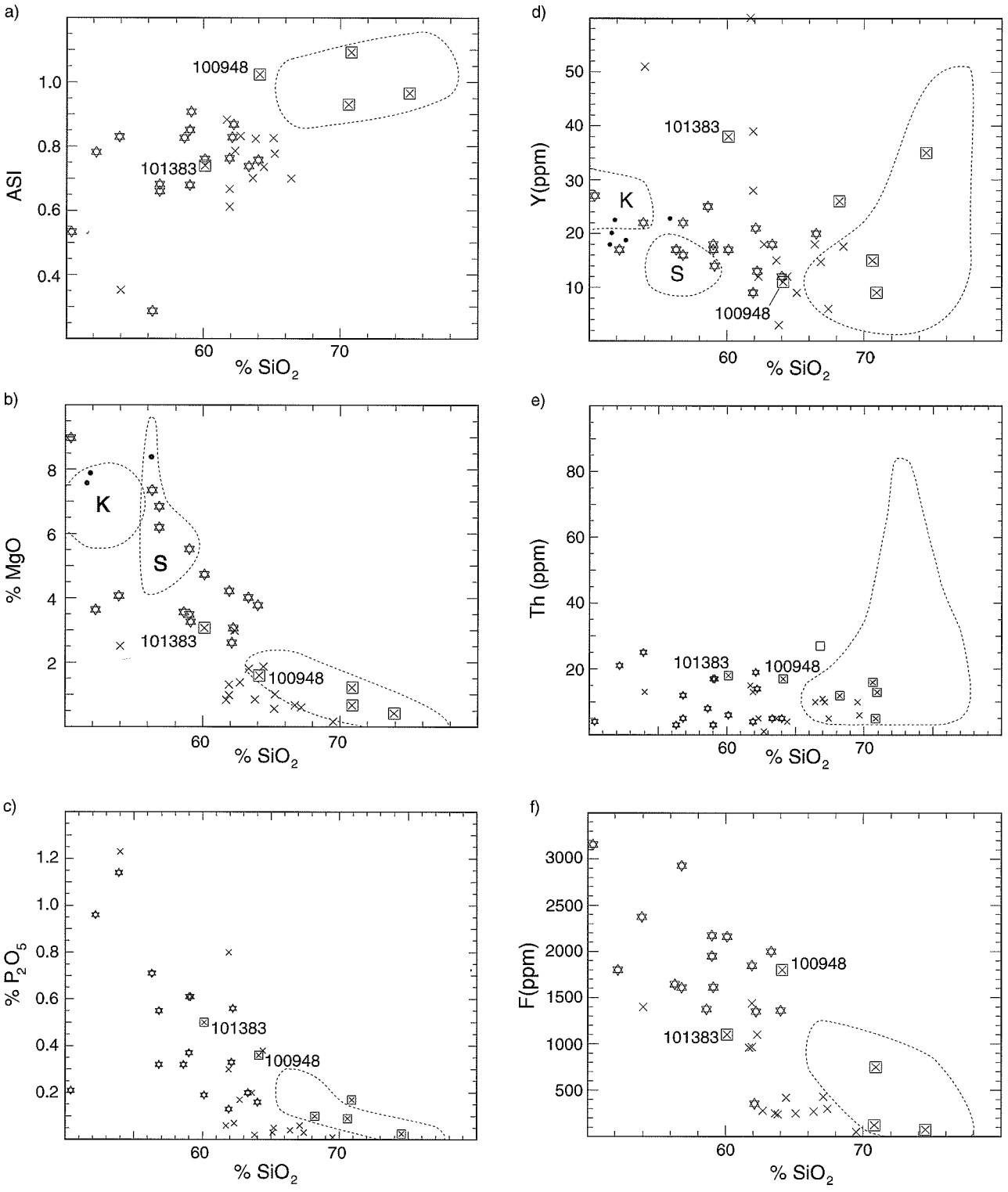

Figure 30. Xenoliths and dykes compared with other granitoids in the SWEGP: (a) ASI versus SiO_2, (b) MgO versus SiO_2, (c) P_2O_5 versus SiO_2, (d) Y versus SiO_2, (e) Th versus SiO_2, (f) F versus SiO_2. Solid dots represent minettes from the Leonora–Laverton area (Hallberg, 1985). Fields outline compositions of kersantites (K) and spessartites (S) from the Kambalda area (Perring, 1988). Unmarked envelopes outline greater than 90% of calc-alkaline granitoids

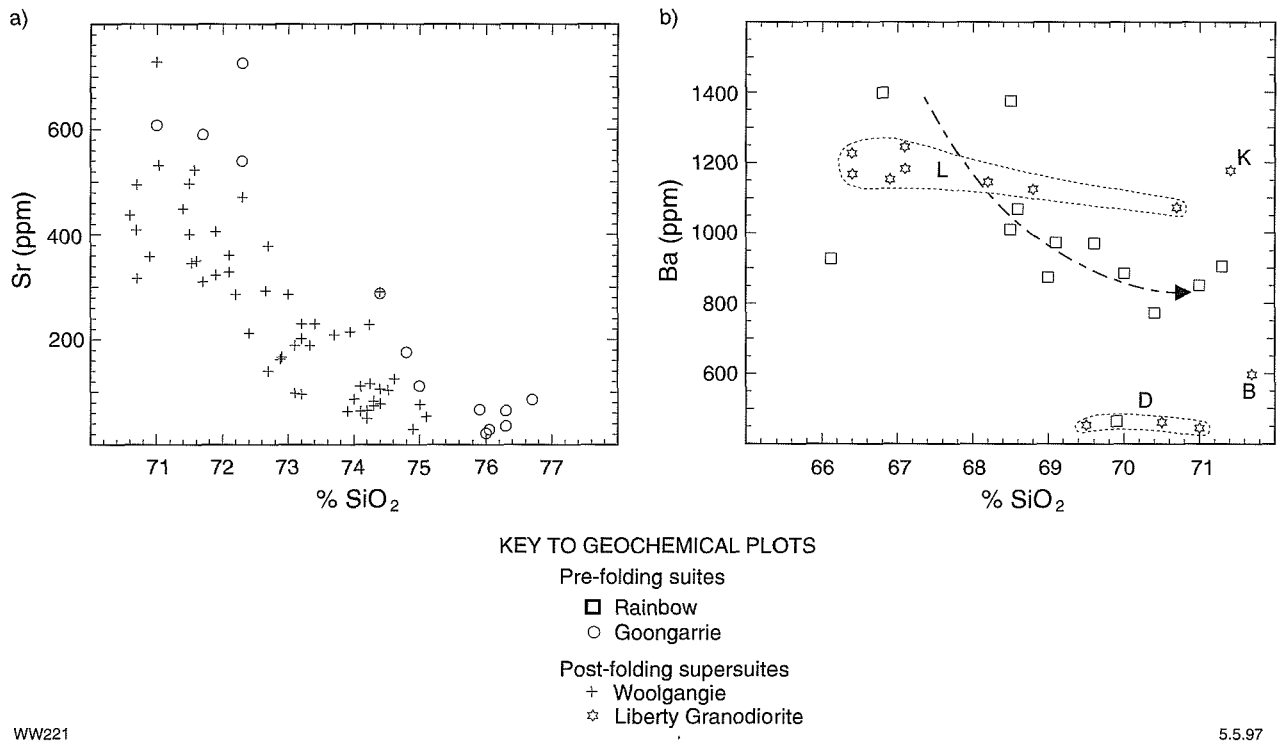

Figure 31. Plots that assist in distinguishing petrographically similar pre-RFGs and post-RFGs: (a) Sr versus SiO_2 for the Goongarrie and Woolgangie (super)suites, (b) Ba versus SiO_2 for the Rainbow suite and Liberty supersuite — Bonnie Vale Tonalite (B), Doyle Dam Granodiorite (D), Kambalda Trondhjemite (K), and Liberty Granodiorite (L)

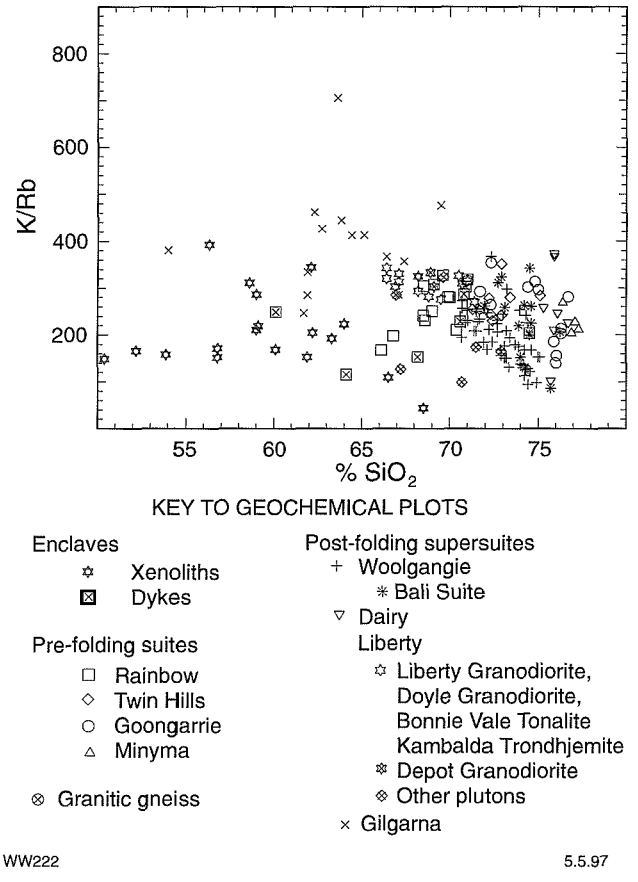

Figure 32. K/Rb versus SiO_2 plot comparing dykes and xenoliths with other granitoids in the SWEGP

granitoids, but are distinguished by plots of FeO*, MgO, P_2O_5, ASI, Ba, Y, Zr and Zn versus SiO_2 (e.g. Fig. 31b).

Xenoliths

Most samples of xenoliths analysed in this study are microgranitoid xenoliths. Two samples of gneiss-textured xenoliths were also analysed. Accidental xenoliths have not been analysed.

The SiO_2 contents for xenoliths range from 50.4 to 68.2% (Fig. 20). They thus overlap the range for calc-alkaline granitoids and alkaline granitoids but are, as a group, less siliceous than both other groups. Figure 30 compares xenoliths with calc-alkaline and alkaline granitoids on selected Harker variation diagrams. Xenoliths contain higher amounts of mafic components (e.g. TiO_2, FeO*, MgO, CaO, Ni, V) and have a lower ASI than the calc-alkaline granitoids. On the other hand, some or all xenoliths are enriched in the incompatible elements (Ce, Li, Nb, Rb, Th, Y) compared to concentrations predicted by projecting calc-alkaline granitoid trends back to low SiO_2 values. Some volatile and incompatible elements (e.g. P_2O_5, F, Th, Li, Zn) are substantially enriched, compared to most calc-alkaline rocks with a comparable SiO_2 content. K/Rb ratios for the xenoliths are approximately equal to, or less than, those for the host granitoids (Fig. 32).

Xenoliths are relatively enriched in REE, especially LREE, compared to the calc-alkaline granitoids that host

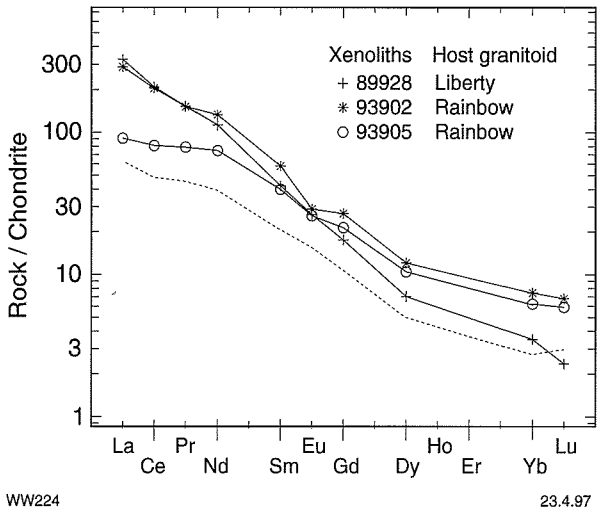

Figure 33. Chondrite-normalized REE plots for xenoliths in the Rainbow suite (93902, 93905) and Liberty Granodiorite (89928). Sample 93904 (Rainbow suite) is shown for reference (dotted line)

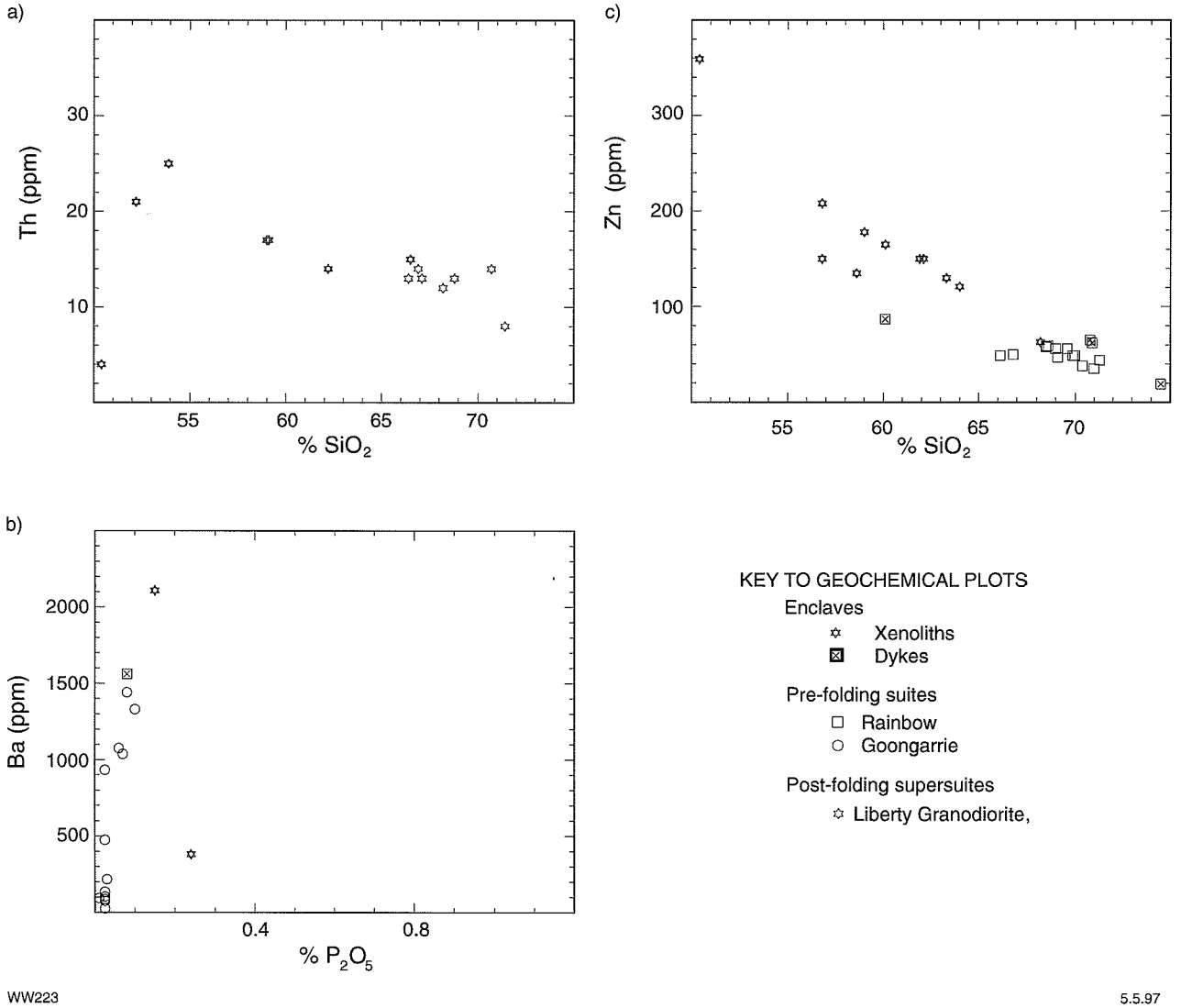

Figure 34. (a) Th versus SiO_2 for xenoliths and host rocks, Liberty Granodiorite, (b) Ba versus P_2O_5 for xenoliths, dykes and host rocks for the Goongarrie suite, (c) Zn versus SiO_2 for xenoliths, dykes and host rocks for the Rainbow suite. These diagrams illustrate non-linear relationships between enclave compositions and the compositions of the host granitoids

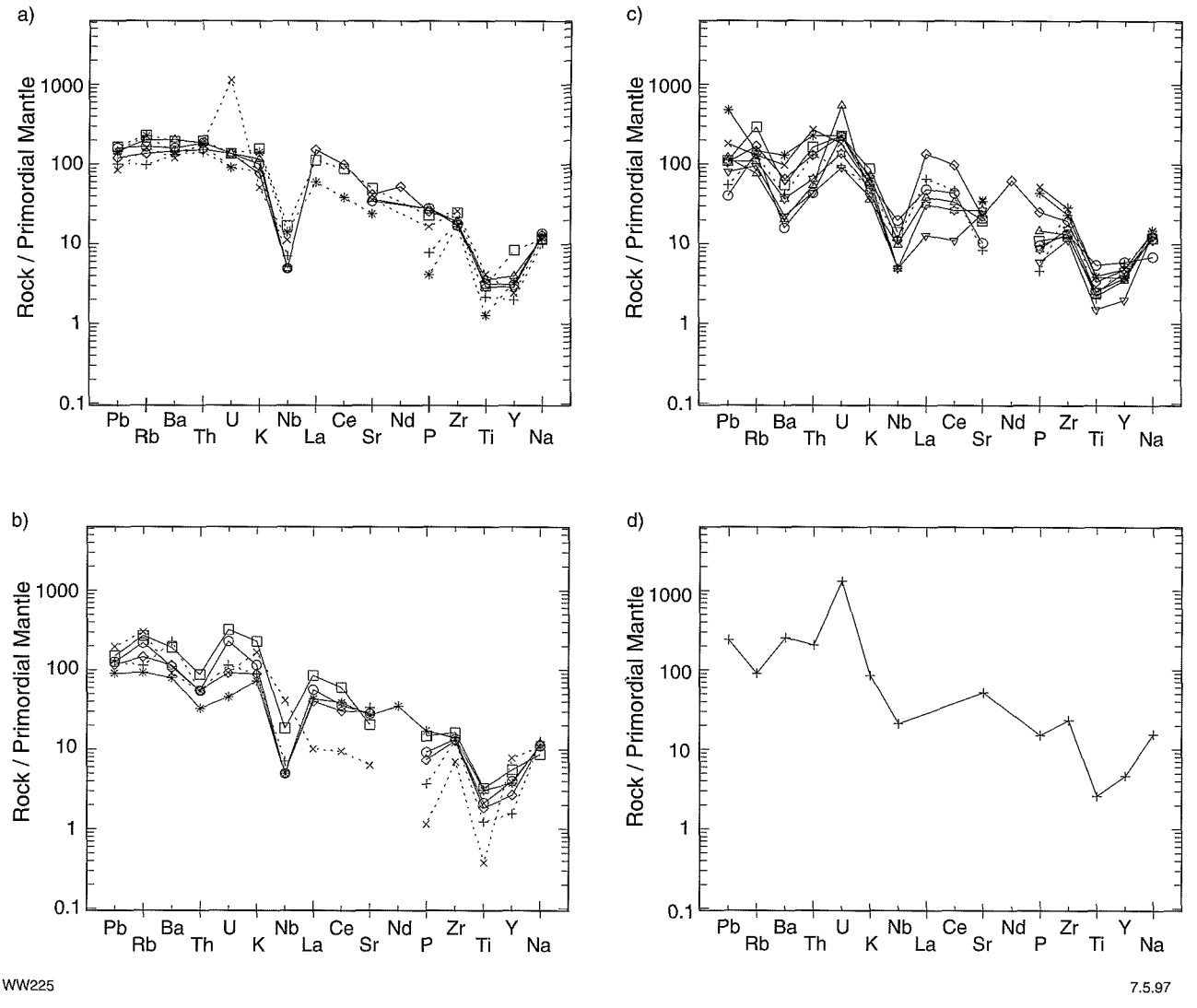

Figure 35. Four groups of dykes and xenoliths as defined by mantle-normalized spidergrams. Dykes are shown as broken lines; xenoliths as solid lines: (a) concave downward Pb–K curves for samples 100930, 100948, 101382, 101383 (dykes); 89928, 97095, 97097, 98251A (xenoliths), (b) curves with negative Th anomalies for samples 98272, 101354 (dykes); 93905, 101356, 101378, 101379 (xenoliths), (c) curves with negative Ba anomalies for samples 101362 (dyke); 97099, 97702, 98253, 93902, 101357, 101374, 101376, 101380 (xenoliths), (d) curve for sample 98279 (xenolith in the Depot Granodiorite)

them. Rare-earth element patterns are strongly fractionated, and have negligible Eu anomalies (Fig. 33).

Although xenoliths plot separately from calc-alkaline host granitoids on most geochemical diagrams, the data are commonly scattered, and rarely display coherent trends. They do not form straight-line relationships with host granitoids (Figs 32 and 34) such as those displayed by restite-controlled granitoid suites of the Lachlan Fold Belt (Chappell et al., 1987).

Four groups of xenoliths are recognized, based on mantle-normalized spidergrams shown in Fig. 35. These groups cut across petrographic trends from quartz-deficient, monzonitic rocks to relatively quartz-rich and feldspar-depleted tonalite and diorite. They do not correlate with the SiO_2 content, Mg-number (100 Mg/(Mg+Fe)), or mafic mineralogy (biotite versus hornblende) of the xenoliths. All xenoliths (with the exception of 98279, Fig. 35d) display prominent negative Nb, Ti and Y anomalies. Small to moderate negative P anomalies are present in some curves but are not specifically associated with any one group. Subdivisions are based mainly on differences in the left hand side of the spidergrams (Pb–K):

1. Group 1 is composed of relatively high-SiO_2 (>55%) xenoliths in the Liberty Granodiorite and a tonalite xenolith from west of Lake Owen that display moderately smooth, convex upward curves, from Pb to K (Fig. 35a).

2. Group 2 contains some other microgranitoid xenoliths in pre-RFG intrusions, and a gneiss-textured xenolith

from the Owen complex (93905), that have similar spidergrams to those described above, but with a prominent negative Th anomaly (Fig. 35b). The pyroxene granofels xenolith in quartz monzonite, south of Princess Bore (101390), has a similar geochemical signature.

3. Most other microgranitoid xenoliths, including low-SiO_2 (<55%) xenoliths from the Liberty Granodiorite and a tonalite xenolith from Bora Rock (98253) that have more irregular curves between Pb and K, including a weak to marked negative Ba anomaly (Fig. 35c), make up group 3. This group tends to have less K_2O and more Na_2O than the other groups.

4. Group 4 contains sample 98279, a xenolith from the Depot Granodiorite, which displays a negative Rb anomaly, and a prominent positive U anomaly, and, like its host rock, is petrographically and geochemically unique amongst the samples studied (Fig. 35d).

Dykes

Dyke compositions are diverse, and overlap both xenolith and calc-alkaline granitoid fields. Some dykes (101383, 100948) display consistent geochemical affinities with xenoliths (Fig. 30). They do not define coherent trends and, individually, they do not show consistent affinities for any of the pre-RFG suites.

Dyke samples have mantle-normalized spidergrams that can generally be assigned to one of the xenolith groups described above (Fig. 35). Most dykes have similar, but less regular curves to group 1 xenoliths. The dyke at Naismith Bore (101362) has a negative Ba anomaly, and low K_2O, and is therefore assigned to group 3. Dyke samples 101354 and 98272, from Rainbow Bore (Birthday complex) and Bald Hill Bore (Goongarrie complex), respectively, display a negative Th anomaly, similar to xenoliths of group 2.

Chapter 6

Petrogenesis of SWEGP granitoids

This chapter describes the petrogenesis of the seven main calc-alkaline granitoid (super)suites, the dykes and xenoliths, and the 'alkaline' Gilgarna supersuite. The petrogenesis of the Liberty Granodiorite is assessed as an example of the compositionally diverse Liberty supersuite. Petrogenesis is addressed in terms of: firstly, the source rocks for each (super)suite; secondly, the origin of the compositional variations within (super)suites; and finally, the petrogenetic relationships between different granitoid (super)suites. Emphasis is placed on the calc-alkaline (super)suites, and the dykes and xenoliths, which constitute the greater part of the database. The Gilgarna supersuite is discussed in less detail because data for this group of rocks are more limited in the SWEGP.

Interpretation of limited geochemical data for granitoid gneiss is complicated due to widespread recrystallization and partial melting in situ. The petrogenesis of granitoid gneiss is therefore not discussed further.

Source rocks for granitoid suites and supersuites

Whereas the compositional variation within granitoid suites can be attributed to a variety of processes, the parent melts for each suite must have been derived by partial melting of a source in the crust. Least fractionated members of granitoid (super)suites are those most likely to retain the characteristics that help identify the nature of the source rocks. The absence of large outcrops of relatively primitive granitoids (tonalite, diorite) in the SWEGP suggests that the least fractionated of the analysed samples may be close to the composition of the parent magma for their respective suites. For most (super)suites, a single representative sample cannot be identified, and the theoretical parent magma is based on two or three of the least fractionated samples. Low Rb and high Sr for most of these least fractionated samples support the hypothesis that they are not fractionated products of deeper, unexposed tonalite or diorite. Some characteristics of hypothetical parent magmas for each of the main calc-alkaline (super)suites and the Liberty Granodiorite are summarized in Table 10.

Implications of high fO_2 magmas

The intrinsically 'oxidized' granitoid magmas of all (super)suites is consistent with derivation from a crustal source (Wones, 1981). Czamanske et al. (1981) further suggested that granitoids that crystallized early magnetite and titanite (e.g. Rainbow suite, Liberty Granodiorite) must

Table 10. Parent melt compositions for granitoid suites and supersuites in the southwest Eastern Goldfields Province

Suite	*Rock type*	*SiO_2 (%)*	*FeO* (%)*	*$Na_2O + K_2O$*	*Na_2O/K_2O*
Pre-RFG suites and supersuites					
Rainbow (a)	Hornblende–biotite granodiorite	67–68.5	3.9	7.4–7.6	1.8–2.0
Twin Hills	Biotite granodiorite (or plagioclase-rich monzogranite)	71–72	1.8–2.0	6.0–7.0	1.5–2.1
Goongarrie	Biotite granodiorite (or plagioclase-rich monzogranite)	71–72	1.6–1.7	7.8–8.4	1.5–1.7
Minyma (b)	Biotite monzogranite	76.5–77	1.5	~8	1.3
Post-RFG suites and supersuites					
Liberty	Biotite–hornblende granodiorite	67	3.3	7.6	1.7
Woolgangie	Biotite monzogranite	70–71	1.6–2.5	7.5–8.5	1.2–1.4
Bali	Biotite monzogranite	72–73	1.1–1.3	8.1–8.3	1.6–1.8
Dairy	Biotite monzogranite	~76	0.5–0.7	8.2	0.9

NOTES:
$FeO^* = FeO + 0.9\ Fe_2O_3$
Rainbow suite — 93901, 101363
Twin Hills suite — 100926, 100927, 100931
Goongarrie suite — 93903, 93906, 93907 (b); 100945
Minyma suite — 101359
Liberty Granodiorite — 97701
Woolgangie supersuite — 101373, 105903, 105904
Bali suite — 77686, 98258, 98267
Dairy supersuite — 98254, 100924
(a) Samples 82114 and 90967099 have been neglected because of possible alteration, but the main effect of their inclusion is to lower SiO_2 in the parent melt to ~66%
(b) Most weight is given to sample 101359 for alkali contents in the parent melt for the Minyma suite, because Na_2O/K_2O is markedly anomalous for sample 100945

have been derived from a crust that has been oxidized (weathered) at the earth's surface (or ocean floor).

Igneous source rocks

All analysed granitoid samples have A/CNK (equivalent to the ASI of Zen, 1986) <1.1, the value that distinguishes most I-type granitoids from most S-type granitoids in the Lachlan Fold Belt (Chappell and White, 1974; Hine et al., 1978). The ASIs of relatively felsic I- and S-type granitoids in the Lachlan Fold Belt overlap, but I-type granitoids display increasing ASI with increasing SiO_2 (Chappell and White, 1992), as do calc-alkaline granitoid (super)suites in the SWEGP (Fig. 30a). Decreasing P_2O_5 with increasing SiO_2 for most (super)suites also indicates an I-type source for the felsic granitoids (Chappell and White, 1992). Rainbow suite granitoids and Liberty supersuite plutons such as the Liberty and Doyle Dam Granodiorites display other features that typify I-type granitoids, including high $Fe^{+3}/(Fe^{+2}+Fe^{+3})$, the presence of microgranitoid xenoliths, igneous-textured hornblende, and an accessory mineral assemblage comprising titanite, magnetite, apatite, zircon and allanite (White and Chappell, 1977; Chappell, 1978; Whalen and Chappell, 1988, in addition to the afore-mentioned references). The Goongarrie suite also contains some microgranitoid xenoliths in less fractionated members. There is no convincing evidence to suggest the presence of S-type granitoids in the study area. Possible metapelitic restite (as surmicaceous xenoliths) occurs in monzogranite near Goongarrie Homestead, but is accompanied by microgranitoid xenoliths and synplutonic dykes, and the host granitoid does not have S-type petrographic or geochemical characteristics. Examination of further thin sections from near Goongarrie Homestead suggests that chabazite and heulandite in surmicaceous xenoliths are alteration products of plagioclase, not of cordierite and andalusite as originally suggested by Witt and Swager (1989) and Witt (1990).

Features described above suggest that most or all granitoids were derived from igneous, or infracrustal, source rocks, or their metamorphosed equivalents (White and Chappell, 1977; Chappell and Stephens, 1988).

Spidergrams and the significance of the negative Y anomaly

Mantle-normalized spidergrams for least fractionated samples of calc-alkaline granitoid suites in the SWEGP are shown in Fig. 36, and the interpreted residual mineralogy is summarized in Table 11. Two main types of spidergram are recognized. Parent melts for most granitoid (super)-suites have a negative Y anomaly, but no Sr anomaly. Parent melts for the Minyma and Dairy (super)suites lack a Y anomaly. Sr is lower in this second group, suggesting more complete spidergrams could display a negative Sr anomaly, although this is difficult to confirm in the absence of La, Ce and Nd data.

Wyborn et al. (1992) and Wyborn (1993) interpreted negative Y anomalies to indicate the presence of residual garnet in the source rocks of granitoids. However, Y partitions strongly into hornblende, as well as garnet (Nash and Crecraft, 1985; Martin, 1987). Lambert and Holland (1974) and Whalen (1985) document the importance of hornblende fractionation in controlling the Y content of igneous rocks. Arth and Barker (1976) and Martin (1986) pointed out that hornblende and garnet partition REEs in essentially the same fashion, in equilibrated silicic liquids. Since Y and HREE behave similarly in igneous systems, negative Y anomalies in primitive members of granitoid suites could reflect the presence of residual hornblende, or garnet (or both), in the source region.

Spidergrams for parent melts of all (super)suites display prominent negative Ti and Nb anomalies, suggesting the presence of a residual titaniferous phase (Hellman and Green, 1979; Green and Pearson, 1987). Similarly, negative P anomalies suggest residual apatite. Residual apatite in the source may have only a minor effect on REE patterns of parent magmas where garnet or hornblende also remain in the source (Watson and Capobianco, 1981). In contrast, residual titanite in the source can have a marked effect on the LREE to medium rare-earth elements in equilibrated melts, even where hornblende and garnet are also residual phases (Hellman and Green, 1979). It is therefore concluded that the residual titaniferous phase was ilmenite or rutile, in view of the marked LREE-enriched, chondrite-normalized patterns for most granitoid (super)suites (Figs 25 and 27).

Identification of source rocks

Source rocks for granitoid (super)suites are discussed here in general terms, in the light of experimental studies, and refined in the light of petrographic and geochemical features of SWEGP granitoids. Rigorous trace-element modelling has not been attempted because specific candidates for source rocks have not been identified. Two types of melting are considered. In vapour-absent (dehydration) melting, hydrous minerals (muscovite, biotite, amphibole) in the source rock break down to yield melt plus an anhydrous residue (Burnham, 1979; Clemens, 1984; Clemens and Vielzeuf, 1987). Under vapour-saturated conditions, source rocks melt in the presence of a free, volatile-rich fluid phase (Wyllie, 1977, 1984).

Early descriptions of relatively potassic granodiorites in the Eastern Goldfields Province suggested they were derived by partial melting of mafic greenstones (Glikson, 1979). However, experimental studies (Beard and Lofgren, 1991) and petrogenetic modelling (Arth and Hanson, 1972) indicate that mafic rocks are too impoverished in K_2O to yield volumetrically significant granodiorite, and that partial melting of mafic rocks yields quartz diorite, trondhjemite and low-K tonalite (<1% K_2O). Other experimental studies cited below indicate that tonalite and granodiorite are more suitable source rocks for the relatively potassic calc-alkaline granitoids in the SWEGP. Of particular interest are the results of Piwinskii and Wyllie (1968) and Piwinskii

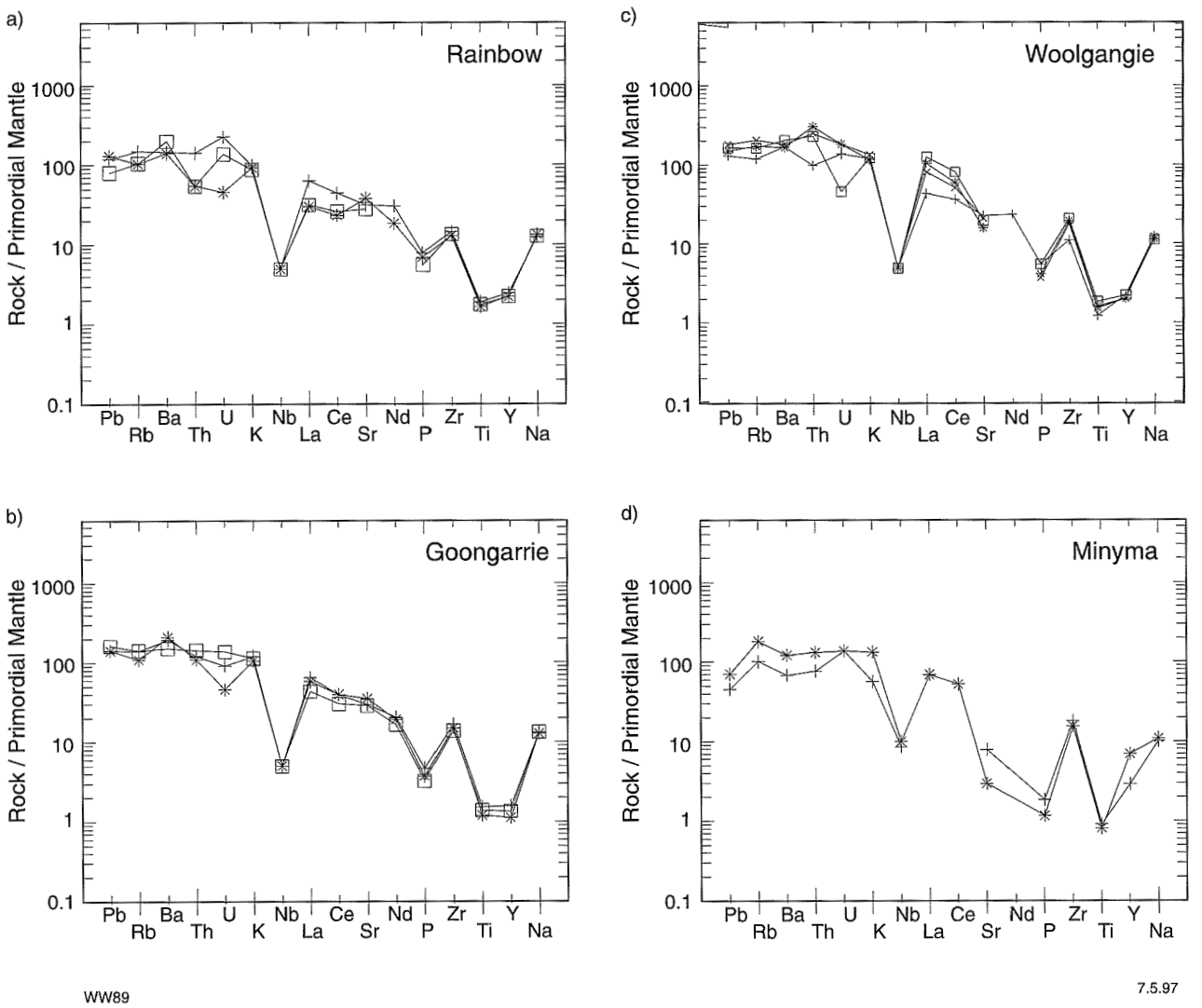

Figure 36. Mantle-normalized spidergrams, for least fractionated samples only, of selected calc-alkaline and alkaline granitoid (super)suites in the SWEGP: (a) Rainbow suite, samples 93901, 93904, 101363; (b) Goongarrie suite, samples 93903, 93906, 93907; (c) Woolgangie supersuite, samples 89950, 101373, 105903, 105904; (d) Minyma suite, samples 100945, 101359

Table 11. Summary of interpreted residual minerals in source rocks for granitoid suites and supersuites in the southwest Eastern Goldfields Province

Residual mineral phase	*Geochemical evidence for residual mineralogy*	*Suites and supersuites*							
		Rainbow	*Goongarrie*	*Twin Hills*	*Minyma*	*Woolgangie*	*Bali*	*Dairy*	*Liberty*
Hornblende and/or garnet	Negative Y anomaly on spidergrams	✓	✓	✓	–	✓	✓	–	✓
Plagioclase	Negative Sr anomaly on spidergrams	–	–	–	✓	–	–	✓	–
Ilmenite, ?rutile	Negative Ti, Nb anomalies on spidergrams	✓	✓	✓	✓	✓	✓	✓	✓
Apatite	Negative P anomaly on spidergrams	✓	✓	✓	✓	✓	✓	✓	✓

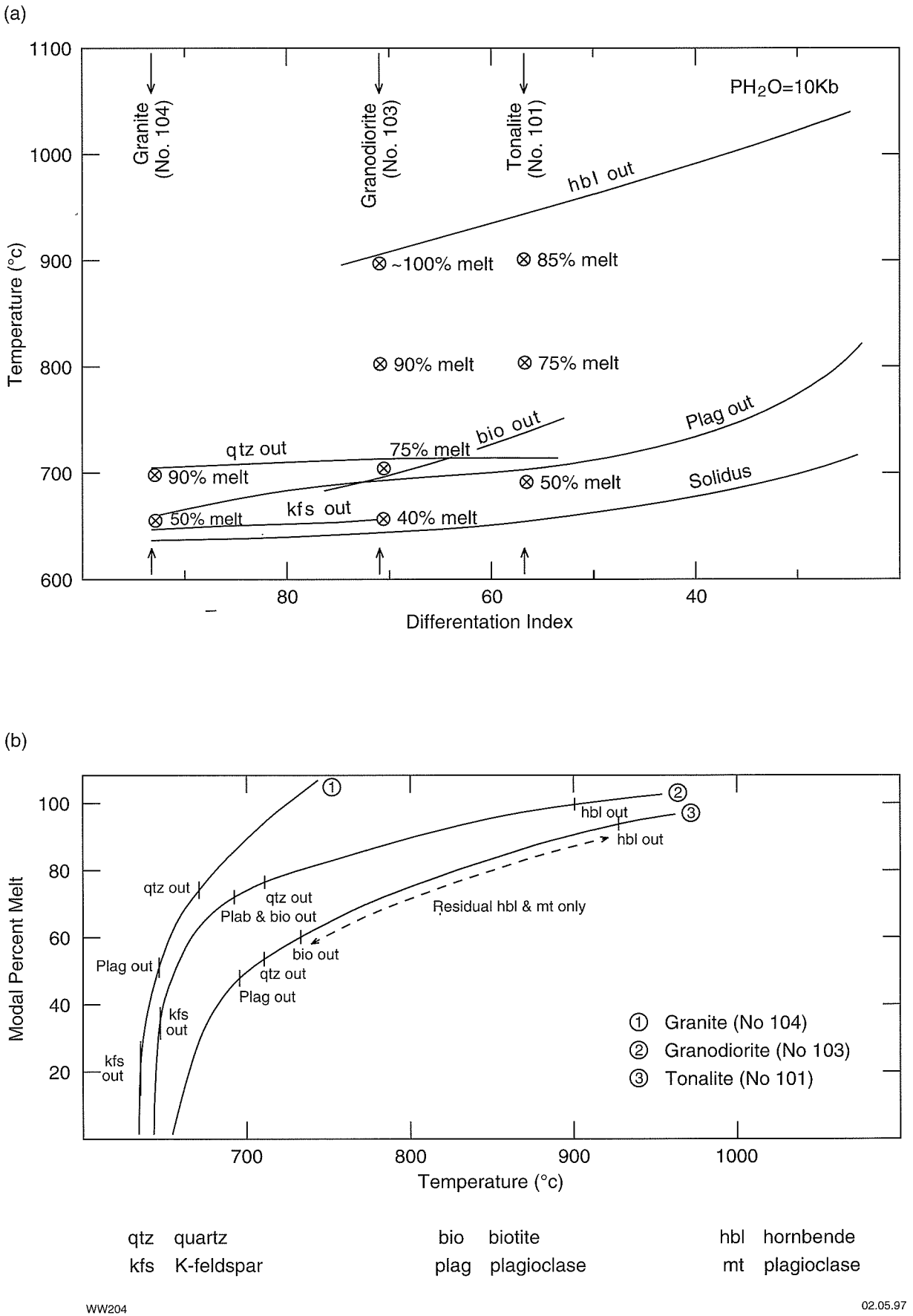

Figure 37. Diagrams showing the results of experimental melting of calc-alkaline granitoids from Sierra Nevada (modified from Piwinskii, 1973): (a) temperature versus differentiation index; (b) modal percent melt versus temperature

(1973), shown in Figure 37, which show that granodioritic to tonalitic rocks yield a large amount of melt for the first 100°C above the solidus, under vapour-saturated conditions. The SiO_2 contents of the early melts (approximately 75% SiO_2) decrease slowly to about 73% SiO_2 at 800°C, when the source rocks are less than 50% melted. Between 800° and 900°C, the percentage of melt formed increases only slowly, but the composition of the melt decreases to about 68% SiO_2, at 900°C.

In the following sections, the petrogenesis of chemically similar pre-RFG suites and post-RFG supersuites are discussed together to avoid repetition. Although some pre-RFG suites and post-RFG supersuites were derived from sources of broadly similar composition, it is not implied that the two are products of the same crustal source region.

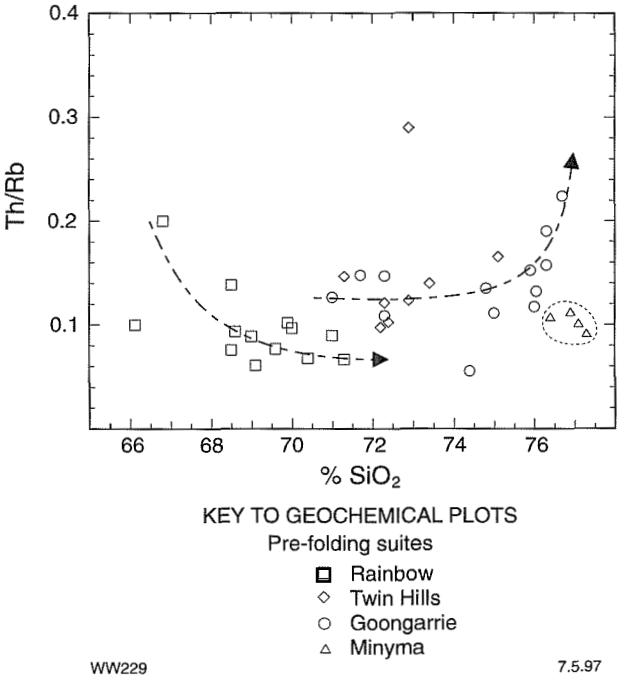

Figure 38. Th/Rb versus SiO_2 for pre-RFGs

Identification of source rocks for Y-depleted, Sr-undepleted, calc-alkaline granitoid suites

Rainbow suite and Liberty Granodiorite

The suggested parent melts for the pre-RFG Rainbow suite and post-RFG Liberty Granodiorite contain 67–68.5% SiO_2, 3–4% FeO* and about 7.5% Na_2O+K_2O (Table 10). Fractionated REE patterns and negative Y anomalies on spidergrams (Figs 25, 27 and 36) require hydrous melting of a tonalitic source rock in order to consume plagioclase and stabilize hornblende in the residue. Under vapour absent conditions, plagioclase is a stable residual phase (to near-liquidus temperatures) and, although hornblende (and garnet) are also residual phases at low melt temperatures, silica values exceed 70%. At the higher temperatures required for the requisite silica (e.g. 1050°C), hornblende and garnet are not residual phases under vapour-absent conditions (Rutter and Wyllie, 1988; Skjerlie and Johnston, 1992).

Hydrous melting of a tonalitic source rock, at 760–960°C and 10 kb, yields 70–80% melt of granodiorite composition, in equilibrium with residual hornblende and magnetite (but not plagioclase). At lower pressures (2–3 kb), temperatures above 900°C are needed to produce melts with about 68% SiO_2 (Piwinskii and Wyllie, 1968; Piwinskii, 1973).

Goongarrie suite and Twin Hills suite

Suggested parent melts for the Goongarrie and Twin Hills suites contain 71–72% SiO_2. The main differences in composition for these melts are the higher Al_2O_3 and alkalis of the Goongarrie suite, and the higher FeO* and Na_2O/K_2O of the Twin Hills suite. These differences are reflected, subsequently, in higher modal feldspar/biotite ratios in the Goongarrie suite.

These melts could have formed by hydrous melting of tonalite or granodiorite at 800–850°C and 10 kb, which yields 60 or 90% of calc-alkaline melt respectively, containing 71–72% SiO_2, and leaves residual hornblende (Piwinskii and Wyllie, 1968; Piwinskii, 1973). A similar melt may be produced by dehydration melting of tonalite (Skjerlie and Johnston, 1992). However, residual hornblende (and garnet) are only stable to about 950°C, and at lower temperatures it may be difficult to separate the small amount of melt produced (~30%) from the source region (Wickham, 1987; Rutter and Wyllie, 1988).

Compositional differences between parent melts for the two suites may reflect slight variations in source-rock composition, in melt proportions, or in fluid content (Carroll and Wyllie, 1989). Incompatible element ratios (e.g. Th/Rb; Fig. 38) for the two suites display considerable overlap, consistent with derivation from the same source rock under slightly different melting conditions. Lower Th/Rb ratios at comparable SiO_2 for most Rainbow suite granitoids suggest that the source for this suite was different to that which produced the Goongarrie and Twin Hills suites.

Woolgangie supersuite

The proposed Woolgangie supersuite parent melt is similar to that for the Goongarrie suite, but has a lower Na_2O/K_2O, and a monzogranitic composition. It may therefore have been derived by hydrous melting of a relatively potassic (?biotite-rich) granodiorite, at temperatures similar to those which produced the Goongarrie suite parent (800–850°C).

Identification of source rocks for Sr-depleted, Y-undepleted calc-alkaline granitoid suites (Minyma suite and Dairy supersuite)

The restricted SiO_2 ranges of the pre-RFG Minyma and post-RFG Dairy (super)suites require some other parameter be used to assess the relative degree of fractionation of samples within these (super)suites. K/Rb is used to assess the relative degree of fractionation for Dairy supersuite granitoids, and indicates that samples 98254 and 100924 most closely approximate the parent melt composition. The restricted range of K/Rb for Minyma suite granitoids renders this parameter inappropriate for determining relative fractionation, and Th/Sr has been chosen as a suitable alternative. Relatively low Th/Sr suggests samples 100945 and 101359 are least fractionated members of the suite.

High-SiO_2 melts are commonly attributed to fractional crystallization of larger volumes of less differentiated magma. However, least evolved members of the Minyma and Dairy (super)suites are not enriched in the incompatible elements Rb, Th and U (Fig. 26), and have low K/Rb and Sr/Rb, comparable to other high-SiO_2 (74–76%) granitoids in the study area (see especially 98254; Fig. 39). It is therefore concluded that the least evolved members of these suites reflect, reasonably accurately, the composition of the source.

Parent melts for the Minyma and Dairy (super)suites were high-SiO_2 (~76% SiO_2) liquids with low Ni, Cr, V, Sr and low Na_2O/K_2O. The Minyma suite parent melt had significantly greater FeO* than the parent Dairy supersuite magma, a feature that is reflected in the greater mafic mineral content, including hornblende, in samples 100945 and 101359.

High-SiO_2 parent melts of the Minyma and Dairy (super)suites may have formed by partial melting of fractionated igneous source rocks. Partial melting of a relatively fractionated, SiO_2-rich source rock, such as biotite monzogranite, avoids problems arising from the difficulty of removing the low volume of high-SiO_2 liquid that can be extracted from a tonalitic source rock. Experimental studies on hydrous melting of muscovite granite (74.7% SiO_2) indicate that, at 15 kb and low H_2O (<5 wt%), plagioclase is stable in the residue to temperatures of approximately 900°C (Huang and Wyllie, 1986), consistent with low Sr in these suites.

Although Minyma suite REE curves are not available, Dairy supersuite REE patterns are different to those of other calc-alkaline granitoid (super)suites. Weakly fractionated REE patterns and the absence of a negative Y anomaly on spidergrams suggest an absence of hornblende or garnet in the source rock. In the absence of residual hornblende or garnet in the source rock, accessory minerals can have a significant effect on the REE patterns. Thus, the relatively LREE-depleted, concave-upward curves of the Dairy supersuite may reflect the presence of

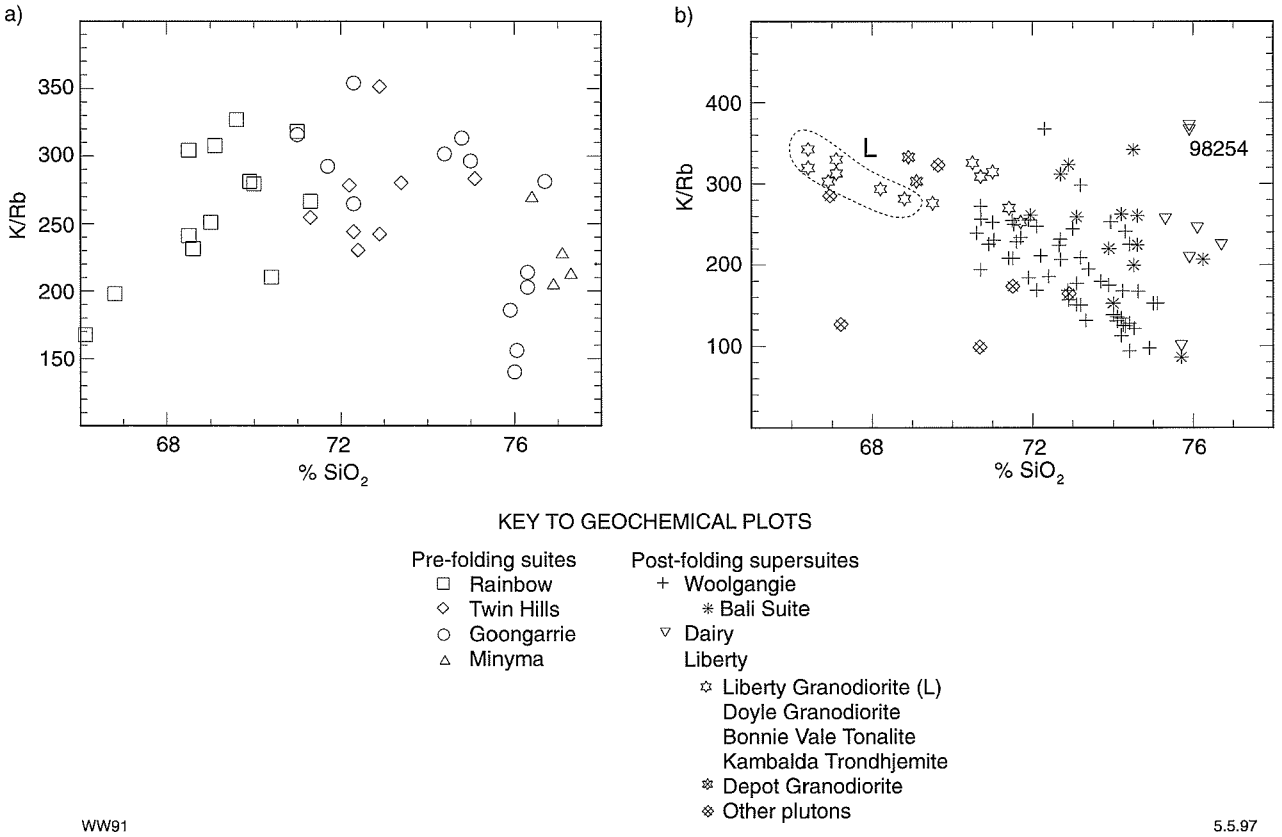

Figure 39. K/Rb versus SiO_2 for: (a) pre-RFGs, and (b) post-RFGs. Liberty Granodiorite (L)

residual apatite and/or titanite in the source, or if the source rocks are relatively felsic, residual monazite (Hanson, 1978; Hellman and Green, 1979).

Compositional variation within calc-alkaline granitoid (super)suites, excluding the Minyma and Dairy (super)suites — assessment of potential mechanisms

First-order compositional variation within granitoid (super)suites can be generated by the following processes: 1) restite separation, 2) progressive partial melting, 3) fractional crystallization, 4) magma mixing and crustal contamination, and 5) metamorphic/metasomatic processes.

Restite separation

Restite-retentive suites are two-component mixes of melt and restite (White and Chappell, 1977; Chappell et al., 1987). Compositional variation in these suites is caused by the relative degree of separation of the two components, which generates linear variation diagrams.

Some low-SiO_2 granitoids of the Rainbow suite and the Liberty Granodiorite contain a small proportion of clots of ferromagnesian minerals (biotite, hornblende), similar to those in microgranitoid xenoliths, which may represent restite (Chappell et al., 1987). However, there is no convincing evidence of a restite component in most SWEGP calc-alkaline granitoids. Calcic cores (approximately An_{30}) in some plagioclase grains are much less calcic than the restitic cores described by Chappell and co-workers (e.g. An_{80} for the Jindabyne suite; Hine et al., 1978) and are more likely to result from mixing of magmas (Hibbard, 1981), a complex growth history in the source region (Huppert and Sparks, 1988), or during ascent and crystallization of the host magma (Vance, 1965).

Well-defined linear trends on variation diagrams are not typical of most granitoid (super)suites in the SWEGP, even those that display possible evidence of a minor restite component (e.g. Figs 24 and 26). Strong, linear trends for only some elements are not diagnostic of restite-controlled suites (Wall et al., 1987).

It is therefore concluded that variable restite separation did not contribute significantly to compositional variation in calc-alkaline granitoid suites of the SWEGP.

Progressive partial melting

The contrasting behaviour of compatible and incompatible trace elements during partial melting and fractional crystallization yields distinctive trends on appropriate geochemical plots (Hanson, 1978). Figure 40 indicates that variable partial melting is an inappropriate or insufficient mechanism for the generation of any of the SWEGP granitoid (super)suites. Very high incompatible-element concentrations, such as those for Y, Nb, Rb, Th and U in SiO_2-rich Woolgangie supersuite granitoids, are normally ascribed to fractional crystallization because it is unlikely that very small partial melts would escape from their source region (Taylor et al., 1968; Halliday et al., 1991).

Fractional crystallization

Calc-alkaline granitoids in the SWEGP have many of the features that characterize fractionation-dominated suites (Wyborn and Chappell, 1986; Wyborn et al., 1992). These include the following:

1. The presence of small leucogranite intrusions (e.g. Mungari Monzogranite, Lone Hand Syenogranite), and many zoned plutons (e.g. Silt Dam Monzogranites, Depot Granodiorite, Liberty Granodiorite, Comet Vale Monzogranite, Menangina Monzogranite) suggestive of fractionation from the pluton margins inwards (Bateman and Chappell, 1979; Perfit et al., 1980). Although poorly exposed, zoned plutons are evident on aeromagnetic images.

2. Curved trends on variation diagrams, with moderate to extreme enrichment of incompatible elements (Rb, Th, U, Nb, Li, Y) for some suites (e.g. the Bali suite and Woolgangie supersuite; Figs 26h–j). For these (super)suites, K/Rb decreases with increasing SiO_2 (Fig. 39b). The scatter on variation diagrams, displayed by many SWEGP suites, is also typical of fractionation-dominated granitoid suites such as the Boggy Plains supersuite in the Lachlan Fold Belt (McCarthy and Hasty, 1976; Wyborn et al., 1987).

3. Rapid depletion of compatible trace elements with increasing SiO_2, which suggests that compositional diversity has been controlled by fractional crystallization of a mafic phase (or phases) and/or feldspars. Suites that display depletion of compatible elements but no significant incompatible-element enrichment (the Rainbow and Twin Hills suites, and the Liberty Granodiorite; Figs 24 and 26) probably underwent less than 40% (approximately) fractional crystallization (Hanson, 1978).

Trace-element modelling (Fig. 41) suggests that most granitoid compositions in the SWEGP can be explained in terms of various combinations of fractional and equilibrium crystallization, possibly superimposed upon progressive partial melting in the case of the Woolgangie supersuite. A semiquantitative aspect to the origin of the suites can be achieved by comparing the degree of enrichment of incompatible trace elements, according to the equation:

$$C_L/C_O = 1/F$$

where C_O and C_L are, respectively, the concentrations of an incompatible element (D = 0) in the least and most fractionated samples of a suite. D is the bulk mineral/melt

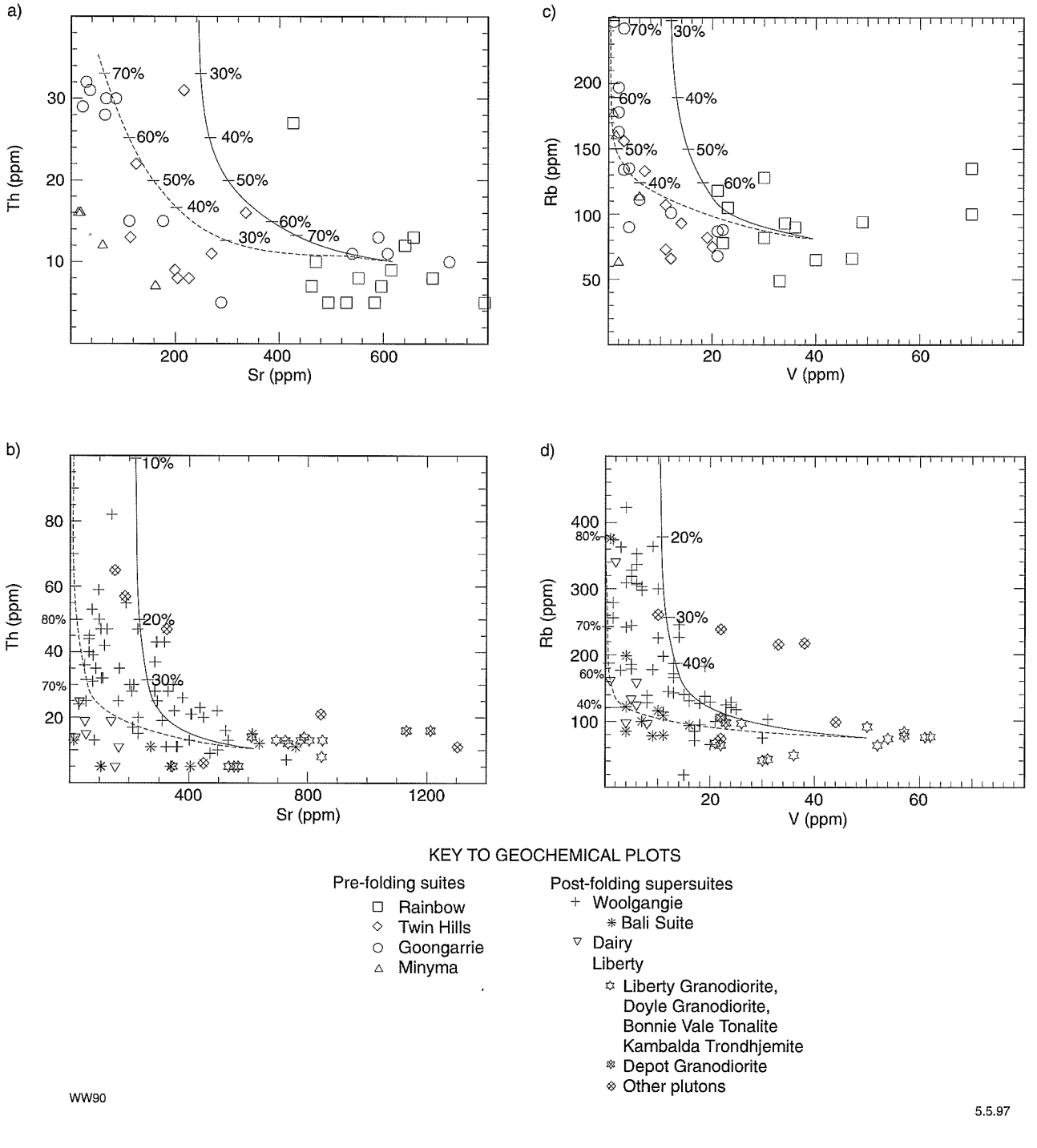

Figure 40. Incompatible versus compatible trace-element plots: (a) Th versus Sr for pre-RFGs; (b) Th versus Sr for post-RFGs; (c) Rb versus V for pre-RFGs; (d) Rb versus V for post-RFGs. Generalized trends for fractional crystallization (broken line) and partial melting (solid line) are shown. These trends are based on hypothetical source-rock compositions of 10 ppm Th, 600 ppm Sr, 50 ppm V, 75 ppm Rb, and bulk partition coefficients of 3.0 (Sr), 5.5 (V), and 0 (Th and Rb). Note that the partial-melting curve is also the equilibrium-crystallization curve, except that compositions move in the opposite direction with progressive crystallization

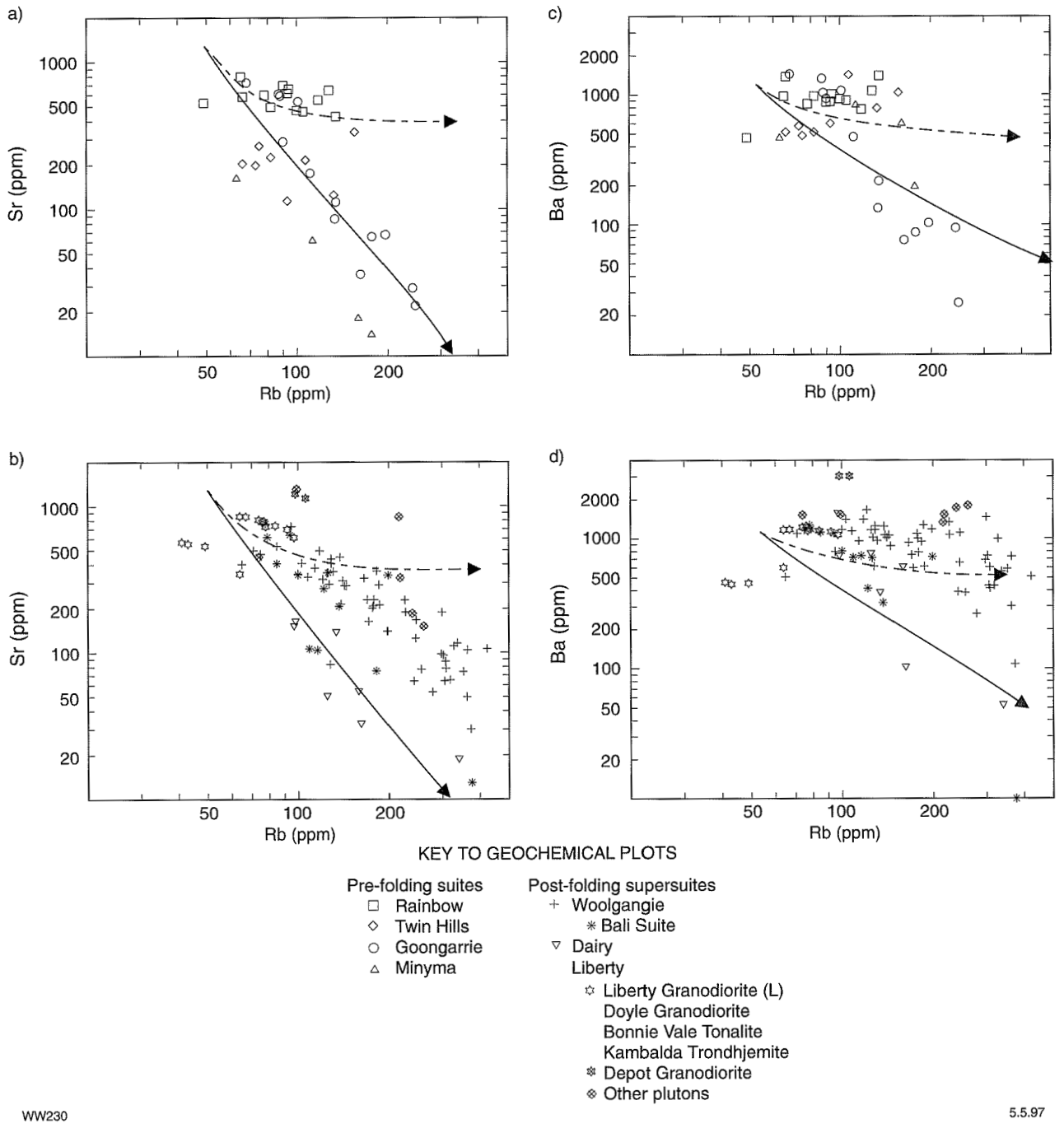

Figure 41. Log Sr versus log Rb plots and log Ba versus log Rb plots (after McCarthy and Hasty, 1976): (a) Log Sr versus log Rb for pre-RFGs; (b) Log Sr versus log Rb for post-RFGs; (c) Log Ba versus log Rb for pre-RFGs; and (d) Log Ba versus log Rb for post-RFGs. Trends shown are for equilibrium crystallization (broken line) and Raleigh fractional crystallization (unbroken line). The trends were modelled using a hypothetical source containing 1000 ppm Sr, 50 ppm Rb, 1000 ppm Ba, and bulk partition coefficients of 2.75 (Sr), 0.26 (Rb) and 2.0 (Ba), based on 30% K-feldspar and 50% plagioclase in the crystallizing assemblage and partition coefficients of McCarthy and Hasty (1976). Note that the trends are given only to indicate the relative importance of fractional crystallization of K-feldspar and plagioclase in various suites and are not intended to accurately model the petrogenesis of the granitoid suites

Table 12. Summary of minerals interpreted to have separated during fractional crystallization of Y-depleted granitoid suites and supersuites in the southwest Eastern Goldfields Province

Fractionating phase	*Geochemical evidence for fractionation*	*Rainbow suite*	*Twin Hills suite*	*Goongarrie suite*	*Liberty Granodiorite*	*Woolgangie supersuite*	*Bali suite*
Biotite	Decreasing MgO, FeO*, TiO_2, Ni, Nb, V, Ba, Zn	✓	✓	✓	✓	✓	✓
Hornblende	Decreasing MgO, FeO*, TiO_2, Cr, Ni, Y	✓	–	–	✓	–	–
Plagioclase	Decreasing CaO, Sr ± Al_2O_3	✓	✓	✓	✓	✓	✓
K-feldspar	Decreasing Ba	–	–	✓	–	–	–
Titanite	Decreasing TiO_2, Ce, La,	?✓	–	–	?✓	–	–
Magnetite	Decreasing V, Zn,	?✓	–	–	?✓	–	–
Apatite	Decreasing P_2O_5, Ce, La	✓	✓	✓	✓	✓	✓
Zircon	Decreasing Zr	–	–	✓	?✓	✓	✓

partition coefficient, and F is the proportion of melt left after the fractionating phases have separated. Using Rb and Th as examples of incompatible elements, it can be calculated that the Goongarrie suite underwent 65–70% fractional crystallization, compared with 75–90% for the Woolgangie supersuite.

Identification of fractionating phases

Some indication of the phases that separated during fractional crystallization of each (super)suite can be obtained by considering variation diagrams in the light of experimentally determined partition coefficients for trace elements (Hanson, 1978; Irving, 1978; Green, 1981; Mahood and Hildreth, 1983; Nash and Crecraft, 1985). Fractionating phases should also appear as texturally early minerals in the granitoids themselves. Mineral phases interpreted to have fractionated during formation of the Y-depleted calc-alkaline granitoid (super)suites in the SWEGP are shown in Table 12, together with the geochemical evidence for the interpretation.

Progressive depletion of TiO_2, FeO*, MgO, Ni and V with increasing SiO_2 (Figs 24b and 26a,b) indicates fractionation of a ferromagnesian mineral, probably mainly biotite, for most suites. Relatively rapid depletion of MgO and Ni in the Rainbow suite and Liberty Granodiorite may be partly related to biotite fractionation, but further suggests a role for clinopyroxene or, more probably, hornblende. The case for hornblende or pyroxene fractionation in the Rainbow suite is supported by the depletion of Cr. The apparent increase of K_2O with SiO_2 requires that biotite was not the main fractionating phase in the Rainbow suite.

Fractionation of plagioclase was important for all calc-alkaline (super)suites (excluding Minyma and Dairy). Relatively flat slopes on Sr and Al_2O_3 versus SiO_2 diagrams (Fig. 24a,f) suggest plagioclase was a less important component of the fractionating assemblage for the Rainbow suite and Liberty Granodiorite, compared with other suites. For the Rainbow suite, plagioclase appears to have begun crystallizing at approximately 68–69% SiO_2, and Sr was incompatible at lower SiO_2 levels. The absence of negative Eu anomalies on REE curves is an insufficient argument against plagioclase fractionation since Eu may exist as Eu^{3+} in these intrinsically oxidized magmas, and because fractionation of hornblende will tend to oppose depletion of Eu^{2+} by plagioclase separation. For the Rainbow suite and Liberty Granodiorite, rapid depletion of CaO may be partly related to hornblende, as well as plagioclase fractionation. K-feldspar fractionation is only evident for the Goongarrie and Woolgangie (including Bali) (super)suites, and only in rocks with SiO_2 greater than 73–74%. Variation diagrams for log concentrations of Ba and Sr, plotted against Rb (Fig. 41), following McCarthy and Hasty (1976), indicate that major fractionation (>50%) of two feldspars occurred only in the Goongarrie suite.

Trace- and major-element trends are consistent with a role for fractionation of several accessory mineral phases. Depletion of REE, especially LREE, in relatively fractionated members of the Rainbow, Goongarrie and Bali suites, is consistent with a role for fractionation of one or more of titanite, apatite and zircon. Rapid depletion of V and Zn is consistent with a role for fractionation of magnetite, another early crystallizing phase, in some suites. Mahood and Hildreth (1983) report strong partitioning of Zn into titanomagnetite in high-SiO_2 melts. Furthermore, trace chalcopyrite has been observed as tiny inclusions in magnetite in the Liberty Granodiorite.

Ilmenite is not considered a significant fractionating phase in any (super)suite, since Nb acts as an incompatible element in all suites.

K/Rb ratios in the pre-RFG suites

In contrast to the Woolgangie supersuite and the Liberty Granodiorite, pre-RFGs such as the Rainbow and Twin Hills suites do not display a negative correlation between K/Rb and SiO_2 (Fig. 39). K/Rb displays a weak positive correlation with SiO_2 for pre-RFG samples containing less than 74% SiO_2, but decreases rapidly at an SiO_2 content greater than 74% (Fig. 39a). The absence of a negative correlation between K/Rb and SiO_2 for the Rainbow and Twin Hills suites probably reflects the importance of biotite rather than feldspar fractionation. Bateman and Chappell (1979) attributed similar trends for K/Rb to the removal of biotite with low K/Rb. In the Tuolomne Intrusive Series, western U.S.A., K/Rb only decreased during the later stages of crystallization, when K-feldspar became a prominent fractionation phase.

Magma mixing and crustal contamination

Magma mixing and crustal contamination are treated together here because they both involve a two-component mixing system and, if unaccompanied by fractional crystallization, should generate consistent linear trends on variation diagrams. Magma mixing and crustal contamination commonly accompany fractional crystallization in granitoid petrogenesis (Barnes et al., 1986, 1990; Frost and Mahood, 1987; Sutcliffe, 1989; Smith et al., 1990). Some scatter on Harker variation diagrams for SWEGP granitoid suites may be related to a secondary role for crustal contamination, acting in conjunction with fractional crystallization.

Oxidizing trends in magmatic suites have been related to loss of H_2 through separation of an aqueous-rich volatile phase, whereas reducing trends have been interpreted to reflect incorporation of carbon, via assimilation of sialic crust (Wones, 1981). Thus, the reducing trends for the Goongarrie, Twin Hills and Woolgangie (super)suites are consistent with a role for crustal contamination in their petrogenesis. However, the role of crustal contamination can be difficult to prove in the absence of isotopic data, especially where there are multiple sources of contamination. Trace-element ratio plots, of the type devised by Langmuir et al. (1978), proved inconclusive when applied to the SWEGP granitoids.

Metamorphic and/or metasomatic fluid–rock interaction

Although broad geochemical coherence within suites suggests that metasomatic fluids have not significantly affected the composition of most samples, granitoids of the Bali suite invite special consideration. These granitoids acted as centres of thermal and fluid flux within a large-scale, synmetamorphic hydrothermal system, which deposited gold in contemporary, active structures (Witt, 1991). Bali suite granitoids are petrographically similar to Woolgangie supersuite granitoids, span a similar SiO_2 range, and display considerable overlap on many variation diagrams. However, there are systematic differences between the two suites for some elements, especially those that might be mobile in a metamorphic or metasomatic environment (Fig. 26). Na_2O and Sr are enriched, and K_2O, Rb, Th and U are relatively depleted in the Bali suite. K_2O, Rb, Th and U are enriched in alteration assemblages adjacent to auriferous structures in the greenstones (Witt, 1993b), suggesting the possibility that the synmetamorphic hydrothermal system mobilized these components from the Bali suite granitoids. There is no supporting petrographic evidence for metasomatism in Bali suite granitoids. However, high-temperature, synmetamorphic reactions would mainly involve the exchange of alkaline and alkaline-earth elements between plagioclase and alkali feldspars. Petrographic evidence for these reactions could be difficult to detect considering alteration was accompanied by progressive recrystallization in the regional stress field.

Compositional variation within the Minyma and Dairy (super)suites

The steep, nearly vertical trends on some Harker variation diagrams for the Minyma and Dairy (super)suites are unusual but similar to those for the garnet–muscovite granite suite in Ontario, Canada. Feng and Kerrich (1992) interpreted these trends to result from fractional crystallization of a high-SiO_2 magma. The Minyma and Dairy (super)suites present difficulties for interpretation, arising from two features. Firstly, the restricted range in SiO_2 content in both suites inhibits recognition of fractionation trends, a problem that is addressed above. Secondly, in both suites, there is a decoupling of elements (e.g. Ni and Cr) that are normally considered compatible in high-SiO_2 melts. This feature indicates that simple fractionation models are inappropriate for the Minyma and Dairy (super)suites.

Dairy supersuite

Strontium and Ba decrease, and Rb increases, with decreasing K/Rb in the Dairy supersuite, consistent with feldspar-dominated fractionation (Fig. 41, 42a). The granitoids are leucocratic, suggesting biotite and other ferromagnesian minerals were not significant fractionating phases.

Overall, Zr and Y increase slightly with decreasing K/Rb, consistent with their status as incompatible elements, but samples 101364 and 101367 are strongly enriched in these elements with respect to this trend (Fig. 42c,d). Data for Th, Zn and F are more scattered but could be similarly interpreted to indicate enrichment of these elements, above a poorly constrained fractionation

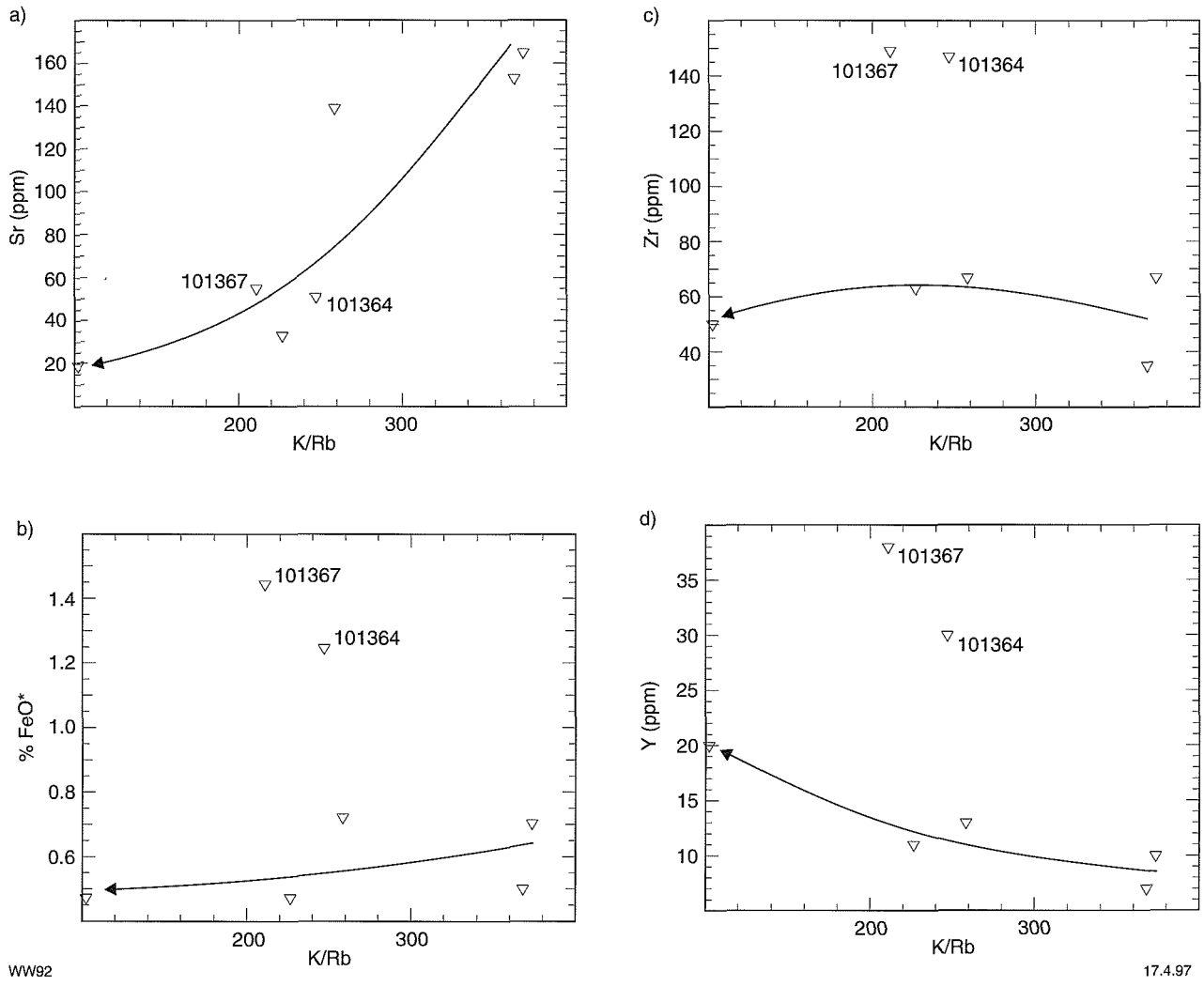

Figure 42. Geochemical plots for Dairy supersuite samples: (a) Sr versus K/Rb, (b) FeO* versus K/Rb, (c) Zr versus K/Rb, and (d) Y versus K/Rb. The solid line with an arrowhead indicates a probable fractional crystallization trend. Positive deviations from this curve reflect a second process, possibly contamination

curve, for samples 98256 and 98255, in addition to 101364 and 101367. The enrichment of Zr, Y, Th, Zn and F, to levels above the proposed fractionation trend, is tentatively ascribed to contamination of the melt. Some samples of granitoid gneiss in the SWEGP contain Th, Y, Zr and Zn concentrations comparable to enriched members of the Dairy supersuite, but more enriched sources of contamination have not been identified.

Titanium dioxide, FeO* and Cr are also variably enriched in some or all Dairy supersuite granitoids, especially 101364 and 101367 (e.g. Fig. 42b). These components would not be enriched by assimilation of predominantly monzogranitic gneiss. They may owe their enrichment to contamination by greenstones, xenoliths of which are common in granitoids from which samples 101364 and 101367 were collected. Although greenstone xenoliths were avoided when collecting geochemical samples, the mafic contaminant may be present as finely dispersed inclusions that have reacted with the granitoid melt to form ferromagnesian minerals.

Minyma suite

Interpretation of the origin of the Minyma suite is hindered by the low number of samples analysed. Mafic minerals are relatively common, suggesting biotite may have been an important fractionating phase, accounting for the restricted range of K/Rb ratios for the Minyma suite. Although Th/Sr has been chosen as an alternative monitor of relative fractionation, it is acknowledged that assimilation of a Th-rich crustal contaminant, similar to that implicated in the origin of the Dairy supersuite, would also increase Th/Sr.

Geochemical plots using Th/Sr as a monitor of fractionation could be interpreted in a similar fashion to that described above for the Dairy supersuite to indicate variable enrichment of Y, Ni and Cr above a fractional crystallization trend. The coarse biotite (± hornblende) clots in Minyma suite granitoids may reflect the presence of a relatively mafic contaminant, possibly partially equilibrated greenstone xenoliths.

Partial melting of a heterogeneous source region may provide an alternative model for the origin of the Minyma and Dairy (super)suites. Additional sampling and isotopic data are required to distinguish this model from the combined fractional crystallization and contamination model.

Relations among diverse pre-RFG suites

Wyborn et al. (1987) interpreted separate geochemical groupings of granitoids with similar SiO_2 contents to belong to a fractional crystallization-controlled supersuite (the Boggy Plains supersuite, Lachlan Fold Belt) derived from a single source. Geochemical groupings within the Boggy Plains supersuite reflect the distribution of different cumulus phases and intercumulus melt. For example, cumulate plagioclase-rich granitoids are enriched in Al_2O_3 and Sr, relative to liquid-rich samples with similar SiO_2. Similarly, MgO and Cr are enriched in cumulate hornblende and pyroxene. CaO does not show the same relationships as Al_2O_3 and Sr in the Boggy Plains supersuite because it enters pyroxene and hornblende as well as plagioclase.

Some similar relationships are evident on variation diagrams for pre-RFGs in the SWEGP (Fig. 24). For example, low-SiO_2 samples of the Goongarrie suite are enriched in Al_2O_3, Na_2O and Sr, relative to Twin Hills and Rainbow suite granitoids with similar SiO_2. Twin Hills suite granitoids are enriched in FeO* and Nb, relative to Goongarrie suite samples. These observations could be used to interpret low-SiO_2 Goongarrie suite samples as plagioclase crystal-rich cumulates, and Twin Hills suite granitoids as enriched in cumulus biotite, but belonging with Rainbow suite granitoids in a pre-RFG supersuite derived by partial melting of a single source rock. However, such interpretations are inconsistent with higher CaO in Twin Hills suite granitoids, relative to the Goongarrie suite (hornblende and pyroxene are not present in either of these suites, and CaO should follow plagioclase). Goongarrie suite granitoids have up to 80 ppm higher Zr than Rainbow and Twin Hills suite granitoids with similar SiO_2 (Fig. 24g), a feature that is difficult to account for by zircon accumulation in the Goongarrie suite. Furthermore, there is no reason to believe cumulus hornblende, biotite and plagioclase would accumulate separately in rocks with a similar SiO_2 content to form, respectively, the Rainbow, Twin Hills and Goongarrie suites. The conclusion is that each of the four pre-RFG suites were derived from compositionally distinct source rocks.

Relationships indicative of magma mixing among the calc-alkaline granitoid suites are not apparent. Isotopic studies are required to assess the possibility of magma mixing between crustal melts and a more mafic, mantle-derived magma in the source region during, or immediately after, partial fusion of the lower crust. Preliminary data (Hill et al., 1989, 1992a; Thom et al., 1991) indicate ε_{Nd} for all granitoids in the Eastern Goldfields Province lies between +2.09 and -2.4, significantly less than values for the depleted mantle at 2700 Ma (+4 to +5). These data suggest a dominantly or purely crustal source for SWEGP granitoids, with little or no input from mantle-derived melts.

Petrogenesis of the Gilgarna supersuite

Identification of source rocks for Gilgarna supersuite granitoids

Libby (1989) reported low initial $^{87}Sr/^{86}Sr$ ratios (0.7012–0.7014) for alkalic granitoids of the Gilgarna supersuite, and suggested they were derived from the mantle, or primitive mafic rocks within the lower crust. Fractionated REE curves suggest the presence of residual garnet or hornblende in the source. Most members of this suite display prominent negative Nb and Ti anomalies on chondrite-normalized spidergrams, suggesting the presence of a residual titaniferous phase. Although initial $^{87}Sr/^{86}Sr$ ratios are low, Gilgarna granitoids are enriched in alkalis, and Y/Nb is mostly between 1 and 3, suggesting a crustal or metasomatized mantle source (Eby, 1990). Comparable low initial $^{87}Sr/^{86}Sr$ ratios, and Y/Nb, are characteristic of the Habd-Aldyahee A-type granites, Saudi Arabia, which are interpreted to have formed by remelting of a depleted crustal source from which I-type granitoid melts have previously been extracted (Jackson et al., 1984; Eby, 1990).

Compositional variation within the Gilgarna supersuite

The Gilgarna supersuite shows a high degree of scatter on Harker diagrams, and nonsystematic variations for K/Rb with SiO_2 (Fig. 32), precluding a simple fractional crystallization relationship between granitoids of the supersuite. Low Ni and Cr suggest that individual plutons have fractionated one or more mafic phases, but collectively plutons of the supersuite cannot be related by fractional crystallization. Progressive partial melting of a uniform source and restite-controlled differentiation are also discounted as possible causes of intrasuite compositional variation, using criteria similar to those described for the calc-alkaline granitoid (super)suites. Libby (1989) described evidence for a metasomatic imprint on alkaline granitoids of the Eastern Goldfields Province, which may have contributed to the scatter on X–Y plots. The relative roles of variable source-rock composition, fractional crystallization, magma mixing and/or contamination, and metasomatism in generating compositional variation within the Gilgarna supersuite require more detailed studies, using a larger database than is presented here.

Petrogenesis of microgranitoid and gneiss-textured enclaves

Nature of the enclaves

Greenstone xenoliths in granitoid intrusions are interpreted herein as accidental xenoliths, incorporated by magmatic stoping. Bettenay (1977) considered monzogranitic to granodioritic gneiss-textured enclaves in post-RFG intrusions to be accidental xenoliths, equivalent to more extensive outcrops of granitoid gneiss shown in Figure 2. Tonalitic granofels was considered as restite.

The more mafic (tonalitic) gneiss xenoliths are not readily correlated with any units in the immediate country rocks and may have been incorporated as accidental, lower to mid-crustal xenoliths during ascent of the host magma. Alternatively, they may be relatively refractory portions of the source region incorporated as a restitic component prior to ascent of the host magma.

Microgranitoid xenoliths do not have compositional equivalents in the country rocks, and there is no evidence to sustain an argument that they are accidental greenstone xenoliths that have been modified by reaction with the host granitoid melt. They are interpreted as cognate xenoliths formed by injection of a mafic to intermediate magma into the incompletely crystallized host granitoid magma (i.e. they have a synplutonic origin). The texturally complex xenolith sample 101019, at Cement Well, probably represents a solid-state xenolith incorporated into hornblende(–clinopyroxene)–quartz monzodiorite melt represented by the microgranitoid-textured domain.

Petrographic evidence for comagmatic mafic and felsic melts

This section assesses the petrographic evidence for the synplutonic origin of microgranitoid dykes and xenoliths in granitoids of the SWEGP. A synplutonic origin involves the injection of the microgranitoid magma into the incompletely crystallized host granitoid magma and hence mingling of two compositionally different magmas. The integrity of the enclaves is retained due to viscosity contrasts between hot enclave magma and cooler host granitoid magma. If thermal equilibration between the two magmas is approached, the viscosity differences are minimized and mixing may occur (Frost and Mahood, 1987).

Although outcrop-scale evidence for large-scale magma mingling and dispersal of xenoliths and dykes, (cf. Walker and Skelhorn, 1966; Frost and Mahood, 1987; Sutcliffe, 1989) is rare in the SWEGP, there is some structural and textural evidence for limited interaction between synplutonic enclave magmas and host granitoid melts.

Dispersal of synplutonic dykes

The most direct evidence for mingling of comagmatic mafic and felsic melts is at Granite Dam where a synplutonic, relatively mafic dyke displays evidence of plastic deformation, disaggregation and dispersal (Figure 2.1a–c, Appendix 2). Elsewhere (e.g. at Goongarrie), a close spatial association suggests many microgranitoid xenoliths may have formed by such disaggregation of synplutonic dykes. Not all microgranitoid xenoliths are spatially associated with synplutonic dykes, but Bacon (1986) and Frost and Mahood (1987) described a variety of mechanisms by which globules of relatively mafic magma can become entrained within a crystallizing granitoid melt.

Gross shape and fabric of enclaves

The gross shape of many enclaves suggest a low viscosity contrast with the host granitoids during emplacement (Figure 2.1, Appendix 2). All microgranitoid xenoliths appear well rounded on outcrop surfaces, in contrast to the angular shapes of most accidental xenoliths. Some rounded xenoliths are extremely thin in the third dimension (pancake-shaped) while retaining only a slightly modified igneous texture. Cuspate to delicately convoluted contacts between microgranitoid enclaves (including some dykes) and host granitoid are common. Some enclaves display a higher degree of deformation and recrystallization compared to the host granitoid. Anomalously high-strain textures and recrystallization in synplutonic dykes and microgranitoid xenoliths are attributed to stress imposed by movements of the incompletely crystallized host granitoid magma (Foster and Hyndman, 1990). However, very strongly deformed and recrystallized (gneiss-textured) xenoliths (e.g. samples 93905, 101390) were more probably entrained as solid xenoliths, incorporated into the granitoid magma, either in the source region or during ascent.

Evidence for quenching of hot enclave magmas against cooler host magmas

Clinopyroxene forms a thin (about 1 mm), discontinuous, monomineralic selvage or rind against the host granitoid at the margin of a clinopyroxene–hornblende diorite dyke at Cement Well. In this dyke, relict clinopyroxene in hornblende is coarsest and most abundant adjacent to thin felsic bands (mainly K-feldspar) interpreted as microveinlets of modified host granitoid magma. At the same locality, a similar rind of clinopyroxene partially envelopes a hornblende diorite xenolith, which otherwise contains only minor clinopyroxene. These observations suggest that clinopyroxene was stabilized (with respect to hornblende) where there was intimate contact between the enclave-forming melt and the host melt. Poli and Tommasini (1991) interpreted similar observations to result from rapid freezing of the more mafic magma globule margins, and subsequent fractionation in situ of the xenolith melt, from the margins inwards. Early-formed clinopyroxene became unstable again, with respect to hornblende, during later stages of enclave crystallization, although monomineralic

rinds were insulated to some degree from further reaction with the microgranitoid melt by an intervening layer of hornblende.

Acicular apatite occurs as inclusions in quartz and plagioclase in microgranitoid xenoliths, but not in the host granitoids (Figure 3.1a, Appendix 3). Acicular apatite in enclaves has also been attributed to quenching of the enclave magma after coming into contact with the relatively cool host granitoid magma (Vernon, 1984).

Modification of modal composition of host granitoid adjacent to microgranitoid enclaves

Some granitoid samples collected adjacent to xenoliths and synplutonic dykes are modally distinct from samples collected several metres or more from these bodies. For example, granodiorite (101375) adjacent to a hornblende–quartz diorite xenolith (101376) at Boundary Well is enriched in hornblende, and depleted in quartz. At Cement Well, granodiorite (101016) adjacent to a synplutonic clinopyroxene–hornblende diorite dyke is enriched in plagioclase and depleted in K-feldspar. It also contains clinopyroxene relicts within hornblende, whereas clinopyroxene is not present in the bulk of the granodiorite. These observations suggest that, although microgranitoid xenoliths, dykes and host granitoids remain physically distinct on an outcrop scale, there has been limited diffusion of chemical components from the enclaves, into the host granitoid, for up to several metres from the granitoid/enclave contact.

Incorporation of host magma and phenocrysts into microgranitoid enclaves

Some microgranitoid xenoliths and synplutonic dykes display irregular, pink to white, leucocratic patches and discontinuous veinlets (typically <3 mm wide and <1 mm long), composed mainly of quartz and K-feldspar (Figure 3.1e,f, Appendix 3; e.g. 89916B, Scotia Bore; 101085, Boundary Well; 101016, 101017, Rainbow Bore). The texture of these irregular bodies varies from hypidiomorphic (igneous) to granoblastic or allotriomorphic (?recrystallized). These leucocratic segregations are interpreted as modified host granitoid melt that infiltrated the more mafic melt while it was still incompletely crystallized (Eberz and Nicholls, 1988). In addition, rare K-feldspar megacrysts, similar to those in the host granitoid, occur in some enclaves, and are interpreted as xenocrysts that were incorporated during the mingling of comagmatic mafic and felsic melts (Eberz and Nicholls, 1988; Holden et al., 1991; Poli and Tommasini, 1991).

Disequilibrium textural features

Several textural features, which are commonly attributed to magma mixing, have been observed in microgranitoid xenoliths, synplutonic dykes and in host granitoid samples.

A range of felsic ocelli, to about 2 mm across, occur mainly in enclaves but also in host granitoids (e.g. 93907, Credo). Some ocelli are composed essentially of quartz surrounded by a narrow, hornblende-rich selvage (Figure 3.1c, Appendix 3; e.g. 101383A). Others are composed of feldspar (± quartz) that is texturally similar to feldspar in the surrounding enclave, but relatively leucocratic because it is depleted in mafic mineral (mainly hornblende) inclusions (Figure 3.1b, Appendix 3; e.g. 101379, 101380, Rainbow Bore). Ocelli similar to those described here have been attributed to mixing or mingling between relatively mafic and felsic magmas by, amongst others, Walker and Skelhorn (1966), Goldie (1978), Cantagrel et al. (1984), Barnes et al. (1986) and Barbarin (1988).

A few grains of plagioclase have a complex internal structure, including calcic cores and oscillatory-zoned margins. These textural types have been observed in granitoids, dykes (101023) and microgranitoid xenoliths. Cores may be rounded (101023), or irregular (skeletal or resorbed), giving rise to patchy zoning and patchy extinction (101376, 101084, 101033). These textures suggest disequilibrium processes during the growth of plagioclase. One possible origin involves undercooling of a relatively mafic magma, following contact with a cooler, felsic magma (Walker and Skelhorn, 1966; Hibbard, 1981).

Rare grains of plagioclase in some calc-alkaline granitoids are mantled by K-feldspar (e.g. 101359). Although other mechanisms have been proposed, Hibbard (1981) has suggested this relationship can be attributed to magma mixing. Rare rapakivi texture (plagioclase mantles on K-feldspar) has also been observed in some calc-alkaline granitoids in the SWEGP (e.g. 98248, 101083). Similarly, two-stage growth of K-feldspar is suggested by the uncommon occurrence of euhedral overgrowths on rounded cores, or irregular overgrowths on euhedral cores (43596, Goongarrie). Rapakivi texture has been attributed to magma mixing by Hibbard (1981) and Cantagrel et al. (1984), although other mechanisms are also possible (Elders, 1968; Stull, 1979).

Geochemical evidence for the origin of microgranitoid enclaves

Dykes and xenoliths have a wide variety of compositions, resulting in scatter on most geochemical plots. Gneiss-textured xenoliths may have been incorporated from various levels of the crust during magma ascent and would not therefore be expected to display geochemical coherence. On the other hand, synplutonic magmas represented by microgranitoid dykes and xenoliths represent a single magmatic event and may therefore be genetically related. Before attempting to interpret the roles of fractionation and source-rock chemistry on the composition of the microgranitoid enclaves it is necessary to assess the degree to which mingling with the host granitoid magma has modified the original composition of the enclaves.

Effect of enclave–host magma interaction on compositions of microgranitoid xenoliths

Holden et al. (1991) assessed the effects of magma mingling on the composition of microgranitoid xenoliths in the Strontian and Criffel plutons, Scotland, by plotting compositions of xenoliths against those of host rock samples. Positive linear correlations were interpreted as the dependence of the concentration of that element in the xenoliths on that within the host, because the granitoid was viewed as an effectively infinite chemical reservoir with respect to xenoliths for the element under consideration. In this study, similar plots for granitoids and xenoliths from the same locality produce steep to vertical trends, parallel to the xenolith axis for most elements, suggesting that the xenolith compositions are largely independent of host granitoid composition (Fig. 43). However, positive correlations were noted for Th, Sr, Li and Zr (excluding xenoliths with Zr >200 ppm). These results contrast with those of Holden et al. (1991) who found the best correlations for K, Rb, Sr and Pb, and poor correlations for Zr.

The results of Holden et al. (1991) probably reflect, at least partly, incorporation of K-feldspar and plagioclase phenocrysts from the host granitoid into the more mafic magma globule that crystallized to form a microgranitoid xenolith. In the SWEGP, K-feldspar megacrysts in xenoliths are relatively uncommon, and were avoided in samples collected for whole-rock analysis. Plagioclase and quartz phenocrysts in the analysed xenoliths are smaller and more common than K-feldspar megacrysts. It is concluded that Sr in the enclaves is at least partly controlled by the physical entrainment of plagioclase crystals from the host granitoid into the enclave magma, but that apart from Sr, Li and possibly Zr, enclave compositions have not been significantly affected by interaction with the host granitoid.

Potential effects of enclave heterogeneity on chemical analyses

Bacon (1986), Eberz and Nicholls (1988, 1990) and Poli and Tommasini (1991) documented chemical zoning from the margins inwards of mafic magmatic enclaves related to fractional crystallization of the enclave magma. Eberz and Nicholls (1990) cautioned that biased sampling of thin enclave margins will yield unrepresentative trace-element data, and scatter of data towards SiO_2-poor compositions. Petrographic observations described above indicate that some microgranitoid xenoliths have narrow cumulate-(pyroxene-) rich margins. Geochemical sample sizes are much greater than the volume represented by mafic-rich margins but none of the samples involve the entire volume of the enclave. If significant inwards fractionation of the enclave magma occurred, some of the scatter on geochemical plots may be caused by unrepresentative sampling of heterogenous enclaves. However, field observations suggest that enclaves in the study area are not markedly heterogeneous beyond the cumulate-rich margins.

Petrogenesis of microgranitoid enclaves

Chemical evidence indicates that the microgranitoid enclaves are not restitic (Fig. 32). Although the compositions of the enclaves (high F, low K/Rb) could be compatible with an origin by disruption of less fractionated, biotite- and apatite-rich marginal zones of plutons (Didier, 1973; Wall et al., 1987), there is no evidence that such zones exist in the relevant plutons and complexes. Instead, the enclaves are interpreted to represent synplutonic magmas that were emplaced into the incompletely crystallized host granitoids.

Source rocks for xenoliths and dykes

The weakly alkalic composition and low SiO_2 contents of most xenoliths and dykes suggests derivation by partial melting of a mantle source. Primitive mantle-derived melts should have an Mg number of 70–74, 250–350 ppm Ni and 500–600 ppm Cr (Cox et al., 1979; Perfit et al., 1980). The relatively low Mg number (Fig. 44), and Ni and Cr abundances for xenoliths and dykes suggest they are not primitive melts. Even the least evolved xenolith compositions (high Mg number, low SiO_2) require fractionation of olivine±pyroxene from a mantle-derived melt. For example, a primitive, mantle-derived melt would have to fractionate approximately 20% olivine in order to reduce Ni contents from 300 to 176 ppm (the Ni content of sample 101357). Note that Cr contents for 101357 approximate those of primitive, mantle-derived melts. Most other xenoliths with a relatively high Mg number (~58) are depleted in both Cr and Ni, requiring fractionation of pyroxene and olivine.

Pearce (1982, 1983) used spidergrams, normalized to average mid-ocean ridge basalt (MORB), to help distinguish various sources for basaltic to andesitic rocks. Fractional crystallization and variable partial melting of a uniform mantle source will not significantly alter the shape of the MORB-normalized spidergrams (Pearce, 1983). The effects of fractional crystallization, and other magma-modifying processes, can be minimized by selectively studying the most primitive samples (high Mg number with low SiO_2). Samples 101357 and 101374 are selected as best fitting these criteria (note that the gneiss-textured xenolith 93902 also fits these criteria). These samples belong to the group with negative Ba anomalies on chondrite-normalized spidergrams. Spidergrams for these least-evolved samples (Fig. 45) are similar to those for shoshonitic and other volcanic rocks erupted at active continental margins on thickened continental lithosphere (Pearce, 1982, 1983). This geochemical signature is believed to incorporate two components. Enrichment of Sr, K, Rb, Ba and Th is probably related to incorporation of a subducted sedimentary component into the source (Pearce, 1983). Relatively high concentrations of REE (Ce, Sm), P, Zr and Nb are understood to reflect an enriched (metasomatized) mantle source. Negative Nb anomalies have been attributed to the enhanced stability of ilmenite or rutile in the subduction-zone environment (Saunders et al., 1980) but this interpretation is controversial (Green and Pearson, 1987; Ryerson and Watson, 1987). The elevated

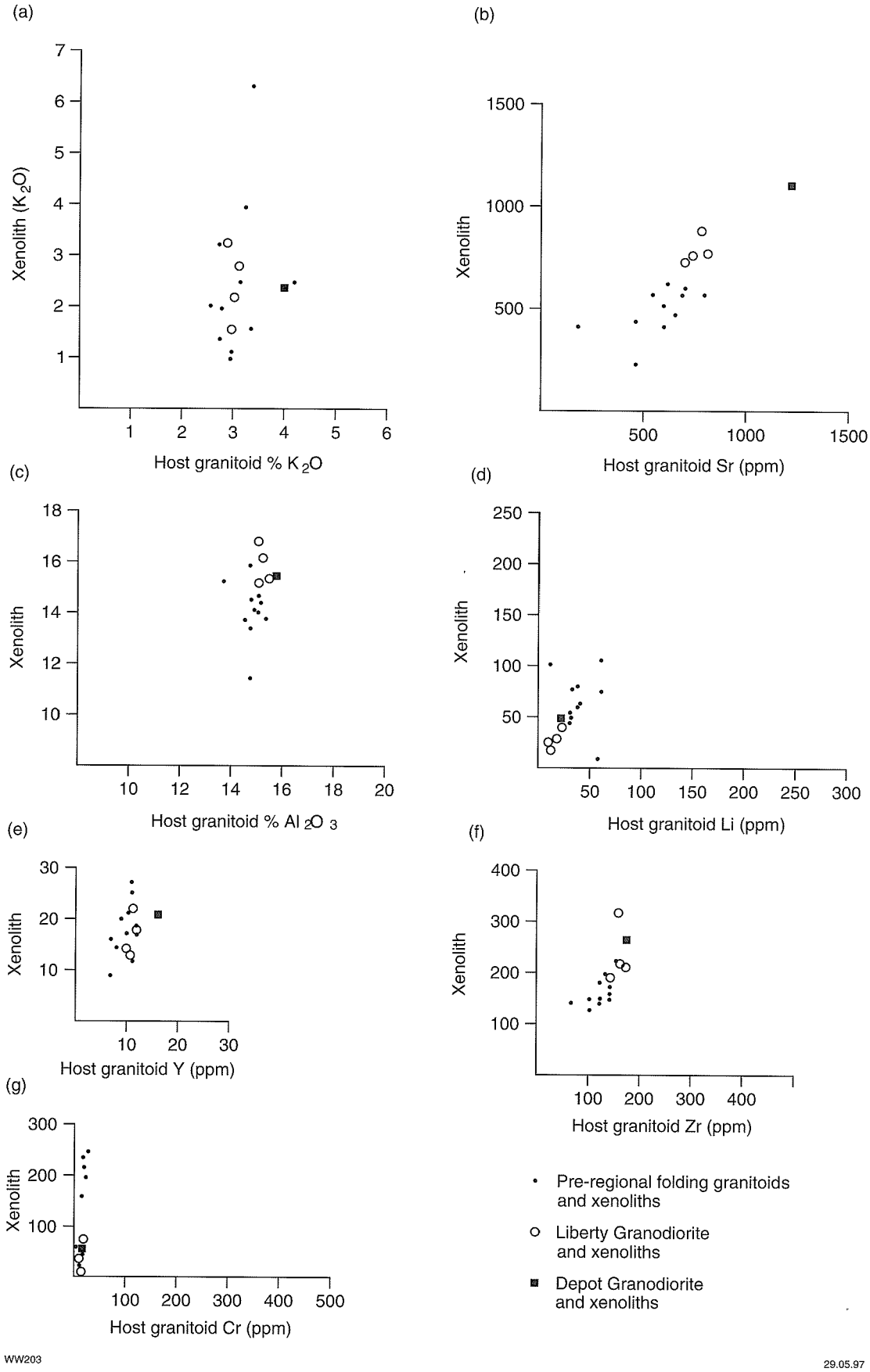

Figure 43. Whole-rock compositions for microgranitoid xenoliths plotted against composition of host rocks at the same locality (after Holden et al., 1991)

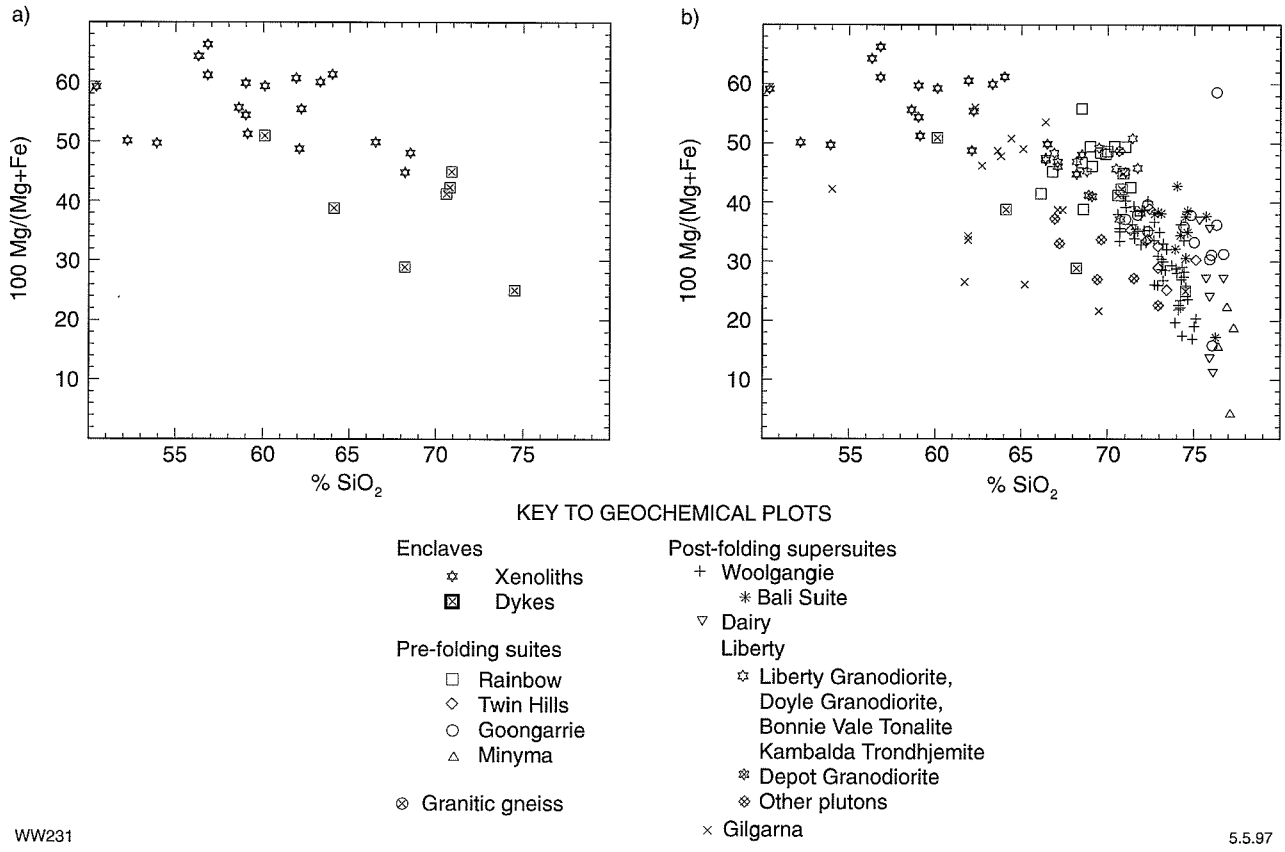

Figure 44. (a) Mg number (100 Mg/(Mg+Fe)) versus SiO_2 for dykes and xenoliths, (b) same plot as for (a) with the addition of calc-alkaline granitoid suites of the SWEGP

P, F and LREE contents of the microgranitoid xenoliths suggests a modally metasomatized mantle source, similar to that which underlies parts of eastern Australia, containing various combinations of apatite, amphibole, spinel, clinopyroxene and mica in veins (Wass, 1979; Wass and Rogers, 1980). The negative Ba anomalies on MORB-normalized spidergrams for the least-evolved xenoliths could reflect fractionation of barium-enriched titanite (Haggerty et al., 1983) at mantle depths, or enrichment of Th from the host granitoid magma as a result of synplutonic mingling.

Compositional variation among the dykes and xenoliths

Progressive partial melting: Incompatible-element versus compatible-element diagrams present some apparent partial-melting curves. However, the curves are 'pseudo partial-melting curves' because the same groups of samples do not define similar trends on other plots (e.g. Th versus Sr, Rb versus Cr).

Restite-controlled differentiation: Mafic aggregates and clots, up to several millimetres across, of ragged hornblende and/or biotite(–magnetite–apatite–titanite–relict cores of clinopyroxene in hornblende) are common in most xenoliths and some dykes. The forms of apatite and titanite in the clots differ from those of the same minerals outside the clots. Apatite forms large, stubby, lozenge-shaped crystals, up to 2 mm across, in contrast to the acicular inclusions in quartz and plagioclase. Titanite is anhedral and interstitial to hornblende, in contrast to the euhedral rhombs that form elsewhere in the xenoliths. These observations indicate that there are two generations of these minerals in the enclaves, and suggest that the minerals in the mafic clots were transported from deeper crustal levels as solid phases. The clots were originally interpreted by Witt and Swager (1989) as restite (refractory minerals from the source rock that became entrained within the mafic melt). However, the clots may alternatively represent aggregates of early-formed phases that crystallized from the melt.

Compositional variation among the enclaves, as a group, is not controlled by restite separation because the appropriate linear trends are not evident on variation diagrams (e.g. Figs 30 and 46).

Fractional crystallization: The broad inverse relationship between Mg number and SiO_2 (Fig. 44) reflects the relative degree of fractionation required to produce the enclave magmas. Fractionation of clinopyroxene, hornblende, magnetite and apatite was responsible for the inverse correlation between SiO_2 and Mg number, TiO_2, FeO*, MgO, CaO, P_2O_5, F (in apatite) and V on Harker variation diagrams (Figs 30a,c,f and 44). In a general sense, relatively evolved xenoliths (Mg number ~58) are enriched

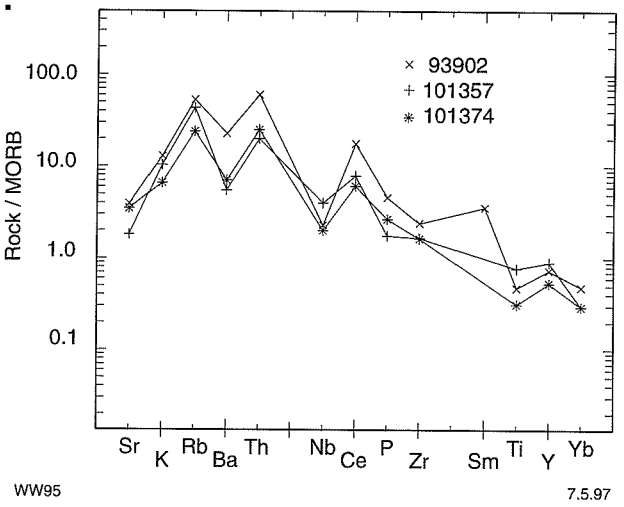

Figure 45. MORB-normalized spidergrams (after Pearce, 1983) for primitive microgranitoid xenolith samples 93902, 101357 and 101374

in K, Rb, Ba and Th, a feature that can reasonably be attributed to fractional crystallization. Although there is some overlap, dyke compositions are commonly more evolved than those of xenoliths. However, plots of Mg number versus Th, Y and Zr are not consistent with synplutonic dykes (excluding 101383) having evolved from xenolith magmas by fractional crystallization (Fig. 46).

Causes of variable SiO_2 at constant Mg number: The marked variation of SiO_2 in less evolved microgranitoid xenoliths (Mg number ~ 58; Fig. 44) must reflect some process other than fractional crystallization. Possible mechanisms are contamination with crustal material (excluding the host granitoid), melting of variably metasomatized mantle, and melting of the mantle at different depths (Frey et al., 1979; Shirey and Hanson, 1984).

The role of crustal contamination can be assessed by plotting Th/Ni against SiO_2 (Fig. 46d). Fractional

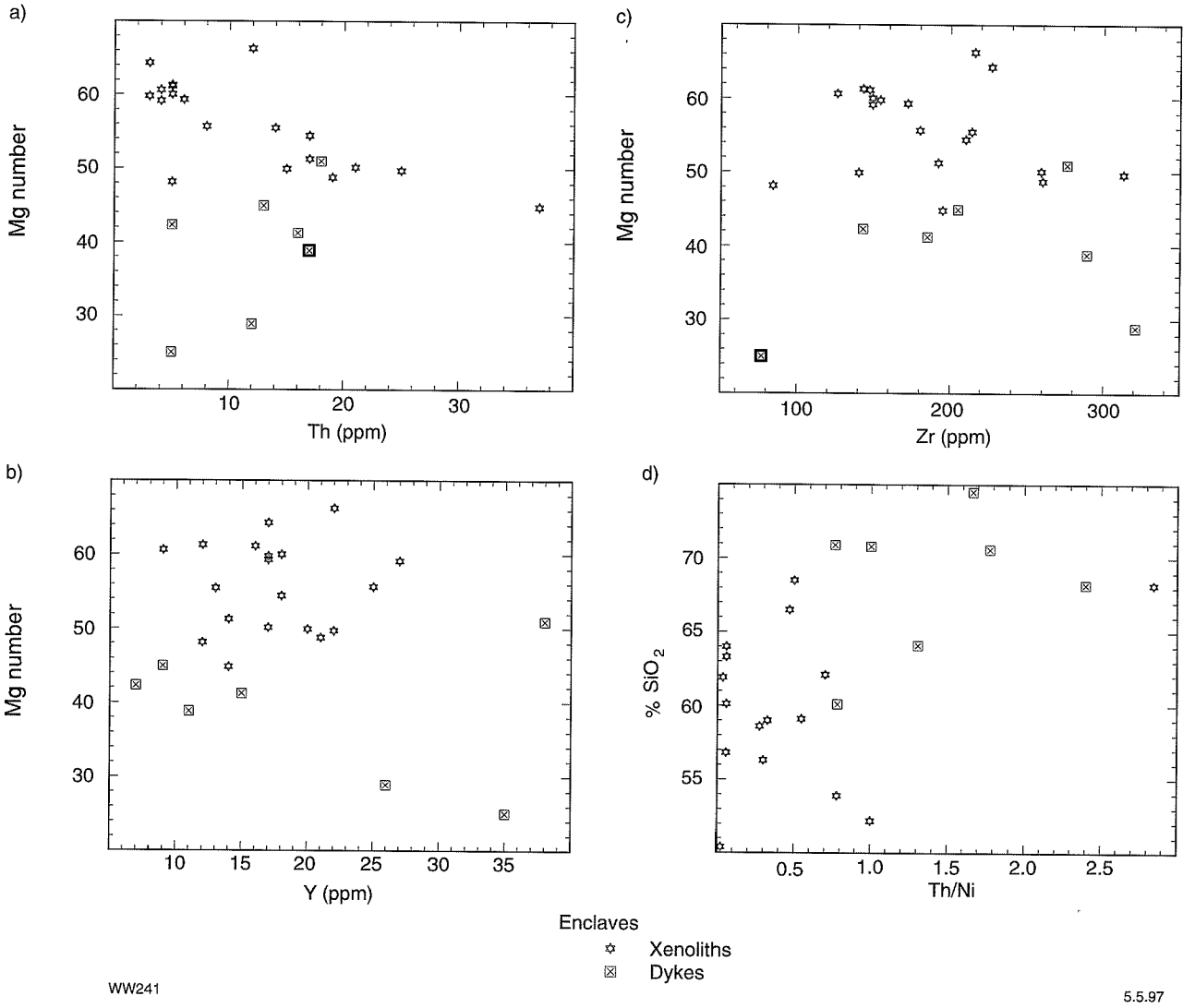

Figure 46. Whole-rock compositions for dykes and xenoliths: (a) Mg number versus Th, (b) Mg number versus Y, (c) Mg number versus Zr, (d) SiO_2 versus Th/Ni

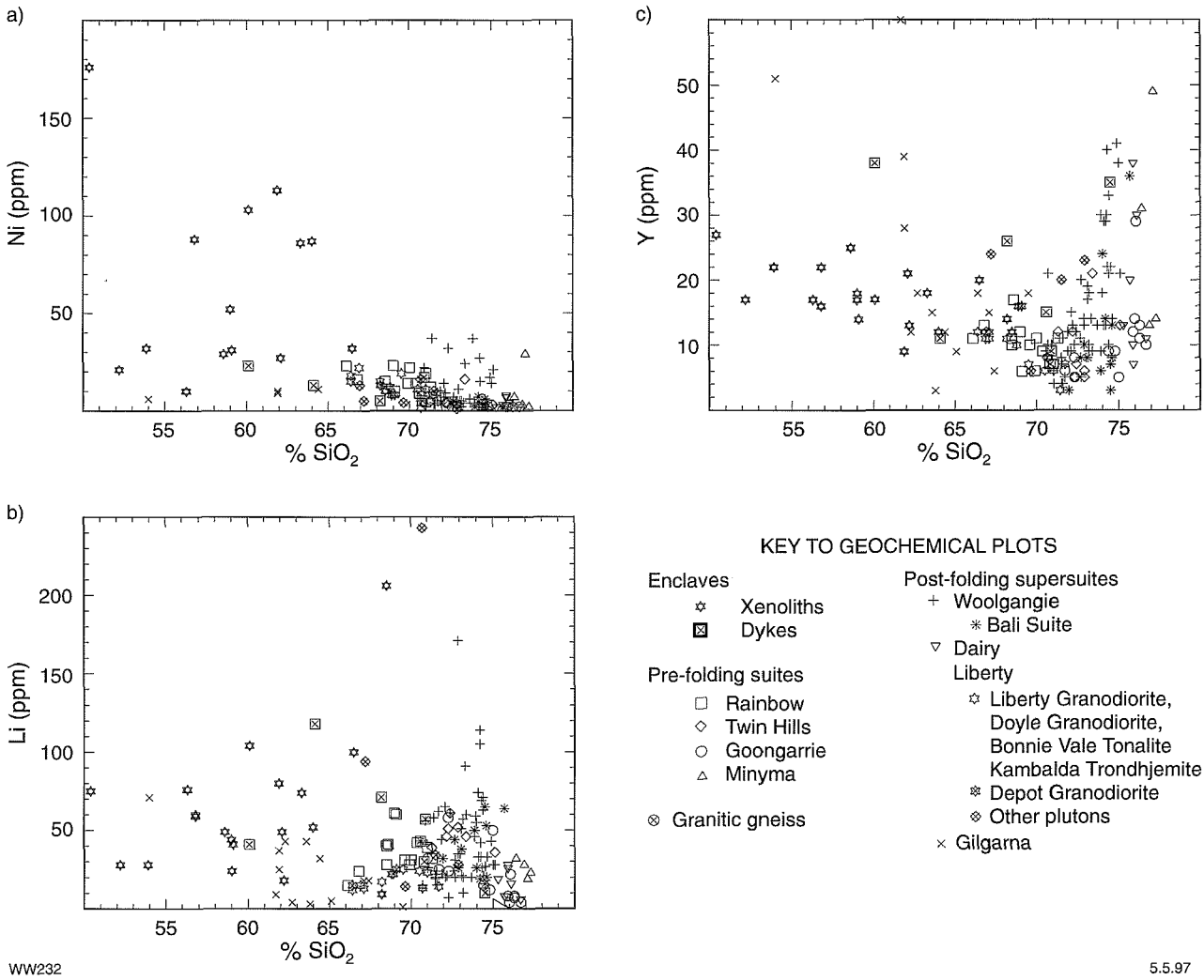

Figure 47. Whole-rock compositions for dykes, microgranitoid xenoliths and granitoid (super)suites: (a) Ni versus SiO_2, (b) Li versus SiO_2, (c) Y versus SiO_2

crystallization and crustal contamination should both produce a positive correlation on this plot. However, high SiO_2 samples do not have consistently higher Th/Ni (or Zr/Ni), suggesting that crustal contamination was not the main cause of variable SiO_2 among the enclaves. Variable SiO_2 is therefore considered to be more probably due to melting of a variably metasomatized mantle source, or a variable depth of melting.

Compositional relations between enclave magmas and calc-alkaline granitoids

Although evolved members of the xenolith/dyke suite overlap with calc-alkaline granitoid compositions on some plots (e.g. SiO_2 vs TiO_2, FeO*, MgO, CaO, P_2O_5, F, V), other trace-element data indicate that the granitoids did not form by continued fractional crystallization of the more mafic magmas (Fig. 47).

Summary

The main pre-RFG and post-RFG calc-alkaline granitoid (super)suites in the SWEGP were derived from a variety of crustal, igneous source-rocks that were tonalitic (for the Rainbow suite and Liberty Granodiorite) to monzogranitic (for the Minyma and Dairy (super)suites). The absence of negative Sr anomalies in spidergrams for most suites, combined with the results of experimental studies of the melting behaviour of appropriate source rocks, suggest parent magmas for each (super)suite were produced by hydrous melting of the source rocks, at temperatures of 800–950°C. Subsequent evolution within most (super)suites was dominated by fractional crystallization. Fractionation was most extreme in the Woolgangie supersuite, which fractionated mainly biotite and plagioclase, and in later stages, K-feldspar. Relatively limited fractionation of biotite and plagioclase (and K-feldspar) controlled compositional variation in the Twin Hills (and Goongarrie) suites. Limited fractionation of biotite, plagioclase, and probably hornblende, controlled evolution of the Rainbow suite and Liberty Granodiorite.

Bali suite granitoids may have been derived from Woolgangie supersuite granitoids by metasomatic interaction with metamorphic fluids, or may have been derived from source rocks similar to, but chemically distinct from, those which yielded other Woolgangie supersuite granitoids.

The origin of compositional variation within the Minyma and Dairy (super)suites is less clear. Limited data and field observations suggest fractional crystallization of a high-SiO_2 melt may have been accompanied by crustal contamination. The inferred contaminants include material comparable to granitoid gneiss and greenstone exposed in the same area. Alternatively, compositional variation within the Minyma and Dairy (super)suites may reflect variation in the chemical composition of the monzogranitic source rocks.

Synplutonic, microgranitoid dykes and xenoliths are interpreted to have been derived from a range of enriched mantle sources, possibly at variable depths, and to have subsequently evolved via fractionation of olivine, pyroxene, hornblende, magnetite and apatite.

Alkaline granitoids of the Gilgarna supersuite were probably derived from a depleted crustal source that had produced earlier I-type granitoids.

Chapter 7

Discussion

Comparisons of the structural subdivision of granitoids in the SWEGP with other classifications of Eastern Goldfields granitoids

Sofoulis (1963) defined 'external granites' as those that lie between major greenstone belts, and 'internal granites' as those enclosed by greenstone sequences. This division has been propagated in several recent descriptions of Eastern Goldfields granitoids (Bettenay, 1988; Hallberg, 1988; Perring et al., 1989; Cassidy et al., 1990, 1991; Hill et al., 1992a,b). In the most general sense, external granitoids are relatively leucocratic whereas internal granitoids comprise a more diverse group of intrusions. However, attempts at rationalizing external versus internal granitoids in terms of petrographic and chemical characteristics have met with limited success. For example, Perring et al. (1989) and Cassidy et al. (1991) noted that post-D_2 to syn-D_3 internal granitoids (mainly Bali suite) along the western margin of the Kalgoorlie Terrane have characteristics akin to external granitoids. Cassidy et al. (1990, 1991) found it necessary to modify the definition of internal granitoids to include some intrusions emplaced in contact zones between greenstones and external granitoids.

On the basis of petrographic and chemical characteristics, the granitoid (super)suites defined in this stuy do not conform to the external/internal granitoid classification. Even using modified definitions, both internal and external granitoid areas, as designated by Cassidy et al. (1990, 1991), contain Woolgangie supersuite intrusions. Areas north and east of Menzies, designated as external granitoid, contain (super)suites as diverse as the Woolgangie, Twin Hills and Minyma (super)suites.

Studies by Gee et al. (1981) and Archibald et al. (1981) did not recognize structural equivalents of pre-RFG complexes (Table 13). Hammond and Nisbet (1992) recognized a similar structural subdivision to that presented here, although there is disagreement on the exact timing of emplacement of the early granitoid complexes.

Recent attempts to subdivide Eastern Goldfields granitoids on geochemical criteria are summarized in Table 14, which also correlates these subdivisions with the suites recognized in this study.

Granitoids studied by Bettenay (1977) were almost exclusively granitoid gneiss and post-RFGs. In the SWEGP, the synkinematic granites of Bettenay (1977) and Archibald et al. (1978, 1981) correspond closely to the post-D_2 to syn-D_3 granitoids along the western margin of the Kalgoorlie Terrane, and are predominantly Bali suite granitoids. Post-kinematic granites belong mainly to the Woolgangie and Dairy supersuites. Some bodies (such as the Owen dome and the Scotia dome) interpreted by Bettenay (1977) as post-kinematic, have been reinterpreted as pre-RFG complexes. The fractionated leuco-adamellites of Bettenay (1977) include members of both the Woolgangie and Dairy supersuites.

Association 1 of Cassidy et al. (1991) is comparable to the pre-RFGs of this study, with the proviso that we cannot confidently identify any synvolcanic bodies. Association 2 is equivalent to post-RFGs of this study, with the exception of the Gilgarna supersuite. Association 3 is equivalent to the Gilgarna supersuite, if synvolcanic peralkaline granitoids (not recognized in this study) are excluded. Sr-depleted, Y-undepleted granitoids of Wyborn (1993) probably correspond to the Dairy supersuite. Of the two Y-depleted granitoid groups of Wyborn (1993), the

Table 13. Comparison of structural subdivisions of granitoids in this Report with subdivisions of previous authors

This Report	*Archibald et al. (1981)*	*Gee et al. (1981)*	*Hammond and Nisbet (1992)*
Post-RFG	Post-kinematic granitoids Synkinematic granitoids	Discordant intrusive granite Tectonically emplaced domal granite	Post-D_2 granitoids
Pre-RFG	Not recognized	Not recognized	Granitic complexes
Granitoid gneiss	Banded gneiss	Banded granitic gneiss	Not recognized

Table 14. Correlations between previously published subdivisions of Eastern Goldfields granitoids, and the granitoid suites and supersuites defined in this study

Bettenay (1977); Archibald et al. (1978, 1981)	**Granitoid gneiss**		**Synkinematic granites**			**Post-kinematic granites and fractioned leuco-adamellites**	
This study	Granitoid gneiss		Bali suite Depot Granodiorite			Woolgangie supersuite Dairy supersuite	
Cassidy et al. (1991)	***Association 1*** **(Synvolcanic to syntectonic, calc-alkaline granitoids)**		***Association 2*** **(Syn- to late-tectonic, calc-alkaline granitoids)**			***Association 3*** **(Late-volcanic to post-tectonic, peralkaline granitoids)**	
This study	Pre-RFG suites		Post-RFG suites, excluding Gilgarna supersuite			Gilgarna supersuite	
Wyborn (1993)	**Granitoid gneiss**		***Sr-undepleted, Y-depleted granitoids***			***Sr-depleted, Y-undepleted granitoids***	
This study	Granitoid gneiss		Granodiorite to granite suite Woolgangie supersuite	Mafic tonalite to granite suite Liberty supersuite		Monzogranite to granite suite Dairy supersuite	
Hill et al. (1992a,b)	**Early granodiorite**	**Porphyritic granodiorite**	**Tonalites**	**Granite and granodiorite associated with 'gneiss domes'**	**Coarse-grained granites**	**Late fractionates**	**Late granites and syenites**
This study	Pre-RFG suites (?Rainbow suite)	Liberty supersuite	Liberty supersuite	Bali suite Depot Granodiorite	Woolgangie supersuite	Dairy supersuite	Gilgarna supersuite Woolgangie supersuite

mafic tonalite to granite suite comprises mainly Liberty supersuite plutons (e.g. Liberty Granodiorite) but also includes the Lawlers Tonalite, a pre-RFG at Agnew, 100 km north of the study area (Platt et al., 1978).

Though not directly comparable, subdivisions applied by Hill et al. (1992a,b) are closest to those proposed in this study. Early granodiorite at Norseman is a pre-RFG and, on petrographic grounds, may belong to the Rainbow suite. Porphyritic granodiorites and tonalites are mostly Liberty supersuite plutons, but also include some porphyry dykes. Late granites and syenites are equivalent mainly to the Gilgarna supersuite, but also include the Mungari Monzogranite, which is assigned to the Woolgangie supersuite in this study.

Comparisons between granitoids and porphyries, and granitoids and felsic volcanic rocks

Although only referred to in passing in earlier sections of this Report, small felsic intrusions, referred to as 'porphyries' (Trendall, 1964; Perring et al., 1991), and felsic volcanic rocks are important components of the greenstones in the SWEGP. There are few detailed published descriptions of felsic volcanic rocks (dominantly dacite and rhyolite) in the SWEGP. Taylor (1984) and Ahmat (1995) described felsic volcanic rocks at Kanowna, and Witt (1994) described rhyolitic and rhyodacitic centres in the Kookynie area. An idea of the petrographic diversity of the porphyry group is given in Perring (1988) and Witt (1992b).

The porphyries are classified into five groups, based on phenocryst content (Table 15). A sixth group of minor intrusions (albitites) comprises massive to porphyritic rocks that approach monomineralic albite in composition. Witt et al. (1996) lists 47 analyses of felsic porphyries and volcanic rocks, and one andesitic volcanic rock (Pipeline Andesite; Witt, 1990) in the Kalgoorlie Terrane.

Although the chemistry of porphyry intrusions has been variably affected by alteration, especially albitization, Witt (1992b) suggested they may be genetically related to some spatially associated granitoids based on analyses of relatively immobile elements (Ti, Zr, Ga, V, Nb). The more-detailed assessment of results presented here is consistent with the conclusions of Witt (1992b) but goes further and attempts to relate the porphyries to specific granitoid (super)suites.

Mantle-normalized spidergrams for porphyries (Fig. 48) display enriched patterns with negative P, Nb, Ti and Y anomalies, similar to those of most granitoid (super)suites. Alteration, particularly albitization in hornblende–plagioclase porphyries, has mobilized several elements (especially K, Rb, Ba) at the left-hand side of the spidergrams, thus masking the Nb anomaly. Plots involving Ti, Zr, Ga, V and Nb for porphyries and granitoids are shown in Figures 49 and 50. Quartz–feldspar porphyries display modal similarities to, and substantial chemical overlap with, Woolgangie supersuite granitoids, and the two groups may be genetically related. Although quartz–feldspar porphyries are also modally similar to Goongarrie suite granitoids, the high Ga and Nb contents of the porphyries are incompatible with a genetic relationship between the two groups. Two quartz–feldspar porphyry samples from the Siberia area, which lie outside the Woolgangie supersuite envelope, have lost TiO_2 due to alteration of biotite (Fig. 49).

All other porphyry groups appear more closely related to Rainbow suite granitoids than to any other group, based on data shown in Figures 49 and 50. Although petrographically similar to some Liberty supersuite plutons such as the Liberty Granodiorite, hornblende-bearing porphyries are depleted in Zr with respect to the Liberty Granodiorite. Hornblende-bearing porphyries are commonly intruded into regional shear zones, such as the Zuleika Fault. The emplacement of porphyries related to pre-RFG suites into these structures supports suggestions that some regional shear zones are long-lived zones of repeated deformation (Williams and Whitaker, 1993; Swager et al., 1995). A plagioclase porphyry sample (from the Broad Arrow area) has much higher TiO_2 (0.62%; Fig. 49) than Rainbow suite granitoids and may belong to a felsic suite that has not been identified amongst the analysed granitoids. The three albitite analyses are quite scattered on geochemical plots, precluding confident recognition of precursor rock types. Spatial associations and some relict petrographic features suggest they were metasomatically derived from hornblende-bearing porphyries (Witt, 1992b).

Hallberg (1985) and Hallberg and Giles (1986) suggested a genetic link between andesitic and rhyolitic volcanic rocks and granitoids, north and east of Kookynie. Felsic volcanic rocks and post-RFGs in the SWEGP are not related since the former were deposited during basin development and the granitoids were emplaced during the latter stages of regional deformation. However, felsic volcanic rocks and pre-RFGs in the Norseman area have similar ages (Hill et al., 1989) and could be genetically related, although this has not been demonstrated. There is only a small amount of published geochemical data for felsic volcanic rocks in the study area at the time of writing this Report. One analysis of Pipeline Andesite, from the Ora Banda area, and several analyses of Melita Rhyolite and Jeedamya Rhyodacite near Kookynie, are plotted with granitoid data in Figures 49 and 50. The data indicate that the analysed volcanic rocks are not genetically related to either pre- or post-RFG (super)suites. The Pipeline Andesite sample has sub-stantially higher TiO_2 than granitoids of similar SiO_2 content. Melita Rhyolite is enriched in Zr compared with all granitoid (super)suites. Jeedamya Rhyodacite exhibits some compositional overlap with Woolgangie supersuite granitoids but does not display the Ga and Nb enrichment trends that are a feature of that supersuite. Hallberg (1985, 1986) reported syenogranite porphyry in the Kookynie area, which chemical data indicate is comagmatic with the Melita Rhyolite. Witt (1994) saw no significant differences between rocks reported as syenogranite porphyry and Melita Rhyolite,

Table 15. Petrographic features of porphyries in the Bardoc–Kalgoorlie area

Magmatic	*Metamorphism*	*Alteration* — *Sodic*	*Alteration* — *Other*
QUARTZ–FELDSPAR PORPHYRY			
Phenocrysts: 5–20%, to 3 mm, rarely to 6 mm			
Quartz: 5–50%, rounded to bypyramidal, evidence of partial resorption common			
Plagioclase: 10–75%, mostly dominant, commonly glomeroporphyritic, subhedral, tabular, ?oligoclase, zoning weak to absent, pericline twinning common; mantled by perthite at Missouri	Variable but mostly minor recrystallization	Variable alteration to albitic plagioclase	Moderate to advanced, dusty sericitization
K-feldspar: 0–60%, mostly subordinate to plagioclase, subhedral, tabular, mostly perthitic	Variable but mostly minor recrystallization	Variable alteration to chessboard albite	Typically minor sericitization
Groundmass: fine-grained to aphanitic (<0.2 mm), quartzofeldspathic	Variable recrystallization to a granoblastic mosaic of subequant anhedral grains		Variable sericitization
Accessory minerals: minor zircon, apatite; rare opaque oxide minerals			
QUARTZ–HORNBLENDE–FELDSPAR PORPHYRY			
Phenocrysts: 5-40%, to 4 mm, less commonly to 10 mm			
Quartz: 5–25%, rounded, subequant; some evidence for partial resorption	Variable pseudomorphous replacement by actinolitic amphibole		Variable alteration to epidote and biotite; variable but mostly minor chloritization
Hornblende: 15–45%, subhedral, prismatic, locally glomeroporphyritic; twinning common in some samples	Variable but mostly minor recrystallization		Mild to moderate sericitization, and epidotization
Plagioclase: 30–60% subhedral to euhedral, commonly glomeroporphyritic; oscillatory zoning common, oligoclase–andesine			Minor alteration to epidote, chlorite
Biotite: 5–10% in some samples only, coarse flakes to 5 mm			
Groundmass: fine-grained to aphanitic, quartzofeldspathic ± hornblende	Variable recrystallization of hornblende to feathery acicular forms; quartzofeldspathic component develops allotriomorphic fabric with sutured grain boundaries	Minor development of feldspathic domains in some samples	
Accessory minerals: apatite, titanite, pyrite; cognate xenoliths of diorite at most localities			
HORNBLENDE–PLAGIOCLASE PORPHYRY			
Phenocrysts: 5–30%, to 3 mm			
Hornblende: 30–70%, subhedral, prismatic; rare relicts display colour zoning with brown cores and green margins	Pseudomorphous replacement by actinolitic amphibole, followed by recrystallization to acicular and fibrous actinolitic amphibole	Partial replacement of actinolitic amphibole by sodic amphibole (magnesioarfvedsonite to magnesio-?riebeckite)	Biotitization, chloritization, carbonation
Plagioclase: 30–70%, subhedral, tabular, commonly glomeroporphyritic, ?oligoclase, unzoned; pericline twinning common	Variable recrystallization	Alteration to albitic plagioclase	Variable sericitization, biotitization
Quartz: rare, mostly absent, ovoid; evidence of partial resorption			
Groundmass: fine-grained to aphanitic, ?quartzofeldspathic	Variable recrystallization to a granoblastic mosaic of subequant anhedral grains	Alteration to quartz-poor, albitic mosaic, variable grain size	Variable sericitization, chloritization, biotitization, carbonation, sulfidization
Accessory minerals: opaque oxide minerals, titanite, rutile and apatite; apatite to ~ 2% in some samples from Mount Percy			

Table 15. (*continued*)

Magmatic	*Metamorphism*	*Alteration*	
		Sodic	*Other*
FELDSPAR PORPHYRY			
Phenocrysts: 5–10%, to 5 mm			
Plagioclase: 85–100%, subhedral, subequant to tabular, glomeroporphyritic, ?oligoclase, unzoned	Variable recrystallization	Variable alteration to albitic plagioclase, advanced alteration to K-feldspar at Sand Queen	Variable sericitization
Quartz: 0–10%, mostly absent			
Hornblende: 0-5%, mostly absent	Alteration to actinolitic ?amphibole		
Groundmass: very fine-grained to aphanitic, quartzofeldspathic	Variable recrystallization to a granoblastic mosaic of subequant, anhedral grains	Alteration to quartz-poor, albitic mosaic in some samples; microclinization at Sand Queen	Variable sericite, chlorite, epidote, pyrite, carbonate; biotite or tremolitic amphibole at higher metamorphic grades
Accessory minerals: rutile, titanite, zircon			
PLAGIOCLASE–HORNBLENDE PORPHYRY			
Phenocrysts: 35–50%, to 4 mm			
Hornblende: 50–60%, subhedral, prismatic, rare relicts are colour zoned from brown cores to green margins, commonly glomeroporphyritic	Pseudomorphed by actinolitic amphibole		Alteration to epidote, chlorite, variable but commonly extensive
Plagioclase: 40–50%, subhedral, subequant to tabular, zoning weak to absent	Variable recrystallization	Alteration to albitic ?plagioclase	Extensive sericitization, epidotization
Quartz: <5%, mostly absent			
Groundmass: fine- to very fine-grained, plagioclase-rich, subordinate quartz and amphibole	Variable recrystallization	Variable alteration to an albite-rich groundmass	Variable, but commonly extensive epidote, chlorite, biotite alteration
Accessory minerals: apatite, titanite, ilmenite; contains irregular xenoliths of diorite and clots of coarse-grained hornblende to several millimetres			

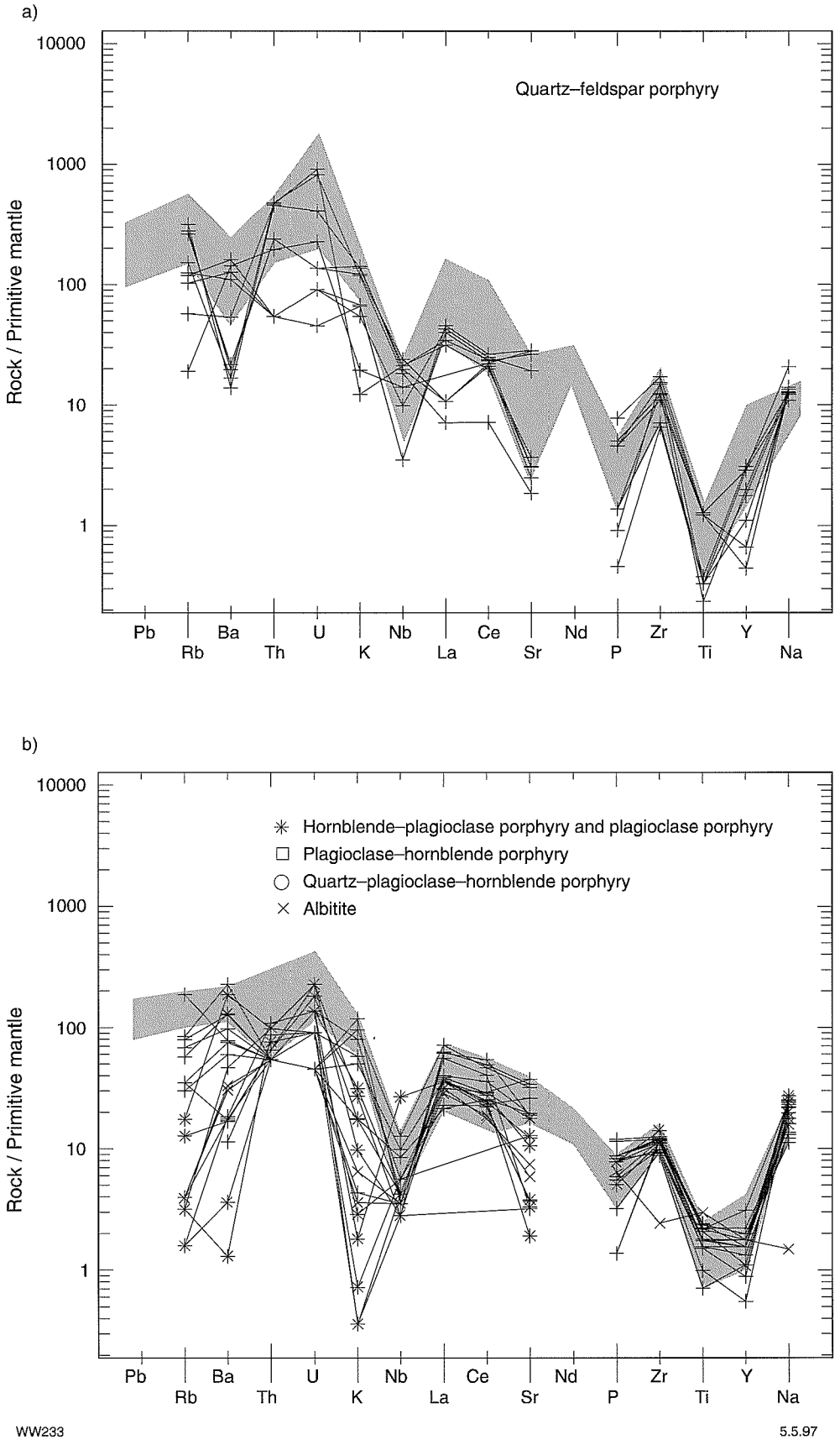

Figure 48. Mantle-normalized spidergrams for porphyries compared to those for selected calc-alkaline granitoid (super)suites: (a) quartz–feldspar porphyries compared to Woolgangie supersuite granitoids, (b) other porphyries compared to Rainbow suite granitoids. Envelopes enclose >90% of granitoids in the Woolgangie supersuite (a) and the Rainbow suite (b)

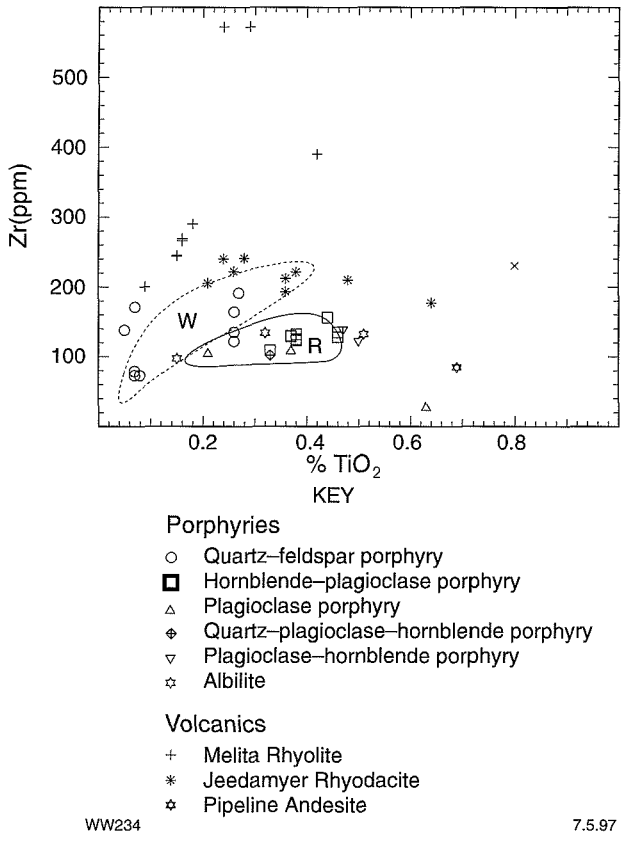

Figure 49. Zr versus TiO_2 for porphyries and felsic volcanic rocks compared to fields for Woolgangie supersuite (W) and Rainbow suite (R) granitoids

and included both groups within the pyroclastic unit. An analysis of granophyre, from Paddys Knob Bore near Ora Banda (Wyche and Witt, 1992), is also reported in Witt et al. (1996). This unit is unrelated to any granitoid (super)suite identified in this study. The geochemistry of felsic volcanic rocks, and their relationship with granitoids in the SWEGP, is currently being investigated by Morris (in prep.). Preliminary results suggest that felsic volcanic rocks of the Black Flag Formation in the Kalgoorlie Terrane are not genetically related to granitoid intrusions in the SWEGP.

Comparisons between microgranitoid enclaves and other enriched, mantle-derived magmas

Most microgranitoid xenoliths and some dykes display enriched, MORB-normalized spidergrams comparable with those generated by mafic to intermediate rocks formed in active continental margins (Pearce, 1983). In this section they are compared with a number of similarly enriched, mantle-derived melts formed in known or proposed subduction-zone environments.

Shoshonites: Shoshonites are typically associated with island-arc and continental-margin environments in which the subduction zone is believed to be steepening or 'flipping' (Morrison, 1980). Although microgranitoid enclaves display some of the major- and trace-element characteristics of basaltic to andesitic shoshonites, most have less K_2O and Rb than typical shoshonites (Fig. 51a) and plagioclase is relatively more sodic.

Sanukitoids: Stern et al. (1989) described Archaean monzodiorite and trachyandesite, associated with larger volumes of granodiorite, in the southwestern Superior Province, Canada. These rocks share the same combinations of high Mg number, Cr and Ni, with enrichment of incompatible, rare-earth and volatile elements that are characteristic of many microgranitoid enclaves in the SWEGP. However, the enclaves in the study area extend to lower Mg number, Cr and Ni suggesting they include more fractionated examples than are present amongst the Canadian sanukitoids.

Appinites: Appinites associated with calc-alkaline granitoids in the Caledonian orogenic belt in Scotland have higher Ba and LREE but are otherwise chemically similar to sanukitoids (Wright and Bowes, 1979). Enriched dioritic dykes and xenoliths in the Lawlers Tonalite, in the northern part of the Eastern Goldfields Province, were identified by Cassidy (1988) as appinites. Microgranitoid enclaves in the SWEGP have some chemical features in common with appinites but appear to be more fractionated because compositions do not extend above 8% MgO, 400 ppm Cr and 800 ppm Sr.

Lamprophyres: Holden et al. (1991) identified microgranitoid xenoliths in the Criffell and Strontian plutons, Scotland, as modified lamprophyres. Small calc-alkaline lamprophyre intrusions are widespread within the greenstones of the Eastern Goldfields Province (Miles, 1945; Hallberg, 1985; Rock et al., 1988). Published analyses of some of these lamprophyres are compared with those of microgranitoid enclaves in Figures 29, 30 and 51. Reasonable overlap between compositions of the two groups is evident. The two rock types are further compared using spidergrams (Fig. 52) in which enclave compositions are normalized to the average global calc-alkaline lamprophyre of Rock (1987). All samples generate moderately flat spidergrams around a ratio of approximately 1.0, demonstrating a general similarity between enclaves and lamprophyres but, in detail, the spidergrams display considerable variability. Most group 1 and 3 xenoliths (Fig. 35a,b) approach the average global calc-alkaline lamprophyre composition. Within each xenolith group, the most lamprophyre-like samples are those with a high Mg number and low SiO_2. More fractionated samples have increased depletion of compatible elements (right-hand side of spidergrams) and variable, negative Nb, Ti and P anomalies.

It is concluded that although the microgranitoid xenoliths display compositional similarities to sanukitoids and appinites, they are most similar to the calc-alkaline lamprophyres.

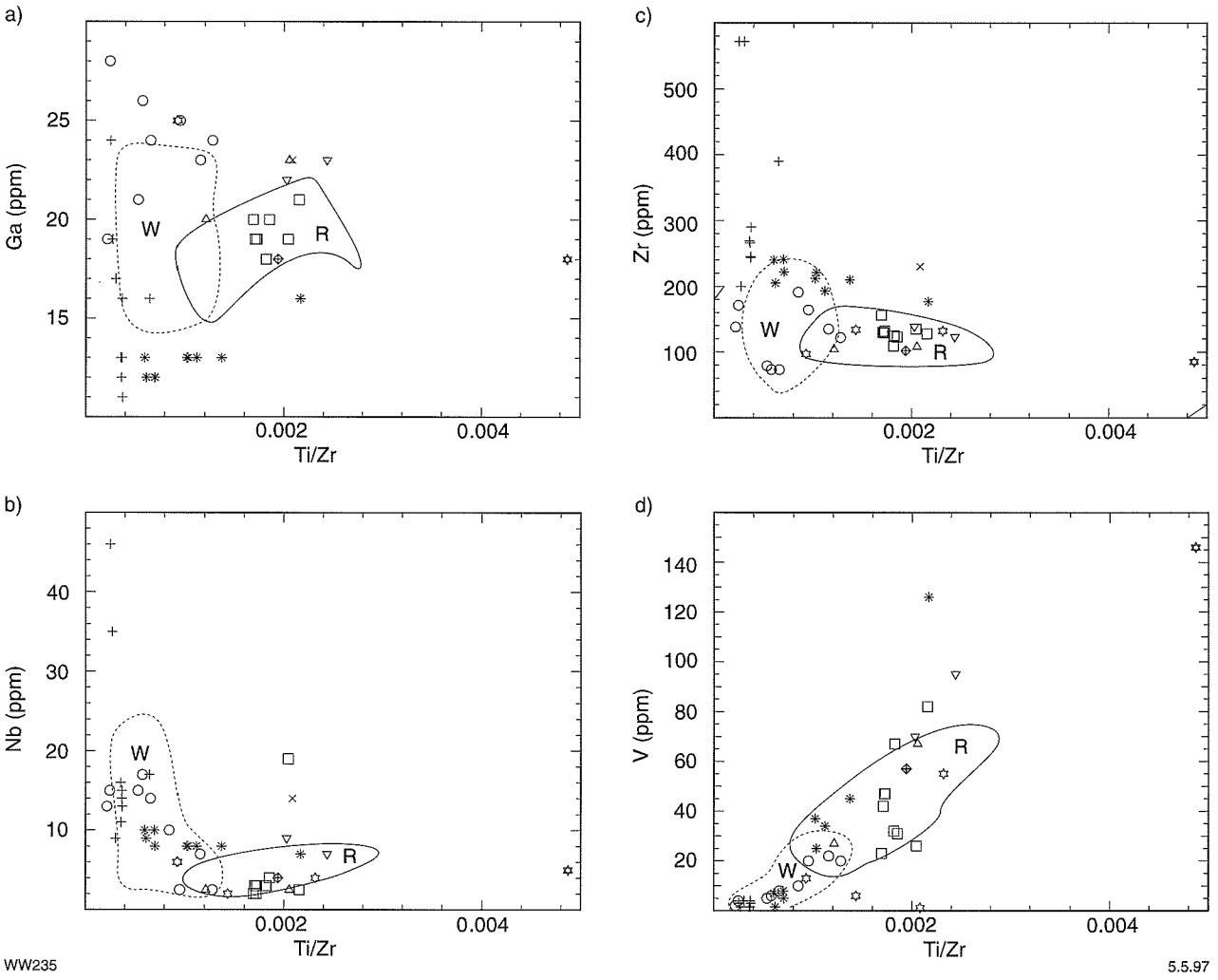

Figure 50. Whole-rock compositions for porphyries and felsic volcanic rocks compared to fields for Woolgangie supersuite (W) and Rainbow suite (R) granitoids (shown as for Figure 49): (a) Ga versus Ti/Zr, (b) Nb versus Ti/Zr, (c) Zr versus Ti/Zr, (d) V versus Ti/Zr. See Figure 49 for key to symbols

Associations between granitoids and mineralization — discussion of relevant factors

There is a very limited association of metallic ore deposits with granitic rocks in the Eastern Goldfields Province.

Witt (1992a) reported a spatial relationship between lithium-rich pegmatites (some with economic concentrations of tantalum and spodumene) and granitoids of the Bali suite. In addition, several gold deposits occur within granitoid host rocks. However, less than 5% of gold produced in the Eastern Goldfields Province has come from felsic rocks, including granitoids, porphyries and volcanic rocks (Groves and Barley, 1988). In the Menzies–Kambalda area, Witt (1993b) reported that granitoids yielded 1% of the total gold produced.

A direct genetic relationship between gold mineralization and granitoids is not readily demonstrated, and most authors assign only a secondary role to granitoids (Groves et al., 1989; Perring et al., 1989; Cassidy et al., 1990; Witt, 1993b). Granitoid bodies may be forcefully emplaced or else act as rigid bodies that resisted regional deformation. In either case, newly formed or reactivated structures may become mineralized (Skwarnecki, 1987; Witt, 1993b,c). Witt (1991) noted the temporal link between gold mineralization and regional metamorphism (M_2) and the emplacement of some granitoid intrusions (mainly Bali suite) in the Menzies–Kambalda area. Spatial relations between Bali suite granitoids, regional metamorphic (M_2) isograds and alteration assemblages in gold deposits indicate that the granitoids may have acted as a source of heat that drove auriferous hydrothermal fluids through a greenstone belt-scale convection cell (Witt, 1991, 1993b).

Bennett (1989) related Pb–Zn–Au–Ag–F mineralization at Black Flag, west of Broad Arrow, to an

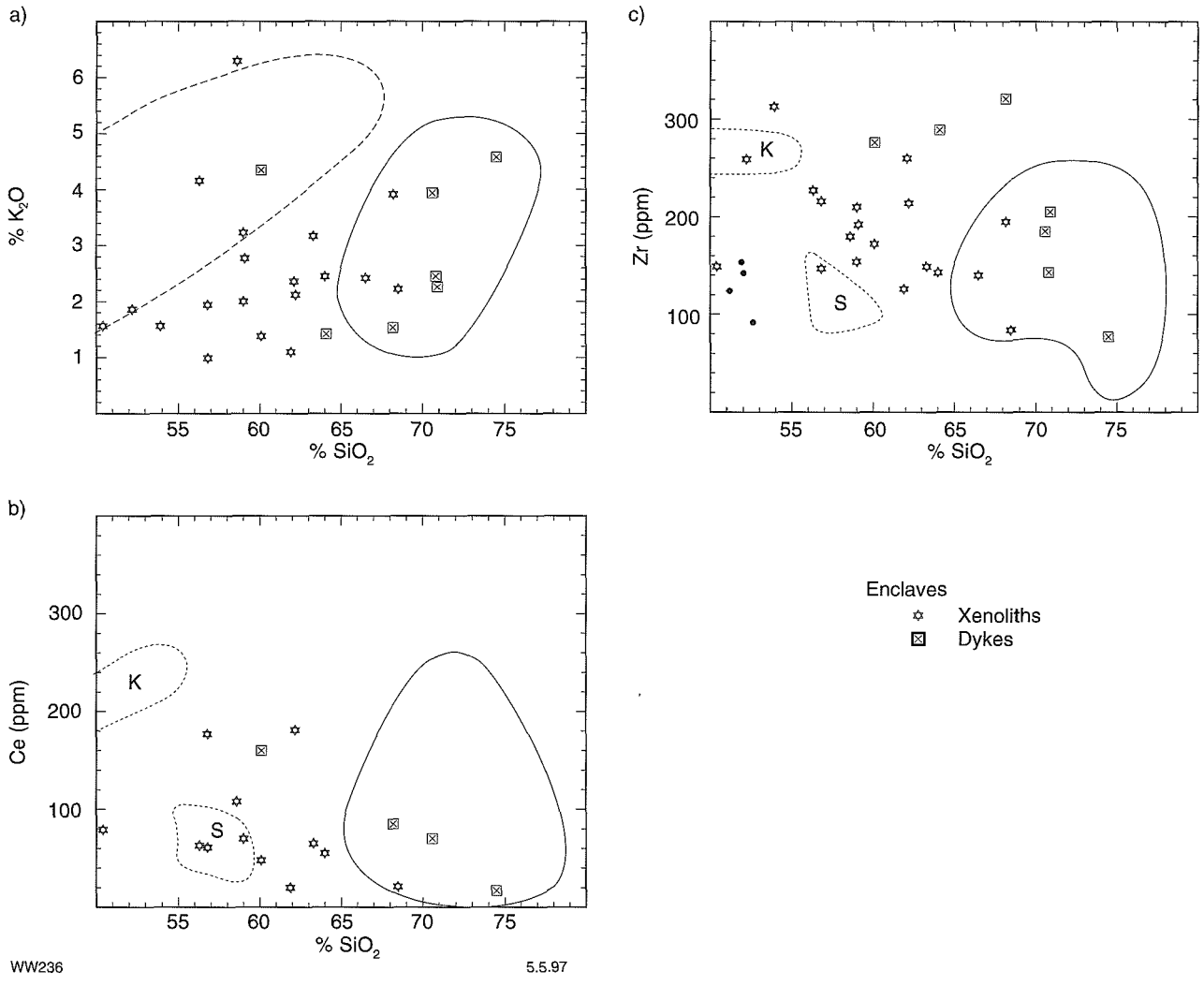

Figure 51. (a) K_2O versus SiO_2 for dykes and xenoliths, compared with calc-alkaline granitoid suites and supersuites. Field of shoshonites (dashed evelopes) is from Morrison (1980), (b) Ce versus SiO_2 (c) Zr versus SiO_2, (b) and (c) show data for dykes, xenoliths and calc-alkaline granitoid suites (solid-line envelopes), as well as fields of kersantites (K) and spessartites (S) from Kambalda (Perring, 1988). Whole-rock compositions of minettes from the Leonora–Laverton area are shown in Figure 51e (Hallberg, 1985)

underlying but unexposed, shallow, subvolcanic stock. However, this deposit is small and has only been mined for its gold content (46 500 t at 11.21 g/t Au).

There is limited potential for other styles of granitoid-related mineralization in the SWEGP. The formation of granite-related ore deposits depends on a complex range of factors, including source rocks, degree of magmatic fractionation, concentration and nature of volatiles, and emplacement level (Burnham and Ohmoto, 1980; Strong, 1985; Hannah and Stein, 1990; Candela, 1992). In the SWEGP, most of these factors do not favour the formation of metalliferous ore deposits.

Source rocks

Many porphyry Cu(–Au) deposits and Fe (Cu, Co, Au) skarns tend to be associated with dioritic to tonalitic rocks in island arcs, or continental margin arcs, nearest the trench (Einaudi et al., 1981; Titley and Beane, 1981; Clark et al., 1990). These granitoids, which are commonly referred to as M-type (Pitcher, 1983; Chappell and Stephens, 1988), are derived from mafic source rocks. In modern subduction-zone settings, the source rocks for granitoids related to porphyry copper mineralization are commonly believed to be oceanic crust and overlying mantle. The continental-crustal sources for granitoids in the SWEGP suggest these styles of mineralization are unlikely to be found. Granitoids from crustal sources are more likely to be associated with Sn, Ta, W, Mo and Pb mineralization.

Degree of magmatic fractionation

Small to moderate amounts of fractional crystallization for pre-RFGs limit the potential for magmatic concentration of incompatible trace metals in these suites. Although some members of the Woolgangie supersuite are strongly

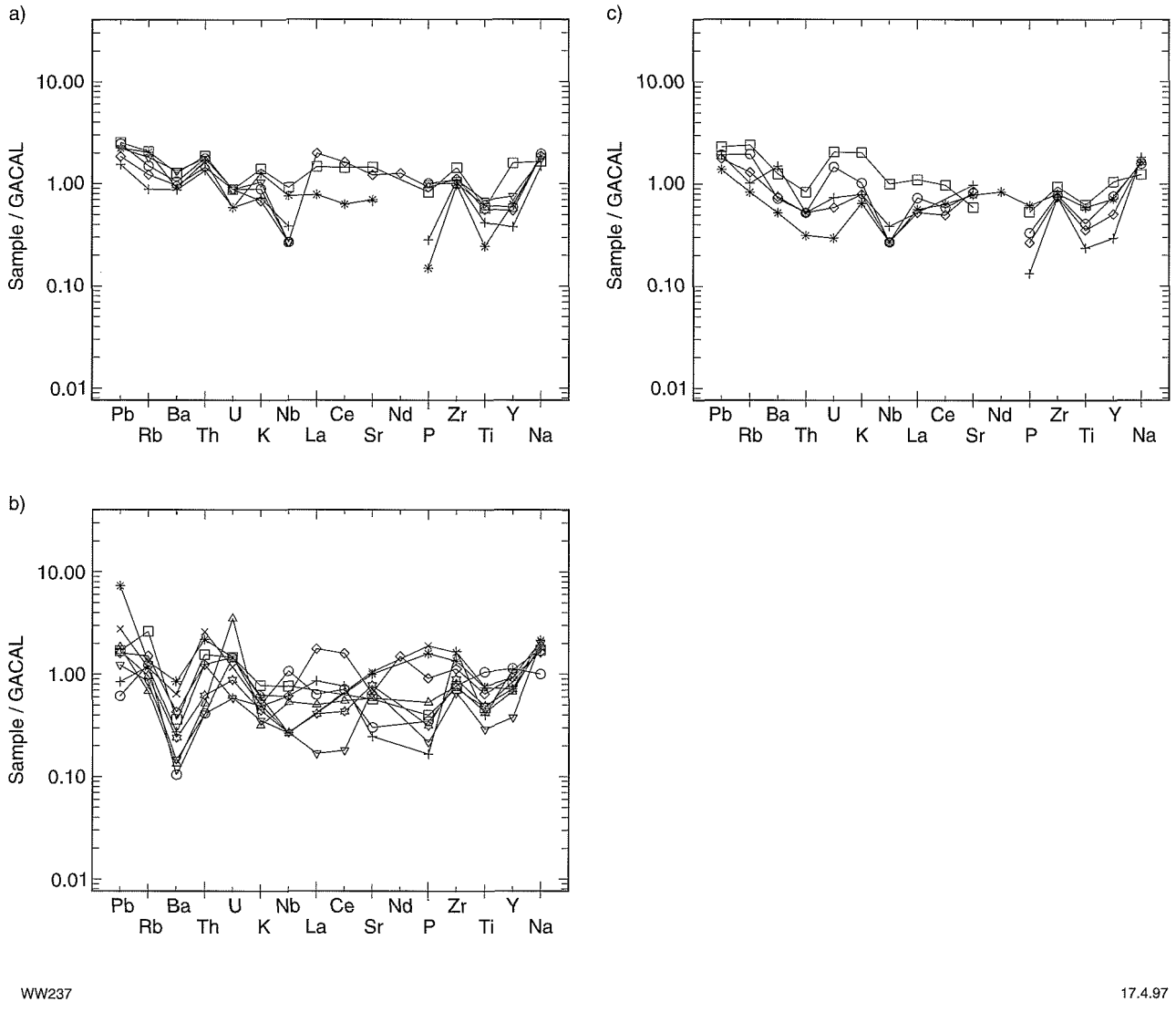

Figure 52. Dyke and xenolith compositions normalized to the global average calc-alkaline lamprophyre (GACAL; Rock, 1987): (a) xenoliths that generate concave downward Pb–K chondrite-normalized spidergrams, (b) xenoliths that generate chondrite-normalized spidergrams with a negative Ba anomaly, (c) xenoliths that generate chondrite-normalized spidergrams with a negative Th anomaly

fractionated, concentrations of metallic trace elements such as Sn and Mo are consistently at or below detection levels. The high fO_2 of the magmas would inhibit concentration of Sn and W, but should favour concentration of Mo, Ta and Nb during fractional crystallization (Ishihara, 1981; Tacker and Candela, 1987; Blevin and Chappell, 1992; Candela, 1992).

Concentration and nature of volatiles

Volatile components, especially H_2O, H_2S, Cl and F, play an important role in granitoid-related ore genesis through depolymerization of the magma and lowering of solidus temperatures, both of which promote efficient magmatic fractionation (Burnham, 1979; Manning et al., 1980; Dingwell, 1985; Manning and Pichavent, 1985). Chlorine is important because it partitions strongly into the aqueous phase, following volatile saturation, and forms complexes that ensure the efficient transfer of Cu, Pb, Zn, Sn, W and Mo from the melt into the hydrothermal fluid (Barnes, 1979; Manning and Pichavent, 1985). Pre-RFGs are characterized by low contents of hydrous minerals (biotite, hornblende), and an absence of internal pegmatite bodies, suggesting that the initial volatile contents of the magmas were relatively low, and that separation of a volumetrically significant volatile phase did not occur. Widespread internal pegmatite segregations in Woolgangie supersuite granitoids indicate crystallization from relatively hydrous magmas. F concentrations in these more hydrous magmas are low (with the exception of the Bullabulling Monzogranite), and Cl contents are unknown. However, large areas of alteration were not observed in any of the granitoid outcrops visited during this study.

Emplacement level

The solubility of H_2O and other volatiles increases with pressure. Therefore, the timing of volatile saturation with respect to extent of crystallization is relatively early in magmas emplaced at shallow depth. Although early aqueous phase saturation favours the formation of porphyry copper deposits, late-stage aqueous phase separation is essential for efficient extraction of incompatible trace metals (Mo, W, Sn) into the hydrothermal fluid (Candela and Holland, 1986). More importantly, the emplacement level of granitoids affects the volume expansion associated with volatile saturation and aqueous phase separation, and therefore has a critical influence on the degree of fracturing and veining in country rocks. A shallow emplacement level (<5 km, approximately) is essential to the formation of large porphyry-style deposits (Phillips, 1973; Burnham, 1979; Burnham and Ohmoto, 1980).

Pressures (3–5 kb) estimated for formation of the thermal aureoles of granitoids in the study area, coupled with the absence of cogenetic volcanic rocks, suggest relatively deep levels of emplacement. Although high pressures would inhibit aqueous phase separation and favour magmatic concentration of Mo, emplacement levels are deeper than those required for optimum development of porphyry Cu and Mo deposits. The depth of emplacement may have been sufficient to preclude immiscible separation of a volatile-rich fluid from fractionated Woolgangie supersuite granitoids, leading to retention of volatiles and metals in late-stage pegmatites (London, 1986).

Potential for undiscovered mineralization genetically related to SWEGP granitoids

It is concluded that the orthomagmatic mineralization potential of granitoids in the SWEGP is low. Apart from the association of Ta–Nb-mineralized, lithium-rich pegmatites with the Bali suite, there is some potential for disseminated Mo and W (scheelite) skarn mineralization (with or without minor precious and base metals) related to fractionated members of the Woolgangie supersuite. Small showings of molybdenite are known in some granitoids in the study area, including the relatively F-rich Bullabulling Monzogranite (Crossley, R., pers. comm., 1992). However, more extensive molybdenite mineralization, if located, is likely to be low grade.

Westra and Keith (1981) recognized two types of intrusion genetically related to porphyry-Mo deposits. A low-F, calc-alkalic group typified by the Kitsault (northwest U.S.A.) and Endako deposits, occurs on continental margins, associated with subduction of oceanic crust. A high-F, alkali-calcic to alkalic group, including the Climax, Henderson–Urad and Mount Emmons deposits (southwest U.S.A.), is associated with crustal extension above a subduction zone (Westra and Keith, 1981; Stein, 1985). Some porphyry copper deposits (e.g. in the southwest U.S.A.) also form in this type of environment (Titley and Beane, 1981). By most of the geochemical criteria established by Westra and Keith (1981), granitoids in the study area are calc-alkalic, and fractionated granitoids have low F. The relatively deep emplacement of granitoids in the study area consign them to the plutonic group of Westra and Keith (1981), which are associated with very low-grade deposits (0.10–0.15% MoS_2), because at these depths boiling of the fluid phase is inhibited and temperature gradients are not steep.

The presence of Pb–Zn mineralization at Black Flag suggests there may be some potential for other small base-metal deposits. However, the data presently available give little indication of the nature of the relevant granitoids.

Tectonic settings — a comparison of the SWEGP with some modern tectonic environments

Although not identified in surface exposures, an ensialic basement to the greenstones in the SWEGP is indicated by the following:

1. Widespread and voluminous dacitic to rhyolitic volcanic and volcaniclastic rocks. The volcanic rocks must have formed by anatexis of a sialic source, because intermediate (andesitic) volcanic rocks are, volumetrically, a minor component of the greenstone sequences.

2. Sedimentary rocks, derived from a felsic (possibly granitoid) source, which occur in the lower part of the greenstone sequence at several localities.

3. Geochemical evidence, and radiogenic zircon xenocrysts, which indicate that some basalt and komatiite units have been contaminated by sialic crust (Arndt and Jenner, 1986; Barley, 1986; Compston et al., 1986; Morris, 1993).

There are currently two main palaeotectonic models for the SWEGP during greenstone formation.

One model envisages a continental margin setting in which the Kalgoorlie Terrane represents a back-arc basin (Barley et al., 1989; Swager et al., 1992, 1995). In this model, andesitic volcanic centres in the Edjudina Terrane (Fig. 2) are interpreted as an ancient volcanic arc. Although rarely stated, this model implies a westward-dipping subduction zone somewhere to the east of the study area. Bimodal volcanic sequences in the Gindalbie Terrane (Fig. 2) have been interpreted as representing rift-margin magmatism along the eastern edge of the back-arc basin (Witt, 1992a, 1994). Other terranes east of the study area may represent smaller, shallower rift basins within a volcanic arc setting (Swager and Ahmat, 1992). Regional deformation is regarded as probably caused by a collisional event between plates with accretion of disparate greenstone terranes (possibly including suspect terranes) to a continental craton to the west.

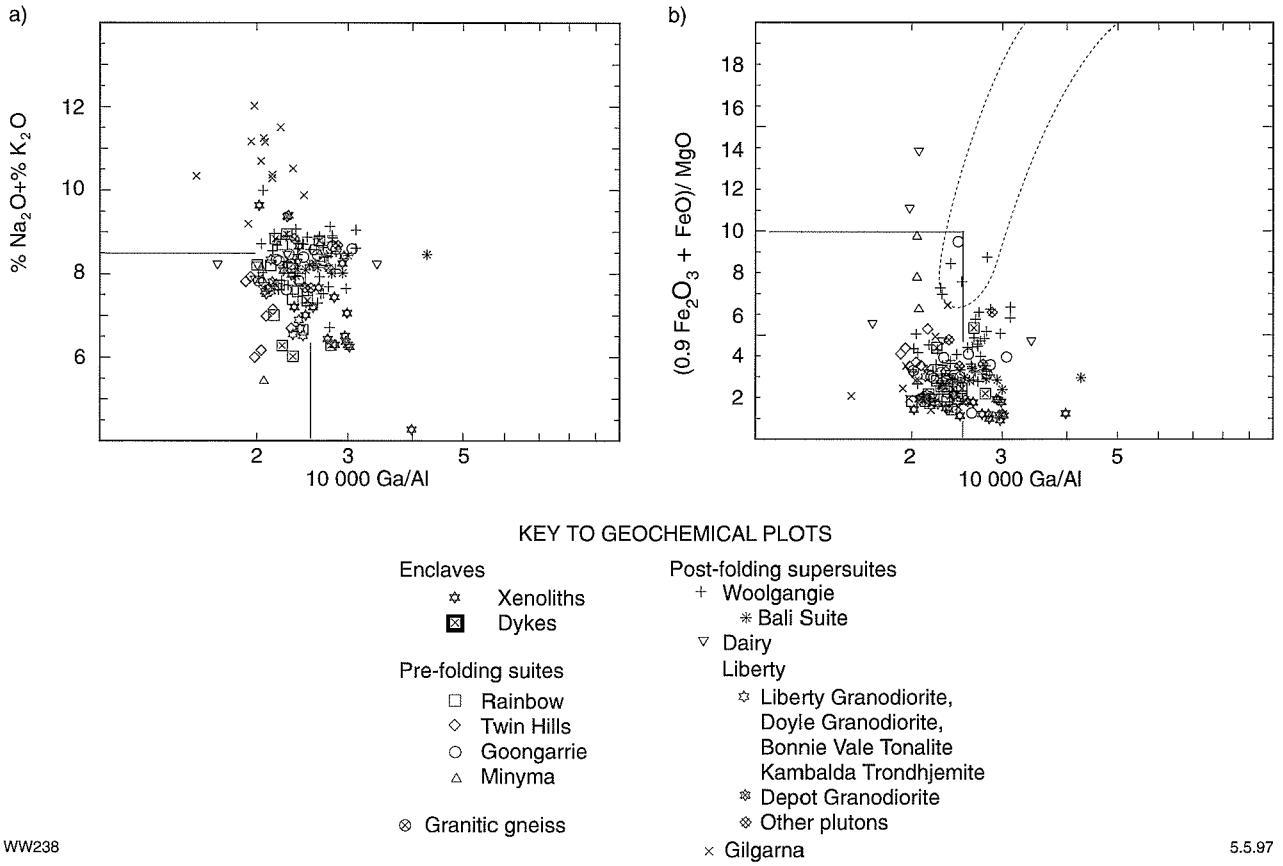

Figure 53. Whole-rock composition of Gilgarna supersuite granitoids compared with calc-alkaline granitoid (super)suites, including dykes and xenoliths: (a) Na_2O+K_2O versus 10 000 Ga/Al; (b) $0.9Fe_2O_3+FeO)/MgO$ versus 10 000 Ga/Al. The lower left-hand box excludes A-type granitoids and some fractionated I-type and S-type granitoids (Whalen et al., 1987). Field of A-type granitoids from Whalen et al. (1987). Broken-line envelope in (b) encloses North American anorogenic granitoids (Anderson, 1983)

The second model relates volcanism in the Eastern Goldfields Province to a large-scale mantle plume and continental rifting (Campbell and Hill, 1988; Campbell et al., 1990). In this model, granitoid magmatism follows conduction of heat from the plume into the base of the crust and regional deformation is related to granitoid emplacement.

This section examines the implications of the structural setting and geochemistry of granitoids in the SWEGP for the wider problem of the tectonic setting of the SWEGP.

Phanerozoic calc-alkaline granitoids are formed in a wide variety of tectonic environments (Pitcher, 1983, 1987): 1) island arcs developed on oceanic crust, 2) anorogenic zones and zones of rifting in continental interiors, 3) continental margins and continental margin arcs, 4) continental areas of post-collision uplift and block faulting, and 5) areas of continental thickening related to collision. In recent literature, the tectonic setting of the Eastern Goldfields Province has been compared favourably to several of these environments. In this section, each environment is assessed in terms of its relevance to the SWEGP during regional deformation, based on the evidence from the granitoids.

Island arcs developed on oceanic crust

The petrogenesis of granitic rocks formed in immature island arcs involves a large component of subducted oceanic crust, and the granitoids are therefore mainly diorite and tonalite (with associated gabbro) characterized by high Na_2O/K_2O (Mason and McDonald, 1978; Pitcher, 1983; Whalen, 1985; Chappell and Stephens, 1988). Island-arc granitoid associations, termed M-type granitoids by Pitcher (1983, 1987), are fundamentally different to the predominant granodiorite and monzogranite described in this Report.

Anorogenic zones and zones of rifting in continental interiors

Wyborn (1993) drew attention to the bimodal distribution of SiO_2 values for Yilgarn Craton granitoids and noted that bimodality is a characteristic of igneous rocks that form in extensional tectonic regimes. However, the character of the SWEGP granitoids is quite unlike that of granitoids associated with rifting of stabilized continental

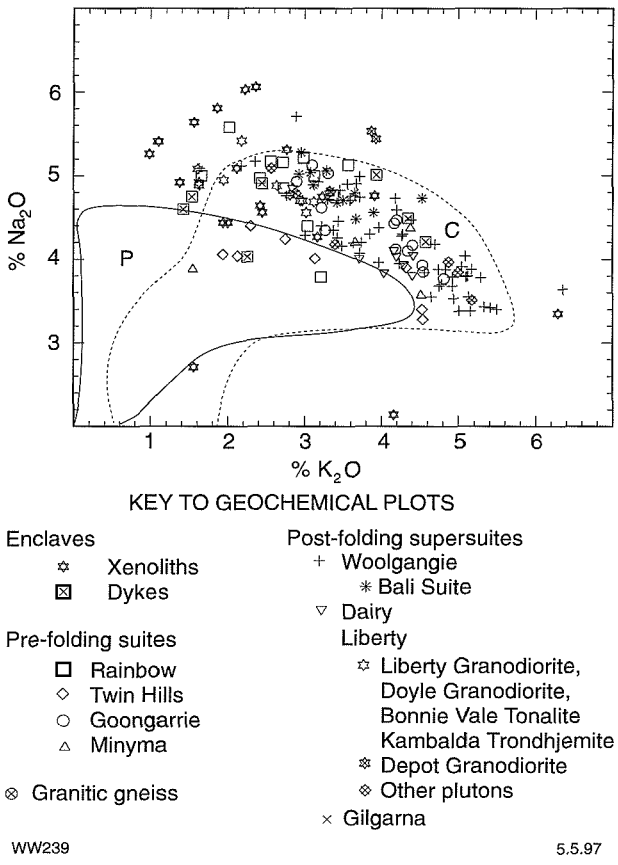

Figure 54. Na_2O versus K_2O for all calc-alkaline granitoids, dykes and xenoliths in the SWEGP. Also shown are the fields enclosing greater than 90% of plutonic rocks from the Peninsular Ranges Batholith, U.S.A. (P), and greater than 90% of plutonic rocks from the Caledonian granitoids (Newer Granites) in Scotland and Ireland (C). Fields are from data published by Chappell and Stephens (1988), and exclude gabbroic rocks

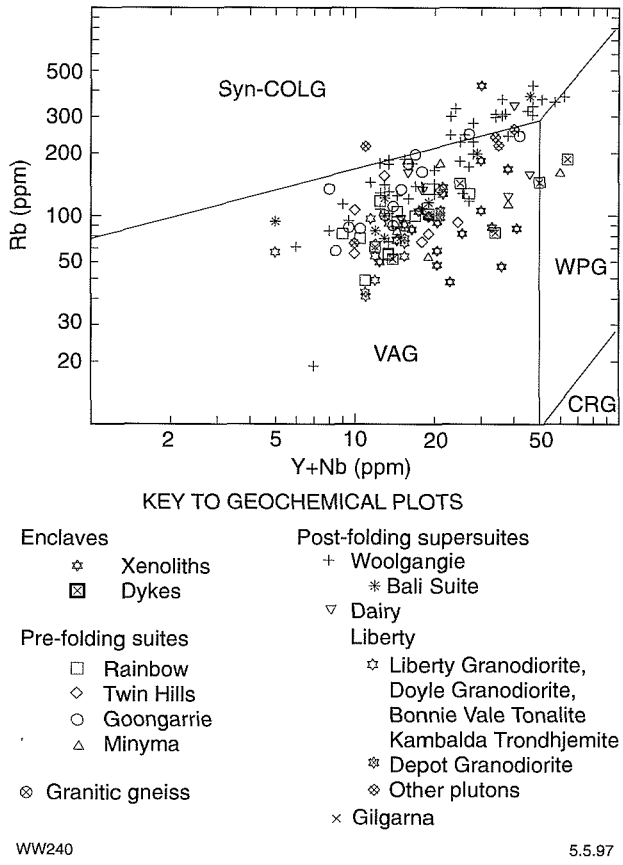

Figure 55. Rb versus Y+Nb (after Pearce et al., 1984) showing whole-rock compositions of all calc-alkaline granitoids, dykes and xenoliths in the SWEGP. SYN-COLG = Syn-collision granitoids, VAG = Volcanic arc granitoids, WPG = Within-plate granitoids, CRG = Continental rift granitoids

crust (e.g. Nigeria, continental North America), which have been termed A-type granites by Whalen et al. (1987) and Eby (1990). Anorogenic granitoids in North America are typically Fe-rich and potassic, metaluminous to peraluminous monzogranite and syenogranite (Anderson, 1983; Whalen et al., 1987). Elsewhere, granitoids associated with continental rifting are commonly anhydrous and slightly to strongly alkaline (Bailey, 1974; Ramberg and Neumann, 1978; Pitcher, 1987). Granitoids in the SWEGP are distinguished from North American anorogenic granitoids, and A-type granitoids overall, on Figure 53. Apart from SiO_2-rich samples (not diagnostic), only the volumetrically minor and distinctly later Gilgarna supersuite granitoids plot in the field of anorogenic granitoids. Gilgarna supersuite granitoids also plot as A-type granitoids on other plots devised by Collins et al. (1982), Whalen et al. (1987) and Eby (1990).

The weak bimodality of SiO_2 values for SWEGP granitoids is not typical of that described for extensional granitoid and volcanic suites. The compositional hiatus for granitoids in the SWEGP is relatively small and occurs at 69–74%, compared with the more pronounced hiatus at 55–60% SiO_2 that separates the felsic and mafic rocks in typical extensional terranes (Bacon, 1982; Wilson, 1989; Cather, 1990). The weakly bimodal character of the granitoids in the study area, if not an artifact of limited sampling, can more probably be attributed to bimodality of source-rock compositions.

Continental margins and continental-margin arcs

Cassidy et al. (1991) suggested similarities between granitoids in the Eastern Goldfields Province and those of the Peninsular Ranges Batholith, in the western U.S.A. Granitoids from the study area are compared with those of the Peninsular Ranges Batholith in Figure 54. The higher alkali (particularly Na_2O) contents of the SWEGP granitoids provides a clear separation of the two groups. A continental-margin setting for SWEGP granitoids has been criticized because plutonic rocks in continental-margin settings, such as the Cordilleran and Andean batholiths, occupy relatively narrow linear belts and

display an extended compositional range that includes a significant proportion of gabbro and tonalite (Hill et al., 1992a). Furthermore, Cordilleran granitoids (referred to as I-(tonalite) type granitoids by Chappell and Stephens, 1988) commonly associated with large volumes of andesitic volcanic rocks, are generally emplaced within a compressional environment, and commonly display evidence (field, geochemical and isotopic) for magma mixing and a variable component of mantle-derived or subducted oceanic crust-derived magma in their petrogenesis (Pitcher, 1983, 1987; Barnes et al., 1986; Fleck, 1990; Foster and Hyndman, 1990; Walawender et al., 1990).

Continental areas of post-collision uplift and block faulting

Pitcher (1983, 1987) associated late Silurian granitoids of the Caledonian fold belt with post-collision uplift and fracturing, which follows crustal thickening. Caledonian granitoids are compositionally similar to those of the Lachlan Fold Belt and Chappell and Stephens (1988) have termed them I-(granodiorite) type granites, in recognition of the dominant rock type. These granitoids are typically emplaced in a relatively short time span, several tens of millions of years after the collisional event. They have a more restricted compositional range than the Cordilleran batholiths, being predominantly granodiorite and monzogranite with a minor component of more mafic rocks represented by the appinite or lamprophyre suite. They are thus broadly similar in composition to granitoids of the SWEGP. Figure 54 supports this comparison, although granitoids in the study area do not extend to the low Na_2O, low K_2O compositions of the Caledonian group. Although compositionally similar, granitoids in the study area were emplaced during regional compression and are thus associated with a fundamentally different tectonic regime.

Areas of continental thickening related to collision

Granitoids in the study area display many regional and physical similarities with the Hercyno-type granitoids of Pitcher (1983, 1987) that formed during continental collision. Both groups were emplaced during a period of crustal thickening and regional shortening, as harmonious or broadly conformable bodies and diapirs, and are associated with regional low-pressure metamorphism. Contemporaneous felsic volcanic rocks are rare to absent in both cases. Hercyno-type granitoid associations comprise mainly leucocratic, peraluminous (commonly S-type) biotite- and two-mica monzogranite, accompanied by subordinate amounts of calc-alkaline I-type granodiorite and monzogranite (Pitcher, 1983; Vidal et al., 1984; Debon et al., 1986; Ortega and Ibarguchi, 1990). Thus, the main difference lies in the absence of abundant S-type granitoids in the SWEGP. As in the SWEGP, late alkaline intrusions were emplaced following stabilization and uplift of the Hercynian orogenic belt (Read and Watson, 1975).

Trace-element discrimination diagrams

Pearce et al. (1984) devised trace-element plots for discriminating between Phanerozoic granitoids generated in different tectonic environments. Data for granitoids in the study area are plotted on a Rb versus Y+Nb diagram in Figure 55. The data lie mainly within the field of volcanic arc granitoids but overlap with syncollision granitoids and, to a lesser extent, within-plate granitoids. The data should be interpreted with caution (Wang and Glover, 1992). Granitoid compositions may be partly inherited from their source rocks (Wyborn, 1993) and, furthermore, Archaean tectonic processes and conditions may not have been identical to those in Phanerozoic times.

Summary

Granitoids in the SWEGP display petrographic and chemical similarity with the Caledonian-type granites of Pitcher (1983, 1987) and the I-(granodiorite) type granites of Chappell and Stephens (1988). Like the granitoids in the study area, the compositions of Caledonian-type granitoids reflect a predominantly igneous crustal source. However, the post-collision, anorogenic to extensional setting for Caledonian-type granitoids cannot be reconciled with those in the SWEGP, where granitoids were emplaced during regional compression, even if most of the granitoids were emplaced towards the end of the orogeny. I-type granitoids similar to the Caledonian examples also occur in some Hercynian-type, syncollisional settings, but the absence of widespread S-type granitoids in the study area requires an explanation. This difference probably reflects the absence of large sedimentary (greywacke, shale) accumulations in the lower crust beneath the study area. Widespread melting of a mainly igneous/metamorphic crust would generate metaluminous granodiorite and monzogranite, which dominates the SWEGP. A predominantly felsic lower crust may be responsible for the absence of low Na_2O, low K_2O granitoids, compared with other crustal-dominated granitoid terranes (e.g. the Caledonides; Fig. 54). The craton-wide scale of the (approximately) 2660 Ma granitoid event (Hill et al., 1992a), represented in the study area mainly by the Woolgangie supersuite, is more consistent with a syncollisional setting than any other tectonic environment. In western Europe, the Hercynian belt is about 2000 km wide (Park, 1988), and in Tibet, crustal deformation and granitoid intrusions occur over a width of about 500 km (Debon et al., 1986). These figures compare with a 700 km width for the Yilgarn Craton at the latitude of the study area.

Although a syncollisional tectonic setting for the granitoids in the SWEGP seems the most appropriate, the full range of granitoids associated with continental collision does not appear to be present. Harris et al. (1986) described four main granitoid groups associated with continental collision zones, which Feng and Kerrich (1992) also identified in the Archaean Superior Province, Ontario. The earliest group comprises pre-collision, calc-alkaline, volcanic-arc batholiths (comprising gabbro, tonalite,

granodiorite) related to subduction. These are represented in the Himalayan collision zone by the Transhimalayan granitoid suite (Debon et al., 1986). This type of granitoid association (the Cordilleran-type of Pitcher (1983, 1987) or the I-(tonalite) type of Chappell and Stephens (1988)) does not occur in the study area.

Potential heat sources for generation of granitic magmatism in the SWEGP

Although identification of the heat source required to initiate granitoid magmatism remains speculative based on the available data, it is possible to report some constraints for thermal models. Five possible mechanisms are assessed below.

A mantle plume or crustal thinning

Recent U–Pb zircon age data have inspired a mantle-plume model to explain the tectonic and magmatic evolution of the Yilgarn Craton (Campbell and Hill, 1988; Campbell et al., 1990; Hill et al., 1989, 1992a,b). The model was originally based on an interpreted 15 Ma time-lag (later revised to 25 Ma; Hill et al., 1992b) between deposition of the lowermost mafic volcanic rocks of the Woolyeenyer Formation, in the Norseman area, and the onset of felsic volcanism represented by the overlying Mount Kirk Formation. The time-lag corresponded to the calculated time for heat from a mantle plume to be transferred by conduction into the base of the crust (Campbell and Hill, 1988). Although it can account for the voluminous, craton-wide magmatic event at approximately 2660 Ma, there are a number of problems with this model.

Firstly, the actual time-lag is poorly constrained since the older date is not derived from the base of the Woolyeenyer Formation, but from a cross-cutting dyke interpreted as a feeder to the basalts. Secondly, the Woolyeenyer Formation is separated from the Mount Kirk Formation by a regional fault, interpreted by Swager et al. (1992, 1995) as a terrane boundary. Therefore, stratigraphic relationships between the Woolyeenyer Formation and the Mount Kirk Formation are equivocal. Although Campbell et al. (1990) apply their model to the entire Yilgarn Craton, the time-lag has not been demonstrated outside the Norseman area and, in fact, the nature of volcanism and volcano-stratigraphic relationships are quite variable, even within the SWEGP (Table 1). Finally, the model does not explain why there appears to have been two main episodes of crustal melting, represented by pre- and post-regional folding granitoids.

Although the plume model appears inappropriate to account for craton-scale magmatic evolution, a model in which heat from the mantle is introduced passively, by conduction, into the lower crust during early extension and lithospheric thinning could account for the melting that produced pre-RFG granitoids in the SWEGP.

Crustal thickening

Early (D_1) thrust stacking of greenstone sequences, in at least some parts of the study area, has been documented by Swager and Griffin (1990), and may have been widespread throughout much of the Eastern Goldfields Province (Hammond and Nisbet, 1992). Structural thickening has been proposed as a mechanism for initiating crustal anatexis (England and Thompson, 1986), and more particularly for the generation of Caledonian and Hercynian-type granitoids (Pitcher, 1983, 1987; Jarpaut and Provost, 1985; Ortega and Ibarguchi, 1990). Thermal modelling suggests the time-lag between thrust stacking and crustal anatexis is measured in tens of millions of years (Zen, 1988). Available geochronological data suggest that the time-lag between thrust stacking and earliest granitoid magmatism in the SWEGP is less than 10 Ma. Thrust stacking therefore cannot account for the thermal perturbation required for pre-RFG magmatism.

There is no evidence for high-pressure metamorphism during D_1, suggesting that D_1 involved thin-skinned thrust stacking of greenstone sequences. Thin-skinned thrust-stacking was unlikely to have modified crustal geotherms sufficiently to cause partial melting of the mid- to lower crust. However, if thin-skinned thrust-stacking was accompanied by more substantial thickening of the crustal basement, the time lag between D_1 (c. 2690 Ma) and post-RFG magmatism (c. 2660 Ma) would have been sufficient for thermal re-equilibration to have provided the initial impetus for this later stage of crustal melting. Alternatively, crustal thickening during D_1 may have been followed by delamination of the underlying lithosphere (cf. Loosveld, 1989), providing a mantle heat-source for post-RFG magmatism similar to that which caused pre-RFG magmatism.

Underplating of the crust by mafic magmas

The common spatial association of mafic igneous rocks with calc-alkaline granitoids has led to the suggestion that emplacement of hot, mafic magmas, derived from the mantle or subducted oceanic crust, into the lower crust may have produced the heat necessary to induce partial melting (Wyllie, 1984; Pitcher, 1987; Huppert and Sparks, 1988; Whitney, 1988). This mechanism is especially relevant to Cordilleran-type granitoids but may also be important for some Caledonian-type associations (Pitcher, 1987). The time-lag between emplacement of the mafic magma and related anatexis is relatively short (Huppert and Sparks, 1988).

The presence of synplutonic dykes and microgranitoid xenoliths in some pre-RFG suites indicates the existence of contemporaneous mafic and granitoid melts. However, the volume of these mafic bodies is very small (<1% of most granitoid complexes). There is no evidence of

contemporaneous mafic magmas in post-RFG supersuites, other than a few Liberty supersuite plutons (e.g. the Depot Granodiorite and the Liberty Granodiorite). Although it is possible that a large body of mafic magma was emplaced at the base of the crust during either or both of the main two magmatic episodes, there is no direct evidence of this. If such a body did exist, field observations suggest there was limited, if any, physical interaction (magma mingling or mixing) between the two. Moreover, preliminary isotopic data (Oversby, 1975; Thom et al., 1991) indicate a predominantly crustal source for granitoids in the study area.

Addition of volatiles

The introduction of water and other volatiles into the lower crust, either directly from the mantle (Bailey, 1970) or transported by hydrous mafic magmas derived from oceanic crust or subcontinental lithosphere (Pitcher, 1987; Whitney, 1988), has been proposed as a viable mechanism for the initiation of partial melting. Volatile components lower the solidus of potential source rocks in the lower crust, and hydrous mafic magmas add heat as well as volatiles to the lower crust. The compositions of enclaves in some pre-RFG suites and post-RFG granitoids indicates that some volatile-enriched, mantle-derived magmas were emplaced into the crust while the granitoid melts were forming. Volatiles such as H_2O and F, derived from these enriched mafic magmas, may have played a role in the origin of those granitoids that contain synplutonic dykes and microgranitoid xenoliths, but it is unlikely that the volatiles introduced from these volumetrically small magmas were sufficient to cause widespread lower crustal melting.

Deeply sourced (lower crust or mantle) H_2O–CO_2 fluids that ascended into the greenstone belts through regional shear zones were responsible for wide spread gold mineralization. These fluids were broadly contemporaneous with post-RFG magmatism (Groves et al., 1989; Witt, 1993b). Recent studies (Peterson and Newton, 1990) indicate that, under some circumstances, a mixed H_2O–CO_2 fluid can be more effective than H_2O alone in lowering the temperature at which rocks begin to melt. The introduction of these deeply sourced fluids may have been a factor in promoting partial melting in the mid- to lower-crust to generate post-RFG magmatism.

A lower crustal 'magma ocean'

Ridley and Kramers (1990) and Ridley (1992) hypothesized that a substantial thickness (about 10 km) of the lower crust would have been partially molten at 2.7 Ga because of higher mantle heat flux, and more especially, higher heat production from radioactive decay within a sialic continental crust. If this was the case, the partially molten layer within the lower crust may have been tapped during episodes of tectonism in the upper crust resulting in widespread emplacement of granitoids. However, according to the model of Ridley and Kramers (1990), the lower crustal melt layer is tonalitic in composition. Open-system fractionation and continuous input of tholeiitic magma from the mantle are required to maintain this layer in its partially molten state. When the system becomes closed, tonalitic magma fractionates to produce widespread monzogranitic granitoids. At this stage, the crust becomes stabilized as a craton.

This model, in its simplest form, is incompatible with the diversity of granitoid (super)suites recognized in the SWEGP, the absence of widespread tonalitic granitoids at the present level of exposure, and the two periods of granitoid magmatism separated by regional folding.

Summary of potential heat sources

In summary, the most likely heat source for pre-RFG magmatism was the mantle. Conduction of heat from the mantle into the lower crust would have followed lithospheric thinning during early, basin-forming extension. The widespread nature of post-RFG magmatism with contemporaneous deformation and low-pressure metamorphism is more difficult to account for in terms of a heat source but is a feature of several ancient orogenic belts (e.g. Loosveld, 1989). A model suggested by Loosveld (1989), which can possibly be applied to the SWEGP, is that regional shortening (D_2 to D_3 in the SWEGP) followed delamination of the thickened lithosphere, thus bringing the base of the crust closer to the mantle. During both periods of granitoid magmatism, melting in the lower crust may have been further promoted by the addition of volatiles.

Toward a tectonic model for the granitoids

The lower, mafic to ultramafic greenstones in the SWEGP were formed in a basin (or basins), within an extensional tectonic regime. The granitoids were emplaced into the greenstones during a period of regional deformation that produced significant shortening of the greenstones. Preliminary observations suggest that the regional asymmetry of greenstone associations that stimulated the continental margin model is also reflected (more subtly) in the distribution of granitoids. Post-RFGs in most of the SWEGP are predominantly leucocratic monzogranite and syenogranite (Woolgangie and Dairy supersuites). East of the study area, many post-tectonic granitoids contain microgranitoid enclaves, and hornblende in addition to biotite (Hallberg, 1985, 1986). They are thus petrographically similar to some Liberty supersuite plutons (e.g. Liberty Granodiorite) in the SWEGP. This suite of post-tectonic granitoids extends onto the southeastern part of the study area, but representative plutons have not been analysed. Davy (1976) also described an east–west asymmetry of granitoid compositions in a northern section of the Eastern Goldfields Province (between Agnew and Laverton; Fig. 1), but one which suggests the relatively mafic granitoids east of the SWEGP are succeeded further east again by more felsic granitoids. In addition to the asymmetry of granitoid compositions and greenstone

associations, a plate margin setting for the granitoids is also suggested by the contemporaneity of lamprophyres (or lamprophyre-like rocks) and granitoids in the SWEGP. Calc-alkaline lamprophyres are commonly considered indicative of plate-margin settings, and more specifically with the terminal stages of subduction (Pearce, 1983; Rock et al., 1988, 1990; Wyman and Kerrich, 1989).

A comprehensive tectonic model for the origin of granitic rocks in the Eastern Goldfields depends upon the results of on-going studies in areas beyond the SWEGP. Nevertheless, the following section presents a provisional model for the study area, which is summarized in Figures 56 and 57.

Tectonic model

The earliest phase of deformation recognized in the SWEGP is an extensional basin-forming event. Extensive basaltic and komatiitic volcanism at c. 2700–2690 Ma filled the basin(s), either as a direct result of rifting (lower pressure, thinner lithosphere), or as a result of heat introduced into the lithosphere by komatiitic magmas from the deep mantle (Morris, 1993). At the margins of the main rift basin (e.g. the Gindalbie Terrane), some mafic magma may have ponded within the crust causing partial melting and bimodal basalt–rhyolite volcanism. If extension and mafic–ultramafic volcanism took place in a destructive continental margin setting, there is no evidence for the formation of contemporaneous, Cordilleran-type granitoid suites at this stage. Either they did not form or they formed but are not exposed at the present level of erosion. However, greenstone belts to the east of the SWEGP contain some andesitic volcanic centres (Hallberg and Giles, 1986; Barley et al., 1989).

The earliest exposed granitoid rocks were emplaced during the first phase of compressive deformation (D_{1c}), and limited geochronological data suggest this was around 2690–2685 Ma. Lithospheric thinning during the extensional, basin-forming event brought the base of the continental crust closer to the underlying mantle causing steep geothermal gradients (Sandiford and Powell, 1986). Heat transferred from the mantle into thinned crust by conduction and the passage of hot mafic magma caused partial melting of the lower continental crust (at point 1 on Figs 56 and 57). Emplacement of pre-RFG magmas into the greenstone succession during D_{1c} may reflect the time required for heat to be conducted from the mantle into the base of the crust. Tectonic disturbance related to crustal thickening during D_{1c} may have mobilized partial melts, which were then emplaced as sheet-like intrusions along active, subhorizontal structures in the upper crust. The diversity of pre-RFG suites, and the overlapping nature of their respective distributions (Plate 1), require a compositionally layered lower-crustal source ranging from monzogranite at least to tonalite. Seismic data indicate a layered lower crust of mainly felsic composition with 20–35% laterally discontinuous layers of more mafic rock, overlain by a more uniformly felsic mid- to upper crust (Drummond, 1988). This arrangement is unlikely to have been modified since the post-RFG event, which was followed by cratonization of the granite–greenstone terranes. During partial melting, the compositionally distinct layers in the lower crust must have remained separate from one another because there is little evidence of mixing between suites. They may have been isolated from one another by relatively refractory layers of more mafic material.

Gravitational collapse of the thickened greenstones (D_{1e}) was followed by regional shortening (at least 50%), crustal thickening and regional metamorphism with peak metamorphic temperatures ocurring at c. 2660 Ma. Lithospheric delamination, bringing the base of the crust, once again, closer to the mantle, is one possible mechanism to explain the second phase of magmatism in the SWEGP. Delamination would have been followed by regional shortening of the attenuated crust, including the greenstones, during D_2 and D_3. Melting of a minor component of more mafic rocks, or deeper tonalitic layers, which escaped melting during the earlier phase of granitoid magmatism, yielded minor tonalite and granodiorite plutons (e.g. Liberty Granodiorite).

Craton stabilization and uplift followed the second phase of granitoid magmatism. Adiabatic decompression caused anhydrous melting of a depleted lower crustal source that had yielded earlier calc-alkaline granitoids. Consequently, A-type granitoids of the Gilgarna supersuite were emplaced as small plugs and dykes along extensional fractures in the stabilized craton.

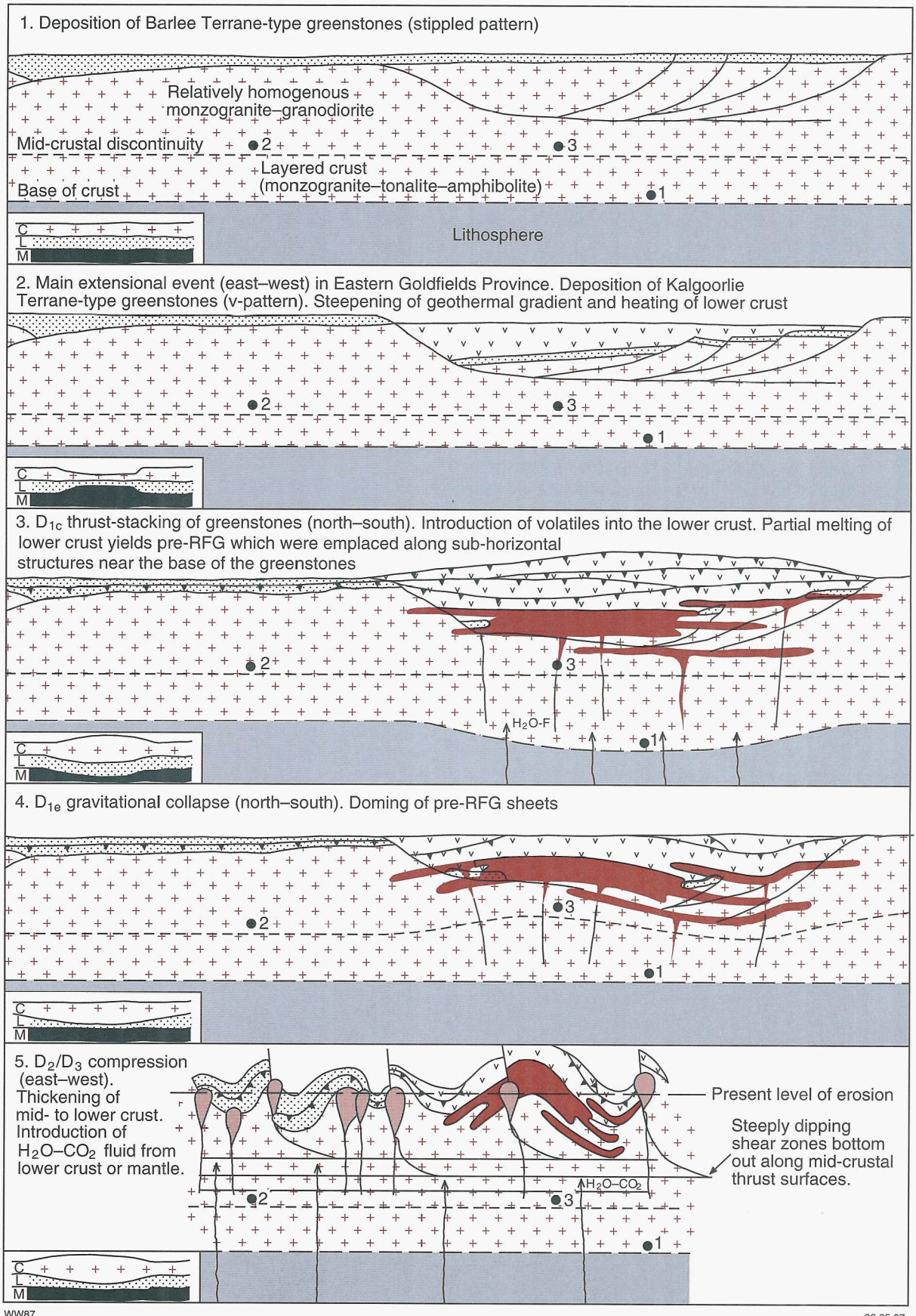
1. Deposition of Barlee Terrane-type greenstones (stippled pattern)
Relatively homogenous monzogranite–granodiorite
Mid-crustal discontinuity
Layered crust (monzogranite–tonalite–amphibolite)
Base of crust
1
2
3
C
L
M
Lithosphere
2. Main extensional event (east–west) in Eastern Goldfields Province. Deposition of Kalgoorlie Terrane-type greenstones (v-pattern). Steepening of geothermal gradient and heating of lower crust
3. D_{1c} thrust-stacking of greenstones (north–south). Introduction of volatiles into the lower crust. Partial melting of lower crust yields pre-RFG which were emplaced along sub-horizontal structures near the base of the greenstones
H_2O-F
4. D_{1e} gravitational collapse (north–south). Doming of pre-RFG sheets
5. D_2/D_3 compression (east–west). Thickening of mid- to lower crust. Introduction of H_2O–CO_2 fluid from lower crust or mantle.
Present level of erosion
Steeply dipping shear zones bottom out along mid-crustal thrust surfaces.
H_2O–CO_2
WW87
02.05.97
Pre-RFG
Post-RFG

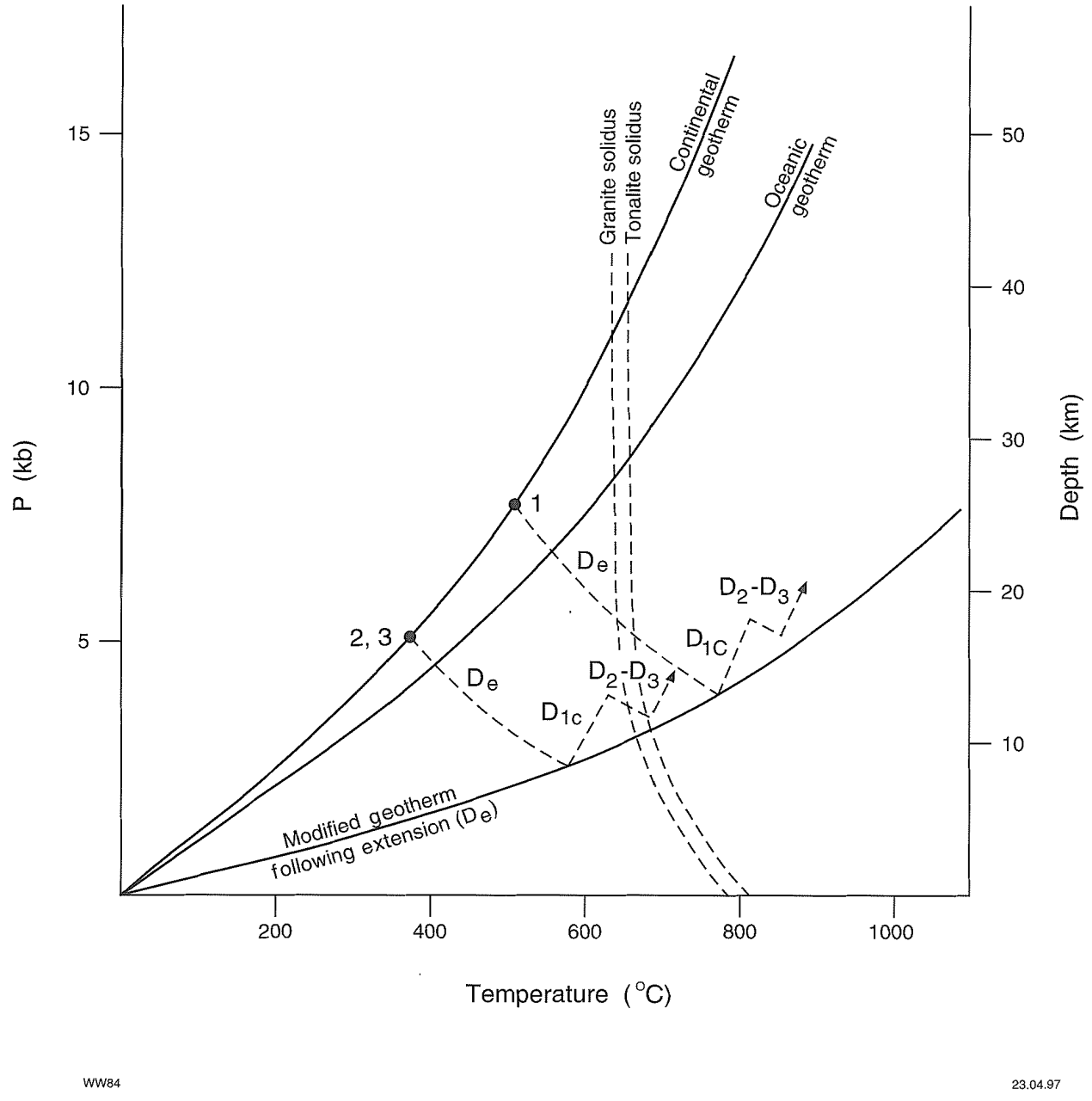

Figure 57. Relations between geotherms and solidi, showing possible P–T–t paths for points 1–3 in Figure 56 in the mid- to lower crust. Continental and oceanic geotherms are from Wilson (1989). Solidi for granite and tonalite are from Piwinskii (1973)

Figure 56. (opposite) Provisional model for the genesis of granitoids with respect to the tectonothermal evolution of the SWEGP. Numbered points are potential sites of melting in the lower crust (1) and middle crust (2,3). Inset shows relations on a larger scale: C — crust, L — lithosphere, M — mantle

Chapter 8

Conclusions

In the southwest Eastern Goldfields Province (SWEGP), intrusive granitoids belong to two major magmatic episodes, separated in time by regional folding (D_2). A third granitoid group, granitoid gneiss, may include a component of basement to the greenstones, but all the geochronological data for gneiss samples to date indicate that they are deformed pre-RFG intrusions.

Pre-regional folding granitoid complexes are regionally concordant with the greenstone country rocks and were probably emplaced as sheet-like bodies at, or near, the base of the exposed greenstone succession, during D_1 thrust stacking and recumbent folding. Limited U–Pb zircon age data suggest emplacement at around 2690–2685 Ma.

There are four pre-RFG suites, based on mineralogy and geochemistry. The suites were derived by hydrous melting of tonalite, granodiorite and monzogranite source rocks in a compositionally layered lower crust. Lower crustal melting was probably a consequence of lithospheric thinning during the extensional event that formed the basin(s) into which greenstones were deposited. Melting may have been assisted by the introduction of volatiles into the lower crust via enriched, mantle-derived melts (lamprophyres), remnants of which are preserved in pre-RFGs as synplutonic, microgranitoid xenoliths and dykes. Subsequent evolution of granitoid magmas was controlled mainly by fractional crystallization. Crustal contamination may have played a significant role in the evolution of the Minyma suite.

Post-regional folding granitoids are mostly circular to ovoid, calc-alkaline plutons, and small, alkaline plugs and dykes, which intruded greenstones and pre-RFG complexes. Calc-alkaline plutons range from syntectonic to late-tectonic but it appears that the times of emplacement of most do not significantly post-date the final stages of regional deformation. The earliest calc-alkaline post-RFG plutons were emplaced in the period 2665–2660 Ma but intrusion continued until around 2600 Ma. There are three calc-alkaline post-RFG supersuites. The volumetrically dominant Woolgangie supersuite, and the Dairy supersuite, were probably derived from granodioritic to monzogranitic source rocks in a relatively homogeneous middle crust. The volumetrically minor Liberty supersuite includes a diverse range of calc-alkaline plutons, including trondhjemite, tonalite, granodiorite and monzogranite. The less leucocratic plutons of the Liberty supersuite may have been derived from a minor mafic to intermediate component of the middle crust, or from parts of the lower crust that had not been subjected to partial melting during the pre-RFG event. There is no readily apparent heat source for this second partial melting event but it is possible that lithospheric delamination following D_1 crustal thickening introduced heat from the mantle into the crust. Hydrous melting may have been promoted by the introduction of deeply-sourced H_2O–CO_2 hydrothermal fluids. Following partial melting, subsequent evolution of calc-alkaline post-RFG supersuites and granitoids was mainly controlled by fractional crystallization, although crustal contamination may have contributed, especially in the case of the Dairy supersuite.

Emplacement of the alkaline, post-RFG Gilgarna supersuite significantly post-dated the final stages of regional deformation. Emplacement ages for these A-type granitoids (c. 2500 ± 100 Ma) suggest they were emplaced during uplift, following craton stabilization. They may have formed as a result of adiabatic decompression and anhydrous melting of residual source rocks in the lower crust.

The structural setting of the granitoids suggests similarities with syn-collisional granitoids (the Hercynotype granitoids of Pitcher (1983, 1987)). The absence of widespread S-type granitoids in the SWEGP is attributed to a lower crust consisting predominantly of igneous material that yielded mainly I-type granodiorite and monzogranite.

Individual pre-RFG suites are not confined by terrane boundaries. It is therefore implicit that source rocks for the suites, in the lower crust, extended beneath two or more greenstone terranes since at least the earliest stages of regional deformation (D_1). Moreover, because granitoid suites reflect the composition of their basement source rocks, the distribution of suites and supersuites suggests similar basement underlies the Kalgoorlie, Gindalbie and Jubilee Terranes. It is unlikely that three unrelated (suspect) terranes all had such similar basement compositions that they each produced granitoids that fell into the same geochemical suites. Thus, the terranes probably did not travel large distances before accretion (that is, they are not suspect terranes). Although there was probably some lateral displacement (shuffling) of terranes with respect to one another, those in the study area were probably already subjacent during greenstone deposition.

Although some post-RFG intrusions played an important role in providing the heat to drive large-scale hydrothermal systems that deposited gold in late-tectonic structures, the potential for orthomagmatic hydrothermal deposits associated with pre-RFG and post-RFG in the SWEGP appears to be limited. However, lithium-rich pegmatites containing Sn and Ta appear to be associated with fractionated Woolgangie supersuite granitoids.

References

AHMAT, A. L., 1994, Kanowna, W.A. Sheet 3236: Western Australia Geological Survey, 1:100 000 Geological Series.

AHMAT, A. L., 1995, Geology of the Kanowna 1:100 000 sheet: Western Australia Geological Survey, 1:100 000 Geological Series Explanatory Notes, 28p.

ALLEN, C. A., 1987, The nature and origin of the Porphyry gold deposit, Western Australia, *in* Recent advances in understanding Precambrian gold deposits *edited by* S. E. HO and D. I. GROVES: Geology Department (Key Centre) and University Extension, University of Western Australia, Publication 11, p. 137–145.

ANDERSON, J. L., 1983, Proterozoic anorogenic granite plutonism of North America: Geological Society of America, Memoir 161, p. 133–154.

ARCHIBALD, N. J., and BETTENAY, L. F., 1977, Indirect evidence for tectonic reactivation of a pre-greenstone sialic basement in Western Australia: Earth and Planetary Science Letters, v. 33, p. 370–378.

ARCHIBALD, N. J., BETTENAY, L. F., BINNS, R. A., GROVES, D. I., and GUNTHORPE, J., 1978, The evolution of Archaean greenstone terrains, Eastern Goldfields Province, Western Australia: Precambrian Research, v. 6, p. 103–131.

ARCHIBALD, N. J., BETTENAY, L. F., BICKLE, M. J., and GROVES, D. I., 1981, Evolution of Archaean crust in the Eastern Goldfields Province of the Yilgarn Block, *in* Archaean Geology *edited by* J. E. GLOVER and D. I. GROVES: International Archaean Symposium, 2nd, Perth, W.A., 1980, Proceedings; Geological Society of Australia, Special Publication, no. 7, p. 491–504.

ARNDT, N. T., and JENNER, G. A., 1986, Crustally contaminated komatiites and basalts from Kambalda, Western Australia: Chemical Geology, v. 56, p. 229–255.

ARTH, J. G., and HANSON, G. N., 1972, Quartz diorites derived by partial melting of eclogite or amphibolite at mantle depths: Contributions to Mineralogy and Petrology, v. 37, p. 161–174.

ARTH, J. G., and BARKER, F., 1976, Rare-earth partitioning between hornblende and dacitic liquid and implications for the genesis of trondhjemitic–tonalitic magmas: Geology, v. 4, p. 534–536.

BACON, C. R., 1982, Time-predictable bimodal volcanism in the Coso Range, California: Geology, v. 10, p. 65–69.

BACON, C. R., 1986, Magmatic inclusions in silicic and intermediate volcanic rocks: Journal of Geophysical Research, v. 91, p. 6091–6112.

BAILEY, D. K., 1970, Volatile flux, heat focussing and the generation of magmas, *in* Mechanisms of Igneous Intrusion *edited by* G. NEWALL and N. RAST: Geological Journal, Special Issue 2, p. 177–186.

BAILEY, D. K., 1974, Origin of alkaline magmas as a result of anatexis, *in* The Alkaline Rocks *edited by* H. SÔRENSON: Wiley and Sons, New York.

BARBARIN, B., 1988, Field evidence for successive mixing and mingling between the Piolard Diorite and the Saint-Julien-la-Vêtre Monzogranite (Nord-Forez, Massif Central, France): Canadian Journal of Earth Sciences, v. 25, p. 49–59.

BARKER, F., 1979, Trondhjemite: definition, environment and hypotheses of origin, *in* Trondhjemites, Dacites and Related Rocks *edited by* F. BARKER: Elsevier, New York, p. 1–12.

BARKER, F., and ARTH, J. G., 1976, Generation of trondhjemitic–tonalitic liquids and Archaean bimodal trondhjemite–basalt suites: Geology, v. 4, p. 596–600.

BARLEY, M. E., 1986, Incompatible-element enrichment in Archean basalts: a consequence of contamination by older sialic crust rather than mantle heterogeneity: Geology, v. 14, p. 947–950.

BARLEY, M. E., EISENLOHR, B. N., GROVES, D. I., PERRING, C. S., and VEARNCOMBE, J. R., 1989, Late Archean convergent margin tectonics and gold mineralization: a new look at the Norseman–Wiluna Belt, Western Australia: Geology, v. 17, p. 826–829.

BARNES, C. G., 1987, Mineralogy of the Wooley Creek batholith, Slinkard pluton, and related dykes, Klamath Mountains, northern California: American Mineralogist, v. 72, p. 879–901.

BARNES, C. G., ALLEN, C. M., and SALEEBY, J. B., 1986, Open- and closed-system characteristics of a tilted plutonic system, Klamath Mountains, California: Journal of Geophysical Research, v. 91, p. 6073–6090.

BARNES, C. G., ALLEN, C. M., HOOVER, J. D., and BRIGHAM, R. H., 1990, Magmatic components of a tilted plutonic system, Klamath Mountains, California, *in* The Nature and Origin of Cordilleran Magmatism *edited by* J. L. ANDERSON: Geological Society of America, Memoir 174, p. 331–346.

BARNES, H. L., 1979, Solubilities of Ore Minerals, *in* Geochemistry of Hydrothermal Ore Deposits (2nd edition) *edited by* H. L. BARNES: Second Edition, John Wiley and Sons, New York, p. 404–460.

BARRIERE, M., 1977, Deformation associated with the Ploumanac'h intrusive complex, Brittany: Geological Society of London, Journal, v. 134, p. 311–324.

BATEMAN, P. C., and CHAPPELL, B. W., 1979, Crystallization, fractionation, and solidification of the Tuolomne Intrusive Series, Yosemite National Park, California: Geological Society of America, Bulletin, v. 90, p. 465–482.

BATEMAN, R., 1985, Aureole deformation by flattening around a diapir during in situ ballooning: the Cannibal Creek Granite: Journal of Geology, v. 93, p. 293–310.

BEARD, J. S., and LOFGREN, G. E., 1991, Dehydration melting and water-saturated melting of basaltic and andesitic greenstones and amphibolites at 1, 3 and 6.9 kb: Journal of Petrology, v. 32, p. 365–401.

BENNETT, J. M., 1989, Comparison of Archaean Pb–Zn(–Au) mineralization at Black Flag and Au mineralization at Lady Bountiful, Mt Pleasant area, Western Australia: University of Western Australia, BSc Honours thesis (unpublished).

BETTENAY, L. F., 1977, Regional geology and petrogenesis of Archaean granitoids in the southeastern Yilgarn Block, Western Australia: University of Western Australia, PhD thesis (unpublished).

BETTENAY, L. F., 1988, Granitoid batholiths of the Eastern Goldfields Province, Yilgarn Block: characteristics and significance to gold

mineralization, *in* Advances in understanding Precambrian gold deposits, Volume II *edited by* S. E. HO and D. I. GROVES: Geology Department (Key Centre) and University Extension, Publication 12, University of Western Australia, p. 227–237.

BICKLE, M. J., and ARCHIBALD, N. J., 1984, Chloritoid and staurolite stability: implications for metamorphism in the Archaean Yilgarn Block in Western Australia: Journal of Metamorphic Geology, v. 2, p. 179–203.

BINNS, R. A., GUNTHORPE, R. J., and GROVES, D. I., 1974, Metamorphic patterns and development of greenstone belts in the eastern Yilgarn Block, *in* The Early History of the Earth *edited by* B. F. WINDLEY: John Wiley and Sons, London, p. 303–313.

BLEVIN, P. L., and CHAPPELL, B. W., 1992, The role of magma sources, oxidation states and fractionation in determining the granite metallogeny of eastern Australia: Transactions of the Royal Society of Edinburgh, Earth Sciences, v. 83, p. 305–316.

BRUN, J. P., and PONS, J., 1981, Strain patterns of pluton emplacement in a crust undergoing non-coaxial deformation, Sierra Morena, Southern Spain: Journal of Structural Geology, v. 3, p. 219–229.

BURNHAM, C. W., 1979, Magmas and hydrothermal fluids, *in* Geochemistry of Hydrothermal Ore Deposits (2nd edition) *edited by* H. L. BARNES: John Wiley and Sons, New York, p. 71–136.

BURNHAM, C. W., and OHMOTO, H., 1980, Late-stage processes of felsic magmatism, *in* Granite Magmatism and Related Mineralization *edited by* S. ISHIHARA and S. TAKENOUCHI: Mining Geology, Special Issue 8, p. 1–11.

CAMPBELL, I. H., and HILL, R. I., 1988, A two-stage model for the formation of the granite–greenstone terrains of the Kalgoorlie–Norseman area, Western Australia: Earth and Planetary Science Letters, v. 90, p. 11–25.

CAMPBELL, I. H., HILL, R. I., CLAOUÉ-LONG, J. C., GRIFFITHS, R. W., and COMPSTON, W., 1990, The evolution of granite–greenstone terranes in the Kalgoorlie–Norseman area of Western Australia, *in* Extended Abstracts Volume, *compiled by* J. E. GLOVER and S. E. HO: Third International Archaean Symposium, Perth, 1990, Extended Abstracts, Geoconferences (W.A.) Inc., Perth, p. 459.

CANDELA, P. A., 1992, Controls on ore metal ratios in granite-related ore systems: an experimental and computational approach: Transactions of the Royal Society of Edinburgh, Earth Sciences, v. 83, p. 317–326.

CANDELA, P. A., and HOLLAND, H. D., 1986, A mass transfer model for copper and molybdenum in magmatic hydrothermal systems: the origin of porphyry-type ore deposits: Economic Geology, v. 81, p. 1–19.

CANTAGREL, J-M, DIDIER, J., and GOURGAUD, A., 1984, Magma mixing: origin of intermediate rocks and "enclaves" from volcanism to plutonism: Physics of the Earth and Planetary Interiors, v. 35, p. 63–76.

CARROLL, M. R., and WYLLIE, P. J., 1989, Experimental phase relations in the system tonalite–peridotite–H_2O at 15 kb; implications for assimilation and differentiation processes near the crust–mantle boundary: Journal of Petrology, v. 30, p. 1351–1382.

CASSIDY, K. F., 1988, Petrology and alteration of an Archaean granitoid-hosted gold deposit, Lawlers, Western Australia, *in* Advances in understanding Precambrian gold deposits, Volume II *edited by* S. E. HO and D. I. GROVES: Geology Department (Key Centre) and University Extension, Publication 12, University of Western Australia, p. 165–183.

CASSIDY, K. F., 1992, Archaean granitoid–hosted gold deposits in greenschist to amphibolite facies terranes: A high P–T depositional continuum equivalent to greenstone-hosted deposits: University of Western Australia, PhD thesis (unpublished).

CASSIDY, K. F., LIBBY, J. W., PERRING, C. S., and HALLBERG, J. A., 1990, Granitoids, *in* Gold deposits of the Archaean Yilgarn Block, Western Australia: nature, genesis and exploration guides *edited by* S. E. HO, D. I. GROVES and J. M. BENNETT: Geology Department (Key Centre) and University Extension, Publication 20, University of Western Australia, p. 102–113.

CASSIDY, K. F., BARLEY, M. E., GROVES, D. I., PERRING, C. S., and HALLBERG, J. A., 1991, An overview of the nature, distribution and inferred tectonic setting of granitoids in the late-Archaean Norseman–Wiluna Belt, Precambrian Research, v. 51, p. 51–83.

CATHER, S. M., 1990, Stress and volcanism in the northern Mogollon–Datil volcanic field, New Mexico: effects of the post-Laramide tectonic transition: Geological Society of America, Bulletin, v. 102, p. 1447–1458.

CHAPPELL, B. W., 1978, Granitoids of the Moonbi district, New England Batholith, eastern Australia: Geological Society of Australia, Journal, v. 25, p. 267–283.

CHAPPELL, B. W., and WHITE, A. J. R., 1974, Two contrasting granite types: Pacific Geology, v. 8, p. 173–174.

CHAPPELL, B. W., and STEPHENS, W. E., 1988, Origin of infracrustal (I-type) granite magmas: Transactions of the Royal Society of Edinburgh, Earth Sciences, v. 79, p. 71–86.

CHAPPELL, B. W., and WHITE, A. J. R., 1992, I- and S-type granites in the Lachlan Fold Belt: Transactions of the Royal Society of Edinburgh, Earth Sciences, v. 83, p. 1–26.

CHAPPELL, B. W., WHITE, A. J. R., and WYBORN, D., 1987, The importance of residual source material (restite) in granite petrogenesis: Journal of Petrology, v. 28, p. 1111–1138.

CLARK, A. H., FARRAR, E., KONTAK, D. J., LANGRIDGE, R. J., ARENAS, M. J., FRANCE, L. J., McBRIDE, S. L., WOODMAN, P. L., WASTENEYS, H. A., SANDEMAN, H. A., and ARCHIBALD, D. A., 1990, Geologic and chronologic constraints on the metallogenic evolution of the Andes of southeastern Peru: Economic Geology, v. 85, p. 1520–1583.

CLAOUÉ-LONG, J. C., COMPSTON, W., and COWDEN, A., 1988, The age of the Kambalda greenstones resolved by ion microprobe: implications for Archaean dating methods: Earth and Planetary Science Letters, v. 89, p. 239–259.

CLEMENS, J. D., 1984, Water contents of silicic to intermediate magmas: Lithos, v. 17, p. 273–287.

CLEMENS, J. D., and VIELZEUF, D., 1987, Constraints on melting and magma production in the crust: Earth and Planetary Science Letters, v. 86, p. 287–306.

COLEMAN, R. G., and DONATO, M. M., 1979, Oceanic plagiogranite revisited, *in* Trondhjemites, Dacites and Related Rocks *edited by* F. BARKER: Elsevier, Amsterdam, p. 149–168.

COLLINS, W. J., BEAMS, S. D., WHITE, A. J. R., and CHAPPELL, B. W., 1982, Nature and origin of A-type granites with particular reference to southeastern Australia: Contributions to Mineralogy and Petrology, v. 80, p. 189–200.

COMPSTON, W., WILLIAMS, I. S., CAMPBELL, I. H., and GRESHAM, J. J., 1986, Zircon xenocrysts from the Kambalda volcanics: age constraints and direct evidence for older continental crust below the Kambalda–Norseman greenstones: Earth and Planetary Science Letters, v. 76, p. 299–311.

COX, K. G., BELL, J. D., and PANKHURST, R. J., 1979, The Interpretation of Igneous Rocks: George Allen and Unwin, London, 450p.

CZAMANSKE, G. K., ISHIHARA, S. , and ATKIN, S. A., 1981, Chemistry of rock-forming minerals of the Cretaceous–Paleocene batholith in southwestern Japan and implication for magma genesis: Journal of Geophysical Research, v. 86, p. 10431–10469.

DAVIS, G. H., 1980, Structural characteristics of metamorphic core complexes, southern Arizona: Geological Society of America, Memoir 153, p. 35–77.

DAVY, R., 1976, Geochemical variations in Archaean granitoids in the northeastern Yilgarn Block, Western Australia: Western Australia Geological Survey, Annual Report 1975, p. 137–142.

DAVY, R., 1978, A comparative study of the geochemistry of Archaean bedrock in part of the northeastern Yilgarn Block: Western Australia Geological Survey, Report 4, 90p.

DEBON, F., and LE FORT, P., 1982, A chemical–mineralogical classification of common plutonic rocks and associations: Transactions of the Royal Society of Edinburgh, Earth Sciences, v. 73, p. 135–149.

DEBON, F., SHEPPARD, S. M. F., and SONET, J., 1986, The four plutonic belts of the Transhimalaya–Himalaya: a chemical, mineralogical, isotopic and chronological synthesis along the Tibet–Nepal section: Journal of Petrology, v. 27, p. 219–250.

DIDIER, J., 1973, Granites and Their Enclaves: The bearing of enclaves on the origin of granites: Developments in Petrology, 3, Elsevier, Amsterdam.

DILLES, J. H., 1987, Petrology of the Yerrington Batholith, Nevada: Evidence for evolution of porphyry copper ore fluids: Economic Geology, v. 82, p. 1750–1789.

DINGWELL, D. B., 1985, The structure and properties of fluorine-rich magmas: a review of experimental studies, *in* Recent Advances in the Geology of Granite-Related Mineral Deposits *edited by* R. P. TAYLOR and D. F. STRONG: Canadian Institute of Mining and Metallurgy, Special Volume 39, p. 1–12.

DIXON, J. M., 1975, Finite strain and progressive deformation in models of diapiric structures: Tectonophysics, v. 28, p. 89–124.

DRUMMOND, B. J., 1988, A review of crust/upper mantle structure in the Precambrian areas of Australia and implications for Precambrian crustal evolution: Precambrian Research, v. 40/41, p. 101–116.

EBERZ, G. W., and NICHOLLS, I. A., 1988, Microgranitoid enclaves from the Swifts Creek Pluton, SE-Australia: textural and physical constraints on the nature of magma mingling processes in the plutonic environment: Geologische Rundschau, v. 77, p. 713–736.

EBERZ, G. W., and NICHOLLS, I. A., 1990, Chemical modification of enclave magma by post-emplacement crystal fractionation, diffusion and metasomatism: Contributions to Mineralogy and Petrology, v. 104, p. 47–55.

EBY, G. N., 1990, The A-type granitoids: a review of their occurrence and chemical characteristics and speculation on their petrogenesis, *in* Alkaline Igneous Rocks and Carbonatites *edited by* A. R. WOOLLEY and M. ROSS: Lithos, v. 26, p. 115–145.

EINAUDI, M. T., MEINERT, L. D., and NEWBERRY, R. J., 1981, Skarn deposits: Economic Geology, 75th Anniversary Volume, p. 317–391.

ELDERS, W. A., 1968, Mantled feldspars from the granites of Wisconsin: Journal of Geology, v. 76, p. 37–49.

ENGLAND, P. C., and RICHARDSON, S. W., 1977, The influence of erosion upon the mineral facies of rocks from different metamorphic environments: Geological Society of London, Journal, v. 134, p. 201–213.

ENGLAND, P. C., and THOMPSON, A., 1986, Some thermal and tectonic models for crustal melting in collision zones, *in* Collision Tectonics *edited by* M. P. COWARD and A. C. RIES: Geological Society of London, Special Publication 19, p. 83–94.

FENG, R., and KERRICH, R., 1992, Geochemical evolution of granitoids from the Archean Abitibi Southern Volcanic Zone and the Pontiac subprovince, Superior Province, Canada: Implications for tectonic history and source regions: Chemical Geology, v. 98, p. 23–70.

FERRY, J. M., 1979, Reaction mechanisms, physical conditions, and mass transfer during hydrothermal alteration of mica and feldspar in granitic rocks from Maine, USA: Contributions to Mineralogy and Petrology, v. 68, p. 125–139.

FLECK, R. J., 1990, Neodynium, strontium, and trace element evidence of crustal anatexis and magma mixing in the Idaho batholith, *in* The Nature and Origin of Cordilleran Magmatism *edited by* J. L. ANDERSON: Geological Society of America, Memoir 174, p. 359–373.

FODEN, J. D., NESBITT, R. W., and RUTLAND, R. W. R., 1984, The geochemistry and crustal origin of the Archaean acid intrusive rocks of the Agnew Dome, Lawlers, Western Australia: Precambrian Research, v. 23, p. 247–272.

FOSTER, D. A., and HYNDMAN, D. W., 1990, Magma mixing and mingling between synplutonic mafic dykes and granite in the Idaho–Bitteroot batholith, *in* The Nature and Origin of Cordilleran Magmatism *edited by* J. L. ANDERSON: Geological Society of America, Memoir 174, p. 347–358.

FREY, F. A., GREEN, D. H., and ROY, S., 1979, Integrated models of basalt petrogenesis: a study of quartz tholeiites to olivine melilites from south eastern Australia utilizing geochemical and experimental petrological data: Journal of Petrology, v. 19, p. 463–513.

FROST, T. P., and MAHOOD, G. A., 1987, Field, chemical and physical constraints on mafic–felsic magma interaction in the Lamarck Granodiorite, Sierra Nevada, California: Geological Society of America, Bulletin, v. 99, p. 272–291.

GASTIL, G., DIAMOND, J., KNAACK, C., WALAWENDER, M., MARSHALL, M., BOYLES, C., CHADWICK, B., and ERSKINE, B., 1990, The problem of the magnetite/ilmenite boundary in southern and Baja California, *in* The Nature and Origin of Cordilleran Magmatism *edited by* J. L. ANDERSON: Geological Society of America, Memoir 174, p. 19–32.

GEE, R. D., BAXTER, J. L., WILDE, S. A., and WILLIAMS, I. R., 1981, Crustal development in the Yilgarn Block, *in* Archaean Geology *edited by* J. E. GLOVER and D. I. GROVES: International Archaean Symposium, 2nd, Perth, W.A., 1980, Proceedings; Geological Society of Australia, Special Publication, no. 7, p. 43–56.

GEOLOGICAL SURVEY OF WESTERN AUSTRALIA, 1990, Geology and mineral resources of Western Australia: Western Australia Geological Survey, Memoir 3, 827p.

GLIKSON, A. Y., 1979, Archaean granite series and the early crust, Kalgoorlie System, Western Australia, *in* Archaean Geochemistry *edited by* B. F. WINDLEY and S. M. NAQVI: Elsevier, Amsterdam, p. 151–173.

GLIKSON, A. Y., and SHERATON, J. W., 1972, Early Precambrian trondhjemitic suites in Western Australia and northwest Scotland, and the geochemical evolution of shields: Earth and Planetary Science Letters, v. 17, p. 227–242.

GOLDIE, R., 1978, Magma mixing in the Flavarian pluton, Noranda area, Quebec: Canadian Journal of Earth Sciences, v. 15, p. 132–144.

GOLEBY, B. R., RATTENBURY, M. S., SWAGER, C. P., DRUMMOND, B. J., WILLIAMS, P. R., SHERATON, J. W., and HEINRICH, C. A., 1993, Archaean crustal structure from seismic reflection profiling, Eastern Goldfields, Western Australia: Results from the Kalgoorlie Seismic Transect: Australian Geological Survey Organisation, Record 1993/15, 54p.

GREEN, T. H., 1981, Experimental evidence for the role of accessory phases in magma genesis: Journal of Volcanology and Geothermal Research, v. 10, p. 405–422.

GREEN, T. H., and PEARSON, N. J., 1987, An experimental study of Nb and Ta partitioning between Ti-rich minerals and silicate liquids at high pressure and temperature: Geochimica et Cosmochimica Acta, v. 51, p. 55–62.

GRESHAM, J. J., and LOFTUS-HILLS, G. D., 1981, The geology of the Kambalda nickel field, Western Australia: Economic Geology, v. 76, p. 1373–1416.

GRIFFIN, T. J., 1990, Southern Cross Province, *in* Geology and mineral resources of Western Australia: Western Australia Geological Survey, Memoir 3, p. 60–77.

GRIFFIN. T. J., WHITE, A. J. R., and CHAPPELL, B. W., 1978, The Moruya Batholith and geochemical contrasts between the Moruya and Jindabyne Suites: Geological Society of Australia, Journal, v. 25, p. 235–247.

GRIFFIN, T. J., HUNTER, W. M., KEATS, W., and QUICK, D. R., 1983, Description of excursion localities, *in* Eastern Goldfields Geological Field Conference *edited by* P. C. MUHLING: Geological Society of Australia (W.A. Division), Abstracts and Excursion Guide, p. 28–53.

GROVES, D. I., and BARLEY, M. E., 1988, Gold mineralization in the Norseman–Wiluna Belt, Eastern Goldfields Province, Western Australia, *in* Western Australian Gold Deposits, Bicentennial Gold 88 Excursion Guidebook *edited by* D. I. GROVES, M. E. BARLEY, S. E. HO and G. M. F. HOPKINS: Geology Department and University Extension, Publication 14, University of Western Australia, p. 47–66.

GROVES, D. I., BARLEY, M. E., and HO, S. E., 1989, Nature, genesis and tectonic setting of mesothermal gold mineralization in the Yilgarn Block, Western Australia, *in* The Geology of Gold Deposits: The Perspective in 1988 *edited by* R. R. KEAYS, W. R. H. RAMSAY and D. I. GROVES: Economic Geology, Monograph 6, p. 71–85.

HAGGERTY, S. E., 1976, Opaque mineral oxides in terrestrial igneous rocks, *in* Oxide Minerals *edited by* D. RUMBLE III: Mineralogical Society of America, Reviews in Mineralogy, Volume 3, p. Hg101–Hg300.

HAGGERTY, S. E., SMYTH, J. R., ERLANK, A. J., RICHARD, R. S., and DANCHIN, R. V., 1983, Lindsleyite (Ba) and mathiasite (K): two new chromium titanites in the crichtonite series from the upper mantle: American Mineralogist, v. 68, p. 494–505.

HALLBERG, J. A., 1982, Kalgoorlie 1:100 000 sheet: Perth, Western Australia, J. Hallberg and Associates.

HALLBERG, J. A., 1985, Geology and mineral deposits of the Leonora–Laverton area, northeastern Yilgarn Block, Western Australia: Perth, Western Australia, Hesperian Press, 140p.

HALLBERG, J. A., 1986, Archaean basin development and crustal extension in the northeastern Yilgarn Block, Western Australia: Precambrian Research, v. 31, p. 133–156.

HALLBERG, J. A., 1988, A reconnaissance view of the internal granitoids of the Norseman–Wiluna Belt: characteristics, lithological and structural associations, and relationships to gold mineralization, *in* Advances in understanding Precambrian gold deposits, Volume II *edited by* S. E. HO and D. I. GROVES: Geology Department (Key Centre) and University Extension, Publication 12, University of Western Australia, p. 239–243.

HALLBERG, J. A., and WILSON, P., 1983, Relative timing of igneous intrusion in the Eucalyptus Well area, northeastern Yilgarn Block, Western Australia: Geological Society of Australia, Journal, v. 30, p. 383–392.

HALLBERG, J. A., and GILES, C. W., 1986, Archaean felsic volcanism in the northeast Yilgarn Block, Western Australia: Precambrian Research, v. 33, p. 413–427.

HALLIDAY, A. N., DAVIDSON, J. P. HILDRETH, W., and HOLDEN, P., 1991, Modelling the petrogenesis of high Rb/Sr silicic magmas: Chemical Geology, v. 92, p. 107–114.

HAMMOND, R. L., and NISBET, B. W., 1992, Towards a structural and tectonic framework for the central Norseman–Wiluna greenstone belt, Western Australia, *in* The Archaean: terrains, processes and metallogeny *edited by* J. E. GLOVER and S. E. HO: Proceedings Volume for the Third International Archaean Symposium, Perth, Western Australia, Geology Department (Key Centre) and University Extension, University of Western Australia, Publication 22, p. 39–49.

HANNAH, J. L., and STEIN, H. J., 1990, Magmatic and hydrothermal processes in ore-bearing systems: Geological Society of America, Special Paper 246, p. 1–9.

HANSON, G. N., 1978, The application of trace elements to the petrogenesis of igneous rocks of granitic composition: Earth and Planetary Science Letters, v. 38, p. 26–43.

HARRIS, N. B. W., PEARCE, J. A., and TINDLE, A. G., 1986, Geochemical characteristics of collision-zone magmatism, *in* Collision Tectonics *edited by* M. P. COWARD and A. C. RIES: Geological Society of London, Special Publication 19, p. 67–81.

HART, S. R., and ALLEGRE, C. J., 1980, Trace element constraints on magma genesis, *in* Physics of Magmatic Processes *edited by* S. R. HARGEAVES: Princeton University Press, p. 121–159.

HELLMAN, P. L., and GREEN, T. H., 1979, The role of sphene as an accessory phase in the high-pressure partial melting of hydrous mafic compositions: Earth and Planetary Science Letters, v. 42, p. 191–201.

HIBBARD, M. J., 1981, The magma mixing origin of mantled feldspars: Contributions to Mineralogy and Petrology, v. 76, p. 158–170.

HILL, R. I., and CAMPBELL, I. H., 1989, A post-metamorphic age for gold mineralization at Lady Bountiful, Yilgarn Block, Western Australia: Australian Journal of Earth Sciences, v. 36, p. 313–316.

HILL, R. I., CAMPBELL, I. H., and COMPSTON, W., 1989, Age and origin of granitic rocks in the Kalgoorlie–Norseman region of Western Australia: Implications for the origin of Archaean crust: Geochimica et Cosmochimica Acta, v. 53, p. 1259–1275.

HILL, R. I., CHAPPELL, B. W., and CAMPBELL, I. H., 1992a, Late Archaean granites of the southeastern Yilgarn Block, Western Australia: age, geochemistry and origin: Royal Society of Edinburgh, Transactions, v. 83, p. 211–226.

HILL, R. I., CAMPBELL, I. H., and CHAPPELL, B. W., 1992b, Crustal growth, crustal reworking and granite genesis in the southeastern Yilgarn Block, Western Australia, *in* The Archaean: terrains, processes and metallogeny *edited by* J. E. GLOVER and S. E. HO: Proceedings Volume for the Third International Archaean Symposium, Perth, Western Australia, Geology Department (Key Centre) and University Extension, University of Western Australia, Publication 22, p. 203–212.

HINE, R., WILLIAMS, I. S., CHAPPELL, B. W., and WHITE, A. J. R., 1978, Contrasts between I- and S-type granitoids of the Kosciusko Batholith: Geological Society of Australia, Journal, v. 25, p. 219–234.

HOLDEN, P., HALLIDAY, A. N., STEPHENS, W. E., and HENNEY, P. J., 1991, Chemical and isotopic evidence for major mass transfer between mafic enclaves and felsic magma: Chemical Geology, v. 92, p. 135–152.

HUANG, W-L., and WYLLIE, P. J., 1986, Phase relationships of gabbro–tonalite–granite–water at 15 kbar with applications to differentiation and anatexis: American Mineralogist, v. 71, p. 301–316.

HUNTER, W. M., 1991, Boorabbin, W.A. Sheet SH51-13 (2nd edition): Western Australia Geological Survey, 1:250 000 Geological Series Explanatory Notes, 46p.

HUNTER, W. M., 1993, Geology of the granite–greenstone terrain of the Kalgoorlie and Yilmia 1:100 000 sheets: Western Australia Geological Survey, Report 35, 80p.

HUPPERT, H. E., and SPARKS, R. S. J., 1988, The fluid dynamics of crustal melting by injection of basaltic sills: Royal Society of Edinburgh, Transactions, Earth Sciences, v. 79, p. 237–243.

IRVING, A. J., 1978, A review of experimental studies of crystal/liquid trace element partitioning: Geochimica et Cosmochimica Acta, v. 42, p. 743–770.

ISHIHARA, S., 1981, The granitoid series and mineralization: Economic Geology, 75th Anniversary Volume, p. 458–484.

JACKSON, N. J., WALSH, J. N., and PEGRAM, E., 1984, Geology, geochemistry and petrogenesis of late Precambrian granitoids in the central Hijaz region of the Arabian Shield: Contributions to Mineralogy and Petrology, v. 87, p. 205–219.

JAUPART, C., and PROVOST, A., 1985, Heat focussing, granite genesis and inverted metamorphic gradients in continental collision zones: Earth and Planetary Science Letters, v. 73, p. 385–397.

JOHNSON, G. I., and COOPER, J. A., 1989, Rb–Sr whole-rock and mineral dating of Gilgarna Rock syenite, Yilgarn Block, Western Australia: Australian Journal of Earth Sciences, v. 36, p. 472–474.

KRIEWALDT, M., 1970, Menzies, W.A., Sheet SH51-5: Western Australia Geological Survey, 1:250 000 Geological Series.

LAGARDE, J. L., OMAR, S. A., and RODDAZ, B., 1990, Structural characteristics of granitic plutons emplaced during weak regional deformation: examples from late Carboniferous plutons, Morocco: Journal of Structural Geology, v. 12, p. 805–821.

LAMBERT, R. S. J., and HOLLAND, J. G., 1974, Yttrium geochemistry applied to petrogenesis utilizing calcium–yttrium relationships in minerals and rocks: Geochimica et Cosmochimica Acta, v. 38, p. 1393–1414.

LANGMUIR, C. H., VOCKE, R. D. Jr, HANSON, G. N., and HART, S. R., 1978, A general mixing equation with applications to Icelandic basalts: Earth and Planetary Science Letters, v. 37, p. 380–392.

LIBBY, W. G., 1989, Chemistry of plutonic felsic rocks in the Eastern Goldfields, Western Australia: Western Australia Geological Survey, Report 26, Professional Papers, p. 83–104.

LONDON, D., 1986, Magmatic–hydrothermal transition in the Tanco rare-element pegmatite: Evidence from fluid inclusions and phase equilibrium experiments: American Mineralogist, v. 71, p. 376–395.

LOOSVELD, R. J. H., 1989, The synchronism of crustal thickening and high T/low P metamorphism in the Mount Isa Inlier, Australia. 1. An example, the central Soldiers Cap belt: Tectonophysics, v. 158, p. 173–190.

MAHOOD, G., and HILDRETH, W., 1983, Large partition coefficients for trace elements in high-silica rhyolites: Geochimica et Cosmochimica Acta, v. 47, p. 11–30.

MANNING, D. A. C., and PICHAVENT, M., 1985, Volatiles and their bearing on the behaviour of metals in granitic systems, *in* Recent Advances in the Geology of Granite-Related Mineral Deposits *edited by* R. P. TAYLOR and D. F. STRONG: Canadian Institute of Mining and Metallurgy, Special Volume 39, p. 13–24.

MANNING, D. A. C., HAMILTON, D. L., HENDERSON, D. M. B., and DEMPSEY, M. J., 1980, The probable occurrence of interstitial Al in hydrous fluorine-bearing and fluorine-free aluminosilicate melts: Contributions to Mineralogy and Petrology, v. 75, p. 257–262.

MARTIN, H., 1986, Effect of steeper Archean geothermal gradient on geochemistry of subduction-zone magmas: Geology, v. 14, p. 753–756.

MARTIN, H., 1987, Petrogenesis of Archaean trondhjemites, tonalites, and granodiorites from eastern Finland: Major and trace element geochemistry: Journal of Petrology, v. 28, p. 921–953.

MASON, D. R., and McDONALD, J. A., 1978, Intrusive rocks and porphyry-copper occurrences of the Papua New Guinea – Solomon Islands region; a reconnaissance study: Economic Geology, v. 73, p. 857–877.

McCULLOCH, M. T., COMPSTON, W., and FROUDE, D., 1983, Sm–Nd and Rb–Sr dating of Archaean gneisses, eastern Yilgarn Block, Western Australia: Geological Society of Australia, Journal, v. 30, p. 149–153.

McCARTHY, T. S., and HASTY, R. A., 1976, Trace element distribution patterns and their relationship to the crystallization of granitic melts: Geochimica et Cosmochimica Acta, v. 40, p. 1351–1358.

McGOLDRICK, P. J., 1993, Norseman, W.A., Sheet 3233: Western Australia Geological Survey, 1:100 000 Geological Series.

McNAUGHTON, N. J., and CASSIDY, K. F., 1990, A reassessment of the age of the Liberty Granodiorite: implications for a model of synchronous mesothermal gold mineralization within the Norseman–Wiluna Belt, Western Australia: Australian Journal of Earth Sciences, v. 37, p. 373–376.

McQUEEN, K. G., 1981, Volcanic-associated nickel deposits from around the Widgiemooltha Dome, Western Australia: Economic Geology, v. 76, p. 1417–1443.

MILES, K. R., 1945, Some Western Australian lamprophyres: Journal of the Royal Society of Western Australia, v. 31, p. 1–15.

MILLER, C. F., WATSON, E. B., and HARRISON, T. M., 1988, Perspectives on the source, segregation and transport of granitoid magmas: Royal Society of Edinburgh, Transactions, v. 79, p. 135–156.

MÖELLER, P., 1989, REE (Y), Nb, and Ta enrichment in pegmatites and carbonatite-alkalic rock complexes, *in* Lanthanides, Tantalum and Niobium *edited by* P. MÖELLER, P. CERNY and F. SAUPÉ: Springer-Verlag, Berlin, p. 103–144.

MORRIS, P. A., 1993, Archaean mafic and ultramafic volcanic rocks, Menzies to Norseman, Western Australia: Western Australia Geological Survey, Report 36, 107p.

MORRIS, P. A., 1994, Mulgabbie, W.A., Sheet 3337: Western Australia Geological Survey, 1:100 000 Geological Series.

MORRIS, P. A., in prep., Felsic volcanic rocks of the Eastern Goldfields Province, Western Australia: Western Australia Geological Survey, Report.

MORRISON, G. W., 1980, Characteristics and tectonic setting of the shoshonite rock association: Lithos, v. 13, p. 97–108.

MYERS, J. S., 1992, Tectonic evolution of the Yilgarn Craton, Western Australia, *in* The Archaean: terranes, processes and metallogeny *edited by* J. E. GLOVER and S. E. HO: Geology Department (Key Centre) and University Extension, University of Western Australia, Publication 22, p. 265–274.

NASH, W. P., and CRECRAFT, H. R., 1985, Partition coefficients for trace elements in silicic magmas: Geochimica et Cosmochimica Acta, v. 49, p. 2309–2322.

NOYES, H. J., WONES, D. R., and FREY, F. A., 1983, A tale of two plutons: petrographic and mineralogic constraints on the petrogenesis of the Red Lake and Eagle Peak plutons, central Sierra Nevada, California: Journal of Geology, v. 91, p. 353–379.

O'BEIRNE, W. R., 1968, The acid porphyries and porphyroid rocks of the Kalgoorlie area: University of Western Australia, PhD thesis (unpublished)

ORTEGA, L. A., and IBARGUCHI, J. I. G., 1990, The genesis of Late Hercynian granitoids from Galicia (northwestern Spain): inferences from REE studies: Journal of Geology, v. 98, p. 189–211.

OVERSBY, V. M., 1975, Lead isotope systematics and ages of Archaean acid intrusives in the Kalgoorlie–Norseman area, Western Australia: Geochimica et Cosmochimica Acta, v. 39, p. 1107–1125.

PARK, R. G., 1988, Geological Structures and Moving Plates: Glasgow, Blackie, 337p.

PEARCE, J. A., 1982, Trace element characteristics of lavas from destructive plate boundaries, *in* Andesites *edited by* R. S. THORPE: London, John Wiley and Sons, p. 526–548.

PEARCE, J. A., 1983, Role of sub-continental lithosphere in magma genesis at active continental margins, *in* Continental Basalts and Mantle Xenoliths *edited by* C. J. HAWKESWORTH and M. J. NORRY: Shiva Publishing Limited (Geology Series), U.K., p. 230–249.

PEARCE, J. A., HARRIS, N. B. W., and TINDLE, A. G., 1984, Trace element discrimination diagrams for the tectonic interpretation of granitic rocks: Journal of Petrology, v. 25, p. 956–983.

PERFIT, M. R., BRUECKNER, H., LAWRENCE, J. R., and KAY, R. W., 1980, Trace element and isotopic variations in a zoned pluton and associated volcanic rocks, Unalaska Island, Alaska: a model for fractionation in the Aleutian calcalkaline suite: Contributions to Mineralogy and Petrology, v. 73, p. 69–87.

PERRING, C. S., 1988, Petrogenesis of the lamprophyre-"porphyry" suite from Kambalda, Western Australia, *in* Advances in understanding Precambrian gold deposits, Volume II *edited by* S. E. HO and D. I. GROVES: Geology Department (Key Centre) and University Extension, Publication 12, University of Western Australia, p. 277–294.

PERRING, C. S., 1989, The significance of "porphyry" intrusions to Archaean gold mineralization in the Norseman–Wiluna Belt of Western Australia: University of Western Australia, PhD thesis (unpublished).

PERRING, C. S., BARLEY, M. E., CASSIDY, K. F., GROVES, D. I., McNAUGHTON, N. J., ROCK, N. M. S., BETTENAY, L. F., GOLDING, S. D., and HALLBERG, J. A., 1989, The association of linear orogenic belts, mantle–crustal magmatism and Archean gold mineralization in the Eastern Yilgarn Block of Western Australia: Economic Geology, Monograph 6, p. 571–584.

PERRING, C. S., GROVES, D. I., SHELLABEAR, J. N., and HALLBERG, J. A., 1991, The "porphyry–gold" association in the Norseman–Wiluna Belt of Western Australia: implications for London models of Archaean gold metallogeny: Precambrian Research, v. 51, p. 85–113.

PETERSON, J. W., and NEWTON, R. C., 1990, Experimental biotite–quartz melting in the KMASH–CO_2 system and the role of CO_2 in the petrogenesis of granites and related rocks: American Mineralogist, v. 75, p. 1029–1042.

PHILLIPS, W. J., 1973, Mechanical effects of retrograde boiling and its probable importance in the formation of some porphyry ore deposits: Institute of Mining and Metallurgy, Transactions, v. 82, p. B90–B98.

PIDGEON, R. T., 1986, The correlation of acid volcanics in the Archaean of Western Australia: Western Australian Mining and Petroleum Research Institute (WAMPRI), Report 27, 102p.

PITCHER, W. S., 1979, The nature, ascent and emplacement of granitic magmas: Geological Society of London, Journal, v. 136, p. 627–662.

PITCHER, W. S., 1983, Granite type and tectonic environment, *in* Mountain Building Processes *edited by* K. J. HSU: London, Academic Press.

PITCHER, W. S., 1987, Granites and yet more granites, forty years on: Geologische Rundschau, v. 76, p. 51–79.

PIWINSKII, A. J., 1968, Experimental studies of igneous rock series, central Sierra Nevada batholith, California: Journal of Geology, v. 76, p. 548–570.

PIWINSKII, A. J., 1973, Experimental studies of igneous rock series, central Sierra Nevada batholith, California: Part II: Neue Jahrbuch für Mineralogie, Monatshefte, v. 5, p. 193–215.

PIWINSKII, A. J., and WYLLIE, P. J., 1968, Experimental studies of igneous rock series: a zoned pluton in the Wallowa Batholith, Oregon: Journal of Geology, v. 76, p. 205–234.

PLATT, J. P., ALLCHURCH, P. D., and RUTLAND, R. W. R., 1978, Archaean tectonics in the Agnew supracrustal belt, Western Australia: Precambrian Research, v. 7, p. 3–30.

POLI, G. E., and TOMMASINI, S., 1991, Model for the origin and significance of microgranular enclaves in calc-alkaline granitoids: Journal of Petrology, v. 32, p. 657–666.

RAMBERG, I. B., and NEUMANN, E. R., 1978, General aspects of rifting, *in* Petrology and Geochemistry of Continental Rifts *edited by* E. R. NEUMANN and I. B. RAMBERG: D. Reidel Publishing Company, Dordrecht, Holland, p. xix–xxvii.

RATTENBURY, M., 1991, Ballard, W.A. (preliminary edition): Australian Geological Survey Organisation, 1:100 000 Geological Series.

READ, H. H., and WATSON, J., 1975, Earth History: Introduction to Geology, Volume 2: Macmillan Press, London, 371p.

RIDLEY, J. R., 1992, The thermal causes and effects of voluminous, late Archaean monzogranite plutonism, *in* The Archaean: terrains, processes and metallogeny *edited by* J. E. GLOVER and S. E. HO: Geology Department (Key Centre) and University Extension, Publication 22, University of Western Australia, p. 275–285.

RIDLEY, J. R., and KRAMERS, J. D., 1990, The evolution and tectonic consequences of a tonalitic magma layer within Archean continents: Canadian Journal of Earth Sciences, v. 27, p. 219–228.

ROCK, N. M. S., 1987, The nature and origin of lamprophyres: an overview, *in* Alkaline Igneous Rocks *edited by* J. G. FITTON and B. G. J. UPTON: Geological Society of London, Special Publication 30, p. 191–226.

ROCK, N. M. S., HALLBERG, J. A., GROVES, D. I., and MATHER, P. J., 1988, Archaean lamprophyres of the goldfields of the Yilgarn Block, Western Australia: new indications of their widespread distribution and significance, *in* Advances in understanding Precambrian gold deposits, Volume II *edited by* S. E. HO and D. I. GROVES: Geology Department (Key Centre) and University Extension, Publication 12, University of Western Australia, p. 245–275.

ROCK, N. M. S., TAYLOR, W. R., and PERRING, C. S., 1990, Lamprophyres, *in* Gold deposits of the Archaean Yilgarn Block, Western Australia: Nature, genesis and exploration guides *edited by* S. E. HO, D. I. GROVES and J. M. BENNETT: Geology Department (Key Centre) and University Extension, Publication 20, University of Western Australia, p. 128–135.

RUTTER, M. J., and WYLLIE, P. J., 1988, Melting of vapour-absent tonalite at 10 kbar to simulate dehydration-melting in the deep crust: Nature, v. 331, p. 159–160.

RYERSON, F. J., and WATSON, E. B., 1987, Rutile saturation in magmas: implications for Ti–Nb–Ta depletion in island-arc basalts: Earth and Planetary Science Letters, v. 86, p. 225–239.

SANDIFORD, M., and POWELL, R., 1986, Deep crustal metamorphism during continental extension: modern and ancient examples: Earth and Planetary Science Letters, v. 79, p. 151–158.

SAUNDERS, A. D., TARNEY, J., and WEAVER, S. D., 1980, Transverse geochemical variations across the Antarctic Peninsula: implications for the genesis of calc-alkaline magmas: Earth and Planetary Science Letters, v. 46, p. 344–360.

SAWYER, E. W., 1991, Disequilibrium melting and the rate of melt-residuum separation during migmatization of mafic rocks from the Grenville Front, Quebec: Journal of Petrology, v. 32, p. 701–738.

SHIREY, S. B., and HANSON, G. N., 1984, Mantle-derived Archaean monzodiorites and trachyandesites: Nature, v. 310, p. 222–224.

SKJERLIE, K. P., and JOHNSTON, A. D., 1992, Vapor-absent melting at 10 kbar of a biotite- and amphibole-bearing tonalitic gneiss: Implications for the generation of A-type granites: Geology, v. 20, p. 263–266.

SKWARNECKI, M. S., 1987, Controls on Archaean gold mineralization in the Leonora district, Western Australia, *in* Recent Advances in Understanding Precambrian Gold Deposits *edited by* S. E. HO and D. I. GROVES: Geology Department and University Extension, Publication 11, University of Western Australia, p. 109–135.

SMITH, E. I., FEUERBACH, D. L., NAUMANN, T. R., and MILLS, J. G., 1990, Mid-Miocene volcanic and plutonic rocks in the Lake Mead area of Nevada and Arizona; Production of intermediate igneous rocks in an extensional environment, *in* The Nature and Origin of Cordilleran Magmatism *edited by* J. L. ANDERSON: Geological Society of America, Memoir 174, p. 169–194.

SOFOULIS, J., 1963, Norseman, W.A. Sheet SI51-2: Western Australia Geological Survey, 1:250 000 Geological Series.

SPRAY, J. G., 1985, Dynamothermal transition zone between Archaean greenstone and granitoid gneiss at Lake Dundas, Western Australia: Journal of Structural Geology, v. 7, p. 187–203.

STEIN, H. J., 1985, Genetic traits of Climax-type granites and molybdenum mineralization, Colorado Mineral Belt, *in* Recent Advances in the Geology of Granite-Related Mineral Deposits *edited by* R. P. TAYLOR and D. F. STRONG: Canadian Institute of Mining and Metallurgy, Special Volume 39, p. 394–401.

STERN, R. A., HANSON, G. N., and SHIREY, S. B., 1989, Petrogenesis of mantle-derived, LILE-enriched Archean monzodiorites and trachyandesites (sanukitoids) in southwestern Superior Province: Canadian Journal of Earth Sciences, v. 26, p. 1688–1712.

STRECKEISEN, A., 1976, To each plutonic rock its proper name: Earth Science Reviews, v. 12, p. 1–33.

STRONG, D. F., 1985, A review and model of granite-related mineral deposits, *in* Recent Advances in the Geology of Granite-Related Mineral Deposits *edited by* R. P. TAYLOR and D. F. STRONG: Canadian Institute of Mining and Metallurgy, Special Volume 39, p. 424–445.

STUDMEISTER, P. A., 1985, The greenschist metamorphism of Archaean synvolcanic stocks near Wawa, Ontario, Canada: Journal of Metamorphic Geology, v. 3, p. 79–90.

STULL, R. J., 1979, Mantled feldspars and synneusis: American Mineralogist, v. 64, p. 514–518.

SUTCLIFFE, R. H., 1989, Magma mixing in late Archean tonalitic and mafic rocks of the Lac des Iles area, western Superior Province: Precambrian Research, v. 44, p. 81–101.

SWAGER, C. P., 1989, Structure of the Kalgoorlie greenstones — regional deformation history and implications for the structural setting of gold deposits within the Golden Mile: Western Australia Geological Survey, Report 25, p. 59–84.

SWAGER, C. P., 1990, Geology of the Dunnsville 1:100 000 sheet, Western Australia: Western Australia Geological Survey, Record 1990/2, 35p.

SWAGER, C. P., 1991, Geology of the Menzies 1:100 000 sheet and adjacent Ghost Rocks area on the Riverina 1:100 000 sheet, Western Australia: Western Australia Geological Survey, Record 1990/4, 66p.

SWAGER, C. P., 1993, Kurnalpi W.A. Sheet 3336: Western Australia Geological Survey, 1:100 000 Geological Series.

SWAGER, C. P., and GRIFFIN, T. J., 1990, An early thrust duplex in the Kalgoorlie–Kambalda greenstone belt, Eastern Goldfields Province, Western Australia: Precambrian Research, v. 48, p. 63–73.

SWAGER, C. P., and AHMAT, A. L., 1992, Greenstone terranes in the southern part of the Eastern Goldfields Province, *in* Mineral Exploration and Mining Geology in the Eastern Goldfields *compiled by* I. ROBERTS, Geology Symposium Proceedings, Western Australian School of Mines, Kalgoorlie, June, 1992, p. 71–72.

SWAGER, C. P., GRIFFIN, T. J., WITT, W. K., WYCHE, S., AHMAT, A. L., HUNTER, W. M., and McGOLDRICK, P. J., 1995, Geology of the Archaean Kalgoorlie Terrane — an explanatory note: Western Australia Geological Survey, Report 48, 26p. (reprint of Record 1990/12).

SWAGER, C. P., WITT, W. K., GRIFFIN, T. J., AHMAT, A. L., HUNTER, W. M., McGOLDRICK, P. J., and WYCHE, S., 1992, Late Archaean granite–greenstones of the Kalgoorlie Terrane, Yilgarn Craton, Western Australia, *in* The Archaean: terrains, processes and metallogeny *edited by* J. E. GLOVER and S. E. HO: Proceedings Volume, Third International Archaean Symposium, Perth, Western Australia, 1990, Geology Department and University Extension Service, University of Western Australia, Publication 22, p. 107–122.

TACKER, R. C., and CANDELA, P. A., 1987, Partitioning of molybdenum between magnetite and melt: a preliminary study of the partitioning between silicic magmas and crystalline phases: Economic Geology, v. 82, p. 1827–1838.

TAIT, R. E., and HARLEY, S. L., 1988, Local processes involved in the generation of migmatites within mafic granulites: Royal Society of Edinburgh, Transactions, v. 79, p. 209–222.

TAYLOR, S. R., EWART, A., and CAPP, A. C., 1968, Leucogranites and rhyolites: trace element evidence for fractional crystallization and partial melting: Lithos, v. 1, p. 179–186.

TAYLOR, T., 1984, The palaeoenvironmental and tectonic setting of Archaean volcanogenic rocks in the Kanowna District, near Kalgoorlie, Western Australia: University of Western Australia, MSc thesis (unpublished).

THOM, A. M., HILL, R. J., CAMPBELL, I. H., McCULLOCH, M. T., and ARNDT, N. T., 1991, Granitoids from the Late Archaean Norseman–Wiluna Belt within the Yilgarn Craton, Western Australia: Geochemical and Isotopic Constraints on Early Crustal Evolution: Research School of Earth Sciences, Annual Report, 1991, Canberra, p. 147–149.

TITLEY, S. R., and BEANE, R. E., 1981, Porphyry copper deposits I. Geologic settings, petrology and tectonogenesis: Economic Geology, 75th Anniversary Volume, p. 214–235.

TRENDALL, A. F., 1964, Notes on the nomenclature and significance of "porphyry" and "porphyrite" in Western Australia: Western Australia Geological Survey, Annual Report 1963, p. 46–50.

VAN DER HOR, F., and WITT, W. K., 1992, Strain partitioning near the Keith–Kilkenny Fault Zone in the central Norseman–Wiluna Belt, Western Australia: Australia BMR, Record 1992/68, 13p.

VANCE, J. A., 1965, Zoning in igneous plagioclase: patchy zoning: Journal of Geology, v. 73, p. 636–651.

VERNON, R. L., 1984, Microgranitoid enclaves in granites — globules of hybrid magma quenched in a plutonic environment: Nature, v. 309, p. 438–439.

VIDAL, P., BERNARD-GRIFFITHS, J., COCHERIE, A., LE FORT, P., PEUCAT, J. J., and SHEPPARD, S. M. F., 1984, Geochemical comparison between Himalayan and Hercynian leucogranites: Physics of the Earth and Planetary Interiors, v. 35, p. 179–190.

WALAWENDER, M. J., GASTIL, R. G., CLINKENBEARD, J. P., McCORMICK, W. V., EASTMAN, B. G., WERNICKE, R. S., WARDLAW, M. S., GUNN, S. H., and SMITH, B. M., 1990, Origin and evolution of the zoned La Posta-type plutons, eastern Peninsular

ranges, southern and Baja California, *in* The Nature and Origin of Cordilleran Magmatism *edited by* J. L. ANDERSON: Geological Society of America, Memoir 174, p. 1–18.

WALKER, G. P. L., 1989, Gravitational controls on volcanism, magma chambers and intrusions: Australian Journal of Earth Sciences, v. 36, p. 149–165.

WALKER, G. P. L., and SKELHORN, R. R., 1966, Some associations of acid and basic igneous rocks: Earth Science Reviews, v. 2, p. 93–109.

WALL, V. J., CLEMENS, J. D., and CLARKE, D. B., 1987, Models for granitoid evolution and source compositions: Journal of Geology, v. 95, p. 731–750.

WALLMACH, T., and MEYER, F. M., 1990, A petrogenetic grid for metamorphosed aluminous Witwatersrand shales: South African Journal of Geology, v. 93, p. 93–102.

WANG, P., and GLOVER, L., 1992, A tectonics test of the most commonly used geochemical discriminant diagrams and patterns: Earth Sciences Reviews, v. 33, p. 111–131.

WASS, S. Y., 1979, Xenoliths from basalts and other volcanics, *in* The Mantle Sample: Inclusions in Kimberlites and other Volcanics *edited by* F. R. BOYD and H. A. MEYER: Proceedings of the Second International Kimberlite Conference, Volume 2, EOS, p. 366–373.

WASS, S. Y., and ROGERS, N. W., 1980, Mantle metasomatism — precursor to continental alkaline volcanism: Geochimica et Cosmochimica Acta, v. 44, p. 1811–1823.

WATSON, E. B., and CAPOBIANCO, C. J., 1981, Phosphorus and the rare earth elements in felsic magmas: an assessment of the role of apatite: Geochimica et Cosmochimica Acta, v. 45, p. 2349–2358.

WESTRA, G., and KEITH, S. B., 1981, Classification and genesis of stockwork molybdenum deposits: Economic Geology, v. 76, p. 844–873.

WHALEN, J. B., 1985, Geochemistry of an island-arc plutonic suite: the Uasilau – Yau Yau Intrusive Complex, New Britain, P.N.G.: Journal of Petrology, v. 26, p. 603–632.

WHALEN, J. B., and CHAPPELL, B. W., 1988, Opaque mineralogy and mafic mineral chemistry of I- and S-type granites of the Lachlan Fold Belt, southeast Australia: American Mineralogist, v. 73, p. 281–296.

WHALEN, J. B., CURRIE, K. L., and CHAPPELL, B. W., 1987, A-type granites: geochemical characteristics, discrimination and petrogenesis: Contributions to Mineralogy and Petrology, v. 95, p. 407–419.

WHITE, A. J. R., and CHAPPELL, B. W., 1977, Ultrametamorphism and granitoid genesis: Tectonophysics, v. 43, p. 7–22.

WHITNEY, J. A., 1988, The origin of granite: the role and source of water in the evolution of granitic magmas: Geological Society of America, Bulletin, v. 100, p. 1886–1897.

WICKHAM, S. M., 1987, The segregation and emplacement of granitic magmas: Geological Society of London, Journal, v. 144, p. 281–297.

WILLIAMS, I. R., 1974, Structural subdivision of the Eastern Goldfields Province, Yilgarn Block: Western Australia Geological Survey, Annual Report 1973, p. 53–59.

WILLIAMS, P. R., 1993, A new hypothesis for the evolution of the Eastern Goldfields Province, *in* An International Conference on Crustal Evolution, Metallogeny and Exploration in the Eastern Goldfields, Extended Abstracts *compiled by* P. R. WILLIAMS and J. A. HALDANE: Australian Geological Survey Organisation, Record 1993/54, p. 77–83.

WILLIAMS, P. R., and WHITAKER, A., 1993, Gneiss domes and extensional deformation in the highly mineralized Archaean Eastern Goldfields Province, Western Australia: Ore Geology Reviews, v. 8, p. 141–162.

WILLIAMS, P. R., and CURRIE, K. L., 1993, Character and regional implications of the sheared Archean granite–greenstone contact near Leonora, Western Australia: Precambrian Research, v. 62, p. 343–365.

WILLIAMS, P. R., NESBIT, B. W., and ETHERIDGE, M. A., 1989, Shear zones, gold mineralization and structural history in the Leonora district, Eastern Goldfields Province, Western Australia: Australian Journal of Earth Sciences, v. 36, p. 383–403.

WILLIAMS, P. R., RATTENBURY, M., and WITT, W. K., 1993, A field guide to the felsic igneous rocks of the northeastern Eastern Goldfields Province, Western Australia: core complexes, batholiths, plutons and supracrustals, *in* An International Conference on Crustal Evolution, Metallogeny and Exploration of the Eastern Goldfields, Excursion Guidebook *compiled by* P. R. WILLIAMS and J. A. HALDANE: Australian Geological Survey Organisation, Record 1993/53, p. 23–74.

WILSON, M., 1989, Igneous Petrogenesis: A Global tectonic Approach: London, Harper Collins Academic, 466p.

WITT, W. K., 1987, Stratigraphy and layered mafic/ultramafic intrusions of the Ora Banda sequence, Bardoc 1:100 000 sheet, Eastern Goldfields: an excursion guide, *in* Second Eastern Goldfields Geological Field Conference, Kalgoorlie, W.A., 1987, Abstracts and Excursion Guide *compiled by* C. P. SWAGER and W. K. WITT: Geological Society of Australia (W.A. Division), Perth, p. 69–83.

WITT, W. K., 1990, The geology of the Bardoc 1:100 000 sheet, Western Australia: Western Australia Geological Survey, Record 1990/14, 111p.

WITT, W. K., 1991, Regional metamorphic controls on alteration associated with gold mineralization in the Eastern Goldfields Province, Western Australia: Implications for the timing and origin of Archean lode-gold deposits: Geology, v. 19, p. 982–985.

WITT, W. K., 1992a, Heavy-mineral characteristics, structural settings, and parental granites of pegmatites in the eastern Yilgarn Craton: Western Australia Geological Survey, Record 1992/10, 54p.

WITT, W. K., 1992b, Porphyry intrusions and albitites in the Bardoc–Kalgoorlie area, Western Australia, and their role in Archean epigenetic gold mineralization: Canadian Journal of Earth Sciences, v. 29, p. 1609–1622.

WITT, W. K., 1993a, Gold deposits of the Menzies and Broad Arrow areas, Western Australia: Western Australia Geological Survey, Record 1992/13, 156p.

WITT, W. K., 1993b, Gold mineralization in the Menzies–Kambalda area, Western Australia: Western Australia Geological Survey, Report 39, 165p.

WITT, W. K., 1993c, Lithological and structural controls on gold mineralization in the Archaean Menzies–Kambalda area, Western Australia: Australian Journal of Earth Sciences, v. 40, p. 65–86.

WITT, W. K., 1994, Geology of the Melita 1:100 000 sheet: Western Australia Geological Survey, 1:100 000 Geological Series Explanatory Notes, 63p.

WITT, W. K., and SWAGER, C. P., 1989, Structural setting and geochemistry of Archaean I-type granites in the Bardoc–Coolgardie area of the Norseman–Wiluna belt, Western Australia: Precambrian Research, v. 44, p. 323–351.

WITT, W. K., DAVY, R., HUNTER, W. M., and PESCUD, L., 1996, Geochemical analyses of Archaean acid to intermediate igneous rocks, including granitoids, minor intrusions, and volcanic rocks, southwest Eastern Goldfields Province, Western Australia: Western Australia Geological Survey, Record 1995/2, 55p.

WONES, D. R., 1981, Mafic silicates as indicators of intensive variables in granitic magmas: Mining Geology (Japan), v. 31, p. 191–212.

WONES, D. R., 1989, Significance of the assemblage titanite + magnetite + quartz in granitic rocks: American Mineralogist, v. 74, p. 744–749.

WRIGHT, A. E., and BOWES, D. R., 1979, Geochemistry of the appinite suite, *in* Caledonides of the British Isles — reviewed *edited by* A. L. HARRIS, C. H. HOLLAND and B. E. LEAKE: Geological Society of London, Special Publication 8, p. 699–703.

WYBORN, D., and CHAPPELL, B. W., 1986, The petrogenetic significance of chemically related plutonic and volcanic rock units: Geological Magazine, v. 123, p. 619–628.

WYBORN, D., TURNER, B. S., and CHAPPELL, B. W., 1987, The Boggy Plain Supersuite: a distinctive belt of I-type igneous rocks of potential economic significance in the Lachlan Fold Belt: Australian Journal of Earth Sciences, v. 34, p. 21–43.

WYBORN, L. A. I., 1993, Constraints on interpretations of lower crustal structure, tectonic setting and metallogeny of the Eastern Goldfields and Southern Cross Provinces provided by granite geochemistry: Ore Geology Reviews, v. 8, p. 125–140.

WYBORN, L. A. I., and PAGE, R. W., 1983, The Proterozoic Kalkadoon and Ewen Batholiths, Mount Isa Inlier, Queensland: source, chemistry, age, and metamorphism: Australia BMR, Journal of Australian Geology and Geophysics, v. 8, p. 53–69.

WYBORN, L. A. I., WYBORN, D., WARREN, R. G., and DRUMMOND, B. J., 1992, Proterozoic granite types in Australia: implications for lower crust composition, structure and evolution: Royal Society of Edinburgh, Transactions, Earth Sciences, v. 83, p. 201–209.

WYCHE, S., 1996, Riverina, W.A. Sheet 3038: Western Australia Geological Survey, 1:100 000 Geological Series.

WYCHE, S., and WITT, W. K., 1992, Geology of the Davyhurst 1:100 000 Sheet, Western Australia: Western Australia Geological Survey, Record 1991/3, 48p.

WYLLIE, P. J., 1977, Crustal anatexis: an experimental review: Tectonophysics, v. 43, p. 41–71.

WYLLIE, P. J., 1984, Sources of granitoid magmas at convergent plate boundaries: Physics of the Earth and Planetary Interiors, v. 35, p. 12–18.

WYMAN D., and KERRICH, R., 1989, Archaean shoshonitic lamprophyres associated with Superior Province gold deposits: distribution, tectonic setting, noble metal abundances, and significance for gold mineralization, *in* The Geology of Gold Deposits: The Perspective in 1988 *edited by* R. R. KEAYS, W. R. H. RAMSAY and D. I. GROVES: Economic Geology, Monograph 6, p. 651–667.

ZEN, E. A., 1986, Aluminium enrichment in silicate melts by fractional crystallization: some mineralogic and petrographic constraints: Journal of Petrology, v. 27, p. 1095–1117.

ZEN, E. A., 1988, Thermal modelling of stepwise anatexis in a thrust-thickened sialic crust: Royal Society of Edinburgh, Transactions, Earth Sciences, v. 79, p. 223–235.

Appendix I

Map references for localities mentioned in text and tables

Location	1:100 000 Sheet	AMG Northing	AMG Easting	Location	1:100 000 Sheet	AMG Northing	AMG Easting
12 Mile Well	EDJUDINA	668750	40850	McAuliffe Well	YERILLA	673730	39540
18 Mile Well	RIVERINA	672500	27200	Melita Railway Siding	MELITA	678530	35260
26 Mile Rock	CAVE HILL	646100	32450	Menangina Homestead	BOYCE	670000	39500
29 Mile Well	RIVERINA	673300	28100	Menzies	MENZIES	671330	30930
50 Mile Rocks	COWAN	647350	37050	Missouri	DAVYHURST	665500	30290
Alexandria Bore	MENZIES	670550	33000	Mount Charlotte	KALGOORLIE	659750	35440
Arrow Lake	KALGOORLIE	662050	34750	Mount Ellis	BARDOC	663050	33280
Barber Well	BOYCE	670900	40550	Mount Hunt	KANOWNA	658640	35720
Bardoc	BARDOC	664250	33550	Mount Ida	BALLARD	678410	25710
Black Flag	KALGOORLIE	661930	33020	Mount Pleasant	KALGOORLIE	662200	33230
Blueys Well (a)	WILBAH	680630	26160	Naismith Bore	BOYCE	673150	36400
Bonnie Vale	KALGOORLIE	658400	32400	Niagara Dam	MELITA	674600	34750
Bora Rock	DAVYHURST	662900	30050	Nine Mile Rock	BARDOC	662790	35170
Boundary Well	EDJUDINA	671600	40380	Ora Banda	BARDOC	663790	31370
Brady Well	BOYCE	670600	39500	Paddington	BARDOC	662630	34120
Breakaway Well	MELITA	677170	31120	Paddys Knob Bore	BARDOC	664390	30930
Broad Arrow	BARDOC	663010	33950	Panglo Mine	KALGOORLIE	662190	34520
Bullabulling	KALGOORLIE	656700	29550	Peters Bore (a)	WILBAH	684240	35880
Celebration	LAKE LEFROY	656930	36560	Princess Bore	BOYCE	668950	40200
Cement Well	BOYCE	671050	39700	Quairnie Rock	YILMIA	653920	31730
Coolgardie	KALGOORLIE	657400	32430	Rainbow Bore	BOYCE	671950	38350
Credo Homestead	DUNNSVILLE	662700	29100	Red Lake	GINDALBIE	668000	39650
Dairy Well	YERILLA	675500	35910	Riverina	RIVERINA	670650	26450
Davyhurst	DAVYHURST	667410	27190	Riverina Homestead	RIVERINA	670600	26450
Democrat	COWAN	649380	38790	Sand Queen	MENZIES	668440	31930
Donkey Rocks	BOYCE	669850	37750	Scotia	BARDOC	665780	33390
Donkey Rocks Well	BOYCE	669900	37700	Scotia Bore	BARDOC	665950	33540
Doyle Dam	DUNNSVILLE	660700	30270	Siberia	DAVYHURST	665250	30400
Fitzgerald Peaks	PEAK CHARLES	636000	32800	Six Mile Rocks	BOYCE	669050	38150
Galah Rockhole	MELITA	674110	33300	Snot Rocks	DAVYHURST	664650	28800
Gilgarna Rock	MULGABBIE	664260	34450	Split Rocks	BARDOC	665200	34300
Goongarrie	BARDOC	667450	32240	Sunday Soak	BARDOC	664550	35050
Goongarrie Homestead	MENZIES	668130	31120	Tassy Well	BOYCE	673400	37500
Granite Dam	MENZIES	668980	33020	Theatre Rocks (a)	NORSEMAN	642800	36370
Hamdorf Bore	BOYCE	671400	40150	Twin Hills	MELITA	674100	31770
Horse Rocks	YILMIA	655550	34770	Twin Peaks	EDJUDINA	668900	41100
Jeedamya Homestead	MELITA	674600	33260	Wangine Soak	DAVYHURST	666170	39240
Jennys Reward	BARDOC	667290	32480	Widgiemooltha	LAKE LEFROY	651470	36450
Jungle Well	YERILLA	673850	37250	Wongi Hill	DAVYHURST	676390	30240
Kookynie	MELITA	675350	35350	Woorana Well (a)	WANGANNOO	675800	32150
Kunanalling	KALGOORLIE	660400	31480	Yerilla Homestead	YERILLA	673950	38550
Lake Owen	BARDOC	666400	31300				

NOTE: (a) Outside area of SWEGP
AMG Australian Map Grid

Appendix 2

Internal relationships within some pre-RFG complexes: outcrop-scale observations

Birthday complex

Outcrops within the Birthday complex commonly display a variety of microgranitoid xenoliths and dykes, some of which are synplutonic dykes. Microgranitoid xenoliths and synplutonic dykes are variably flattened in the plane of the regional S_2/S_3 foliation. Limited three-dimensional exposures of xenoliths, which display no evidence of east-northeast–west-southwest flattening, indicate some are extremely thin in the vertical dimension (pancake-shaped; Figure 2.1g).

One of the more interesting exposures of pre-RFGs occupies about 1 km^2, between Cement Well and Barber Well, 11 km north-northwest of Menangina Homestead. The volumetrically dominant component at this locality is foliated granodiorite and monzogranite of the Rainbow suite, containing up to about 10% mafic minerals (biotite and hornblende), and tabular K-feldspar phenocrysts up to several centimetres long. Variations in grain size and composition, based on relatively minor differences in the abundance of mafic minerals, produces large-scale banding (tens of metres or more). Contacts or transitions between bands are rarely exposed. However, at one locality a sharp contact between coarse-grained (1–4 mm) granodiorite (5–10% mafic minerals) and relatively fine-grained (0.5–2 mm), leucocratic (3–4% mafic minerals) monzogranite is exposed. The more leucocratic unit displays a slight concentration of biotite, and a fine-grained margin, against this contact.

Rounded, relatively mafic clots and cognate xenoliths, up to 1 m across, are abundant and compositionally diverse, ranging from hornblende(–clinopyroxene–biotite–quartz) monzonite to monzodiorite. Mesocratic xenoliths commonly contain smaller, darker enclaves and mafic mineral clots to about 5 mm (Figure 2.1d). Small (to a few centimetres across), relatively mafic synplutonic dykes (including clinopyroxene–biotite–hornblende granodiorite) have cuspate margins, and display evidence of plastic deformation (Figure 2.1e,f). Synplutonic dykes and xenoliths are both back-veined by the host granodiorite. The abundance of xenoliths, clots and synplutonic dykes appears to vary directly with the colour index of the host granitoid. However, contacts between enclaves and host are typically sharp, and structures suggesting dispersal of enclaves have not been observed.

In addition to small, synplutonic dykes, there are some larger dykes (to several metres across). One of the two largest dykes is leucocratic quartz monzonite containing biotite and hornblende, and the other is mesocratic monzonite containing hornblende and clinopyroxene. The leucocratic quartz monzonite dyke contains phenocrysts of tabular plagioclase (~1 cm), rounded quartz (~5 mm), hornblende and biotite, in a very fine-grained groundmass. It also contains fine-grained, hornblende-rich, dioritic xenoliths up to several centimetres across (Figure 2.2a). The dyke has a thin chilled margin against the granodiorite and monzogranite country rocks. This leucocratic dyke is cut by the mesocratic monzonite dyke that contains abundant rounded xenoliths, up to about 20 cm across, of a type and variety similar to those contained in the host granodiorite and monzogranite (Figure 2.2b). The colour index of the dyke is variable, on many scales, with irregular, sharp and gradational transitions. It contains xenoliths of the host granodiorite/monzogranite, but is also cut by numerous narrow, irregular, discontinuous, leucocratic veinlets (Figure 2.2c) which are interpreted to have crystallized from a modified host granitoid magma.

Granodiorite and monzogranite display a north to north-northwesterly S_2/S_3 foliation, defined mainly by the alignment of mafic minerals, and, to a lesser degree, by elongate quartz grains. The foliation is more strongly developed in zones. The outcrops in the vicinity of the large dykes are massive to weakly foliated, but synplutonic dykes and mafic xenoliths in the leucocratic quartz monzonite dyke are strongly flattened and smeared out subparallel to the regional foliation. These observations suggest that the dyke locality was a low-strain domain for the granodiorite and monzogranite during regional compression, and that strain may have been partitioned into the quartz monzonite dyke.

Two syenitic units belonging to the Gilgarna supersuite intrude Rainbow suite granitoids a few hundred metres south of the above locality. The main Gilgarna phase consists predominantly of massive, coarse-grained (2–6 mm), tabular K-feldspar, with interstitial clinopyroxene. Igneous banding, defined by alternating layers of feldspar and mafic minerals, and irregular pipe-like bodies of very coarse-grained (?pegmatoid) syenite, are developed locally. The coarse-grained syenite is cut by a moderately to strongly foliated (trending 170°) dyke of porphyritic quartz monzonite composed of phenocrysts (<4 mm) of clinopyroxene, hornblende and plagioclase in a very fine-grained, pink groundmass. There are also small, rounded, relatively mafic syenitic xenoliths, to about 5 cm, in the coarse-grained syenite. Both syenite and quartz monzonite dyke are cut by a fine-grained alkaline complex

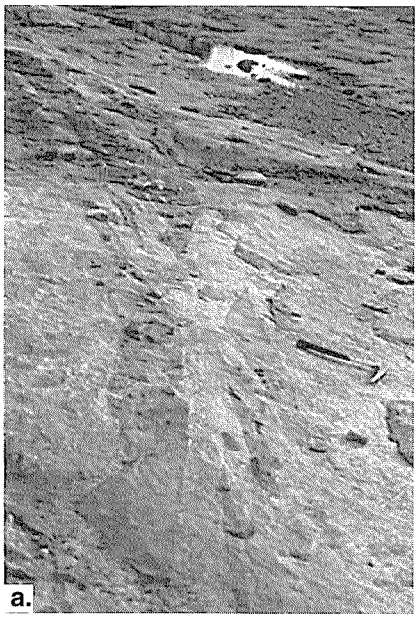

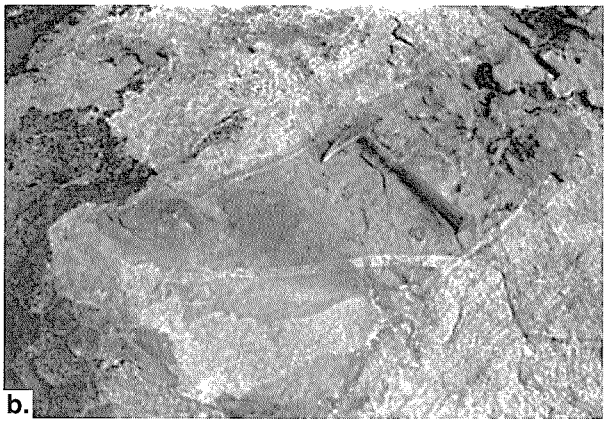

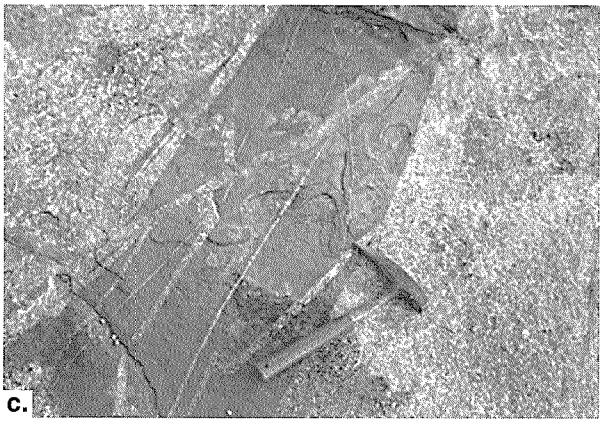

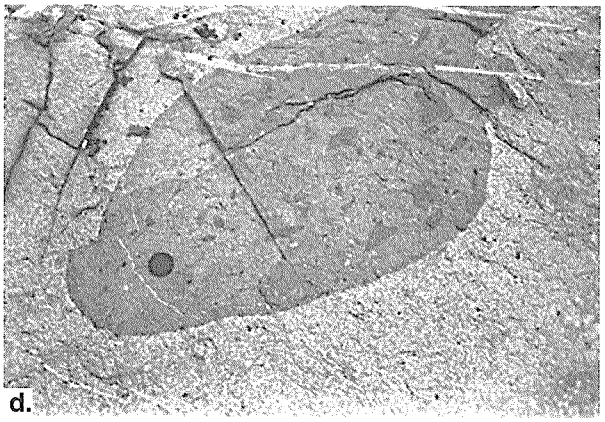

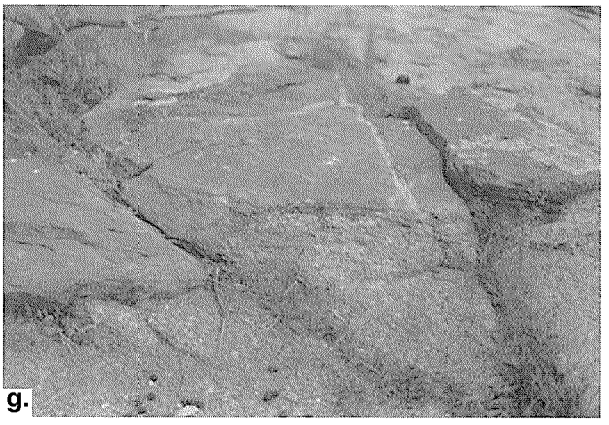

WW 295

13.05.97

Figure 2.1a Back-veining of a microgranitoid dyke by the Twin Hills suite monzogranite, Granite Dam. Note the irregular, convoluted contact between the dyke and monzogranite in the left foreground. The width of thickest dyke fragment is approximately 20 cm

Figure 2.1b Convoluted contacts at terminations of dyke fragments where the dyke has been pulled apart and back-veined by the host monzogranite, Granite Dam. The width of the dyke is approximately 20 cm

Figure 2.1c Close-up photograph of back-veining of a microgranitoid dyke by the Twin Hills monzogranite host rock. Dyke is approximately 25 cm wide

Figure 2.1d A rounded microgranitoid xenolith in the Rainbow suite granodiorite, Cement Well. Note the darker microgranitoid enclaves within the xenolith, the convolute contact with the granodiorite at lower left, a cross-cutting aplitic dyke, and the small offset of xenolith/granodiorite contacts by a late, dextral fault. The xenolith measures approximately 1 m in the long dimension

Figure 2.1e A pull-apart structure in a microgranitoid, synplutonic dyke in the Rainbow suite granodiorite, Cement Well. Note the back-veining of the dyke pull-apart by the host granodiorite, and cuspate contacts between the dyke and granodiorite. The dyke is approximately 4 cm wide

Figure 2.1f An irregular, microgranitoid xenolith in the Rainbow suite granodiorite, Cement Well. Note the delicately convoluted contacts between the xenolith and granodiorite. The xenolith measures approximately 1 m in the long dimension

Figure 2.1g A microgranitoid xenolith in the Rainbow suite granodiorite, Cement Well. Note the flat lower contact of the xenolith with the granodiorite and high aspect ratio ('pancake shape') of the xenolith. The xenolith is approximately 2 m long

that displays stromatic, swirling and other complex mixing structures between relatively mesocratic and leucocratic components. Coarse-grained (?pegmatoid) quartz syenite segregations containing black melanitic garnet occur in the main zone of mixing. Similar mixing structures with melanitic garnet occur in alkaline rocks at Twin Peaks.

Scotia complex

Rainbow suite granitoids occur in the Scotia complex at Nine Mile Rock, Sunday Soak and Split Rocks. Granodiorite and monzogranite at these localities display a pervasive north to north-northwesterly S_2/S_3 foliation, defined by oriented hornblende and biotite, elongate quartz grains, and a weak mineral segregation. Orientation of hornblende at Split Rock defines a weak subhorizontal lineation. Tabular K-feldspar phenocrysts up to 7 cm long are common, especially at Sunday Soak. They are mostly aligned subparallel to the regional foliation, but local concentrations of unoriented K-feldspar, up to several metres across, suggest accumulation due to eddying currents in the flow pattern of the original magma.

Rounded, cognate xenoliths (tonalite, diorite) up to about 1 m across are common and contain the same foliation as the host granitoid. Grainsize and colour index are variable, and at Split Rocks, darker enclaves within xenoliths are common. At Sunday Soak rounded xenoliths are variably flattened in the plane of the regional foliation. Angular, slab-like xenoliths (length to width ratio up to approximately 20:1) with a distinct gneissic fabric are oriented with their long axes subparallel to the regional foliation.

Both xenoliths and host granitoids are cut by a network of aplitic dykes, and, less commonly, later intermediate to mafic porphyry dykes. Dykes trend north to north-northwest, and approximately 120°.

A contact between Rainbow suite granodiorite and Goongarrie suite monzogranite at Split Rocks is characterized by alternating bands of the two intrusive units. The bands are up to several metres across, and are oriented approximately normal to the gross east–west trend of the contact. Prior to F_2, this would have been a subhorizontal, interfingering contact, consistent with the interpretation of pre-RFG units as sheet-like bodies (**Chapter 3**).

Mulliberry complex

All pre-RFG suites are represented in the Mulliberry complex. Good exposures occur at several localities, including Granite Dam, east of Menzies, and in the Niagara–Kookynie area. Synplutonic dykes and cognate xenoliths are present at some localities, but are less common than in most Birthday complex outcrops. Intrusive porphyry dykes are also fairly common, and there is some compositional variation within the predominant medium- to coarse-grained monzogranite and granodiorite.

Granite Dam

At Granite Dam there are two biotite-monzogranite bodies with tabular K-feldspar phenocrysts separated by a sharp, roughly north-trending intrusive contact. The more mafic unit (5–10% biotite) belongs to the Twin Hills suite whereas the more leucocratic body (<5% biotite) is assigned to the Goongarrie suite. The Twin Hills suite monzogranite displays igneous banding, on the scale of tens of centimetres, subparallel to the intrusive contact, defined by variations in the proportions of biotite and K-feldspar, and in the size of the phenocrysts. Some bands consist almost entirely of K-feldspar and biotite. Biotite schlieren are common, and rounded mafic xenoliths are present, but not widespread. The Twin Hills suite monzogranite is cut by several finer grained, mesocratic dykes, in a variety of orientations. Some have sharp contacts with the host monzogranite, but the largest dyke (about 1 m wide) is apparently synplutonic. The dyke is back-veined by the monzogranite, and locally displays evidence of streaking out and partial disaggregation and dispersal (Figure 2.1a–c). Some dykes contain biotite-rich clots and lenses, and more mafic bands and xenoliths, in varying stages of flattening and plastic deformation. The relatively mafic components tend to concentrate toward the margins of the dykes. A pervasive northwesterly trending foliation passes through all units, and is refracted slightly across some dykes. It is defined by oriented biotite and biotite-rich aggregates, elongate quartz grains, and variably flattened xenoliths. K-feldspar phenocrysts are commonly oriented within the regional foliation, and define a subhorizontal linear fabric. Minor aplite and pegmatite dykes cut all other phases but do not contain a distinct foliation.

Alexandria Bore

Two intrusive members of the Minyma suite are exposed near Alexandria Bore, east of Menzies. Biotite monzogranite has a fine-grained margin against a sharp but irregular intrusive contact with hornblende–biotite monzogranite. Both granitoids are coarse-grained (1–3 mm) and quartz-rich, but the biotite monzogranite is relatively leucocratic. The fine-grained margin of the biotite monzogranite is finely banded and biotite increases from about 2% in the main body of the intrusion to about 50% at the contact. Xenoliths and synplutonic dykes have not been observed. A north-northwesterly trending foliation is developed in zones, in both phases.

Niagara–Kookynie area

Pre-RFG exposures south of Niagara and Kookynie have not been analysed but possess petrographic characteristics that suggest they are dominantly members of the Twin Hills suite. Biotite monzogranite and granodiorite are dominant but are extensively interleaved with diverse greenstone lithologies and narrow zones of mylonitized granitoid schist. Greenstone lenses and mylonitic zones are mostly oriented parallel to the margins of the Mulliberry complex. Granodiorite and monzogranite display a pervasive, contact-parallel foliation that is locally overprinted by a north-northwesterly trending S_2/S_3 foliation. The contact-parallel foliation contains a north–south to northwesterly trending lineation (L_1) defined by oriented, elongate aggregates of recrystallized biotite. A synplutonic dyke of weakly porphyritic biotite tonalite, and some microgranitoid xenoliths, outcrop south of Kookynie. Locally abundant lenses and slices of tonalitic to dioritic composition are isoclinally folded by F_1 south of Niagara mining centre and probably represent strained cognate xenoliths and synplutonic dykes.

Raeside complex

The best exposures of the Raeside complex in the study area outcrop immediately east of Twin Hills, north of Menzies. A north to north-northwesterly trending banding, on a scale of several metres, is defined by three main intrusive phases, all belonging to the Twin Hills suite. The earliest and volumetrically dominant phase is coarse-grained (1–4 mm), equigranular monzogranite containing 5–15% biotite. Lit-par-lit intrusive contacts with relatively leucocratic (<5% biotite) and finer grained (0.5–2 mm) monzogranite and syenogranite have been observed. Medium-grained (0.5–1 mm), weakly plagioclase-phyric biotite-granodiorite bands contain accidental xenoliths of coarse-grained monzogranite, but timing relationships with leucocratic monzogranite and syenogranite are not known. The granodiorite phase contains small mafic clots, up to several millimetres across. The colour index varies, but only the darkest bands have (minor) hornblende. Synplutonic dykes and rounded mafic xenoliths were not recognized at this locality.

All three phases contain a northerly trending, upright regional foliation oriented at a small angle to the compositional banding. The foliation is best developed in the main monzogranite phase, which also preserves a shallow southerly plunging linear fabric, defined by stretched biotite aggregates. This locality was mapped as granitic gneiss by Kreiwaldt (1970) but is assigned to the pre-RFG intrusions in this study because granoblastic textures are not prevalent and compositional banding is recognizably attributable to multiple intrusive episodes.

The three granitoid phases are intruded by narrow, unfoliated pegmatite dykes up to 30 cm wide. Most dykes are oriented subparallel to the igneous banding, although a few are oblique. Although not observed in-situ, minor amphibolite and banded iron-formation float are interpreted as greenstone screens that were probably interleaved with the granitoids during D_1 movements on the granite–greenstone contact.

Similar banded, intrusive units, with interleaved greenstone screens, outcrop around the northern margin of the Raeside complex, near Leonora, where banding is oriented subparallel to the margin of the dome (Williams, 1993). Two foliations are present — a contact-parallel S_1 is crenulated by the north to north-northwesterly trending S_2. The banding at this locality is correlated with that near Twin Hills. This contact-parallel compositional banding suggests the Raeside complex was a flat-lying association of sheet-like intrusive units before F_2 folding.

Figure 2.2a **Strongly flattened hornblende-rich dioritic xenoliths in a leucocratic quartz-monzonite dyke, intrusive into the Rainbow suite granodiorite, Cement Well. The largest xenolith is approximately 7 cm long**

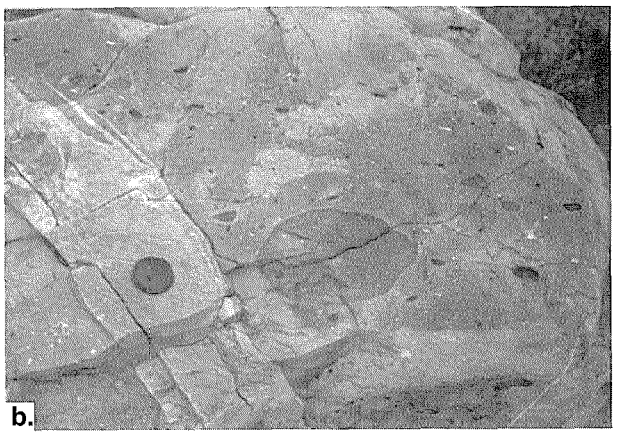

Figure 2.2b **Abundant microgranitoid xenoliths in a mesocratic monzonite dyke, intrusive into the Rainbow suite granodiorite, Cement Well. The largest xenolith is about 20 cm in diameter. Note the lens cap on a cross-cutting aplitic dyke**

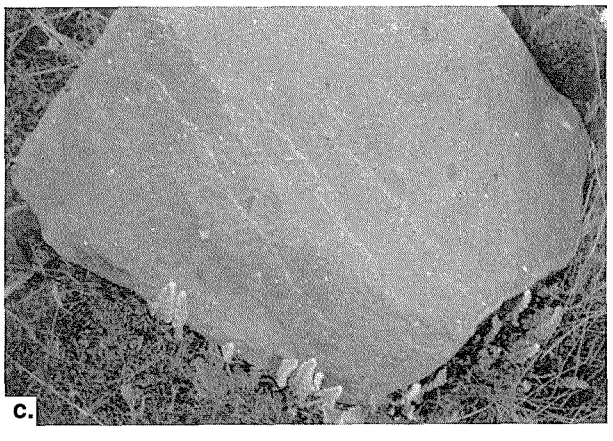

WW 296 13.05.97

Figure 2.2c **Thin, diffuse bands of leucocratic granitoid (northwest to southeast across photo) in a mesocratic monzonite dyke, Cement Well. The monzonite block is approximately 1 m across**

Owen complex

The Owen complex is dominated by granitoids of the Goongarrie suite, the best exposures of which are in the Goongarrie Homestead area and west of Goongarrie. Medium- to coarse-grained (0.5–3 mm) monzogranite, containing up to 10% biotite and <5% tabular K-feldspar phenocrysts (~2 cm), is the dominant phase. Oriented biotite forms a weak to moderate north-northwesterly trending foliation, but K-feldspar phenocrysts are unoriented to only weakly aligned. Biotite-rich schlieren are common. Synplutonic dykes and rounded cognate xenoliths are locally common, but not widespread. Xenoliths are mainly biotite diorite and biotite quartz diorite, with minor biotite-rich syenogranite. These, and elongate xenoliths of biotite-rich (?pelitic) schist, are back-veined by the host granodiorite and variably flattened in the plane of the foliation. The north-northwesterly trending foliation passes through xenoliths, dykes and monzogranite, but some xenoliths also retain a distinct (?gneissic) foliation oblique to the regional foliation. Pegmatite dykes are variably oriented and cut all other phases. They are weakly foliated or unfoliated. Xenoliths and synplutonic dykes are sparse or absent at exposures elsewhere in the Owen complex (Bora Rock, west of Mount Ellis, and along the western margin of the dome).

References

KRIEWALDT, M., 1970, Menzies, W.A. Sheet SH51-5: Western Australia Geological Survey, 1:250 000 Geological Series.

WILLIAMS, P. R., 1993, A new hypothesis for the evolution of the Eastern Goldfields Province, *in* An International Conference on Crustal Evolution, Metallogeny and Exploration in the Eastern Goldfields, Extended Abstracts *compiled by* P. R. WILLIAMS and J. A. HALDANE: Australian Geological Survey Organisation, Record 1993/54, p. 77–83.

Appendix 3

Late-magmatic and metamorphic mineralogical and textural modifications of the granitoids

Quartz

Quartz is present in almost all granitoid samples, but comprises <20%, and mostly <10%, of the alkaline granitoids, and also of many of the microgranitoid xenoliths. It is rarely a phenocryst phase, except in some microgranitoid xenoliths (e.g. 100957, Goongarrie).

Quartz is subequant and anhedral in undeformed granitoids. Recrystallization has caused strained extinction and minor to extensive subgrain growth in all samples. Progressive recrystallization causes suturing of grain boundaries. Strongly deformed granitoids, particularly those around the margins of pre-regional folding complexes and post-D_2 to syn-D_3 diapirs, contain elongate ribbons of recrystallized quartz with a length to width ratio of up to 6:1. A granoblastic texture is dominant in gneiss samples.

K-feldspar

Anhedral K-feldspar is interstitial to other essential minerals in unrecrystallized calc-alkaline granitoids. Tabular K-feldspar phenocrysts, to several centimetres (mostly 1–2 cm), are common and locally abundant. Phenocrysts contain inclusions of most other minerals, especially quartz and plagioclase. The inclusions are commonly concentrated in the outer margins of the phenocrysts, may be zonally arranged, and are oriented with respect to crystallographic axes of the host K-feldspar. Although apparently euhedral in hand specimen, phenocryst grain-boundaries are very irregular in detail. These observations suggest that K-feldspar was a late-crystallizing phase, even in rocks with coarse, tabular K-feldspar phenocrysts (cf. Hibbard, 1965).

K-feldspar is weakly to moderately perthitic, with up to about 30% film, vein and patch albite (terminology of Smith, 1974). A perthitic texture is normally better-developed, or preserved, in phenocrysts, and interstitial groundmass K-feldspar is commonly non-perthitic. Cross-hatch twinning is widespread, indicating the K-feldspar is microcline. Rarely, individual grains are mantled by plagioclase.

Recrystallization of K-feldspar results in grainsize reduction, and ultimately produces anhedral, subequant grains of non-perthitic microcline, commonly with 120° triple points. Swapped albite rims (Rogers, 1961; Smith, 1974) are well-developed in some high-SiO_2 (>75% SiO_2) granitoids (mainly a few small, late-tectonic intrusions such as the Old Monzogranite). These intrusions also contain coarse-grained albite replacing perthitic intergrowths. Minor sericitization of microcline occurs in some calc-alkaline granitoids, but K-feldspar is commonly less susceptible to alteration than is plagioclase in the same sample.

K-feldspar has a similar form in most enclaves and dykes, but phenocrysts are rare, and it is generally less abundant than in the calc-alkaline granitoid host rocks, and non-perthitic. In quartz-poor, monzodioritic to syenitic microgranitoid xenoliths at Cement Well, K-feldspar is allotriomorphic, commonly displaying 120° triple points.

Subhedral, tabular grains, from 1–10 mm, of mesoperthitic K-feldspar are common in the alkaline granitoids of the Gilgarna supersuite. Recrystallization is variable, producing swapped rims and coarse-grained albite, which replaces the mesoperthitic intergrowth (e.g. 101047, Hamdorf Bore). An enigmatic, euhedral zoning of alternating albite and K-feldspar has been noted in K-feldspar from syenitic rocks at McAuliffe Well (see also Libby, 1989). Finer grained, microsyenitic granitoids contain discrete anhedral grains of albite and non-perthitic K-feldspar with cross-hatch twinning.

Plagioclase

Subhedral, tabular plagioclase is characteristic of calc-alkaline granitoids and dykes. Minor antiperthitic inclusions of K-feldspar occur in some samples. Myrmekitic intergrowths at grain boundaries are common, and may form large, bulbous protrusions into adjacent K-feldspar. Less commonly, plagioclase displays narrow, clear albitic rims. Inclusions of mafic minerals and accessory minerals have been noted in some samples, but are rare compared to those in K-feldspar.

Normal to oscillatory zoning is weak to pronounced, with stronger zoning in more mafic granitoids (e.g. Rainbow suite, Liberty Granodiorite). Unconformities within the oscillatory-zoned plagioclase indicate a complex growth history. Calc-alkaline granitoids with <74% SiO_2 (approximately) also display a number of other features, but only within a relatively few grains. These include: euhedral to irregular calcic cores, mantles of K-feldspar (e.g. 101359), and patchy extinction and patchy zoning (Vance, 1965) in the cores of some larger grains.

In some samples (e.g. 101377), oscillatory zoning in plagioclase is cut by narrow, irregular veins of unzoned plagioclase. This probably reflects local equilibration of plagioclase with metamorphic fluids adjacent to fine fractures. More commonly, plagioclase is variably altered to fine- or medium-grained muscovite (sericite) with lesser amounts of epidote and carbonate. This type of alteration is commonly concentrated in cores and zones within the feldspar, suggesting preferential replacement of relatively calcic plagioclase. Coarse, secondary muscovite is common in some of the more leucocratic post-regional folding monzogranite and granodiorite.

Plagioclase is less susceptible to recrystallization than is K-feldspar. It is commonly cracked and fractured, or has bent twinning planes, but in strongly recrystallized zones, plagioclase forms anhedral, granoblastic grains. In Depot Granodiorite, 120° triple points among plagioclase grains are common, suggesting substantial strain-free recrystallization.

Plagioclase in microgranitoid xenoliths displays many of the features of that in the host granitoid, but is more anhedral or lath-like in form. Although there are exceptions, zoning tends to be less distinct than in the more mafic granitoid host rocks. Subhedral to euhedral, tabular plagioclase phenocrysts, with weak to moderate oscillatory zoning, occur in some dykes and microgranitoid xenoliths.

Plagioclase in alkaline granitoids is anhedral to subhedral, and rarely zoned.

Compositions have been determined from extinction on twin planes normal to (010). Calc-alkaline granitoid plagioclase compositions vary between An_5 and An_{20}, with core compositions of An_{27}–An_{32}. Dykes contain plagioclase with compositions in the range An_9 to An_{30}, with most more calcic than An_{14}. Plagioclase in microgranitoid xenoliths varies from An_{15} to An_{30}. Libby (1989) reported the presence of albite and sodic oligoclase in alkaline granitoids of the Gilgarna supersuite. Granitoid gneiss samples contain plagioclase within the range of compositions for plagioclase in calc-alkaline granitoids.

Biotite

Biotite forms anhedral to subhedral, tabular to platy grains, but is commonly recrystallized to aggregates of smaller, irregularly-shaped grains. In foliated granitoids these aggregates are elongate, and define an anastamosing foliation. Microgranitoid xenoliths contain a similar form of biotite, although in some cases elongate laths (length to width ratio up to about 6:1) are characteristic (e.g. 100955). Inclusions of zircon and/or apatite are common in some granitoids, but are minor to absent in microgranitoid xenoliths. Biotite within biotite-rich (?surmicaceous) xenoliths in the Owen complex contains abundant apatite inclusions with metamict halos.

Biotite is typically pleochroic from very pale brown, to brown, to dark brown. In many calc-alkaline granitoids with less than 74% SiO_2, biotite displays distinctly green-brown tints; however, green biotite is less common in microgranitoid xenoliths. Green biotite is associated with fine, granular, secondary titanite, or needle-like inclusions of ilmenite. This relationship suggests metamorphic replacement of a brown (Ti, Fe^{+2}-rich) biotite by Fe^{+3}-rich biotite (Deer, Howie and Zussman, 1970), with titanite or ilmenite expelled as a byproduct of the reaction. Green and brown biotite is variably altered (minor to extensive, even within a single thin section) to epidote and/or chlorite. Secondary muscovite after biotite is common in many granitoids containing greater than 74% SiO_2. Altered biotite is associated with secondary titanite, rutile, ilmenite or hematite, and in some cases fluorite, which presumably formed from titanium and fluorine expelled from the original biotite.

Small flakes of biotite with ragged terminations are concentrated in mafic clots in some xenoliths. In some cases these clots contain relict hornblende. The alkaline granitoids do not contain primary biotite.

Although some biotite in amphibole-bearing granitoids and microgranitoid xenoliths is late- to post-magmatic (see **Amphiboles**, below), most biotite has a primary igneous origin. The presence of biotite inclusions in the cores and margins of feldspar phenocrysts (101015, 101035) indicates that it crystallized directly from the melt from the earliest stages of solidification.

Amphiboles

Amphiboles in calc-alkaline granitoids and dykes are mostly subhedral, prismatic and pleochroic from pale yellow-green, to green or olive green, to brown-green, dark green or blue-green. Optical properties are consistent with compositions corresponding to magnesio-hornblende or actinolitic hornblende. They are commonly associated in irregular aggregates with biotite and accessory phases (opaque oxides, titanite, apatite). Inclusions of apatite and magnetite are common.

Amphiboles contain little evidence of recrystallization, except in highly deformed contact zones of intrusions, but are variably altered to biotite and pale yellow epidote (pistacite). Hornblende also displays irregular colour zoning and evidence for patchy replacement by actinolitic (?metamorphic) amphibole (101375). In some of the more mafic calc-alkaline granitoids of the Birthday complex, some amphibole grains have relict clinopyroxene cores. However, much amphibole, even in these rocks, is subhedral to euhedral and appears to be a primary igneous phase. The stability of hornblende, from the earliest stages of crystallization, is indicated by its presence as inclusions in K-feldspar, and in other phenocrysts, in many calc-alkaline granitoids.

Amphibole in the Depot Granodiorite is interstitial to all other silicate minerals, and contains inclusions of plagioclase and zircon.

In microgranitoid xenoliths, hornblende has a similar form to that in the host granitoid, but more commonly has ragged terminations. In some cases, it occurs as aggregates in subparallel layers, defining a weak foliation. In gneiss-textured xenoliths (e.g. 89997) the amphibole is oriented parallel to the foliation. Hornblende-rich clots are common

in hornblende-bearing xenoliths, and consist of aggregates of subhedral grains, in some cases crowded with fine, dusty inclusions of magnetite (Figure 3.1g).

Primary amphibole is modally subordinate to pyroxene in most alkaline granitoids. It has a similar form and optical properties to amphibole in calc-alkaline granitoids. Libby (1989) suggested that it is most common in samples that are transitional towards calc-alkaline granitoids, and decreases in abundance in more alkaline rocks containing distinctly pleochroic pyroxene (aegerine–augite). Rare hornblende megacrysts, containing apatite and titanite inclusions, occur in some alkaline granitoids (e.g. south of Tassy Well, 101078).

Replacement of hornblende by biotite in calc-alkaline granitoids and microgranitoid xenoliths could be attributed to late-magmatic (Speer, 1987) or metamorphic (Wyborn and Page, 1983) processes. Biotite that replaces hornblende along cleavage planes and grain boundaries is clearly post-magmatic, and possibly metamorphic in origin. In some granitoids (e.g. 101069 from Rainbow Bore) and biotite-bearing xenoliths (100953, 100955 from Goongarrie) hornblende occurs only as inclusions in plagioclase and quartz phenocrysts, and as rare relicts in biotite-rich aggregates, suggesting it was stable at an early stage of crystallization, but reacted with the melt unless protected by its inclusion in a larger grain.

Pyroxene

Clinopyroxene occurs only as relicts within amphibole grains in calc-alkaline granitoid samples of the Rainbow suite that were collected adjacent to large, clinopyroxene-bearing microgranitoid xenoliths. The presence of clinopyroxene, mainly as relict grains in amphiboles, suggests a process that could be attributed to either late-magmatic reaction between pyroxene and the melt, or to post-magmatic metamorphism. Fine, dusty magnetite inclusions in the cores of some amphibole grains could be interpreted to indicate late-magmatic equilibration of pyroxene and melt to form hornblende. A reaction of this type has been proposed to describe similar relationships in the Bullenbalong supersuite in the Lachlan Fold Belt of New South Wales (Chappell et al., 1987) and the Liberty Hill pluton in South Carolina (Speer, 1987).

Clinopyroxene is more common in some microgranitoid xenoliths, where it is weakly pleochroic, pale green, and partly altered to green amphibole. Relatively pristine clinopyroxene has been preserved in a gneiss-textured monzonitic xenolith (101019). Rare clinopyroxene-rich clots, and cumulate-textured pyroxene (rounded clinopyroxene to about 0.5 mm with interstitial hornblende) occur in some hornblende- and pyroxene-rich xenoliths (e.g. 101031, 101033).

Weakly to distinctly pleochroic clinopyroxene is the dominant mafic silicate in alkaline granitoids. The pleochroic scheme is pale green to olive green to emerald green. Libby (1989) reported two pyroxene compositions in alkaline granitoids. Sodian ferrosalite to sodian augite, containing up to about 2% Na_2O is more widespread, but aegerine–augite (7–9% Na_2O) occurs in intrusions with higher alkalinity (e.g. McAuliffe Well). Pyroxenes are commonly altered to amphibole, including magnesio-reibeckite and richterite (Libby, 1989).

Orthopyroxene has been identified only as a single grain in a sample from south of Princess Bore (the Red Lake locality; Libby, 1989).

Muscovite

Secondary muscovite, after plagioclase and biotite, occurs in relatively leucocratic calc-alkaline granitoids, mostly post-regional folding monzogranite and syenogranite. Although much is secondary, some colourless mica, intergrown with biotite, displays many of the features characteristic of primary muscovite (Miller et al., 1981). These include: clean grain boundaries against biotite, coarse grainsize, absence of relict biotite, and weak pleochroism (colourless to pale brown) suggesting a phengitic composition. Primary muscovite is practically confined to post-RFGs, and is not greatly recrystallized in most samples. However, probable primary muscovite was observed in a pre-regional folding, two-mica monzogranite in the Mulliberry complex (101006). Recrystallization of muscovite involves grain-size reduction, and orientation of grains in foliated samples.

Garnet

Minor garnet was identified in a few post-regional folding, muscovite–biotite monzogranite samples, including an aplitic phase at the margin of the Bali Monzogranite. Garnetiferous samples were also collected west of Jungle Well, and near Donkey Rocks (in the monzogranite and in an associated pegmatite dyke). Hunter (1991) reports the presence of garnet in the Calooli Monzogranite. The garnet is typically subequant, subhedral to anhedral, and forms relatively coarse, but sparse, grains to about 4 mm. In the aplite, garnet occurs in bands parallel to the contact. Garnet is commonly restricted to two-mica granitoids (exclusive of hornblende). Although the three minerals have not been observed in the same thin section, two petrographically similar samples from west of Jungle Well contain biotite–garnet and biotite–hornblende.

Melanite garnet is a minor phase of some alkaline granitoids of the Gilgarna supersuite. Coarse-grained (to several millimetres), anhedral garnet is particularly abundant in pegmatitic segregations associated with mixing of relatively mafic and felsic alkaline magmas (e.g. Twin Peaks, Cement Well).

Titanite

Salmon pink to red-brown, subhedral to euhedral rhombs of titanite, to about 1 mm, are common in many of the calc-alkaline granitoids. Crystal overgrowths are common, and indicate a multistage growth history. A few samples contain inclusions of opaque minerals, apatite and/or zircon. Primary titanite is commonly well-preserved but is extensively altered to leucoxene in some samples.

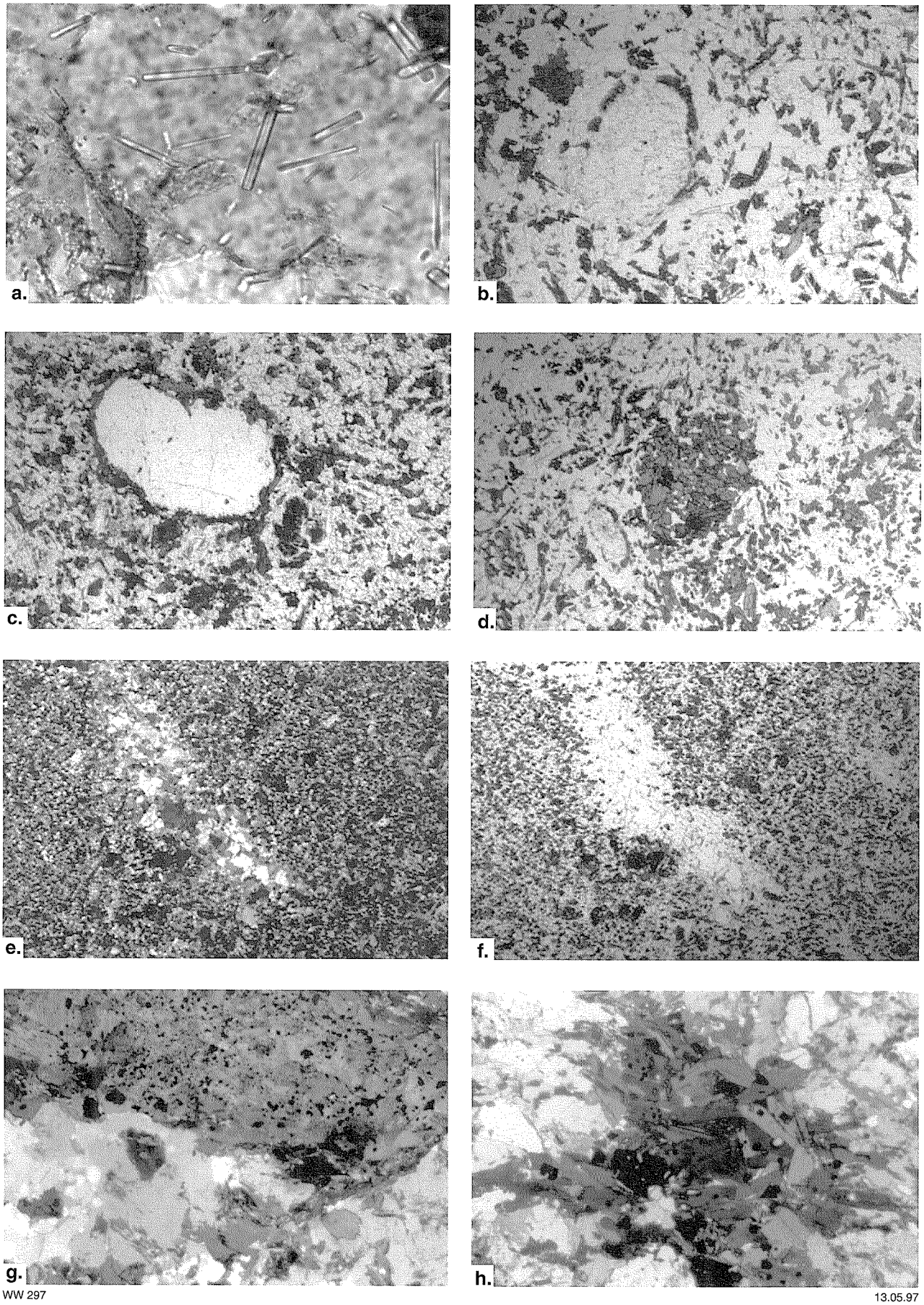

WW 297

13.05.97

Figure 3.1a Acicular apatite inclusions in quartz, micrograniteoid xenolith in a Rainbow suite granitoid, Boundary Bore. GSWA 101084, plane-polarized light. Width of field approximately 0.05 mm

Figure 3.1b K-feldspar ocellus with a mantle of amphibole, microgranitoid xenolith in a Rainbow suite granitoid, Cement Well. GSWA 101380, plane-polarized light, width of field approximately 4 mm

Figure 3.1c Quartz ocellus with a mantle of amphibole, microgranitoid xenolith in a Rainbow suite granitoid, Cement Well. GSWA 101383A, plane-polarized light, width of field approximately 4 mm

Figure 3.1d Biotite–amphibole clot in a microgranitoid xenolith in a Rainbow suite granitoid, Cement Well. Note K-feldspar ocellus near lower left margin of clot. GSWA 101380, plane-polarized light, width of field approximately 4 mm

Figure 3.1e Leucocratic patch (quartz–K-feldspar) in mesocratic monzonite dyke, Cement Well. GSWA 101025, crossed polars, width of field approximately 10 mm

Figure 3.1f Same field of view as in (e) but in plane-polarized light

Figure 3.1g Amphibole-rich clot with abundant magnetite inclusions, from a microgranitoid xenolith in a Rainbow suite granitoid, Split Rock. GSWA 89993, plane-polarized light, width of field approximately 2 mm

Figure 3.1h Biotite-rich clot (with minor magnetite and apatite) from a microgranitoid xenolith in a Rainbow suite granitoid, Split Rock. GSWA 89916B, plane-polarized light, width of field approximately 2 mm

Primary titanite is readily distinguished from pale yellow-brown to colourless, fine-grained, granular, secondary titanite associated with altered biotite.

Primary titanite is very common in some micro-granitoid xenoliths, but is rare or absent in others. In some xenoliths, it occurs as anhedral grains, interstitial to plagioclase and hornblende, rather than as euhedral rhombs (e.g. 93902).

In the alkaline granitoids, titanite is a distinct orange colour.

Opaque oxide minerals

The oxide-mineral assemblage is particularly important because it imparts a characteristic magnetic signature that can assist the mapping of intrusive units based on aeromagnetic data.

The main primary assemblages are: magnetite only; magnetite and ilmenite–hematite solid solution; and magnetite and ilmenite. Magnetite is subequant and subhedral to euhedral. Ilmenite and ilmenite–hematite solid solution are subequant and anhedral.

Opaque minerals display evidence of subsolidus re-equilibration, possibly during regional metamorphism. Magnetite displays variable, but mostly minor, cleavage-controlled alteration to hematite. Subsolvus exsolution of ilmenite–hematite solid solution has produced intergrowths between ilmenite and titaniferous hematite (Haggerty, 1976). Magnetite and ilmenite commonly occur as independent but spatially associated grains. Less commonly, 'oxidation exsolution' of titanomagnetite has produced compound, sandwich and trellis magnetite–ilmenite intergrowths (Haggerty, 1976).

Primary titanite is a minor to very common accessory mineral in granitoids that contain only magnetite. However, it is commonly absent in samples containing ilmenite or ilmenite–hematite solid solution. Relicts of ilmenite or ilmenite–hematite solid solution in primary titanite, in some granitoids, suggest a late-magmatic reaction relationship. Similarly, ilmenite–hematite intergrowths are included in plagioclase, but are otherwise absent in a dyke sample from Granite Dam (100948), a sample in which titanite is a common accessory mineral. Coronas of fine-grained granular, secondary titanite around opaque oxide cores are more likely attributable to metamorphism.

Magnetite is common to abundant, and unaccompanied by other oxide phases, in the alkaline granitoids of the Gilgarna supersuite.

Apatite

Stubby, subequant to lozenge-shaped, subhedral apatite is a common accessory mineral in many of the granitoids. It commonly occurs in small aggregates with, or as inclusions in, hornblende and/or biotite. It is locally concentrated (up to about 6%) in microgranitoid and surmicaceous xenoliths, especially in mafic mineral clots, where grains can be up to 2 mm in size. Apatite also occurs as acicular inclusions in quartz and feldspar in many microgranitoid xenoliths Figure 3.1a), a habit that has not been observed in the host granitoids.

In the alkaline granitoids, apatite is common to abundant, forming several percent of the mode, and is commonly concentrated in clots or elongate aggregates with pyroxene and/or garnet.

Zircon

Small grains of zircon are an almost ubiquitous accessory phase in calc-alkaline and alkaline granitoids. They are abundant in a few samples of quartz-poor, microgranitoid xenoliths and dykes in the Birthday complex (e.g. 101031, 10132). Zoning and multiple overgrowths attest to a complex crystallization history.

Allanite

Coarse-grained (to several millimetres), subhedral to euhedral pseudomorphs of allanite occur in a few samples of calc-alkaline granitoid and microgranitoid xenoliths (e.g. Liberty Granodiorite; 100956, 98253). The allanite is rarely preserved, except as fine-grained, secondary mineral pseudomorphs surrounded by metamict decay halos.

References

CHAPPELL, B. W., WHITE, A. J. R., and WYBORN, D., 1987, The importance of residual source material (restite) in granite petrogenesis: Journal of Petrology, v. 28, p. 1111–1138.

DEER, W. A., HOWIE, R. A., and ZUSSMAN, J., 1970, An introduction to the rock-forming minerals: London, Longman.

HAGGERTY, S. E., 1976, Opaque mineral oxides in terrestrial igneous rocks, *in* Oxide Minerals *edited by* D. RUMBLE III: Mineralogical Society of America, Reviews in Mineralogy, Volume 3, p. Hg101–Hg300.

HIBBARD, M. J., 1965, Origin of some alkali feldspar phenocrysts and their bearing on petrogenesis: American Journal of Science, v. 263, p. 245–261.

HUNTER, W. M., 1991, Boorabbin, W.A. Sheet SH51-13 (2nd editions): Western Australia Geological Survey, 1:250 000 Geological Series Explanatory Notes, 46p.

LIBBY, W. G., 1989, Chemistry of plutonic felsic rocks in the Eastern Goldfields, Western Australia: Western Australia Geological Survey, Report 26, Professional Papers, p. 83–104.

MILLER, C. F., STODDART, E. F., BRADFISH, L. J., and DOLLASE, W. A., 1981, Composition of plutonic muscovite: genetic implications: American Mineralogist, v 19, p. 25–34.

ROGERS, J. J. W., 1961, Origin of albite in granitic rocks: American Journal of Science, v. 259, p. 186–193.

SMITH, J. V., 1974, Feldspar Minerals, Volume 2: Berlin, Springer-Verlag.

SPEER, J. A., 1987, Evolution of magmatic AFM mineral assemblages in granitoid rocks: the hornblende + melt = biotite reaction in the Liberty Hill pluton, South Carolina: American Mineralogist, v. 72, p. 863–878.

VANCE, J. A., 1965, Zoning in igneous plagioclase: patchy zoning: Journal of Geology, v. 73, p. 636–651.

WYBORN, L. A. I., and PAGE, R. W., 1983, The Proterozoic Kalkadoon and Ewen Batholiths, Mount Isa Inlier, Queensland: source, chemistry, age, and metamorphism: Australia BMR, Journal of Australian Geology and Geophysics, v. 8, p. 53–69.

Appendix 4

Summary of petrographic and geochemical data for SWEGP whole-rock analytical samples, by suite and supersuite

Notes for tables

Samples are arranged in approximate order, from least fractionated to most fractionated within each suite

Qualifying minerals mentioned in order of increasing abundance

Minerals in parentheses are rare, or occur in only minor amounts

Samples not included where polished thin section not available for analyses

– means opaque oxide minerals not observed

Abbreviations

bio	biotite	ilm–hm	ilmenite–hematite intergrowth
hbl	hornblende	musc	muscovite
mt	magnetite	gt	garnet
ti	titanite	ASI	Aluminium saturation index
ilm	ilmenite		

Rainbow suite

Distribution: Mainly in the Scotia and Birthday complexes

Sample no.	*Lithology*	*Opaque oxides*	*SiO_2 (%)*	*TiO_2 (%)*	*V (ppm)*
93901	Hbl–bio granodiorite	Mt, ti	68.5	0.40	49
101363	Hbl–bio granodiorite	Mt, ti, (ilm)	68.5	0.37	47
93904	Bio–hbl granodiorite	Mt, ti	69.6	0.35	40
101381	Bio–hbl monzogranite	Mt, ti	69.0	0.32	36
101377	Bio–hbl monzogranite	Mt, ti	70.0	0.28	34
98266	Bio–hbl tonalite	Mt, ti	69.9	0.29	33
101384	Hbl–bio monzogranite	Mt, ti	68.6	0.33	30
100942	(Hbl–)bio granodiorite	Mt, ti, (ilm)	69.1	0.30	30
101355	(Hbl–)bio granodiorite	Mt, ti, (ilm)	71.3	0.28	23
101375	Bio–hbl granodiorite	Mt, ti	71.0	0.20	22
101365	Bio–hbl granodiorite	Mt, ti	70.4	0.19	21

Main outliers:	90967099	low for MgO, CaO, P_2O_5, Ba; ?high for Al_2O_3
	82114	low for Na_2O, Cr, Zr; high for K_2O, Th, U
	98266	low for K_2O, Ba
	101384	low for MgO, CaO, Cr, Ni, V; high for K_2O, Nb, Y, Zr
	100942	low for CaO, Na_2O, Cr, Ni, Zr, V; high for ASL

Twin Hills suite

Distribution: Raeside and Mulliberry complexes

Sample no.	*Lithology*	*Opaque oxides*	*SiO_2 %*	*MgO %*	*Ga (ppm)*	*V (ppm)*
100931	Bio monzogranite (M)	Mt, ti	71.3	0.62	18	20
100927	Bio monzogranite (M)	Mt, ti	72.2	0.56	16	19
100926	Bio granodiorite (D)	Absent	72.3	0.53	15	12
100929	Bio granodiorite (D)	Absent	72.9	0.48	15	11
101361	Hbl–bio monzogranite	Mt, (ilm)	73.4	0.42	15	14
100946	Hbl–bio monzogranite	Mt, ilm–hm	72.4	0.33	17	3
100932	Bio monzogranite (L)	Mt, (ilm)	72.9	0.34	14	11
100928	Bio syenogranite (L)	Mt	75.1	0.25	13	7

Twin Hills locality: M — main phase (mesocratic); D — dark, fine-grained phase; L — leucocratic phase

Main outliers:

100931	?low for Li; ?high for Y
100927	?high for Y
100926	high for Zn
100929	high for Zn
101361	low for Nb; high for FeO*, TiO_2 , Y, Zn
100946	low for TiO_2, FeO*, CaO, MgO, V; high for K_2O, Ba, Rb
100932	low for CaO, MgO, Na_2O, Li; high for K_2O, Ba, Th

Goongarrie suite

Distribution: Mainly in the Goongarrie complex; also in the Scotia and Mulliberry complexes

Sample no.	*Lithology*	*Opaque oxides*	*SiO_2 (%)*	*Sr (ppm)*	*Ba (ppm)*
93906	Bio monzogranite	Mt, ti, ilm–hm	72.3	726	1 440
93903	Bio monzogranite	Mt, ti	71.0	608	1 330
93907	Bio granodiorite	Mt, ti	71.7	590	1 037
98251	Bio monzogranite	Mt, ti, (ilm)	72.3	540	1 075
98271	Bio monzogranite	Mt, ilm–hm, ilm	74.4	288	933
100949	Bio monzogranite	Mt, ilm–hm	75.0	112	217
98247	Bio monzogranite	(Mt)	76.7	86	134
98248	Bio monzogranite	(Mt)	75.9	67	103
98249	Bio monzogranite	(Mt)	76.3	65	87
90967150	Bio monzogranite	–	76.0	29	94
98250	Bio monzogranite	(Mt)	76.0	22	25

Main outliers:

98251	high for Li
100949	high for Li, U
98247	low for Rb
90967150	high for FeO*

Minyma suite

Distribution: Mainly within the Mulliberry complex

Sample no.	*Lithology*	*Opaque oxides*	*SiO_2 %*	*Rb (ppm)*	*Sr (ppm)*	*Th/Sr*
100945	Hbl–bio monzogranite	Mt, ilm	76.9	63	162	0.04
101359	Hbl–bio monzogranite	Mt, ilm	76.4	113	61	0.20
101358	Hbl–bio syenogranite	Mt, ilm	77.1	160	18	0.89
100944	Bio monzogranite	Mt	77.3	177	14	1.14

Outliers: The uniformly high SiO_2 contents obscure the identification of outliers

Woolgangie supersuite

Distribution: Widespread plutons, mostly in large batholithic masses that separate greenstone belts

Sample no.	*Lithology*	*Opaque oxides*	*SiO_2 %*	*Sr (ppm)*	*Y (ppm)*	*V (ppm)*
89950	Bio monzogranite	Ti	72.3	471	10	30
105904	Bio monzogranite	–	70.7	409	10	31
101373	Bio monzogranite	Mt, Ilm–hm	70.6	437	9	24
105903	Bio monzogranite	–	72.1	329	9	23
105905	Bio monzogranite	–	71.6	350	11	23
101388	Bio monzogranite	Mt, Ilm–hm (ti)	71.0	728	6	18
101369	Bio monzogranite	Mt, Ilm–hm	71.4	449	11	19
101371	Bio monzogranite	Mt, Ilm–hm	71.9	406	9	20
101348	Bio monzogranite	Mt, (ti)	72.1	361	15	19
101353	Bio monzogranite	Mt, ti	70.9	358	10	16
100950	Bio monzogranite	Mt, ilm–hm	71.7	310	5	15
105910	Bio monzogranite	–	72.2	286	13	13
101366	Bio granodiorite	Mt	71.9	323	12	13
100941	Musc–bio syenogranite	Mt, ilm–hm	72.9	167	13	14
90967423	Bio monzogranite	–	72.9	163	14	13
105902	Bio monzogranite	–	73.1	189	17	14
101346	Musc–bio monzogranite	Mt, ilm–hm	72.4	212	12	13
101372	Bio monzogranite	Mt	73.0	286	8	12
105901	Bio monzogranite	–	73.7	209	13	9
90967541	Bio monzogranite	–	73.3	189	14	10
105907	Bio monzogranite	–	72.7	140	20	11
101360	(Hb–)bio monzogranite	Mt, ti	74.3	83	22	8
100938	Musc–bio monzograntie	Mt, ilm	73.2	96	18	7
100939	Musc–bio monzogranite	Mt, ilm–hm	73.1	98	19	7
100937	Musc–bio monzogranite	Mt	74.0	87	18	6
101368	Musc–bio syenogranite	Mt, ilm	74.3	74	40	6
100934	Musc–bio monzogranite	Mt, (ilm)	74.1	64	29	6
90967589	Bio monzogranite	–	74.1	111	13	5
105906	Bio monzogranite	–	74.4	291	10	5
101347	Bio monzogranite	Mt, ilm–hm	73.4	230	9	5
198280	Bio monzogranite	Mt	74.4	106	33	4
100940	Bio monzogranite	Mt, ilm–hm	74.4	78	21	4
101351	Musc–bio monzogranite	Mt, ilm–hm	73.9	64	30	4
100933	Musc monzogranite	Mt	74.2	65	29	5
105908	Bio monzogranite	–	73.2	202	10	3
101350	Musc–bio monzogranite	Mt	75.1	54	21	<3
100936	Musc–bio monzogranite	Mt	74.2	50	29	3
101349	Musc–bio monzogranite	Mt	75.0	77	38	<3
101352	Gt–musc–bio monzogranite	Mt	74.9	30	41	<3

Main outliers:

89950	low for Rb
105904	low for F
101388	high for Sr
101360	low for Rb, Th; high for FeO*
105906	?low for Y; high for Ba, Sr
101351	low for Nb
105908	low for Cao; high for K_2O
101350	low for Nb

Bali suite

Distribution: Along the western margin of the Kalgoorlie (greenstone) Terrane

Sample no.	*Lithology*	*Opaque oxides*	*SiO_2 (%)*	*Al_2O_3 (%)*	*Zr (ppm)*
98267	Bio monzogranite	Mt, ilm–hm, (ti)	72.9	15.0	140
98258	Bio monzogranite	Mt	72.7	15.1	124
77686	Bio granodiorite	–	72.0	15.3	108
98273	Bio–musc monzogranite	Mt, ilm–hm	73.1	14.9	97
82130	Musc–bio monzogranite	–	73.9	14.7	96
98260	Bio–musc monzogranite	Mt, ilm–hm	74.6	14.2	80
98257	Bio monzogranite	Mt, ilm	74.0	14.5	75
98268	Bio monzogranite	Mt	74.5	14.2	70
82131	Musc–bio monzogranite	–	74.5	14.3	67
98275	Bio–musc monzogranite	Mt	74.2	13.7	65
98274	Bio–musc monzogranite	Mt	74.6	13.7	68
82132	Musc–bio monzogranite	rare to absent	76.2	13.8	–
98261	Gt–musc microgranite	rare to absent	75.7	14.2	40

Main outliers:
98257 high for Rb
98268 high for Ba
98261 high for F, Li, Zn

Dairy supersuite

Distribution: Small plutons, distributed along linear trends

Sample no.	*Lithology*	*Opaque oxides*	*SiO_2 %*	*TiO_2 (%)*	*Zr (ppm)*	*K/Rb*
100924	Musc–bio monzogranite	Mt	75.9	0.04	35	368
98254	Bio monzogranite	Mt, (ti)	75.9	0.07	67	373
98255	Musc–bio monzogranite	Mt, ilm	75.3	0.10	67	258
101364	Hbl–bio monzogranite	Mt, ilm	76.1	0.14	147	247
98256	Bio monzogranite	Mt, ilm	76.7	0.05	63	226
101367	Bio monzogranite	Mt	75.9	0.17	149	211
100925	Musc–bio monzogranite	Mt	75.7	0.04	50	102

Main outliers: The uniformly high SiO_2 contents obscure the identification of outliers

Liberty supersuite

Distribution: Widespread

Sample no.	*Lithology*	*Opaque oxides*	SiO_2 %	TiO_2 (%)	*Sr* (ppm)	*V* (ppm)
Liberty Granodiorite						
97098	Bio–hbl granodiorite	Mt, ti	66.4	0.47	850	52
97096	Bio–hbl granodiorite	Mt, ti	66.4	0.48	805	54
97701	Bio–hbl granodiorite	Mt, ti	66.9	0.48	788	62
89930	Bio–hbl granodiorite	Mt, ti	67.1	0.46	777	61
89910	Bio–hbl granodiorite	Mt, ti	67.1	0.46	725	57
97100	Bio–hbl granodiorite	Mt, ti	68.2	0.46	734	57
97094	Bio–hbl granodiorite	Mt, ti	68.8	0.42	694	50
97093	Bio micromonzogranite	Mt, ti	70.7	0.37	611	26
Doyle Dam Granodiorite						
98263	Bio–hbl granodiorite	Mt, ti	70.5	0.29	566	30
98265	Bio–hbl granodiorite	Mt, ti	71.0	0.29	552	31
98264	Bio–hbl granodiorite	Mt, ti	69.5	0.33	534	36
Bonnie Vale Tonalite						
98259	Bio tonalite	–	71.7	0.22	344	22
Depot Granodiorite						
98276	Hbl granodiorite	Mt, ti	68.9	0.18	1 212	23
98278	Hbl granodiorite	Mt, ti	69.1	0.19	1 131	22

Main outliers: 97098 low for V
97096 low for V

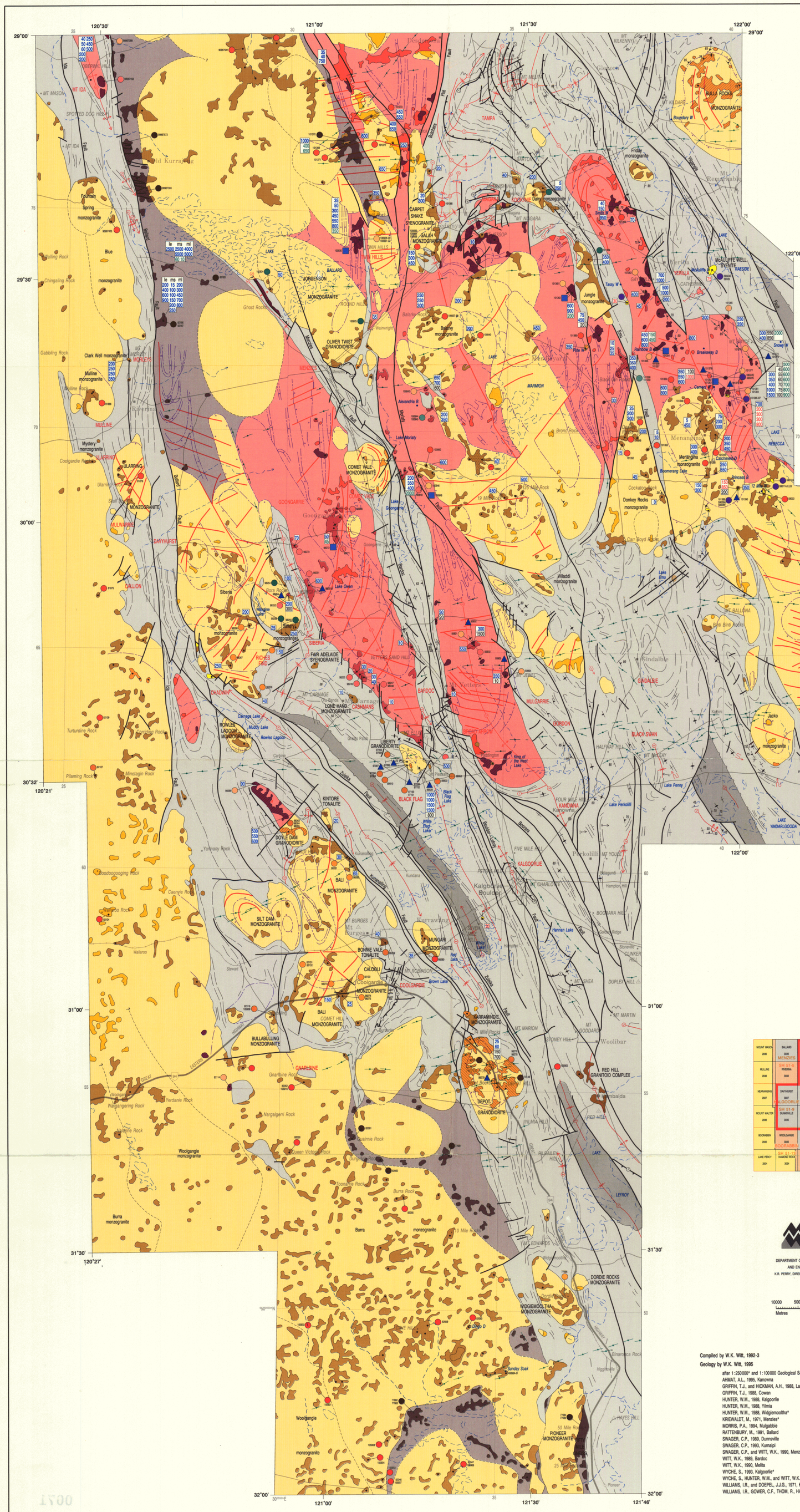

Compiled by W.K. Witt, 1992-3

Geology by W.K. Witt, 1995

after 1:250000* and 1:100000 Geological Series maps
AHMAT, A.L., 1995, Kanowna
GRIFFIN, T.J., and HICKMAN, A.H., 1988, Lake Lefroy
GRIFFIN, T.J., 1988, Cowan
HUNTER, W.M., 1988, Kalgoorlie
HUNTER, W.M., 1988, Yilmia
HUNTER, W.M., 1988, Widgiemooltha*
KRIEWALDT, M., 1971, Menzies*
MORRIS, P.A., 1994, Mulgabbie
RATTENBURY, M., 1991, Ballard
SWAGER, C.P., 1989, Dunnsville
SWAGER, C.P., 1993, Kurnalpi
SWAGER, C.P., and WITT, W.K., 1990, Menzies
WITT, W.K., 1989, Bardoc
WITT, W.K., 1990, Melita
WYCHE, S., 1993, Kalgoorlie*
WYCHE, S., HUNTER, W.M., and WITT, W.K., 1992, Davyhurst
WILLIAMS, I.R., and DOEPEL, J.J.G., 1971, Kurnalpi* (1st ed.)
WILLIAMS, I.R., GOWER, C.F., THOM, R., HARLEY, A.S., and KOEHN, P.R., 1973, Edjudina*

Edited by C. Strong, S. Willis and G. Loan

Cartography by S. Collopy

Topography from the Department of Land Administration, with modifications from geological field survey

Published by the Geological Survey of Western Australia. Copies available from the Mining Information Centre, Department of Minerals and Energy, 100 Plain Street, East Perth, WA, 6004. Phone (09) 222 3459, Fax (09) 222 3444

Printed by Allwest Print, Western Australia

The recommended reference for this map is: WITT, W.K., 1996, Granitoid geology of the southwest Eastern Goldfields: Western Australia Geological Survey, Report 49, Plate 1

REPORT 49 PLATE 1

GRANITOID GEOLOGY

OF THE SOUTHWEST

EASTERN GOLDFIELDS